SENSITIVITY OF PROBABLE MAXIMUM FLOOD ESTIMATES IN THE LOWER NELSON RIVER BASIN

By

Kevin Andrew Barlishen Sagan

A Thesis submitted to the Faculty of Graduate Studies of

The University of Manitoba

In partial fulfillment of the requirement for the degree of

MASTER OF SCIENCE

Department of Civil Engineering

University of Manitoba

Winnipeg, Manitoba, Canada

December 2017

ABSTRACT

The sensitivity of Probable Maximum Flood (PMF) estimates in the Lower Nelson River Basin (LNRB) was tested to hydrological model choice, parameterization, and climate change impacts on PMF inputs. Three hydrological models were employed in the analysis: an existing PMF model in SSARR, and HEC-HMS and WATFLOOD models that were recalibrated for PMF conditions. The impact of model choice was less significant than that of choice of calibration period. Model parameter uncertainty was explored in a limited capacity using Monte Carlo-based sampling; parameterization was also more impactful than choice of model. Regional Climate Model (RCM) data was used to project climate change impacts on PMF inputs. RCM projections were highly variable and produced the greatest range of uncertainty about the baseline. PMF is a critical dam design and safety consideration; this research improves the understanding of PMF estimates in the context of climate change and advancements in hydrological modelling.

ACKNOWLEDGEMENTS

Thank you to my advisor, Dr. Trish Stadnyk, for your guidance and your patience, for challenging me, and ensuring that I was prepared every step of the way. Thank you especially for your positive reinforcement over my part-time studies – you prevented an (isotopic) decay of my productivity! Thank you as well to Dr. Masoud Asadzadeh and Dr. Ronald Stewart for giving of your time to serve on my examining committee.

A big thank you to the Hydrologic and Hydroclimatic Studies Section at Manitoba Hydro (Ms. Kristina Koenig, Mr. Phil Slota, Mr. Mike Vieira, Mr. Mark Gervais, Mr. Shane Wruth) and Mr. Efrem Teklemariam for your support and for involving me in such an intriguing topic. I truly appreciated the opportunity to learn from each of you. Your creativity is contagious. Thanks for giving me a place to sit once a week!

Merci to Ms. Anne Frigon, Ms. Jacinthe Clavet-Gaumont, Mr. Blaise St. Denis-Gauvin, and the rest of the team at Ouranos – for your support, insights, and for providing data from the Canadian Regional Climate Model (CRCM4) used in this research. Your understanding of climate science and uncertainty was invaluable. Thanks too for welcoming me to Montreal! I hope we have the opportunity to collaborate in the future.

Thank you to Mr. Joe Groeneveld of Hatch Ltd. for your mentorship on the intricacies of the SSARR model and of PMF. I appreciated your generosity in supporting a young engineer.

Thank you to Ms. Abby Scaletta, for all of your hard work in Summer 2015. Thank you also to everyone in the CWRA-SYP team, and all the upstairs and downstairs grad students. It was a blast, and an honour to be elected as “Pope”. I wish you all the best.

My project received support from Manitoba Hydro, the Natural Sciences and Engineering Research Council (NSERC), Ouranos, the Canadian Dam Association, and the University of Manitoba. I am honoured to have been supported by such noteworthy organizations.

I must also recognize the study, *Probable Maximum Floods and Dam Safety in the 21st Century Climate*, which was made possible by support from Natural Resources Canada through the Adaptation Platform Energy, through financial support of Fonds Vert Québec, Ontario Power Generation, Manitoba Hydro, and with technical support from Hydro-Québec, Rio Tinto, INRS-ETE and the Ministère du Développement durable, de l'Environnement et de la Lutte contre les changements climatiques (MDDELCC). That study provided input data used in my research and gave me the opportunity to interact with subject matter experts from across Canada.

The North American Regional Climate Change Assessment Program (NARCCAP) provided data used in this research. NARCCAP is funded by the National Science Foundation (NSF), the U.S. Department of Energy (DoE), the National Oceanic and Atmospheric Administration (NOAA), and the U.S. Environmental Protection Agency Office of Research and Development (EPA).

I am lucky to have tremendous family and friends who I could look forward to at the end of a long day. Thank you to my parents for all you have done to guide and encourage me; and thank you to my sisters for keeping things light and making me laugh. You all know how to keep things in perspective – this would be deserving of something like, "Well aren't I special".

Finally, to my fiancée, Laura: throughout the last three years (and more), thank you for brightening my day and reminding me to have fun.

TABLE OF CONTENTS

LIST OF TABLES

LIST OF FIGURES

1.0. INTRODUCTION

The Probable Maximum Precipitation (PMP) and Probable Maximum Flood (PMF) play an important role in safe dam design (Environment Canada, 2004). The PMF is used as the inflow design flood for dams or related infrastructure classified to have an extreme consequence of failure in Canada (CDA, 2007) and the United States (England, 2011). The PMF is considered to be the "most severe flood that may reasonably be expected to occur at a particular location" (CDA, 2007 p. 12), and is simulated based on the combination of severe meteorological, hydrological, and antecedent inputs that are then used as forcing to a hydrologic model (FERC, 2001; Whitfield, 2012).

PMP and PMF are often provided only as design values, with little exploration of sources of uncertainty (Alberta Transportation, 2004; Chernet, Alfredsen, & Midttømme, 2014), and PMP estimates in particular are often out of date (England, 2011). However, the need has been recognized for re-evaluation of extreme meteorological inputs in the face of climate change (Beauchamp, Leconte, Trudel, et al., 2013; Chernet et al., 2014; Environment Canada, 2004; Veijalainen & Vehviläinen, 2008), and for comparison of multiple models and calibrations when considering high flow scenarios (Vansteenkiste, Tavakoli, Ntegeka, et al., 2014). This research was intended to contribute to these areas and to explore a wider range of plausible PMF scenarios.

1.1. PROJECT MOTIVATION

Natural Resources Canada (NRCan) commissioned a study in 2013 to review PMF estimation methods in various jurisdictions, and to incorporate climate change projections into

the estimation of PMP and PMF. As part of the study, several dam owners, including Manitoba Hydro, assessed possible changes in PMF events using hydrological models of their respective study basins and future climate scenarios compiled by the Ouranos Consortium and the Water Earth Environment Centre of the National Institute of Scientific Research (Institut national de la recherche scientifique, Eau Terre Environnement; INRS-ETE). The methodology and findings were intended as a step towards standardizing the incorporation of climate change information into PMF estimates in Canada. A public report (Ouranos, 2015) from the study was published in 2015 and is available online (https://www.ouranos.ca/en/publications/); the public report is referenced here when referring to the study in general. An article on the study was also recently published (Clavet-Gaumont et al., 2017) and will be referenced for details on methodology and climate model projections. The study is generally referred here as "the NRCan PMP/PMF study" for simplicity.

The NRCan PMP/PMF study noted a high level of uncertainty related to projected changes in PMF inputs (i.e., PMP, snowpack), concluded that "climate change may increase future PMF values", and suggested various regulatory or non-invasive adaptation methods (Ouranos, 2015). However, just as climate change projections have led to projected changes in PMF inputs, so too have advancements in computing and engineering led to more complex hydrological models and more robust methods to optimize those models. Older hydrological models traditionally used in PMF studies may, in fact, no longer be supported. By testing different hydrological models, a range of multi-model uncertainty around PMF estimates can be produced that may be similar to the variability caused by climate change (Steinschneider, Wi, & Brown, 2014). This justifies that further research is warranted to evaluate and compare the PMF

ranges resulting from climate change and from other forms of uncertainty such as the hydrological model and its parameterization.

Support was provided by Manitoba Hydro in the form of a study basin of interest for PMF purposes (the Lower Nelson River Basin in northern Manitoba), as well as existing hydrological models and modelling experience with the basin that could be adapted for PMF purposes. The timing of this research proved to be advantageous; climate model data from the NRCan PMP/PMF study was available to be applied here, while initial PMF model results from this research were available to contribute to the NRCan study.

1.2. OBJECTIVES

This research has two primary objectives: (1) to estimate the sensitivity of PMF estimates in the Lower Nelson River Basin (LNRB) to projected inputs under climate change; and (2) to explore uncertainty in these estimates related to hydrological model selection and parameterization. The first objective is achieved by (a) acquiring climate change projections for some PMF inputs (i.e., PMP, temperature and snowpack) developed by Ouranos and INRS-ETE for the LNRB as part of the NRCan PMP/PMF study, and (b) deriving change factors for other PMF inputs using raw climate model data in order to consider additional PMF scenarios. As part of this research, existing calibration and uncertainty analysis methodologies were applied to a PMF application. The projected climate change impacts were incorporated into PMF scenarios, the critical PMF was defined in the baseline and future periods, and the sensitivity of PMF was evaluated to changes in each individual input.

The second objective is achieved by estimating baseline and future PMF using multiple hydrological models of varying structure and complexity. An existing PMF model used by

Manitoba Hydro (i.e., SSARR) was compared to two additional PMF models developed as part of this research (i.e., HEC-HMS and WATFLOOD) to assess the effect of model structure and parameterization on PMF estimates, and the sensitivity of each model structure to projected changes in climate. In order to accomplish the second objective, and due to a lack of existing literature on the subject, methods were applied for calibrating more complex models (i.e., HEC-HMS and WATFLOOD) to PMF conditions. This calibration of additional models for PMF simulation represents an additional objective for the project and also provides for a comparison to the baseline, historical PMF model calibration (i.e., in SSARR) using a more recent (wider) range of high flow years in HEC-HMS and WATFLOOD.

This research is intended to advance the study of sensitivity of PMF estimates to several commonly-acknowledged sources of uncertainty that have not previously been well explored in PMF studies. The exploration around PMF is limited by the factors noted below; however, it is considered sufficient to assess the significance of each uncertainty source. Although this research may lead to a more robust understanding of PMF (present and future) in the LNRB, the intent is that the application is transferable to other basins where PMF is a dam safety consideration. Indeed, applying the study parameters to other basins is encouraged.

1.3. SCOPE

This research represents a first step in quantifying the sensitivity and, in some cases, the uncertainty of PMF estimates from a variety of plausible changes and sources of uncertainty. The project objectives were accomplished through results that explore PMF estimates in four ways:

(1) Through comparison between baseline and future projected simulations to assess sensitivity of PMF to climate change;

(2) Through stepped incorporation of changes to PMF inputs, in order to determine the sensitivity of PMF to each type of forcing (i.e., precipitation, snow cover, temperature, and upstream contributions);

(3) Through comparison of multiple hydrologic models in order to evaluate sensitivity of PMF to the choice of hydrologic model, calibration period, and the sensitivity of each model to projected changes in climate; and

(4) Through evaluation in each hydrologic model of the significance of individual model parameters in producing PMF estimates, and the range of PMF estimates that develop from each model.

The results and conclusions of this research are structured to address each of these areas, in order to satisfy the research objectives.

The following discussion highlights the limitations associated with the methodology developed to achieve these results. Limitations to the methodology are best framed in the context of the following caveat from the U.S. Federal Energy Regulatory Commission (FERC, 2001 p. 4) – *"No single method of PMF analysis is without limitations"*.

This study considers only spring PMF scenarios, in particular the two scenarios recommended by the Canadian Dam Association in its Dam Safety Guidelines 2007 (revised 2013). Uncertainty in summer/fall PMF was not considered due to time constraints related to analyzing additional climate change projections, the potential need for model re-calibration, and that summer/fall PMF (rainfall-dominated) has not historically been a critical PMF scenario in the basin of interest.

Spring PMF inputs used in this study as "baseline" values are those developed in previous PMF studies for the Lower Nelson River Basin (LNRB). These inputs (e.g. PMP,

snowpack) have been periodically reviewed or updated in the context of additional meteorological data, most recently in 2013 (Hatch Ltd., 2013b), and continue to be used for PMF studies at Manitoba Hydro. As such, the assumption is made that the historically estimated inputs are representative for the baseline period (in this case, taken as 1971-2000). In addition, the Canadian Dam Association Hydrotechnical Considerations for Dam Safety (2007, p. 13) recommend, at least for PMP, that "estimates should be developed from suitable mapped PMP values, in preference to initiating project-specific studies". In keeping to this guideline, no re-analysis of baseline inputs was conducted for this study, and climate change projections are applied as relative perturbations to the previously-derived baseline values. This also assumes that PMF inputs in the future period will maintain the same characteristics as in the baseline (e.g. a 48-hour PMP storm, with the same temporal and spatial distribution), with only changes in magnitude considered. This assumption is necessary in that current methods and climate model data are unable to capture all the necessary assumptions (e.g. worst-case orientation) required for traditional PMP estimation (Rousseau et al., 2014).

The incorporation of climate change impacts on baseline PMF inputs relies heavily on the methodology used in the NRCan PMP/PMF study (Ouranos, 2015). This methodology is recognized as a first step in exploring that form of PMF uncertainty. More recent advancements in the methodology, plus suggestions for future work, are noted in this document. Relative projected changes to some inputs (i.e., PMP, 1/100 year snowpack, daily temperature) were provided directly from Ouranos. For additional PMF inputs not considered in the NRCan PMP/PMF study (i.e., 1/100 year rainfall, Probable Maximum Snow Accumulation), raw climate model data was compiled and provided by Ouranos and then converted into change factors as part of this research. Methodologies in this latter case were assisted by recommendations from

Ouranos and Manitoba Hydro. As well, the ensemble of climate model simulations used in this study includes only those used in the NRCan PMP/PMF study; there were no attempts to acquire additional model simulations. It is recognized that there may be additional climate model runs or members available to allow for a more robust study. However, as the simulations in the NRCan PMP/PMF study were previously quality-checked by others (as applied by Clavet-Gaumont et al., 2017), only those climate model simulations are used here.

A lack of standardized guidance for appropriate PMF modelling assumptions and setups is a recognized issue for consistent PMF estimation (Nathan & Weinmann, 2015). Similarly, whether or not PMF assumptions are reasonable is subjective and specific to the watershed of interest (FERC, 2001). The methodology for PMF simulations (i.e. initial conditions and modelling assumptions), therefore, is based as closely as possible on that historically used for PMF modelling on the Lower Nelson River. This provides a closer comparison to previous PMF estimates in the LNRB and is more appropriate given that the existing PMF assumptions were developed specifically for this basin and continue to be used in PMF review studies.

Calibration to an updated time period, and a limited uncertainty analysis surrounding that calibration for the HEC-HMS and WATFLOOD PMF models was undertaken as part of this research. A similar analysis was not conducted for the existing PMF model in SSARR. Given the age and unsupported nature of the model, the existing calibration in SSARR was only validated in (not adjusted to) more recent high flow years. Additionally, due to the archaic nature of the model interface and files (owing to its age), setup and parameterization of the model for the purposes of conducting uncertainty analyses were prohibitive. Analyses were instead limited to a local sensitivity study of the existing parameter set. The SSARR model PMF estimates are therefore used in this study as a "baseline" PMF model for comparison to the HEC-HMS and

WATFLOOD PMF models. The existing SSARR PMF model is still validated over historical high flow years, as per a suggestion of FERC (2001), but there was no attempt to adjust the existing SSARR model if this performance is poor.

Finally, the forms of uncertainty addressed in this research have only been explored, and not definitively quantified. Projected future PMF simulations were limited by the spread, uncertainty, and at times, non-consensus in climate model projections. Additional model projections, particularly multi-member runs, may yield different results. Similarly, intra-model uncertainty assessment (i.e., related to calibration and parameterization) was limited by computational and time constraints: a larger number of model runs would yield more confident uncertainty bounds and parameter identifiability. The PMF ranges shown here consist only of plausible PMF scenarios (i.e., "plausible" based on the best methodology available at the time), but do not include all plausible scenarios. Ranges provided around the baseline PMF do not represent full uncertainty ranges, but rather a range depicting the impact of a plausible set of changes on the PMF.

2.0. LITERATURE REVIEW

Climate change and other areas of uncertainty have been identified as having potentially significant impacts on water resources planning decisions (Steinschneider et al., 2014), including the estimation of Probable Maximum Precipitation (PMP) and Probable Maximum Flood (PMF) (Rousseau et al., 2014). Changes in meteorological extremes have already been observed and documented (Cunderlik & Simonovic, 2005), with the expectation that changes to intensity and frequency of precipitation may impact streamflow extremes (Poitras, Sushama, Seglenieks et al., 2011), and that projected warmer temperatures could lead to increased moisture uplift and carrying capacity that will affect the variability and intensity of extreme precipitation (Trenberth, Dai, Rasmussen, et al., 2003). In short, "existing and new dams are likely to be exposed to climatic conditions during their lifetime different from those that have been experienced in the recent past" (Chernet et al., 2014, p. 569). Other areas of uncertainty in PMF (due to modelling, calibration, and inputs) have been recognized but rarely quantified; often, PMP and PMF are provided only as single design values (Alberta Transportation, 2004).

This research is intended to address some of these knowledge gaps. The following review will provide background on PMP and PMF, climate change and climate modelling, previous studies of climate change impacts on extreme meteorological and hydrological variables, and previous PMF simulations and the subsequent uncertainty in modelling extreme high flows.

2.1. BACKGROUND ON PMP/PMF

The Probable Maximum Precipitation (PMP) is "the greatest accumulation of precipitation for a given duration meteorologically possible for an area" (Kunkel, Karl, Easterling, et al., 2013, p. 1402), but more specifically, also for a given time of the year (Alberta

Transportation, 2004). It is a physically-based estimate of the theoretical maximum precipitation and has traditionally been estimated only for historical conditions (WMO, 2009). The PMP was first defined by the American Meteorological Society in 1959; during this time, limiting rates for precipitation were being developed to estimate these maximum storms (FEMA, 2012). The World Meteorological Organization (WMO) now publishes guidelines on the estimation of PMP using a moisture maximization approach, which is considered the most widely used method of estimation in North America (Rousseau et al., 2014). Although other methods have been developed for PMP estimation, including statistical and regional estimates, the baseline PMP estimates in this research were developed based on the moisture maximization approach, and therefore will be discussed in further detail.

The maximization approach commonly involves three steps that are generally agreed upon in regulatory guidelines (e.g. Alberta Transportation, 2004; CDA, 2007; WMO, 2009). First, extreme historically observed precipitation events that have occurred on the basin, or in an area that could be transposed to the basin, are selected. Second, the precipitable water available during that storm event is estimated, as is the maximum precipitable water that could have been available during the event. Precipitable water refers to the amount of water vapour available for condensation into precipitation at that time and location, and is commonly estimated based on observations of humidity or of surface dew point temperature (Rousseau et al., 2014; WMO, 2009). Maximum precipitable water refers to the most amount of moisture that could physically be available in the atmospheric column at that time and location, and is commonly estimated as the 1/100 year precipitable water (Rousseau et al., 2014). The observed storm is then maximized based on the following equation (Kunkel, Karl, Easterling, et al., 2013):

$$PMP_{estimated} = Precipitation_{storm}\, x\, \frac{Precipitable\ Water_{max}}{Precipitable\ Water_{storm}}$$

Finally, the maximized storm (with known isohyets) is transposed to the basin and oriented for maximum effect. This maximization method allows for consideration of storm isohyets, orientation, and basin-specific factors, and does not require the amount of rainfall data that statistically-based methods would require (Kulkarni, Nandargi, & Mulye, 2010).

An additional step of depth-area-duration analysis can be considered, particularly when using gridded precipitation data (i.e. the climate model outputs used for PMP estimation in this research). PMP estimates are done at a gridpoint scale, then expanded incrementally to include additional gridpoints until reaching the basin scale (Bingeman, 2001). These varying storm depths and areas, along with varying durations, can be tested to find the most critical storm. Although gridded climate model outputs can be used to estimate PMP using the maximization approach, Rousseau et al. (2014) suggest that these are not intended to replace historical PMPs; rather, they allow for change analysis between baseline and future periods that can then be applied to the existing PMP values.

The Probable Maximum Flood (PMF) is intended to be a realistic but most extreme hydrological value, used in the design of large dams. It is simulated based on the combination of severe meteorological, hydrological, and antecedent inputs that are then used as forcing to a hydrologic model (FERC, 2001; Whitfield, 2012). The concept of PMF was first mentioned in a 1964 report by the United States Army Corps of Engineers (USACE) as a guideline for the design of dams where failure could not be tolerated (FEMA, 2012). After a series of dam safety incidents in the 1970s in the United States, FEMA also specified PMF as the required spillway design flood for existing dams where significant human or economic losses were expected if failure occurred (classified as “High Hazard” dams). The Canadian Dam Association (CDA, 2007) has also defined five consequence classifications for dams, where dams with the highest

potential consequences of failure (i.e. the "Extreme" category) should be designed to pass the PMF.

The PMF can be estimated using a statistically-based or a modelling-based approach. Statistical estimation of the PMF is highly uncertain given the need to estimate a flood with a return period much larger than 1/1000 years based on short observed streamflow records, thus many jurisdictions recommend the modelling-based approach (Alberta Transportation, 2004; FEMA, 2012). The CDA (2007) recommends PMF be estimated by estimating extreme precipitation and snowpack inputs, developing a rainfall-runoff model, and defining initial conditions in the model to maximize soil moisture prior to the design storm. The unit hydrograph has been a popular rainfall-runoff tool for PMF in the past (FEMA, 2012); although regardless of method, Alberta Transportation (2004) recommends calibrating to extreme historically observed floods. The reliability of the model calibration will be based on the magnitude of difference between the calibrated events and the simulated PMF.

The PMF is not a maximum possible flood, but instead the largest flood that is still probable. This can involve a scenario where the extreme precipitation input and wet antecedent conditions lead to a ratio of runoff volume to moisture input of 75% or greater, often much larger than any previously observed event (Alberta Transportation, 2004). North American guidelines agree that initial and basin conditions and specified inputs should not each be estimated as a probable maximum, as such a combination of very extreme inputs is too severe and overly-conservative (CDA, 2007; FEMA, 2012). The most recent Dam Safety Guidelines (2007 and revised in 2013) from the Canadian Dam Association recommend that several input scenarios be tested to find the most severe PMF, including:

1. A summer-autumn PMP;

2. A spring PMP and 1/100 year snowpack;
3. A spring 1/100 year rainfall and a Probable Maximum Snow Accumulation (PMSA).

The PMSA has previously been estimated as a factored 1/100 year snowpack (Alberta Transportation, 2004) or the 1/500 year snowpack (CEA, 1994), and is explained further in Section 2.5.

In suggesting that the PMF is intended to retain some probability of occurrence, experts have found it difficult to quantify this probability, or the level of conservatism in the estimate (Alberta Transportation, 2004). A review by England (2011) found that some jurisdictions in the USA estimate PMF at rarer than $1/(1x10^8)$ years. The USACE have applied a probability of 1/10,000 years in the past (FEMA, 2012), while Bingeman (2001) presumed a probability of between 1/1,000,000 to 1/10,000 years in British Columbia. However, the probability of exceedance of the PMF is intended to be exactly (i.e. just reaching) zero in order to ensure protection to the largest plausible flood event without costly over-design (Debs, Sparks, & Birikundavyi, 1999; FEMA, 2012; E. Watt & Marsalek, 2013; Whitfield, 2012).

2.2. CLIMATE CHANGE AND CLIMATE MODELLING

Climate change is defined by the Intergovernmental Panel on Climate Change (IPCC) in their Fifth Assessment Report (AR5) as "a change in the state of the climate that can be identified…by changes in the mean and/or the variability of its properties" (Cubasch et al., 2013, p. 126). Climate refers to the mean and variability of meteorological activity, such as precipitation and temperature (Cubasch et al., 2013). Changes in the climate system are of such importance that the IPCC was formed to study all aspects of observed and projected changes, mitigation, and adaptation. The work of the IPCC is disseminated through assessment reports, of

which the two most recent are the Fourth Assessment Report (AR4; IPCC, 2007) and the AR5 (IPCC, 2014). The AR5 (IPCC, 2014, p. 40) concluded, among other things, that (a) warming of the global climate is "unequivocal", and (b) both natural and human systems are sensitive to changing climate. More specific to the area of this research, the IPCC has also noted that climate change has resulted in changes in the occurrence or strength of extreme events (Cubasch et al., 2013). The potential for changes in extreme events, such as those related to PMP/PMF, have prompted a number of studies that are synthesized in Section 2.3. Looking ahead to the future, the IPCC (2014, p. 64) projects that climate change will "create new risks" for human systems that can be reduced via adaptation. This research is an example of an adaptation measure to understand the scope of climate change that could be expected in the future.

The primary method of representing atmospheric processes in the past and projecting into the future is the use of three-dimensional climate models; which solve the mass, energy, and momentum conservation equations over a grid with many vertical layers (Cubasch et al., 2013). This has traditionally involved Atmosphere-Ocean General Circulation Models (AOGCMs; also referred to as Global Climate Models, GCMs) but recently has shifted to more advanced Earth System Models (ESMs), both of which simulate processes at low resolution across the globe (Flato et al., 2013). In either case, climate models have demonstrated an ability to accurately simulate the past observed climate and climate changes (Randall et al., 2007). This allows the models to be used for sensitivity studies and for short and long term climate projections (Flato et al., 2013). Best noted by the IPCC in the AR4, there is "considerable confidence that [climate models] provide credible quantitative estimates of future climate change" (Randall et al., 2007, p. 591).

Although climate models are based on laws of physics, they also involve approximations of the complex physical system, and mathematical representations for some processes (Randall et al., 2007). Parameterization of models is also required, with only some parameters being measurable (Randall et al., 2007). Therefore, climate models are based on similar principles but include different approximations that impact any resulting simulations, leading to uncertainty or a "model spread" (Cubasch et al., 2013, p. 138). It is important to note here that the unique structure of each climate model, driven by a set of initial and boundary conditions and an emissions scenario, represents one physically-based, plausible future climate scenario (Whitfield, 2012). All scenarios are equally likely, and their spread indicates the "potential range of future climate change" (Whitfield, 2012, p. 18).

To quantify model spread in a uniform manner, climate models are most commonly applied as ensembles to common experiments organized by the World Climate Research Programme (WCRP); these studies are referred to as phases of the Coupled Model Intercomparison Project (CMIP). The two most recent such studies have been CMIP3 (twenty-four models; e.g. Meehl et al., 2007) and CMIP5 (over fifty models; e.g. Taylor, Stouffer, & Meehl, 2012). Although CMIP5 is the latest study to be conducted, Knutti et al. (2010, p. 5) acknowledge that, "in many cases it may be appropriate to consider simulations from CMIP3". This is the case here. The climate projections applied in this research are based on a subset of six GCMs from CMIP3 – a limitation resulting from the Regional Climate Model ensembles available at the time of this study for the basin of interest. As such, further references to these models will be as GCMs, and not as the more advanced ESMs.

Climate models are forced by two components: a set of initial conditions, and a future greenhouse gas emissions scenario. GCMs are run over a number of experiment periods, most

notably a pre-industrial control period (pre-1850), a historical period (1850-2005), and a projection period (post-2005) (Taylor et al., 2012). Multiple members of the same GCM, initialized with different conditions (e.g. on different dates), lead to different "climate trajectories" that are all equally likely (Taylor et al., 2012, p. 495). For example, Deser, Knutti, Solomon, et al. (2012) initialized the atmospheric components of separate CCSM3 GCM runs on different days between December ,1999 and January, 2000, and analyzed the subsequent range of climate projections for the future period. The spread between these members illustrates inherent variability (a.k.a., "climate noise", irreducible uncertainty) that occurs naturally in the climate system (Taylor et al., 2012). The "signal" of climate change impacts can be clouded by the "noise" of natural climate variability, and thus multiple members of the same GCM with varied initial conditions are vital to better isolate the signal of interest (Deser et al., 2012).

Emissions scenarios can represent an additional form of variability in future climate projections, and have recently taken several forms. Three Socio-Economic Driven SRES Scenarios were used in the CMIP3 simulations (B1, A1B, A2, from the Special Report on Emission Scenarios, SRES; Nakicenovic & Swart, 2000). The SRES scenarios involved different "storylines" of future societal, economic, and technological changes and the impact of those actions on greenhouse gas emissions (Cubasch et al., 2013). In contrast, four Representative Concentration Pathway (RCP) scenarios (RCP2.6, RCP4.5, RCP6, RCP8.5; see Van Vuuren et al., 2011) were used in the more recent CMIP5 simulations; their fundamental difference is in having less basis on "storylines" and defining scenarios based on the peak radiative forcing in W/m^2 in the 21^{st} century. (Cubasch et al., 2013, p. 147). The RCPs were required as an input to more advanced climate models, and to account for a wider array of potential climate policies (i.e. the RCPs have a wider spread, particularly in the directions of lower emissions), and to

incorporate greenhouse gas concentrations, emissions, and potential land use changes (Van Vuuren et al., 2011). The three SRES scenarios and four RCPs are not directly comparable (Knutti & Sedláček, 2012). Although the SRES scenarios are considered to have more shortcomings than the RCPs (Cubasch et al., 2013), the climate model simulations compiled by Ouranos and INRS-ETE for the NRCan PMP/PMF study used the SRES A2 forcing. In justifying the use of SRES A2 forcing, Clavet-Gaumont et al. (2017) note that the choice of emissions scenario is expected to have little impact when considering the 2050s period.

Downscaling is a further component of climate modelling that scales GCM simulations to a finer grid, often resulting in a higher resolution over a more limited area and thus more useful inputs to hydrological models in impact studies (Chen, Brissette, & Leconte, 2011; Flato et al., 2013). A higher resolution also allows for better representation of extreme events that depend on finer-scale processes (Mladjic et al., 2011). Downscaling is conducted by two methods: statistical and dynamical. Statistical downscaling involves finding empirical relationships that allow for predicting regional climate variables based on large-scale (i.e. GCM) output (Chen, Brissette, & Leconte, 2011; Flato et al., 2013); it was not applied as part of any data used in this research and will not be discussed further. Dynamical downscaling involves the use of Regional Climate Models (RCMs) that utilize a finer grid of a limited area and take GCM data as boundary inputs (Chen, Brissette, & Leconte, 2011). Climate change projections used in this research were produced using RCMs; as such, this form of downscaling will be described in further detail.

Similar to GCMs, RCMs are based on fundamental laws of physics and attempt to model physical climate processes (Flato et al., 2013). RCMs offer a benefit of greater spatial in both present and future simulations; however, they also have an additional source of uncertainty due

to forcing data (often from GCMs) that is required at the model boundaries (De Elía & Côté, 2010; Music & Caya, 2007). Déqué et al. (2007) suggested to use at least as many GCMs for boundary conditions as the number of RCMs being studied, given the significance of uncertainty from boundary conditions. This is the case in this research: RCMs are preferred for studies of extremes given that smaller scale, as the benefit of this scale will be more significant when attempting to represent more extreme, isolated events (Feser, Rockel, von Storch et al., 2011). For example, Kawazoe & Gutowski Jr. (2013) determined that simulations from a group of six RCMs were able to accurately reproduce high-resolution observations for low-frequency rainfall events (95^{th} to 99.5^{th} percentiles). The IPCC also has "high confidence" in this improved skill in simulating extremes of "relatively small spatial or temporal character" (Flato et al., 2013, p. 815). Clavet-Gaumont et al. (2017) similarly utilized RCMs in the NRCan PMP/PMF study due to their finer scale.

A final consideration of literature in this field is the body of recommendations from the IPCC in relation to the study of extreme precipitation events, and how these recommendations are addressed in this research. IPCC (2007) concluded that GCMs do not have fine enough resolution to accurately simulate extreme events. Then, (Flato et al., 2013) synthesized that (a) simulation of extreme precipitation is sensitive to model resolution, and (b) that models with a resolution of 50km or finer have been found to sufficiently reproduce historical extreme precipitation. In addition, Doherty et al. (2009) recommended that multiple GCMs (i.e. a representative set) be used as boundary conditions for RCMs. The ensemble of simulations in this study is based on five GCMs (eleven total members) and four RCMs. This represents only a sample of available GCMs and RCMs currently available; Knutti et al. (2010, p. 2) acknowledge that such an "ensemble of opportunity" is often a necessary limitation of climate change studies

(e.g. limiting uncertainty analysis) but recommend to explicitly describe the reasoning behind an ensemble's selection.

Both recent IPCC assessment reports - IPCC (2007) and Flato et al. (2013) – as well as other literature (Veijalainen & Vehviläinen, 2008; Whitfield, 2012) acknowledge the difficulty in representing extreme events in climate models and in assessing relative changes to extremes in future projections. However, this cannot discourage the study of extremes given the IPCC's confidence in the AR5 (IPCC, 2014, p. 53) that the "frequency and intensity of heavy precipitation events has *likely* increased in North America…," and that it is very likely that "extreme precipitation events will become more intense and frequent in many regions."

2.3. PROJECTIONS OF CLIMATE EXTREMES IN NORTHERN MANITOBA

Numerous studies have been conducted on past and projected changes to extreme meteorological and hydrologic variables in Canada, including in the study area of northern Manitoba. Only studies of extreme precipitation events are discussed here, as these extreme events are expected to change by different, often larger magnitudes, than average precipitation (Veijalainen & Vehviläinen, 2008). Whitfield (2012) synthesized a number of studies that concluded there has likely been a global increase in heavy precipitation frequency and intensity, and that projections are for this heavy precipitation to become more frequent, and of increased intensity at high latitudes. Increased water vapour holding capacity in the atmosphere as temperatures increase is also connected to projected increases in extreme precipitation (Wehner, 2013). Snowmelt is generally projected to be earlier and of lower magnitude, though with a greater frequency of rain-on-snow events (Whitfield, 2012).

Mladjic et al. (2011) used five members of the CRCM4 ensemble and projected annual maximum precipitation to the 2080s (2071-2100) of varying durations over Canada. CRCM in general underestimated extreme precipitation events in the historical period, and the analysis was found to be difficult based on short historical records and 30-year baseline and future periods. The authors suggested that a regional frequency analysis approach to the gridded data may help to overcome this issue. In this approach, extremes are analyzed over a larger region of grid cells to compensate for a shorter sampling period. This method is mentioned here as it is also the method that was used to estimate PMPs from climate models in the NRCan PMP/PMF project (Clavet-Gaumont et al., 2017).

In a study of 20-year daily maximum precipitation between the baseline and the 2050s (2041-2070) over Canada using the NARCCAP ensemble, the RCMs were found to adequately represent the spatial behaviour of extreme precipitation over the historical period (Mailhot, Beauregard, Talbot et al., 2012). A similar study of extreme precipitation was conducted using the NARCCAP ensemble for the Canadian prairie watersheds (Khaliq, Sushama, Monette et al., 2014). Ensemble average projected changes in north-central Manitoba were approximately +15% for 1/50 year daily extreme rainfall and +20% for 1/50 year daily extreme snowfall (Khaliq et al., 2015). This was of a similar magnitude to a +10% projected change in 3-day, 1/100 year extreme precipitation in northern Manitoba by Mladjic et al. (2011). Although the ensemble averages showed positive changes, individual large negative projected extreme rainfall changes in the 0% to -15% range did occur, with more instances of negative projected changes as the return period of extreme rainfall increased (Khaliq et al., 2015; Mailhot et al., 2012). Both studies, as well as that by Wehner (2013) for the United States, also concluded that there was greater dispersion and lower confidence in extreme precipitation projections as the return period increased. This

widening of the uncertainty envelope with return period is important when projecting changes to extreme PMP.

Estimates of maximum precipitable water and its impact on extreme precipitation have also been conducted. A study of seven GCMs showed a projected increase in maximum precipitable water in nearly all grid cells across the globe, with an increase of 20-25% in northern Manitoba (Kunkel, Karl, Easterling, et al., 2013). The same study projected a 10-20% increase in daily maximum precipitation to the 2080s in northern Manitoba, suggesting that increased water vapour availability will drive increased extreme precipitation events in the future.

Finally, the runoff output variable from climate models have also been used to project changes in extreme discharge at various scales, including in the Nelson River Basin. Poitras et al. (2011) used Canadian Regional Climate Model (CRCM) output and projected an earlier and slightly lower 1-day maximum peak flow in the Nelson basin for the 2041-2070 period, with no significant trend in changes to the 1/10 year return period of 1-day maximum flows. A similar trend for the spring freshet and weak signal for annual runoff in the LNRB was found by Sushama et al. (2006). GCM-based studies have also been conducted. Arnell & Gosling (2013) forced a global hydrological model using CMIP3 projections to 2050 and found (a) increased 1/100 year daily streamflow in some parts of the LNRB, and (b) an insignificant signal in other areas of the basin. In contrast, the runoff variable from eleven CMIP5 GCMs analyzed by Koirala et al. (2014) for the 2071-2100 period predominantly showed decreased high flows in the LNRB, with sporadic pockets of marginal increases. Using the runoff variable from a subset of five CMIP5 GCMs, Vieira (2016) found no significant trend in maximum monthly streamflow over the much larger Nelson-Churchill watershed. The variability of these results speaks to the

uncertainty that surrounds projections of future floods. Note too that none of the studies that directly used climate model runoff data attempted to estimate flows comparable to PMF-level events; such extreme estimations are primarily done using an impact approach that utilizes a hydrological model forced by meteorological climate model output.

2.4. HYDROLOGICAL MODELLING AND PMF SIMULATIONS

Hydrological (or watershed, or rainfall-runoff) models simplify and simulate the natural processes of precipitation, snowpack, and other moisture inputs being converted into runoff in a basin, and then the flow of water through the basin (Moradkhani & Sorooshian, 2009; Singh & Frevert, 2005). Model simulations can then be applied for both design and analysis of water resources applications, such as the effect of anthropogenic or climatic changes (Singh & Frevert, 2005). Hydrological models have two major components: a representation or structure of the natural processes and a set of variables (parameters) that can be modified for the system of interest (Moradkhani & Sorooshian, 2009). A great deal of freedom exists in selecting a model that has a structure and parameterization appropriate for the application and watershed of interest (Vansteenkiste, Tavakoli, Van Steenbergen, et al., 2014).

The structure of a hydrological model (based on a modeller's "perceptualization" of the system, as coined by Beven, 2001) can be classified in several ways. The most significant classification is the degree to which the watershed is discretized. Lumped models represent the watershed as a single unit, thereby neglecting any spatial variability and considering all forcing data and rainfall-runoff processes in the basin as empirically averaged values (Aral & Gunduz, 2005; Boyle et al., 2001; Moradkhani & Sorooshian, 2009; Refsgaard & Knudsen, 1996). In contrast, distributed models discretize the basin into a system of cells (often gridded) that

considers the spatial variability of basin characteristics and meteorological forcing in the area (Aral & Gunduz, 2005; Moradkhani & Sorooshian, 2009; Refsgaard & Knudsen, 1996). A middle ground between the two is the semi-lumped model which separates the basin into a connected system of lumped elements (sub-basins), and each element averages the hydrometeorological processes for the area it represents (Boyle et al., 2001; Refsgaard & Knudsen, 1996). There is a clear trade-off of improved spatial representation with greater complexity when moving from lumped towards distributed models, which should be expected to impact model results (Ajami, Gupta, Wagener, & Sorooshian, 2004; Aral & Gunduz, 2005; Boyle et al., 2001).

In addition, the complexity of the hydrological model structure can be differentiated between conceptual and physically-based representations (Aral & Gunduz, 2005; Beven, 2001). Conceptual models use empirical parameters and equations to simplify physical processes, and often represent the watershed as a vertical system of storage elements to convert rainfall to runoff (Boyle et al., 2001; Vansteenkiste, Tavakoli, Van Steenbergen, et al., 2014). In contrast, physically-based models have parameters that are often measurable and tied more directly to physical characteristics, and try to represent processes using conservation-based physics (Ajami et al., 2004; Refsgaard & Knudsen, 1996). The complexity of a model is not the only sign of its skill – indeed, conceptual models have historically been successful at simulating observed hydrographs (Refsgaard & Knudsen, 1996). Finally, there is differentiation between models that are intended to simulate for a short period (event-based) and models that update internal parameters throughout the simulation and are stable for longer runs (continuous) (Alberta Transportation, 2004).

PMF is commonly simulated by inputting a design storm (often the PMP) and other inputs into a hydrological model. This method, which applies frequency or maximization analysis to meteorological inputs and not to historically observed runoff, is considered to have reduced uncertainty compared to estimates based on statistical analysis of streamflow records (Chernet et al., 2014). Hydrological modelling for PMF studies has historically been done using conceptual, lumped models, often event-based and built around the unit hydrograph concept, such as the HEC-1 and HEC-HMS models from the USACE (England, Velleux, & Julien, 2007). In fact, guidelines in the 1990s in the UK specified the unit hydrograph method for PMF estimation (England et al., 2007). However, Alberta Transportation (2004) notes that both event-based and continuous models have been used for PMF in their jurisdiction.

Lumped, conceptual models have been used for estimating PMF or similar low-probability design floods in Norway (PQFLOM; Chernet et al., 2014), in Quebec (HSAMI; Beauchamp, Leconte, Trudel, & Brissette, 2013), and for high flow frequency analysis in England (PDM; Lamb, 1999). Semi-lumped, conceptual models have also been used in Finland (WSFS; Veijalainen & Vehviläinen, 2008), Sweden (HBV; Harlin & Kung, 1992), Germany (HEC-HMS; Haberlandt & Radtke, 2014), and in the Nelson River basin in northern Manitoba (SSARR; Crippen Acres Wardrop, 1990). Increasing complexity in the model with additional degrees of freedom may be expected to achieve fit better to historical data, but also would introduce more uncertainty into simulations, particularly when extrapolating to much more extreme PMF conditions (Ajami et al., 2004; Alberta Transportation, 2007; Seibert, 2003; Van Steenbergen & Willems, 2012).

There are limited applications of distributed hydrological models for PMF conditions; however, both applications successfully applied the more complex model setup. Bingeman

(2001) simulated PMF in the Columbia River basin of B.C. using the WATFLOOD model forced by a PMP at a 10km grid cell resolution. England et al. (2007) also tested the Two-dimensional, Runoff, Erosion, and Export (TREX) model for simulating PMF in a semi-arid watershed in Colorado. The latter study concluded that the distributed TREX model adequately simulated spatial and temporal behaviour of past high flow events, produced an expected PMF response, and was thus an alternative to conceptual or unit hydrograph models for PMF. In both studies, the PMP could be input as a gridded spatial storm, instead of being interpolated to selected points in the basin (as it would be in a lumped or semi-lumped model).

2.5. HYDROLOGICAL MODEL CALIBRATION & UNCERTAINTY

The second component of a hydrological model is a set of parameters that can be adjusted to the watershed of interest. Some parameters are measurable (e.g. area, landcover percentages), while the majority are empirically-based and must be determined through calibration (Moradkhani & Sorooshian, 2009). Calibration is an inductive process in which parameter values are adjusted while simulated streamflow from the model is compared to an observed historical record in the basin (Beven & Young, 2013; Moradkhani & Sorooshian, 2009).

Many forms of calibration exist, ranging from manual trial and error adjustment of parameter values to automated methods that search the parameter space for an optimal solution (Moradkhani & Sorooshian, 2009). In general, any calibration method is defined by four requirements (Singh & Frevert, 2005): an objective function (that quantifies the similarity between simulated and observed streamflow), an optimization algorithm (whether trial and error or more sophisticated), termination criteria (what skill of solution is acceptable), and calibration data (meteorological data to force the model and discharge data of the same period to adjust to).

A great deal of uncertainty exists in the calibration process, particularly as the number of parameters increases, and it is generally acknowledged that care must be taken to understand that parameters may not be completely identifiable (Beven, Buytaert, & Smith, 2012) and to ensure that the model fits the observed response "for the right reasons" (Kirchner, 2006, p. 1). Both of these areas are also addressed later in this report.

Multiple studies have noted that calibration to a short number of extreme peak flow periods provide sufficient results for PMF estimation (Haberlandt & Radtke, 2014; Lamb, 1999). Length of calibration periods have varied in PMF studies, from five complete years (1981-1985, considered representative of baseline conditions; Bingeman, 2001), to the full period of record (Harlin & Kung, 1992), to a single storm event (England et al., 2007; Salas, Gavilán, Salas, et al., 2014), and to select high flow years in the period of record in the existing PMF model of the Nelson River basin (Crippen Acres Wardrop, 1990). A guidance document from Alberta Transportation (2004) recommended calibration to at least two years, with a reduction in uncertainty as the number of calibration years increases. Calibration to specific seasons in the calibration period has also been performed; the conceptual HSAMI model used by Beauchamp et al. (2013) was calibrated to summer-fall periods only, as that was the main period of concern for PMF in their study basin.

More broadly, modelling applications of flood frequency analysis with future climate projections can also be considered. Studies on this topic used calibration periods ranging from a single summer period (Kang & Ramírez, 2007), to four discontinuous years (Dankers & Feyen, 2009), to longer period of 11-17 years (Coulibaly & Dibike, 2004; Kay & Jones, 2012). Coulibaly & Dibike (2004, p. 21), in their consideration of both lumped and distributed models, chose a period to be representative of the "current climate condition" of the region. Van

Steenbergen & Willems (2012, p. 425) similarly advise that calibration should "represent the hydrological regime".

Both manual and automated calibration techniques have been applied, individually or in tandem, for PMF models. Manual calibration has the benefits of human interaction to visually inspect and learn from errors (Moradkhani & Sorooshian, 2009; Van Steenbergen & Willems, 2012), and is guided by experience that is either passed on heuristically or in explicitly documented (Boyle, Gupta, & Sorooshian, 2000). However, such calibration can be labour intensive (Moradkhani & Sorooshian, 2009) and may not be successful as the number of non-physically-based parameters and complexity of processes increase (Boyle et al., 2001). PMF models have, at times, relied on manual calibration alone - for lumped models (Harlin & Kung, 1992), distributed models (England et al., 2007), and from guidance documents (Alberta Transportation, 2004). This is representative of modelling in the latter part of the 20th century - Boyle, Gupta, & Sorooshian (2000, p. 3663) described the hesitance to accept automated calibration at the operational scale given the "excellent" results historically obtained from manual adjustment.

Hydrological models for PMF or extreme flow simulations have also utilized automatic calibration techniques, in recognition of improvements in computing power (Boyle et al., 2000) and the increasing parameterization and complexity of watershed models (Boyle et al., 2001). In some early cases, this involved locally optimizing direct search methods – in HBV (Harlin & Kung, 1992) and WATFLOOD (Bingeman, 2001). The use of local search methods is reflective of extensive use of similar methods for most early watershed model calibrations (Duan, 2003). Random search (e.g. Monte Carlo) methods were also being applied to PMF models during the same period (Barker, Schaefer, Mumford et al., 1997; Bingeman, 2001; Harlin & Kung, 1992),

albeit primarily for uncertainty analyses. Duan (2003, p. 93) characterizes random search techniques as "crude and computationally inefficient", while Moradkhani & Sorooshian (2009) notes an improved exploration in the presence of multiple local optima and discontinuities.

There are limited examples of PMF models calibrated with more recent global optimization methods. Beauchamp et al. (2013) calibrated a lumped HSAMI model for PMF using Shuffled Complex Evolution (SCE), and Haberlandt & Radtke (2014) calibrated a HEC-HMS model for flood frequency analysis using PEST. The infrequent use of global optimization methods is not indicative of the efficacy of these methods. Indeed, many global optimization methods have been used extensively and successfully; Duan (2003) provides a summary of a number of techniques. Two in particular are SCE, recognized as "robust, effect, and efficient" (Duan, 2003, p. 100) over a large number of model evaluations, and Dynamically Dimensioned Search (DDS), which has proven to be similarly effective over fewer evaluations for more complex models (Tolson & Shoemaker, 2007). Global optimization methods have proven to be robust and effective; their infrequent use for PMF models may be reflective of the age of previous PMF models and studies, and the special consideration required of peak flows.

Global optimization algorithms intend to find a best parameter set; however, previous studies have raised concerns with equifinality, or instability as a result of multiple solutions producing similar performance during the calibration period (Beven & Freer, 2001). Uncertainty analysis techniques have been developed to attempt to quantify the resulting range of model outputs. A number of techniques are Monte Carlo-based: randomly sampling candidate solutions from among parameter distributions (Moradkhani & Sorooshian, 2009). At their simplest, the range of model results can be compared directly to the baseline result, as in the PMF uncertainty study by Barker et al. (1997). Generalized Likelihood Uncertainty Estimation (GLUE) follows a

similar approach, except that candidate solutions have a likelihood value based on performance, and confidence intervals about the baseline are developed based on those likelihood values (Beven & Freer, 2001; Moradkhani & Sorooshian, 2009). Importantly, GLUE, and other methods like it, are highly dependent on the choice of likelihood function (Yang, Reichert, Abbaspour, Xia, & Yang, 2008). A further advancement was that of Markov Chain Monte Carlo (MCMC) methods in which samples can be generated over a high dimensional space without a probability distribution (Moradkhani & Sorooshian, 2009), and each new solution is dependent on the previous one (Yang et al., 2008). The Metropolis algorithm, as applied for example by Kuczera & Parent (1998) for watershed studies, is one example of an MCMC method that attempts a "random walk" through the parameter space that is drawn to areas of high probability while still exploring areas of lower probability. The Metropolis algorithm has also been incorporated into global optimization techniques, namely the Shuffled Complex Evolution Metropolis algorithm (SCEM-UA) of Vrugt, Gupta, Bouten, & Sorooshian (2003).

Separate from uncertainty analyses are those methods intended only to quantify the impact of individual model parameters, and not for producing uncertainty bounds about the prediction. The most basic is the one-at-a-time (OAT) method in which one parameter is changed while others are held constant (van Griensven et al., 2006). OAT methods are limited to a local search around the starting point. An advancement to this approach, and a shift from local to global sensitivity, was the random OAT method of Morris (1991) in which multiple starting points are used and the mean and variance of changes are used to assess the significance of a parameter (Yang, 2011). A more recent global sensitivity approach is ANOVA (Analysis Of Variance), a numerical approach that decomposes model variance into the partial effects from one or groups of variables (van Griensven et al., 2006; Yang, 2011).

Perhaps the most common global sensitivity analysis approaches are those that rely on the generation of a number of samples throughout the decision space; their generality and ability to handle instability in the objective function is popular (Moradkhani & Sorooshian, 2009). In particular, Monte Carlo approaches sample randomly from parameter distributions, while Latin Hypercube sampling discretizes the parameter distributions as a more efficient way to represent the entire range of solutions (van Griensven et al., 2006). Both methods, however, require a second phase to assess the sensitivity of the decision variables. Two examples are a Kolmogorov-Smirnov test on the samples (e.g. applied by Harlin & Kung (1992) for sensitivity analysis of a design flood model) and a Regional (or Regionalized) Sensitivity Analysis that compares the distribution of results between behavioural and non-behavioural samples (Yang, 2011). The choice of parameter sensitivity analysis is dependent on available computational resources and the expected magnitude of interaction between variables, among others.

2.6. INCORPORATING CLIMATE CHANGE INTO PMP/PMF ESTIMATION

Previous studies have attempted to incorporate climate change projections into the estimation of PMP and PMF based on recommendations from a number of sources. Both Environment Canada (2004) and Watt & Marsalek (2013) suggest that there is a need to revisit historical PMF estimates and to consider climate change impacts. Historical meteorological and hydrometric data that previous inputs to PMF estimation and assumptions were based off may have shifted already, be in the process of shifting, or could shift in the future. The danger of continuing to use PMP/PMF estimates based on this historical data without considering changing climate conditions, especially if these changes lead to increased PMF peak flow, volume, and insufficient reservoir capacity (Chernet et al., 2014). Advances in the fields of precipitation data

and hydrological modelling now allow for the re-examination of historical extreme flood estimates (FEMA, 2012).

The simplest form of accounting for climate change impacts is to suggest, as summarized by Kunkel et al. (2013), that increased temperatures in the future would lead to increased evaporation from the oceans, leading to greater atmospheric water vapour content. Meanwhile, the maximum moisture-carrying capacity of the atmosphere would also increase with temperature (i.e., 7% increase per 1°C of warming) as per the Clausius-Clapeyron relationship (Stratz & Hossain, 2014). An extension of this method is to represent projected climate changes by increasing historical dew point temperatures that are used in the PMF estimates. Le Clerc & Garros-Berthet (2011) used historically observed temperature changes to estimate corresponding changes in dew point temperature, resulting in estimated increases in moisture availability and maximized PMP magnitude. Stratz & Hossain (2014) estimated an increase of 2°F in dew point temperatures over an observed 111-year period for an eastern US watershed, which resulted in a 10% increase in maximization of PMP. The same study also incorporated changes to surface persisting dew point temperatures as a result of non-stationary land cover in a regional atmospheric modelling system, and found that increased irrigation and reservoir impoundment increased PMP maximization from pre-dam to current conditions by at least 2.7% for several dam sites in the USA.

A common and more complex method of incorporating projected changes to PMF is via the impact approach summarized in several studies (Chen, Brissette, Poulin, et al., 2011; Cunderlik & Simonovic, 2005). The method involves developing a hydrological model, developing baseline and projected future variables based on climate model output, downscaling these inputs to an appropriate scale, and running the hydrological model forced by these new

inputs. In order to use this approach, however, methods of using climate models to estimate PMP need to be developed. The method of estimating PMP based on climate models also has the advantages of not relying on observed storm magnitudes and maximization, calculating maximization based on simulated physical processes (Bingeman, 2001), and providing a greater number of precipitation events to study (Rousseau et al., 2014).

An intermediate version of the impact approach that does not use climate model output directly was utilized by Cunderlik & Simonovic (2005) to project changes in hydrological extremes (not necessarily PMF) for a basin in southwestern Ontario. Future climate scenarios were developed based on GCM outputs but then simplified to a temperature change scenario (1°C increase) and a precipitation change scenario (100mm increase in average annual precipitation). A HEC-HMS model was then forced with these adjusted inputs, which resulted in a decrease in the magnitude of annual maximum snowmelt peaks, an increase in annual maximum rainfall peaks, and in general, greater variability in the magnitude, occurrence, and timing of annual maximum flows. Cunderlik & Simonovic (2005) note an important limitation of the impact approach: that the model parameters are invariant with climate change, based on the assumption that the impact of climate change will be much larger on the climate inputs to the model than on the processes governed by the model parameters.

The first attempts at estimating PMP via physically-based atmospheric models, in order to consider PMP in a non-stationary climate, were done by Abbs (1999), Bingeman (2001) and then Ohara et al. (2011). In the former study, temperatures in the atmospheric model were increased while leaving relative humidity at its original values, in order to keep the system in balance while increasing precipitation water. In contrast, Ohara et al. (2011) maintained atmospheric boundary conditions at equilibrium but maximized relative humidity in the

atmospheric model and changed conditions to drive moisture movement towards the watershed of interest. Bingeman (2001) also used an atmospheric model, MC2, to estimate PMP for the Columbia River basin in British Columbia. That research found that PMP estimated by maximization in the atmospheric model was larger than any previously observed storm, but less than traditional estimates of PMP for the basin.

Estimation of PMP via atmospheric models has drawbacks. The resolution of GCMs is too coarse for simulating PMP events (Rousseau et al., 2014), particularly given that model resolutions coarser than 50km are shown to simulate extreme precipitation rates that are significantly lower than observed (Wehner, Smith, Bala, et al., 2009). At the same time, statistical downscaling of GCM outputs does not provide necessary humidity data; thus the only reasonable method for PMP estimation is dynamical downscaling (i.e. RCMs) (Rousseau et al., 2014). The finer scale of RCMs (45-50km for those used in this research) also better represents topography and processes that play a role in extreme precipitation (Mladjic et al., 2011). In particular, an ensemble of RCMs is preferred due to uncertainty related to model processes, initial conditions, and GCM boundary forcing (Monette, Sushama, Khaliq, et al., 2012). Rousseau et al. (2014) found that CRCM was sufficiently able to simulate precipitable water and sufficiently estimate PMP values (though at times underestimated PMP), but acknowledged that RCMs cannot account for some conservative assumptions involved in traditional PMP estimation. (This is not surprising given that some conservative PMP assumptions require human judgment). Therefore, climate model-derived PMP estimates are expected to be smaller than historically estimated PMPs; however, the comparison of RCM-derived historical and future PMPs for calculating relative change factors in this research should not be impacted.

The first comprehensive study to utilize RCMs for PMP/PMF purposes was that of Beauchamp et al. (2013). That study applied the WMO maximization method to outputs from CRCM4 for a watershed in Quebec. This was done by extracting individual extreme precipitation events and the corresponding precipitable water variable from the RCM time series (at the grid point scale), maximizing based on maximum precipitable water, then adjusting via depth-area analysis to the basin-scale. Importantly, maximum precipitable water was analyzed separately and defined as the minimum of (a) the 1/100 year value of precipitable water for the given season, and (b) the precipitable water value assuming a saturated atmospheric column. Climate change impacts were also incorporated by inserting the estimated PMP into time series of simulated baseline and future precipitation, at different points in each time series, to determine the most critical resulting PMFs in each period. Increases of 0.5-6% in 48- to 72-hour PMP magnitudes for the Manic-5 watershed in Quebec to the 2080s were projected.

An extension of the Beauchamp et al. (2013) study was conducted by Rousseau et al. (2014) under a similar methodology of applying the WMO maximization method, with two differences. First, a moving window technique was used for maximizing storms, as opposed to individual selection of events. Second, non-stationarity was accounted for in the frequency analysis of precipitable water, so that 1/100 year values used to estimate maximum precipitable water also shifted with time. Precipitation was maximized and the largest precipitation event in a given time period was selected to represent the PMP. Finally, seasonality was accounted for by defining a spring PMP as that occurring when 10mm or more of snow water equivalent was on the ground. This is an additional method of accounting for climate change, as snowmelt was projected to occur earlier in the future period, and was incorporated in the RCM analysis in this

research. The result of the study was an increasing trend in PMP from baseline to 2080s in Quebec, with an especially significant signal for Summer/Fall PMP.

Veijalainen & Vehviläinen (2008) conducted another version of the impact approach to assess climate change impacts to the 2080s on high-hazard design floods (1/5000 to 1/10000 year) in Finland. In the baseline case, the timing of a 14-day design precipitation event was varied throughout a 40 year period of observed temperature and precipitation to find the most severe event. To incorporate climate change, projected percent changes ("deltas") to average temperature and precipitation were applied to the 40 year observed time series. The design storm was also adjusted; distributions were fit to baseline and future maximum precipitation, and the percentage change between 1/10,000 year precipitation events was extracted and applied to the design storm. The study found that results varied by basin; the timing of the design flood changed for some reservoirs (from spring to summer or from spring to winter), the range of changes in design flood magnitudes was large (and included both increases and decreases), and that in general, a 1:1 relationship occurred between design precipitation changes and design flood changes. The results from this and the previous studies illustrate the sensitivity of PMP/PMF to climate change, but also the difficulty in hypothesizing the potential effect of those changes for a watershed of interest.

2.7. UNCERTAINTY IN HYDROLOGICAL MODELLING

Previous studies have attempted to compare the effects of uncertainty in hydrological modelling and climate change impact studies. Since this research involves the comparison of multiple hydrological models simulating PMF, and forced by multiple climate change projections, it is important to review the methodology and results of past multi-model studies

under climate change. Studies that incorporate multiple models, multiple realizations of physical processes, and multiple scenarios allow for consideration of uncertainty in future hydrological extremes and the impact of each of those areas (Dankers & Feyen, 2009). The use of multiple techniques, climate models and initializations, impact models, and parameterizations is also advocated for by Chen et al. (2011) and by Exbrayat, Buytaert, Timbe, et al. (2014), especially given that the relative effects of each area of uncertainty are expected to vary based on the hydrological variable of interest.

There are widely considered to be four sources of uncertainty in the process of calibrating, forcing, and applying a hydrological model (Butts, Payne, Kristensen, et al., 2004; Renard, Kavetski, Kuczera, et al., 2010):

- Errors associated with historical inputs (meteorological input data);
- Errors in observed discharge measurements that are calibrated to;
- Hydrological model structure, as an approximation of physical processes;
- Model parameterization, resulting from limiting simulations to a single "best" parameter set.

In addition, when applying a hydrological model as part of a climate change impact study (as in this research), additional sources of uncertainty are introduced in the production of climate change forcing (Hawkins & Sutton, 2011):

- Choice of projected future emissions scenario;
- Climate model structure, as an approximation of physical processes;
- Natural variability associated with the climate system.

Each of these sources contribute to the total uncertainty envelope of a climate change impact study, and as such will be described below in detail and relative to each other.

Uncertainty in historical data (observed meteorological and discharge data) exists due to measurement errors inherent in rainfall measurement and discharge estimation, which are rarely reported with available data (Renard et al., 2010). Both sources can have significant impacts during model calibration and limit the effectiveness of that step. The treatment of observed discharge as a measured rather than a "virtual" variable, and the lack of quantifiable data on the effect of this is issue, is especially concerning to Beven et al. (2012). Having made these concerns clear, a study by Butts et al. (2004) concluded that historical rainfall errors contribute relatively less to the total uncertainty when compared to the other sources described below.

General Circulation Models (GCMs) are the "primary tools available" for quantifying atmospheric responses to different forcing and for projecting changes in the climate over short to long range scales (Flato et al., 2013, p. 746); thus they are also generally used for climate change impact studies on water resources (Bae, Jung, & Lettenmaier, 2011). Uncertainty is introduced in that many models exist, and each model is an imperfect and different representation of physical processes (Tebaldi & Knutti, 2007). Therefore, each model will respond differently to the same forcing and contribute to a range of future climate scenarios (i.e. uncertainty), whose size will be dependent on the number and types of GCMs considered (Hawkins & Sutton, 2011; Veijalainen & Vehviläinen, 2008). GCM structural uncertainty is estimated then by utilizing a number of models all equally weighted – an ensemble - and quantifying the range of projections that develop about the center of that ensemble (Flato et al., 2013; Hawkins & Sutton, 2011; Tebaldi & Knutti, 2007). The choice of GCM (i.e. GCM structural uncertainty) is commonly considered to be the largest source of uncertainty in impact studies (Kay & Jones, 2012); more specifically, and over a variety of applications, it can be larger than hydrological model uncertainty (Bastola, Murphy, & Sweeney, 2011; Exbrayat et al., 2014; Najafi, Moradkhani, & Jung, 2011;

Steinschneider et al., 2014; Wilby & Harris, 2006), or similar in size (Bae et al., 2011; Ludwig et al., 2009).

There are also uncertainties related to the future emissions scenario that is assumed and used to drive the GCM (Chernet et al., 2014). The emissions scenario represents an outlook of future radiative forcing, which is uncertain given potential societal changes that could occur (Hawkins & Sutton, 2011). This form of uncertainty is typically estimated by forcing GCMs with multiple future emissions scenarios (e.g. Hawkins & Sutton, 2011). Uncertainty studies using this methodology have found that, contrary to the historical belief that the choice of emissions scenarios is a key source of uncertainty (Hawkins & Sutton, 2011), it is less significant than other sources such as choice of GCM, internal variability, or the choice of hydrological model (Bastola et al., 2011; Chen, Brissette, Poulin, et al., 2011).

Natural climate or internal variability occurs as a result of fluctuations in short-term climate processes, as well as when initial conditions for the GCM are slightly perturbed (Hawkins & Sutton, 2011; Knutti & Sedláček, 2012). This form of uncertainty is quantifiable but difficult to reduce, as such it is termed "irreducible" (Deser et al., 2012; Knutti & Sedláček, 2012). Internal variability is commonly estimated by considering multiple members of a GCM, where each member has different initial conditions (Chen, Brissette, Poulin, et al., 2011; Knutti & Sedláček, 2012). Studies that have estimated irreducible uncertainty in this way have found that it can contribute significant uncertainty to climate modelling – less significant than the choice of GCM, but equivalent in magnitude to uncertainty from the hydrological model for extreme flows (Steinschneider et al., 2014) and a critically important component when considering precipitation projections (Chen, Brissette, Poulin, et al., 2011; Deser et al., 2012; Hawkins & Sutton, 2011).

Finally, GCM data is commonly downscaled to a higher resolution for hydrological model impact studies, due to the difference between GCM grid size and the typical size of watersheds that are studied (Chen, Brissette, & Leconte, 2011). Regardless of the downscaling method chosen (statistical, or dynamical/RCM), there is additional uncertainty related to the use of downscaling and continued uncertainty related to scaling issues even at a finer scale (Veijalainen & Vehviläinen, 2008; Whitfield, 2012). Downscaling uncertainty can be measured through the use of multiple methods/RCM (e.g. see Chen, Brissette, & Leconte, 2011), and has previously been found to contribute an envelope of uncertainty that is similar in size to that from GCMs alone.

A number of factors are involved in PMF estimation, including PMP characteristics such as depth, duration, spatial distribution, and storm center, model processes such as rainfall-runoff and routing parameters, and assumptions in the method such as initial watershed conditions prior to the PMP (Salas et al., 2014). Each factor adds a degree of uncertainty. Put another way, PMF simulations are "always linked to much uncertainty, regardless of the method" (Veijalainen & Vehviläinen, 2008, p. 467), particularly when incorporating climate change projections. This section addresses these areas of uncertainty – related to climate models, hydrological model structure, calibration, parameterization, and PMF assumptions - and their relative impacts as found in previous studies.

The next step in the "cascade of uncertainty" (Bastola et al., 2011, p. 573) for a climate change impact study is the selection of a hydrological model. A number of hydrological models exist, and uncertainty is introduced in terms of (a) a model's formulation - structural assumptions made in attempting to represent physical processes - and (b) a model's spatial and temporal representation of a watershed, such as lumped versus distributed models (Renard et al., 2010).

The accuracy of the rainfall-runoff processes in the model, relative to the watershed of interest, also plays a significant role in the model's ability to extend to PMF conditions (Vansteenkiste, Tavakoli, Ntegeka, et al., 2014). Despite its inherent uncertainties, the hydrological modelling approach for PMF continues to be the preferred method, with recommendations to quantify sensitivity to model uncertainties and other assumptions in the method (Alberta Transportation, 2004; FEMA, 2012).

Model structural uncertainty, neglecting lumped versus distributed spatial representation, can be "remarkably high" according to Bastola et al. (2011, p. 562) in a study of four conceptual models. Similarly, Jiang et al. (2007, p. 329) caution that a hydrological model must be carefully selected for any application and that "water resources scenarios predicted by any particular hydrological model represent only the results of that model". This can generally be traced back to varied mathematical approximations, each of which have different sensitivities and will respond differently to future climate scenarios (e.g. Kay & Jones, 2012; Vansteenkiste, Tavakoli, Ntegeka, et al., 2014). This results in a model uncertainty envelope that widens as the outlook of the future scenario increases, despite similar model performance in the historical calibration & validation periods (Bae et al., 2011; Jiang et al., 2007; Najafi et al., 2011). The uncertainty envelope has led some studies to advocate for quantifying this range of uncertainty and in some cases to use ensemble responses as opposed to simulations from individual models (Butts et al., 2004; Ludwig et al., 2009).

Literature routinely suggests that hydrological modelling uncertainty is less significant than that from GCMs (Chen, Brissette, Poulin, et al., 2011; Kay & Jones, 2012), but a wide and significant uncertainty envelope still exists (Exbrayat et al., 2014; Van Steenbergen & Willems, 2012). When compared to uncertainty due to model parameterization, Vansteenkiste et al. (2014)

found conflicting conclusions among past studies: the impact of model structure can be more significant than uncertainty in model parameters, but the impact of model calibration can be significant when considered in climate change studies.

Finally, uncertainty is introduced in the parameterization of the hydrological model(s), specifically in the attempt to isolate an optimum parameter set for the basin of interest. An example is the concept of equifinality, which states that there are often many sets of parameters that perform equally well in a historical period and it may be impossible to identify a single "best" solution (Beven & Freer, 2001). This is a difficult problem, as Seibert (2003) noted that improved calibration techniques may not alleviate this issue. Parameter uncertainty has previously been estimated in several ways. Butts et al. (2004) and Bastola et al. (2011) estimated uncertainty by quantifying the range of model simulations produced by parameter sets that meet a given behavioural threshold. Similar analyses specifically for PMF purposes are more limited; however, Barker et al. (1997) used Monte Carlo sampling of 500 sets of HEC-1 model parameters and PMF inputs and was able to quantify a plausible range of simulations about the baseline PMF hydrograph (whereas Harlin & Kung (1992) used similar Monte Carlo sampling for a conceptual PMF model to consider parameter sensitivity only). The relative impact of hydrological model parameter uncertainty has previously been estimated to be smaller than the other forms of uncertainty listed above (Chen, Brissette, Poulin, et al., 2011; Steinschneider et al., 2014); however, Bastola et al. (2011) found that uncertainty related to multiple behavioural solutions can still amount to a range of nearly 40% of average discharge in the historical period. The magnitude of parameter uncertainty is also expected to increase when extrapolating a model to future periods and more extreme conditions (Bastola et al., 2011; Vaze et al., 2010; Wilby & Harris, 2006).

Many studies have compared the impact of these sources of uncertainty on hydrological model simulations, varying from average or extreme conditions, high or low flows, and climate change impacts. The following relative behaviour can be generally expected, based on previous literature:

- The GCM is often the most significant source of uncertainty (Bastola et al., 2011; Najafi et al., 2011; Wilby & Harris, 2006);
- If downscaling is used, the choice of RCM incorporates additional uncertainty that can be similar in magnitude to uncertainty from the GCM alone (Chen, Brissette, & Leconte, 2011);
- Uncertainty related to the hydrological model structure can also be as significant as that from the GCM (Bae et al., 2011; Ludwig et al., 2009), or can be a lesser but still significant source (Butts et al., 2004);
- Uncertainty related to hydrological model parameterization is less significant than that from the other major sources listed above.

Finally, it is widely acknowledged that extrapolating a hydrological model to projected future conditions will increase uncertainty related to the model structure and parameterization (Jiang et al., 2007; Vaze et al., 2010).

3.0. STUDY AREA & HYDROLOGICAL MODELS

The following section provides background on the study area and hydrological models used in this study, and the reasons for their inclusion. This information provides important context for the parameterization and calibration of the hydrological models and the assumptions made in PMF simulations.

3.1. STUDY AREA

The basin of interest in this study is the Lower Nelson River Basin (LNRB) in northern Manitoba. The LNRB refers to an approximately 81,000 km^2 local watershed that drains into Hudson Bay. There are two main channels in the basin: the Burntwood and the Nelson Rivers, where the Burntwood drains into the Nelson River at Split Lake. Both channels receive upstream contributions from outside the watershed, including from Lake Winnipeg (which drains an area of approximately 1.1 million km^2). For the purposes of this study, only the local drainage area (approximately 73,500 km^2) upstream of a prospective Manitoba Hydro generating station (Conawapa G.S.) is considered. The area is additionally bounded at the upstream end by several control structures and/or streamflow gauges, which can be used as boundary forcing to the model. Figure 1 shows the total drainage area, the drainage area considered in this study, the main channels and waterbodies, and the locations of upstream contributions.

The LNRB is of particular importance to Manitoba Hydro for this PMF study because it contains five existing hydroelectric generating stations and another under construction, with potential future development options available. The majority of generation is concentrated in the Lower Nelson River Complex (denoted in Figure 1), a group of three existing stations (Kettle , Long Spruce, and Limestone generating stations (G.S.)) that combine to provide over 65% of the

province's current hydroelectric generating capacity with an additional station (Keeyask G.S.) under construction (Manitoba Hydro, 2016b). All existing and prospective generating stations in the complex fall under the CDA category of "Extreme" consequence of failure and thus are designed to pass the PMF flow (KGS Acres Ltd., 2010).

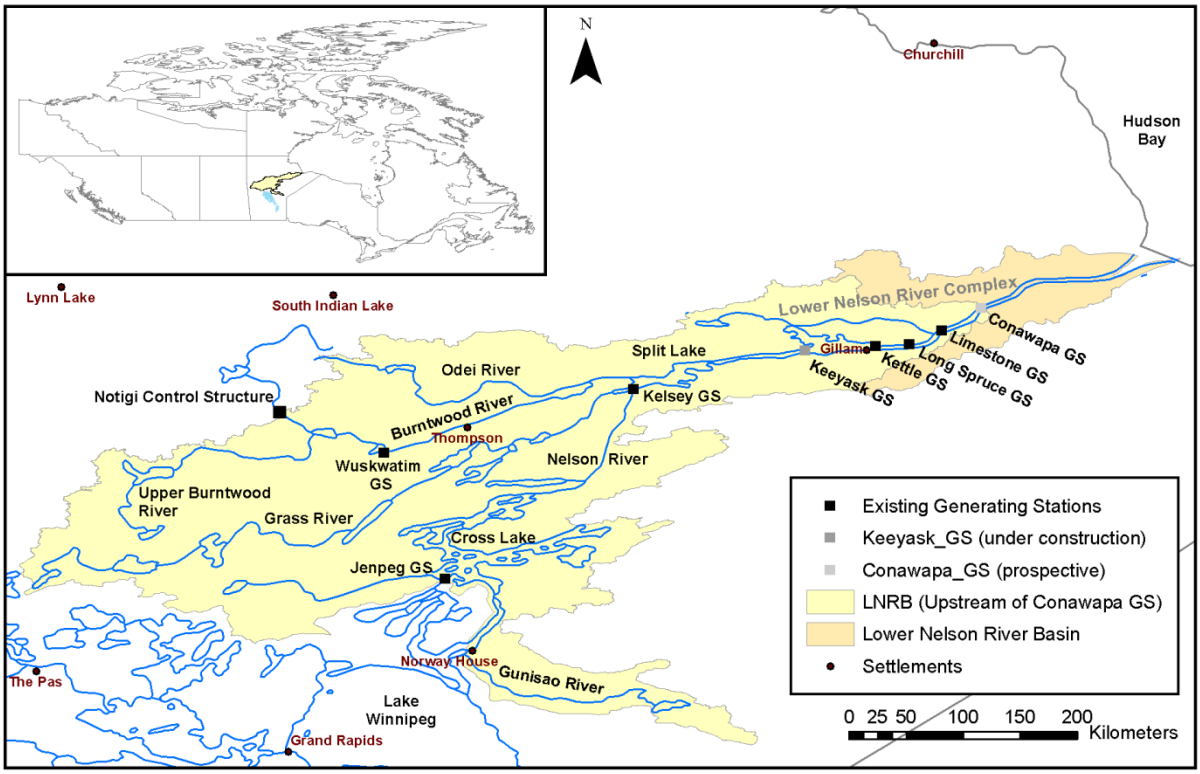

Figure 1: Lower Nelson River Basin (LNRB) Study Area

Two regulated, upstream sources provide a significant portion of the flow in the Lower Nelson River Complex: the Churchill River Diversion (CRD), and Lake Winnipeg. The CRD to the northwest diverts a portion of flow from the Churchill River (draining an area of 283,350 km^2) into the LNRB to increase generation capacity in the basin (Manitoba Hydro, 2016a). Flows through the diversion are regulated at the Notigi Control Structure (C.S.), and eventually merge with the main channel of the Burntwood River. Second, Lake Winnipeg drains into the LNRB via two channels: a smaller, natural, east channel; and through Jenpeg G.S. to the west. Jenpeg G.S. regulates the majority of outflows from Lake Winnipeg, which can be a significant

amount of flow given the large area of the Lake Winnipeg watershed. The study area shown in Figure 1 therefore extends only upstream to these three locations, given that discharge at all three points can be specified as a boundary forcing for a hydrological model.

Upstream contributions through both Notigi and Jenpeg are important parts of the PMF scenario (the model domain begins downstream of these points, visible in Figure 1). To illustrate the importance of regulated inflows to the basin under average conditions, Table 1 describes mean streamflow at all three inflow points and at select downstream locations. There is similarly significant contribution from these boundary forcing locations during the PMF scenario.

Table 1: Mean daily streamflow (1979-2014) of LNRB inflows (data from Manitoba Hydro and Water Survey of Canada, 2014)

Location	Mean Discharge (m^3/s)
Upstream Contributions	
Notigi C.S. Outflows	790
Jenpeg G.S. Outflows	1925
Nelson River East Channel at Sea River Falls	345
Total Inflows	3060
Downstream	
Nelson River at Kettle G.S.	3382

The LNRB is located in the Boreal forest region and is dominated by coniferous forest, ranging from a closed cover in the southern parts of the basin to a sparse cover mixed with shrubland in the northern areas (Beke, Veldhuis, & Thie, 1973). These two dominant land classes are visible in the classification of landcover shown in Figure 2. The basin, at one time glaciated and then submerged by the extensive post-glacial Lake Agassiz, has a subdued surface topography and slope and is predominantly covered in lacustrine clay (Beke et al., 1973). Surface depressions are extensive, and are typically filled by organic materials; these areas have

formed wetlands that vary in type and drainage behaviour. This mild slope and depressional terrain has also produced a landscape marked by small lakes (Beke et al., 1973), as well as larger surface water bodies that make lake storage and outflows especially important to consider. As a final note, Beke et al. (1973, p. 36) note that much of the LNRB is at the "wet end of the moisture scale", and warn that "site conditions change rapidly over relatively short distances".

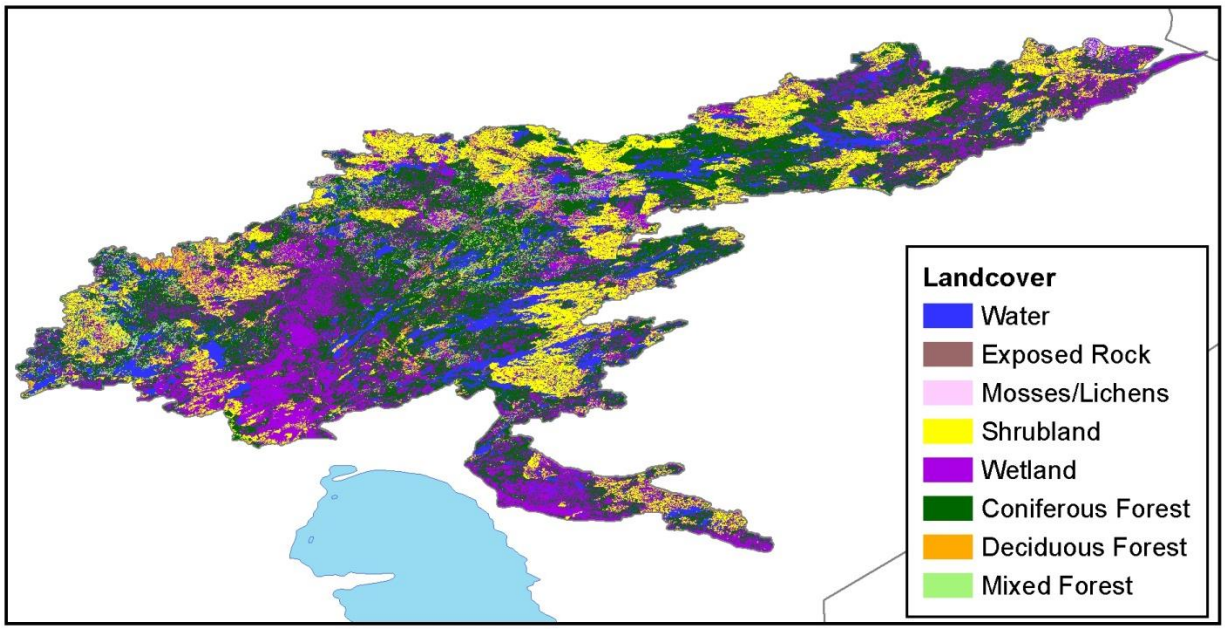

Figure 2: Landcover in the Lower Nelson River Basin (data from Geobase, 2000)

Figure 2, based on Landsat 5 and Landsat 7 satellite images from GeoBase (2000) and classified as per Wulder & Nelson (2003), depicts significant variation in landcover among the major tributaries in the basin; this leads to noticeable differences in hydrological response. For example, the Grass River basin has significant wetland area (approximately 30% wetlands) that contributes to a more attenuated outflow hydrograph. In contrast, northern tributaries are heavily shrubland-dominated (approximately 40%), resulting in a more rapid hydrograph response and recession. There is significant spatial variation within sub-basins as well, with alternating areas of coniferous forest, treed bedrock, and wetlands in the Burntwood River system, for example,

that leads to a more complex and difficult hydrologic response to simulate. This intra-basin physiography may be an important factor in differentiating the skill of a semi-lumped model (HEC-HMS) versus a distributed model (WATFLOOD).

The LNRB is primarily underlain by formations of lacustrine clay that display moderate or imperfect drainage (Ehrlich, Pratt, Barr, et al., 1959; Mills, Veldhuis, & Forrester, 1976; Veldhuis, Mills, & Forrester, 1979). In the upper parts of the basin, this is commonly overlain by flat bog-like, very poorly drained organics and peat deposits of varying thickness (Ehrlich et al., 1959; Mills et al., 1976). As stated previously, some areas in the upper and central regions also include isolated bedrock outcrops (Beke et al., 1973). Towards the lower part of the basin, layers of better drained loam/sand and layers of poorly drained silt/loam more commonly surround the clay horizon (Mills et al., 1976). For another perspective based on the NRCS soil classification system (ranging from A-D; Natural Resources Conservation Service, 2007), this variability includes infrequent areas of Type B soils (moderately low runoff potential, high transmissivity) and large areas of soils expected to have Type C (moderately high runoff potential, moderate transmissivity) and Type D (high runoff potential, restricted transmissivity) behaviour.

Climate in the LNRB is characterized as continental with short summers, long winters, and generally cooler temperatures; but a very large range in annual temperature (Beke et al., 1973). As an example, basin average meteorological statistics from 1981-2010 (for seven long-term meteorological gauges in or near the basin), are provided in Table 2.

Table 2: LNRB basin average climate normals (1981-2010)
(based on data from Environment Canada, 2015)

Daily Average Temperature	-1.1°C
Average Annual Precipitation	353 mm
Average Annual Snowfall	172 mm (49%)

The LNRB represents a relatively complex watershed to simulate in hydrological models. The highly variable physiography, significant surface water and depressional storage, and wetland storage/release require careful parameterization and model setup to account for effects on runoff generation (particularly snowmelt-dominated runoff). Similarly, the large proportion of precipitation as snowfall makes accurate simulation of snowmelt processes of critical importance. Finally, the significant upstream (regulated inflow) contributions make it essential to isolate local inflows when considering historical high flow years.

3.2. HYDROLOGICAL MODELS

Three hydrological models are selected for this study. The SSARR model is currently used for PMF studies on the LNRB and was selected as a baseline model for this study. Support for the SSARR PMF model was available from Joe Groeneveld at Hatch Ltd. HEC-HMS and WATFLOOD are currently used in other modelling capacities at Manitoba Hydro, and the corporation has developed in-house expertise with those models. Given this experience with the models, there was interest in potentially extending these models to PMF purposes in the future. Significant expertise with the WATFLOOD model was also available in the Water Resources (Hydrology) group in the Department of Civil Engineering at the University of Manitoba. Finally, the three models represent a significant range in model structure and complexity – as detailed in the remainder of this section.

3.2.1. SSARR

The Streamflow Synthesis and Reservoir Regulation (SSARR) model was developed in 1956 by the United States Army Corps of Engineers (Crippen Acres Wardrop, 1990), and is the platform used by Manitoba Hydro for the existing LNRB PMF model. It is a semi-lumped,

conceptual and mathematical model, capable of simulating all major hydrological processes in a northern basin, including snowmelt, evapotranspiration, and surface and subsurface processes (Debs et al., 1999). The model has two components: a watershed model, and a river routing model (USACE, 1991), which are described in detail below. This version of the SSARR model was previously tested by SNC-Shawinigan Inc. (1993) for its applicability in Quebec to an extreme flood scenario like the PMF. That report concluded that model parameters behave consistently even under extreme inputs, and thus the model (as described below) can be used with confidence for PMF modelling.

The existing PMF model uses the depletion curve watershed model, selected due to the flat topography of the basin (Crippen Acres Wardrop, 1990). In this setup, precipitation inputs are provided to a given basin element by a weighted average of selected stations at the centroid of the basin (USACE, 1991). These are provided at a daily scale in the PMF model due to data availability limitations, and because the large drainage area and slow response of the LNRB allows the model to be run at a daily time step (Crippen Acres Wardrop, 1990). Moisture input to a basin has three destinations: runoff, soil moisture, or evapotranspiration losses; no loss as a result of subsurface percolation to deep groundwater systems is incorporated (USACE, 1991). A schematic of the depletion-curve watershed model is provided in Figure 3 and explained below.

At the air-surface interface, moisture input is converted to runoff as a function of the soil moisture index (SMI) based on a specified tabular relationship between SMI and runoff percentage (USACE, 1991). Runoff is then simulated by three sets of linear reservoirs, which differ based on the time of storage (Crippen Acres Wardrop, 1990). Separation between direct runoff and baseflow is done based on the baseflow infiltration index (BII). Similar to SMI, a given basin will have a specified tabular relationship of BII versus baseflow runoff percentage;

as the BII increases, there is reduced subsurface runoff capacity and increased direct runoff (USACE, 1991).

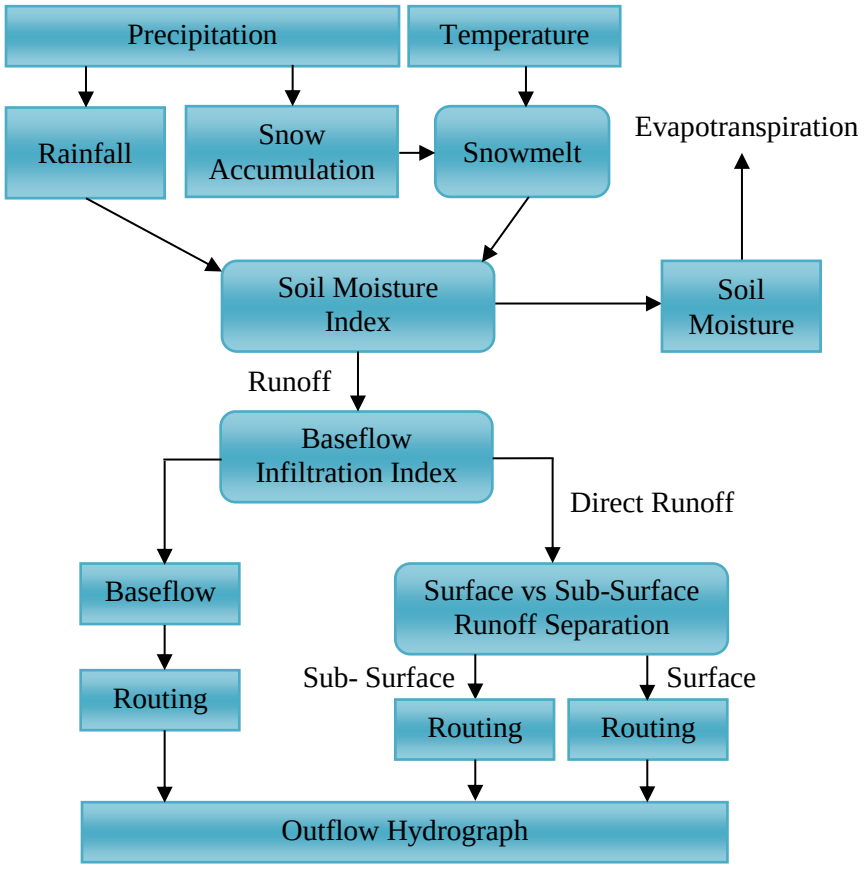

Figure 3: Schematic of SSARR model processes, adapted from USACE (1991)

The direct runoff portion is also split up into surface and interflow components, again by a specified tabular relationship of total direct runoff versus surface runoff; this conceptualizes that under heavier moisture input, wetter conditions will result in less infiltration (USACE, 1991). Debs et al. (1999) explain that the SMI-runoff relationship is important for accurate modelling on a seasonal scale, while the other two relationships are more important for fitting observed hydrographs on a shorter daily scale. Remaining moisture input then fills the soil storage reservoir (SMI), where it can only be lost via evapotranspiration (no downwards percolation – unlike HEC-HMS). Potential evapotranspiration is specified as monthly average

values, then reduced to actual evapotranspiration based on available SMI and whether precipitation is occurring (USACE, 1991).

Snowmelt is modelled in SSARR using a temperature-index approach due to a lack of energy budget input data (Crippen Acres Wardrop, 1990). Snowmelt rate is a function of snow covered area depletion and daily average temperature (USACE, 1991), which helps to represent slower melt during the early ripening phase, and faster melt later as the ground surface is exposed. Individual sub-basins can also be specified with different snowmelt relationships to account for varying physiographic effects on snowmelt. These points are important to note as they differ considerably from the snowmelt functions in HEC-HMS and WATFLOOD.

Finally, the routing portion of the model represents channel reaches as a "chain of lakes", whereby attenuation is achieved by passing portions of basin outflows through many lake elements (USACE, 1991, p. 44). Lake elements are programmed with stage-storage-discharge relationships, which can be calibrated or specified based on known behaviour. The routing component has two additional features that are unique to SSARR among the models in this study: backwater relationships (used for two lakes in the LNRB model), and target elevation controls for regulated reservoirs (as opposed to free-outflow behaviour; used for several regulated reservoirs in the model).

Given this parameterization, the SSARR model was selected for the PMF study in the LNRB for several reasons, originally given by Crippen Acres Wardrop (1990) and reiterated here:

- SSARR was developed for large, data sparse basins comparable to the LNRB and was capable of simulating all relevant processes in the LNRB;
- SSARR was also widely accepted and applied for similar applications in other places;

- Assistance from USACE model developers was available at that time.

Since the LNRB PMF model was completed, additional studies have been conducted of the SSARR model applied to PMF conditions (Debs et al., 1999; SNC-Shawinigan Inc., 1993). As well, although model support was available at the time, SSARR was last updated in 1991 and has not been supported for some time. This lack of support is justification to consider the two additional, supported models in this study.

3.2.2. HEC-HMS

The Hydrologic Modeling System developed by the Hydrologic Engineering Center (HEC-HMS) of the United States Army Corps of Engineers was created as a successor to the HEC-1 program in 1998 (Bennett & Peters, 2000), and is used in this study in Version 3.5 released in 2010. More recent versions of HEC-HMS have since been released, but had not yet been tested for the LNRB at the time of this study. HEC-HMS is a semi-lumped, conceptual model (Feldman, 2000) with a great deal of flexibility in that it can combine various sub-process methods together based on what is most reasonable for the basin of interest (García et al., 2008).

The LNRB PMF model in HEC-HMS uses Soil Moisture Accounting (SMA) to simulate rainfall-runoff processes. SMA is a continuous method, meaning it is stable over long term, continuous simulations (Bennett & Peters, 2000; Fleming & Neary, 2004). Although event-based methods have often been applied historically for dam safety simulations (England, Velleux, & Julien, 2007; FERC, 2001; Salas, Gavilán, Salas et al., 2014), more recent studies on high flow simulations in HEC-HMS have applied the SMA method (Cunderlik & Simonovic, 2005; Haberlandt & Radtke, 2014). The SMA method was selected for this study, as opposed to an event-based approach, for a number of reasons:

- Continuous simulation was more useful for simulating the calibration period (a long historical period, concerned with only certain high flow years) in a single run and to also append a spin-up year to the beginning of the simulation;
- SMA has greater complexity and parameterization compared to the event-based methods, and thus acts as a moderate level of complexity between SSARR and WATFLOOD;
- SMA allows for specification of initial saturation percentages of all five vertical reservoirs, which is important for setting antecedent conditions in the PMF simulation;
- Fleming & Neary (2004) provided a methodology for estimating SMA parameters using GIS, soil texture, and streamflow data that could be applied to the LNRB model.

SMA simulates five vertical reservoirs: canopy, surface storage, soil storage, and upper and lower baseflow storages (Bennett & Peters, 2000; Fleming & Neary, 2004; Figure 4). This setup is parameterized based on (a) maximum storage sizes; (b) maximum downward percolation rates; and (c) lateral baseflow runoff rates (Feldman, 2000). Impervious surface area percentage is also specified, for a maximum of thirteen rainfall-runoff parameters for a given basin element. Baseflow contributions are modelled in this study by linear reservoirs, where each layer has an empirical storage coefficient that can be estimated by recession analysis. This method is most conducive to the SMA method (García et al., 2008). Most basins in the LNRB model use both upper and lower baseflow reservoirs, as per the recommendation from Moore, Hamilton, & Scibek (2002) that two linear reservoirs best fit the low flow recession curve in northern Canada.

The Clark Unit Hydrograph was selected to transform direct runoff into an outflow hydrograph. This method builds a time-area histogram of the basin using a time of concentration parameter and an empirical basin storage coefficient (Feldman, 2000). Time of concentration

represents the longest time required for the entire basin to contribute runoff (FERC, 2001), while the storage coefficient is a proxy to the recession constant of the hydrograph's falling limb (Fleming & Neary, 2004). The method was selected as it was used in the existing HEC-HMS forecasting model for the LNRB and because both parameters were easily estimated by empirical methods (described further in Appendix A). This resulted in a maximum of fifteen parameters for any given basin element.

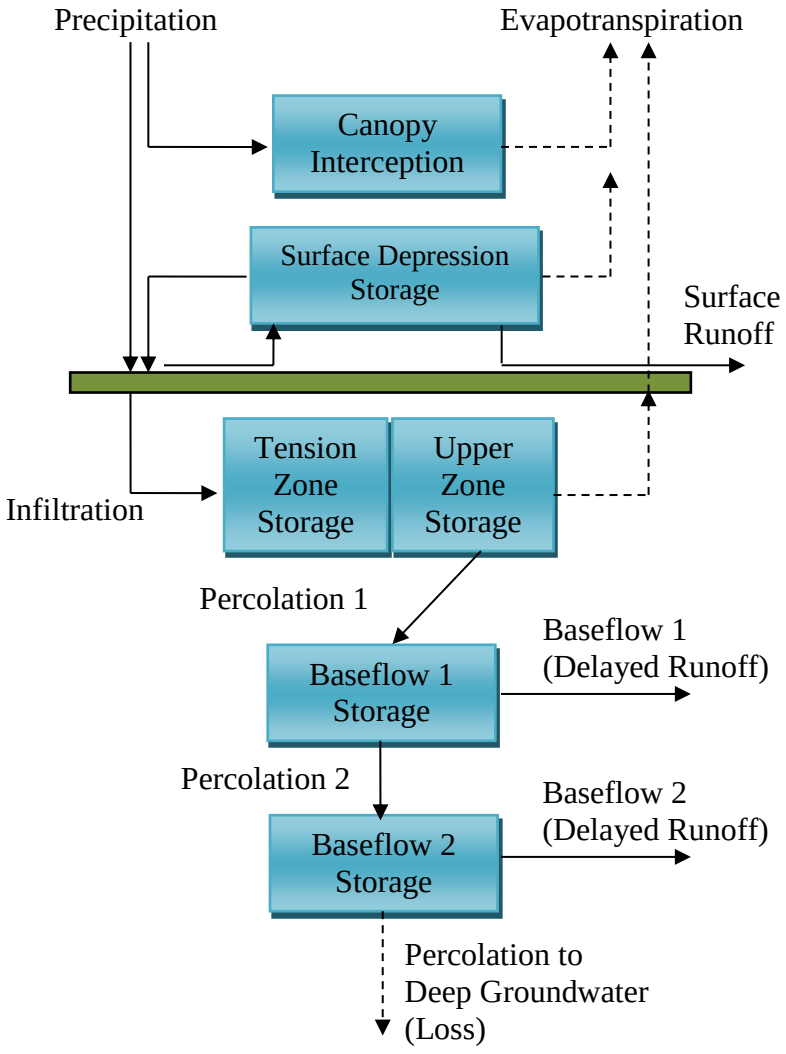

Figure 4: Soil moisture accounting process in HEC-HMS (adapted from Bennett & Peters, 2000; Feldman, 2000)

Snowmelt is simulated using an antecedent temperature-index (ATI) approach, whereby daily melt rate is a function of accumulated degree-days and the mean temperature relative to a base melt temperature (Feldman, 2000). The relationship is specified in a stepped table format (similar to SSARR), but limits all sub-basins in the model to the same melt rate relationship (neglecting any physiographic effects in different basins).

SMA simulates moisture losses through two processes: deep percolation and evapotranspiration. Deep percolation represents downward water movement from the lowest baseflow reservoir to a "deep aquifer" that responds so slowly that there is a negligible outflow (Bennett & Peters, 2000, p. 6). This process is unique to HEC-HMS among the models in this study. Evapotranspiration is modelled similarly in HEC-HMS as SSARR; potential evapotranspiration is provided as an average monthly depth of evaporation (Feldman, 2000). A pan coefficient (less than 1; in this study 0.7) is used to convert this to actual evapotranspiration. Actual evapotranspiration occurs first from canopy storage, then surface storage, then soil storage, and is only dependent on level of saturation if soil moisture is below field capacity (Bennett & Peters, 2000).

Finally, channel flow is routed in reaches using the Muskingum method on a daily time step. The Muskingum method is a finite difference approximation whereby reach storage is representing by an additional prism storage on the reach (Feldman, 2000). It includes two parameters: "K" or a travel time parameter, and "X" or a storage weighting parameter; this method is chosen based on the ability to estimate these parameters without calibration. The selection of these two parameters is discussed further in Appendix A.

The HEC-HMS model was selected for this study as it is currently used for inflow forecasting by Manitoba Hydro in the LNRB. An existing model, calibrated for average

conditions, was available from Manitoba Hydro and was previously recalibrated for an undergraduate thesis on PMF modelling in HEC-HMS (Sagan, 2014). That model was repurposed for this study and improved upon, as described in Section 4.1.3.

3.2.3. WATFLOOD

WATFLOOD is a distributed hydrological model with both physically-based and mathematical representations of hydrologic processes. The model takes gridded spatial data (e.g. digital elevation models, satellite-based landcover imagery, gridded meteorological data) as input and performs process calculations on a grid (Dibike & Coulibaly, 2007; Kouwen et al., 2005). Grid size is specified by the user based on watershed size, data availability, and the computational budget (Kouwen, 2014). A 10km grid size was used in an existing WATFLOOD model of the LNRB, and is continued to be used in this study.

WATFLOOD discretizes a watershed into Grouped Response Units (GRUs) - areas of similar landcover or physiography that are expected to respond hydrologically similar to meteorological forcing (Kouwen et al., 2005). All pixels of a given GRU inside of a grid cell then respond identically to forcing data on the grid cell, and the outflow from a grid is then calculated as the weighted average of the GRU responses within it (Kouwen, 2014; Kouwen et al., 2005). The use of GRUs has several advantages that have been recognized in literature (Kouwen et al., 2005; Pietroniro & Soulis, 2003):

- GRUs are more efficient for discretizing large watersheds (e.g. the LNRB) because the same calculations do not need to be repeated for all GRU pixels in a given grid cell; and
- GRUs are tied to physiography as opposed to sub-basins, meaning parameters should be more physically-based and more transferable between hydrologically similar areas.

The WATFLOOD model used in this study includes nine GRUs (also termed land classes, and described further in Section 4.1.4).

WATFLOOD also simultaneously discretizes the watershed by river classes, whereby each grid cell is assigned to a river class (Kouwen, 2014). Often, river classes are classified based on major tributaries or sub-basins. Parameters for certain processes are divided by river class (i.e. are more tied to unique physiographic regions or subsurface units than a particular land cover type), including those for baseflow, wetland routing, and flow roughness. The LNRB model in this study also included nine river classes (described in Section 4.1.4).

The representation of hydrological processes in WATFLOOD has been described by Roberts, Pryse-Phillips, & Snelgrove (2012, p. 235) as "intermediate complexity" due to its lack of energy-budget incorporation. Earlier work by Kouwen et al. (2005) showed confidence in the model's ability to simulate the surface water balance, and noted that the model uses commonly-used and recognized representations of hydrological processes (Figure 5).

WATFLOOD considers five vertical layers: canopy interception, surface storage, upper zone saturated soil storage, intermediate zone unsaturated storage, and lower zone baseflow storage (Kouwen, 2014; Kouwen et al., 2005). Canopy interception is modeled based on specified monthly average depths of interception for each land class, and surface depressional storage is modelled based on a maximum storage depth parameter (Kouwen, 2014). Infiltration uses the Philip Formula (Dibike & Coulibaly, 2007), and can differentiate between bare ground and snow-covered infiltration (Kouwen, 2014). Infiltration entering the upper soil zone is then either lost upwards to evapotranspiration, moves vertically to the lower zone (recharge) or moves horizontally (interflow) based on separate storage-discharge functions (Kouwen et al., 2005). Finally, baseflow from the lower zone reservoir is modelled with a two-parameter exponential

depletion function, differentiated by river class (Dibike & Coulibaly, 2007). No losses associated with percolation to deeper groundwater are considered.

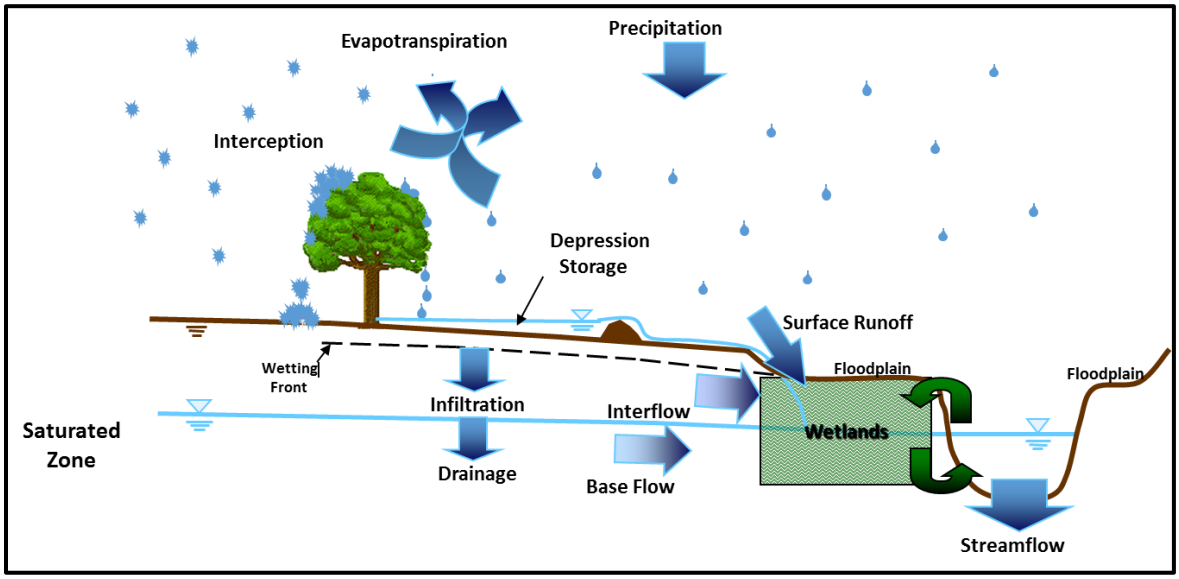

Figure 5: WATFLOOD representation of watershed processes, modified from Stadnyk-Falcone (2008)

Snowmelt is represented by a temperature-index approach, similar to the other models in this study. The base melt temperature and an average melt rate are parameterized for each land class (Kouwen et al., 2005). However, unlike SSARR and HEC-HMS, sublimation over winter is also incorporated using an average daily depth of sublimation for each land class.

Potential evapotranspiration is estimated using the Hargreaves and Samani equation, which requires only temperature data as input (Kouwen, 2014). Actual evapotranspiration is calculated based on reductions for upper zone soil moisture, daily temperature, and vegetation height and roughness in each land class (Kouwen, 2014). This represents greater complexity than in SSARR and HEC-HMS, which only use monthly average depths for potential evapotranspiration and cannot explicitly account for physiographic effects on evapotranspiration.

WATFLOOD also differs from the other models in that it uses two separate physically-based routing methods: a dedicated wetland routing model and a channel routing model. Wetland

routing acts on all fluxes from the portion of a grid cell classified as a connected wetland class (i.e., fen), and allows for the flow direction between the wetland and channel to change direction based on the hydraulic gradient (Kouwen, 2014). The wetland model has a storage component associated with it, taking in all surface, sub-surface and snowmelt inflows and precipitation, and losing evapotranspiration, which determines the water level relative to the channel and ultimately determines the hydraulic gradient and flow direction. The wetland porosity and hydraulic conductivity are parameterized and can be unique to each river class.

Outflows from the rest of a grid cell are routed in a channel. GRU discretization assumes that every grid cell has at least one channel, which connects to a neighbouring, downstream grid (Dibike & Coulibaly, 2007). Flows are routed in both the channel and overbank/overland areas based on average slope and the Manning equation, with different roughness values for overland versus in-channel flow (Kouwen et al., 2005). Each river class in the watershed model has its own roughness parameters to account for varying physiography effects on routing.

WATFLOOD has been previously utilized by Manitoba Hydro for climate change impact studies and thus was of interest to use here. Furthermore, the distributed representation, more physically-based climate-hydrologic feedback, and increased complexity (compared to the other two models in the study) made it advantageous to include as part of a PMF study. An existing model of the LNRB, developed in 2010 and calibrated to a limited period of average conditions, was available from the University of Manitoba to be repurposed for this study.

4.0. DATA AND METHODS

This chapter describes the application of existing methods to a large-scale study of sources of uncertainty in PMF estimates. Works conducted as part of this research are clearly distinguished from results produced by others that are used in the study.

This study sets up and forces multiple PMF models for the same basin, over baseline and future periods, and with an analysis of input and parameter sensitivity. A PMF study that considers all of these components could not be found in the current body of literature. This scope requires a number of supporting elements, which in their entirety would have been prohibitive to derive in this study. Instead, the study utilizes supporting elements from works that have previously been conducted, peer reviewed, and agreed upon by external sources. This includes repurposing existing hydrological models of the LNRB, attempting to mimic baseline PMF inputs and assumptions for the LNRB, and using climate change projections from the NRCan study on PMF in a changing climate (Ouranos, 2015). This approach is best justified by the following remark from the advanced draft version of *Australian Rainfall and Runoff: A Guide to Flood Estimation* (a comparable document to the Canadian Dam Association's *Dam Safety Guidelines*):

> "Improving the consistency of the manner in which such assumptions are applied in practice will thus minimise the potential for differences in the results obtained by different hydrologists… In addition, prescriptive procedures relating to the estimation of floods beyond the credible limit of extrapolation are justifiable as without empirical evidence or scientific justification there can be little rational basis for departing from a consensus approach." (Nathan & Weinmann, 2015, §6.5 para. 3)

4.1. PMF Model Setup

The three hydrological models in this study are set up for simulation in high flow years over the period of record for the basin (approximately 1976-2014, varying by hydrometric gauge) and over a hypothetical PMF simulation (a spring-summer period of approximately April to August). Historical high flow simulations require observed meteorological forcing data (i.e. temperature, precipitation) and observed discharge records at a sufficient number of locations throughout the basin. The PMF simulation also requires forcing data, which is outlined in Section 4.4 and Appendix B. Both simulations require the models to adequately represent the LNRB in terms of basin areas and major physiographic features - such as lakes and main river channels. The parameterization of the models, optional model processes to include, and default values for some meteorological process parameters were also tested as part of this setup to ensure the models reasonably represent LNRB hydrology.

4.1.1. Historical Input Data

The LNRB is a relatively data sparse region (Coulibaly, Samuel, Pietroniro, et al., 2013); however, sufficient meteorological forcing data for hydrologic modelling is available from several long-term meteorological stations inside and surrounding the basin, which are operated and disseminated by Environment and Climate Change Canada (ECCC) through the National Climate Data Archive (Environment Canada, 2015). The data was used to force the hydrological models during the high flow calibration and validation periods.

ECCC historical archived data is used; at the time of this study, adjusted precipitation data was also available (Mekis & Vincent, 2011). In the area of the LNRB, Mekis & Vincent (2011) found that adjustment on average resulted in a 10-15% increase in total precipitation. Use of the adjusted data may have improved the underestimation of peak flow magnitudes during the

calibration period for WATFLOOD and HEC-HMS. Further, higher precipitation may have resulted in less extreme model parameters, and in turn reduced PMF estimates by HEC-HMS and WATFLOOD.

Meteorological stations used as part of the project are listed in Table 3 and shown on Figure 6. The distribution of stations about the basin is sparse, particularly in the northern portion where much of the area relies only on the Thompson A or Gillam A gauges. Thiessen polygons, previously developed by Crippen Acres Wardrop (1990) and Manitoba Hydro, use these stations and are used in this study to create precipitation input for sub-basins in the semi-lumped models (SSARR and HEC-HMS).

Table 3: Meteorological stations used for hydrologic model forcing

Station	Period of Record	Frequency of Data	Data of Interest	% Missing in Period of Interest[a]
Cross Lake Jenpeg	1972-Present	Daily	Mean Temp., Total Precip.	0.8%
Flin Flon	1927-Present	Daily	Mean Temp., Total Precip.	1.2%
Gillam A	1970-Present *(to Oct 1st, 2014)*	Daily	Mean Temp., Total Precip.	1.7%
Island Lake A	1970-Present	Daily	Mean Temp., Total Precip.	0.8%
Norway House A, Norway House	1973-2005, 2005 - Present	Daily	Mean Temp., Total Precip.	3.3%
The Pas A	1943-Present	Daily	Mean Temp., Total Precip.	0.7%
Thompson A	1967-Present	Daily	Mean Temp., Total Precip.	1.3%

[a] Period of Interest = available years between 1972 and 2014

Missing data are gap filled as necessary using an average from neighbouring stations. Of more concern is a n undercatch bias in winter precipitation measurements at the Norway House

gauge after 2004 that is not observed at nearby gauges (i.e. Island Lake A, Cross Lake, and Jenpeg). There is much less snowfall recorded at the gauge after this time, which may be the result of gauge movement or issues with data collection at the gauge. Snowfall measurements prior to 2005 are acceptable (and comparable to nearby gauges), and summer precipitation did not show similar discontinuity. Therefore, Norway House winter precipitation measurements (October-March) after 2004 are replaced with those from the nearby Island Lake A gauge. This methodology is considered most appropriate for modelling because it preserves Norway House measurements in spring/summer for adequate coverage of convective rainfall events, but prevents underestimation error associated with known, erroneous snowfall undercatch after 2004.

Hydrometric streamflow records are extracted for all major tributaries and main channel gauge locations in the basin. Streamflow records for tributaries and some main channel locations are available from Water Survey of Canada (WSC) records (Water Survey of Canada, 2014). Manitoba Hydro provided proprietary best-estimate outflow records at generating stations and upstream control structures. Streamflow gauges used in hydrologic model calibration are displayed in Table 4 and shown on Figure 6.

Note that the Churchill River Diversion (regulated at Notigi C.S.) was completed in 1975, and that Lake Winnipeg Regulation (regulated at Jenpeg G.S.) was completed in 1976, which limits the period of record available for this study on the lower Nelson River. Also note that two tributary gauges were moved during the period of record – the Upper Burntwood River gauge was moved upstream in 1985, and the Gunisao River gauge was moved downstream in 1992. For ease of modelling, calibration periods for these gauges include only years after their respective movement. The validation period, however, is more flexible and considers years both pre- and post-movement for these gauges.

Table 4: Hydrometric gauges used in hydrologic model calibration

Gauge Name	WSC Designation	Drainage Area (km^2)	Period of Record	Mean Annual Flow (m^3/s)[c]
Tributary Gauges (used in calibration)				
Grass River at Standing Stone Falls	05TD001	15,400	1960-Present	60.4
Gunisao River at Jam Rapids	05UA003	4,610 4,400	1992-2014 1971-1992[a]	18.9
Kettle River at Gillam	05UF004	1,950	1963-Present	13.2
Limestone River at Bird	05UG001	3,270	1963-Present	20.2
Odei River near Thompson	05TG003	6,110	1979-Present	34.0
Burntwood River -Above Leaf Rapids -Above Threepoint Lake	 05TE002 05TE001	 5,810 6,670	 1985-Present 1977-1985[b]	 22.4 24.8
Downstream Gauges				
Nelson River at Kelsey G.S.	05UE005 [e]	25,514	1961-Present	2338
Burntwood River near Thompson	05TG001 [e]	12,360	1958-Present	866
Nelson River at Kettle G.S.	05UF006 [e]	68,183	1976-Present	3334
Upstream Contributions (Model Forcing Locations)				
Notigi Control Structure (Outflows)	N/A [e]	N/A	1976-Present	783
Nelson River (West Channel) at Jenpeg	05UB009 [e]	N/A	1976-Present	1889
Nelson River (East Channel) below Sea River Falls	05UB008 [e]	N/A	1968-Present	340

[a] Gauge moved downstream in 1992
[b] Gauge moved upstream in 1985
[c] Mean annual flow calculated based on period of interest – available years between 1977-2014
[d] Shaded cells indicate locations with regulated flows
[e] Data provided by Manitoba Hydro (all other data available from Water Survey of Canada)

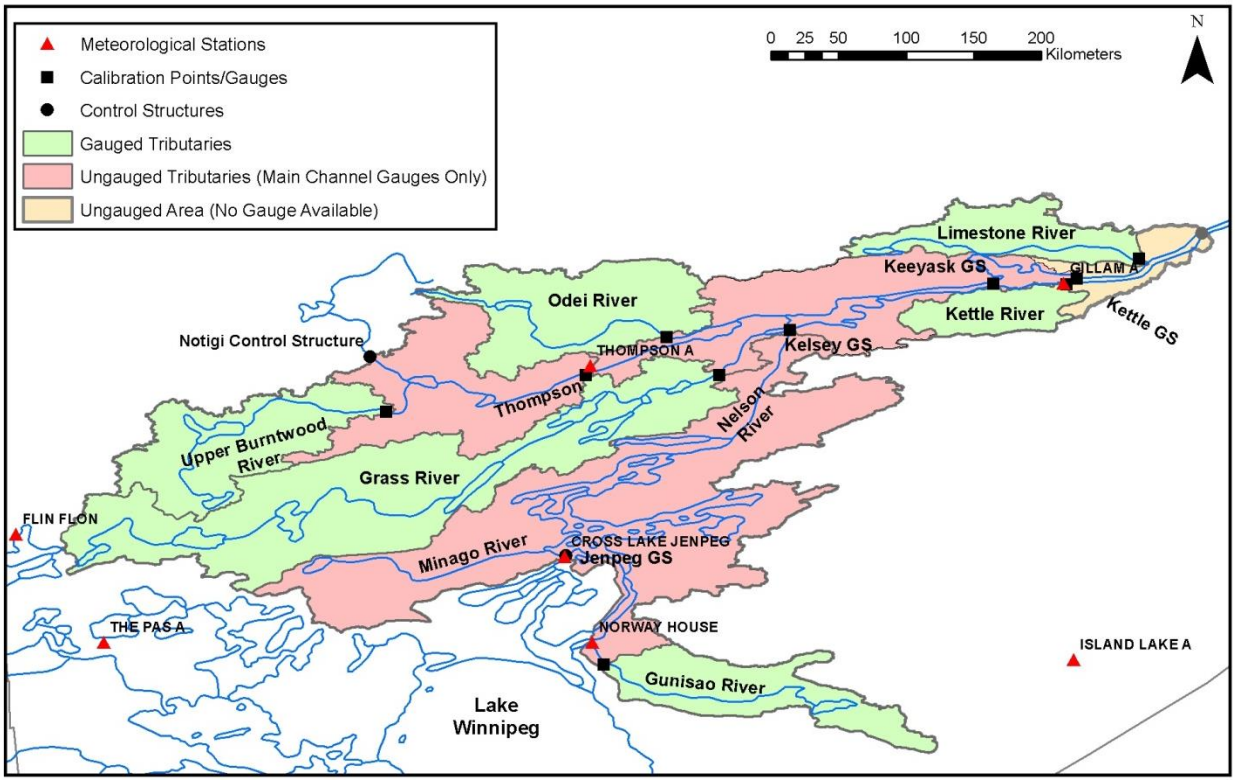

Figure 6: Meteorological and hydrometric gauges within the LNRB

The spatial distribution of hydrometric gauges is sufficient to calibrate all major regions of the LNRB that are expected to have varying physiography, and main channel gauges are available to calibrate areas without tributary gauges. Any ungauged areas between Kettle G.S. and Conawapa G.S. (i.e. no available downstream calibration point) are parameterized based on the Kettle and Limestone Rivers.

4.1.2. SSARR

The existing SSARR model used by Manitoba Hydro for PMF studies of the LNRB has been acquired and resurrected for this study. The model consists of twenty-one sub-basin elements and twenty-six lake routing elements (Acres Manitoba Ltd., 2006). The model is first run with baseline inputs to ensure that results match those provided in the latest PMF update study by Hatch Ltd. (2013b). An important note, in the event of future work, is that the model

requires a 32-bit operating system - or in this case, a 32-bit emulator on a 64-bit machine - in order to run.

The existing PMF model is modified to run historical high flow (non-PMF) years. This extension of the PMF model is important in order to validate the performance of SSARR relative to HEC-HMS and WATFLOOD simulations over the historical period. Results from a simulation in 1979 are visually compared to calibration hydrographs of the same year provided in the Crippen Acres Wardrop (1990) study, and are found to match those results. Lacking any quantitative calibration results from the 1990 study, the visual comparison provides enough confidence that the model is properly set up for historical high flow simulation in this study.

Historical high flow runs in SSARR (hereafter called validation runs) begin in March 1st of a given year and require initial snowpack (SWE), soil moisture, and baseflow infiltration index values. Values of these initial conditions from Crippen Acres Wardrop (1990) are available only for 1979 (the primary calibration year). Lacking any source of data to initialize SMI and BII in other years, these values are held constant in subsequent years.

The initial value of SWE in 1979 is a calibrated parameter in Crippen Acres Wardrop (1990) that accounts for over-winter snowpack losses; it is not an absolute depth of SWE. Therefore, it cannot easily be initialized for other years based on winter precipitation records. Instead, initial SWE in other years is estimated relative to the 1979 SWE input as a ratio of recorded over-winter SWE in a desired year to the recorded SWE in 1979. This notably assumes that any calibration for snowpack losses in 1979 also holds true in other historical years. Without more detailed information on the rationale behind initial SWE parameterization in Crippen Acres Wardrop (1990), this approach is deemed acceptable. Two sources of over-winter snowpack values are averaged as part of this approach: winter precipitation measurements at

meteorological stations (October 1 – March 1), and simulated SWE on March 1st from the HEC-HMS model. Averaging these two sources prevents excessive bias from any one estimate being introduced into the study. This approach produces values of initial SWE that are of expected magnitudes and perform sufficiently for the majority of years; poor performance in some years is associated with the SSARR model parameters and not due to significant error in the initial SWE input (further described in Section 5.1.1).

4.1.3. HEC-HMS

As stated previously, an existing PMF model in HEC-HMS is repurposed for this project. The model was initially developed by Manitoba Hydro for the LNRB as an inflow forecasting model, and was later recalibrated for a preliminary PMF study as an undergraduate thesis (Sagan, 2014). Several issues exist with the initial PMF model: calibration was done by manual adjustments only, the model was calibrated to the same years as SSARR (i.e. not representative of contemporary conditions), and the model did not use the same PMF assumptions as the original SSARR model. Therefore, a more robust calibration of the model and an improved PMF setup is undertaken in this study.

The PMF model in HEC-HMS covers the entire study area (LNRB upstream of Conawapa G.S.) using thirty-three basin elements, nine lake/reservoir elements, and a number of routing reaches. This setup is left largely unchanged from that used by Manitoba Hydro for inflow forecasting, with the exception that some gauged tributaries are further discretized into finer sub-basin elements to allow for more accurate simulation (not uncommon for design flood model setup, see Nathan & Weinmann, 2015). Precipitation forcing is distributed to each basin element based on Thiessen polygon weights for nearby gauges. These weights are a combination of those used in the existing LNRB model and those used in the SSARR PMF model (as reported

by Crippen Acres Wardrop, 1990). Temperature forcing for each basin element is provided from the closest meteorological station only.

A HEC-HMS model setup includes a number of global variables, such as meteorological parameters and snowmelt that apply to the model as a whole. Sensitivity to these parameters is tested prior to calibration. Historical high flows are insensitive to global meteorological parameters (e.g. rain-snow separation temperature) so those are set at values previously used in the LNRB forecasting model (in most cases, default HEC-HMS values). Snowmelt parameters (base snowmelt temperature and the stepped table of cumulative degree-days versus melt rate) are extremely sensitive and require calibration. Discussion on the adjustment of these parameters is included with other calibrated parameters in Section 4.2.2.

High flow years also show moderate sensitivity to evaporation. HEC-HMS uses average monthly depths as evaporation input, so these are easily estimated based on published values (and thus are not calibrated). Average monthly potential evaporations amounts using the Penman method are available from the National Ecological Framework (Agriculture and Agri-Food Canada, 2013a). These estimates are also compared to those available from NEF using the Thornthewaite equation, and compared to Environment Canada monthly evaporation normals at Island Lake A and Thompson A. The NEF-Penman monthly values produce the best performance in terms of the timing and magnitude of simulated flow during the calibration period, and compare conservatively to evaporation rates programmed in the SSARR model.

This setup provides confidence that model performance in historical high flow years can be attributed to watershed parameters, and not affected by errors in meteorological variables. The parameterization and calibration of watershed parameters is explained in detail in Section 4.2.2.

4.1.4. WATFLOOD

The WATFLOOD PMF model for the LNRB is a modification of an existing model that has been previously developed at the University of Manitoba and used in previous studies at Manitoba Hydro. Elements of the model, including watershed delineation, topography (via digital elevation model), and landcover (via remotely sensed imagery) were originally developed by others in 2010. More recent updates of these elements are unavailable and continue to accurately represent the basin. The WATFLOOD model covers the entire area of the LNRB (i.e. to the outlet at Hudson Bay), distributed on an approximately 11 km grid, and includes 20 defined lakes and reservoirs (Figure 7).

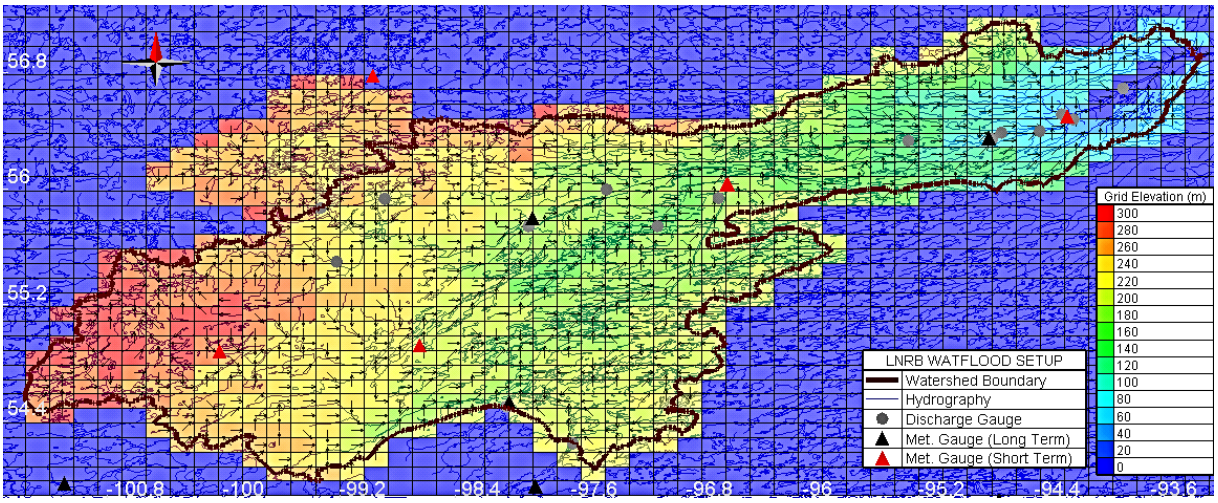

Figure 7: Lower Nelson River Basin WATFLOOD model setup, with gridded elevation and drainage directions visible

Originally twenty-one GRUs (herein, land classes) existed in the LNRB model. For this study, these are reduced to nine land classes by harmonizing redundant or insignificant (based on area) classes, which significantly reduces the runtime of the model. The nine land classes are listed in Table 5, along with their respective areas in the LNRB. Land cover classes conform to the EOSD classification used in land cover (LCC2000-V) data provided by the Government of Canada (Wulder & Nelson, 2003), with the exception of a "Treed Rock" class that has been

included in the model since 2010 (and differentiates areas of forest underlain by rock). Wetland areas are divided 65% to 35% between non-connected wetlands (bogs) and connected wetlands (fens); this ratio is a parameter previously calibrated for the model. Nine land classes are considered appropriate for the LNRB, and no significant loss in performance is expected; indeed, Haghnegahdar, Tolson, Craig et al. (2015) found that a discretization of seven GRUs performed comparably and more efficiently to a discretization of 16 GRUs in a similar hydrological model. Landcover in the LNRB is also shown on Figure 2.

Table 5: Land and river classes included in the LNRB WATFLOOD model

	Land Class	% of WATFLOOD Model Area		River Class	% of WATFLOOD Model Area
1	Coniferous Forest	33.7%	1	Rat/Burntwood	12.2%
2	Mixed Forest	6.1%	2	Nelson	9.5%
3	Treed Rock	5.9%	3	Upper Burntwood	9.7%
4	Shrubland	16.3%	4	Grass/Split Lake	30.2%
5	Bogs (Herb Wetlands)	4.6%	5	Minago/ Cross Lake	10.7%
6	Non-Connected Wetlands	12.9%	6	Kettle River	2.6%
7	Connected Wetlands	6.9%	7	Odei River	10.3%
8	Water	13.1%	8	Limestone River	12.9%
9	Impervious Area	0.5%	9	Footprint River	1.9%

The model is also separated into nine river classes – areas expected to have similar geomorphological characteristics, such as roughness, wetlands, and baseflow properties – also shown with their respective areas in Table 5. The river classes are defined based on major gauged tributaries in the basin (Upper Burntwood, Odei, Grass, Kettle, Limestone Rivers), two ungauged tributaries (the Minago and Footprint Rivers), and the main stem Burntwood and

Nelson Rivers. This allows for more flexible calibration of tributary gauges. The Footprint River class is negligible compared to the basin area; it is not included as part of the model calibration and instead is parameterized prior to (and after) calibration based on the Burntwood river class.

The WATFLOOD model incorporates several additional short-term meteorological gauges within the basin for historical precipitation and temperature forcing. For certain years, assuming the gauge has adequate record length and data quality, this increases the density of point precipitation data being distributed to a gridded input. This is important for attempting to catch localized precipitation events that may impact high spring/summer historical flows. In contrast, the semi-lumped models are limited to long-term meteorological gauges only.

Importantly, the existing PMF methodology for the LNRB includes the Gunisao River basin and some downstream local drainage area (i.e. these areas are subject to extreme rainfall/snowpack and contribute to flows downstream); however, this area was missing from the existing WATFLOOD LNRB model. Rebuilding the foundation of the LNRB model was deemed to be too time intensive, and would be more uncertain than the existing model (i.e. every aspect of the model would need to be re-verified). Instead, a separate WATFLOOD model for this study is developed for the Gunisao River basin upstream of the hydrometric gauge (05UA003; 4610 km^2). To incorporate this second model into PMF simulations, the resulting model outflows are (a) prorated for additional local area downstream of the gauge that is also not included in the original LNRB model (909 km^2 extra), and then (b) input into the LNRB model as an upstream forcing into the Nelson River east channel.

The Gunisao River model is on a 10 km grid scale (Figure 8) built using the digital elevation model (DEM) and landcover data used in the LNRB model. More specifically, the land surface was created from a 1:250,000 scale Canadian Digital Elevation Data DEM from

GeoBase (Natural Resources Canada, 2000a) – this coarser resolution is considered more appropriate for watershed delineation (Charrier & Li, 2012).

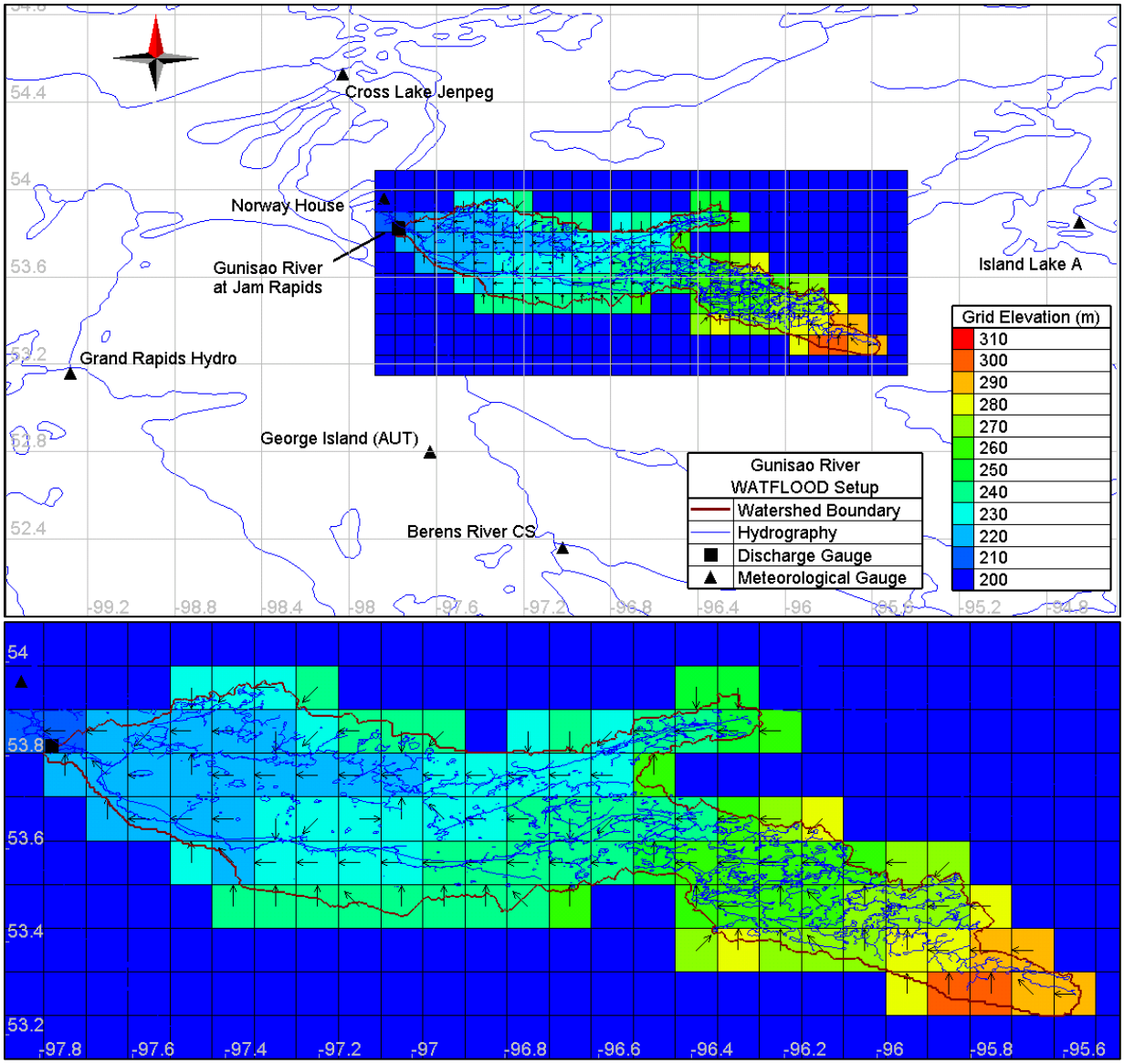

Figure 8: Gunisao River WATFLOOD model setup, with close-up of gridded representation and basin hydrography

The model includes eight land classes (a ninth – mixed forest – was negligible in the basin and thus harmonized with coniferous forest), and three river classes that define an upstream wetland and lake-dominated area, a mid-basin treed rock dominated area, and a downstream wetland dominated area. A single lake element is programmed in the model,

representing a major lake area in the upstream portion of the watershed. The Gunisao River model is run separate from the LNRB model throughout all historical and PMF simulations.

The setup of the existing LNRB WATFLOOD model has been verified and updated as part of this study, improving runtime and reducing the number of decision variables. Similar setup and verification of the Gunisao River model is also performed. Testing of both models determines that high flow years are adequately simulated (i.e. no structural or process problems), and that the models are suitable for PMF calibration (Section 4.2.3).

4.1.5. Model Setup Comparison

Basin areas are compared in all three models to Water Survey of Canada (WSC) and PFRA reported drainage areas to ensure the models are (a) accurate, and (b) comparable for a multi-model study. All three models compare favourably (i.e. within 5%) to reported sub-basin drainage areas. Several gauged sub-basins in SSARR, however, are slightly larger than in the other two models or the drainage area reported by WSC, as the SSARR modellers simplified the basin setup and included some downstream tributary area with the gauged sub-basins. The models also compare well at downstream locations (Table 6). Reported basin areas are based on delineations of incremental drainage area from the Watersheds Project first created by the Prairie Farm Rehabilitation Association (Agriculture and Agri-Food Canada, 2013b). Based on this, all three models are deemed to be (a) accurate enough, and (b) sufficiently comparable to have confidence that any major differences in simulations are the result of differences in model structure or parameterizations, and not due to errors in model setup.

Table 6: Comparison of modelled and reported drainage areas, with percent error from reported drainage area shown in brackets.

Location	SSARR (km^2)	HEC-HMS (km^2)	WATFLOOD LNRB + Gunisao (km^2)	Reported (km^2)
Nelson River at Keeyask G.S.	64,379 (-0.9%)	65,044 (+0.2%)	65,504 (+0.9%)	64,940
Nelson River at Conawapa G.S. (Total Study Area)	73,177 (-1.4%)	74,216 (-0.0%)	74,042 (-0.3%)	74,220

All three hydrologic models include several setup assumptions regarding lake/reservoir elements. Namely, no forebay reservoirs are simulated at Keeyask G.S., Limestone G.S., and Conawapa G.S. This is in line with an assumption made for the existing SSARR model (Crippen Acres Wardrop, 1990), and is made for two reasons: the reservoirs in reality provide very little attenuation, and their exclusion is more conservative. Of the regulated reservoirs in the basin, only Stephen's Lake (the forebay of Kettle G.S.) is large enough to create enough attenuation to warrant consideration of both inflows and outflows in PMF results.

To allow for potential modelling of larger PMFs in the future climate simulations, the storage discharge curves of lake/reservoir elements in all of the models were extended. Regulated reservoirs programmed in the models (i.e. Kelsey G.S., Kettle G.S., Long Spruce G.S.) assume that dams act as free overflow weirs, if overtopped. This theoretically leads to more extreme peak flows downstream when an upstream dam on the Nelson River is overtopped. For non-regulated lakes, a simple polynomial extrapolation of the existing storage-discharge curve is assumed to allow for the occurrence of higher flows. Both of these assumptions were developed previously as part of a similar PMF study for Manitoba Hydro using GCM projections (Hatch Ltd., 2013a), and are used here for consistency in PMF simulations.

With their setups verified, the HEC-HMS and WATFLOOD models as described here are then moved forward for calibration and parameter adjustment; while the SSARR model was run without additional adjustment using the same historical years for validation purposes only.

4.2. PMF Model Calibration

Calibration and independent validation of model parameters are integral to hydrological modelling (Debs et al., 1999), particularly when using a conceptual model whose parameters are not necessarily physically-based (Nathan & Weinmann, 2015). This section describes the calibration and validation of the PMF models in this study, keeping in mind two points from PMF guidance documents: (a) that the calibrated models will need to be extrapolated to conditions much more extreme than those used for calibration (Alberta Transportation, 2004; Nathan & Weinmann, 2015), and therefore (b) that the calibration must involve a sufficient number and severity of high flow events to have more confidence in this extrapolation (Alberta Transportation, 2004; FERC, 2001; Nathan & Weinmann, 2015). In addition, calibration techniques were applied in this research in the context of the previous PMF models and guidance described in Section 2.4.

4.2.1. Calibration Methodology

The existing SSARR model was developed in the late 1980s, and calibrated to select high flow years prior to that. Often, gauged tributaries in SSARR were calibrated to only one or two years. Streamflow records up to present, however, show that there have been higher flow years in the basin since that time (e.g., see Figure 9) and that the years used in the SSARR calibration generally differ from the magnitude or timing of peak flows occurring more recently (and frequently) in the record. The decision is therefore made to use the existing calibration of the

SSARR model as a baseline scenario, and in keeping with point (b) above from PMF guidance documents and the recommendation of Alberta Transportation (2004), to calibrate the HEC-HMS and WATFLOOD PMF models to a longer (and wetter, capturing at least two high flow years) period than the SSARR calibration period.

4.2.1.1. Calibration Period

The HEC-HMS and WATFLOOD models are calibrated to select high flow years throughout the period of record, prioritizing the highest flow years with varying dates of occurrence and including years spread throughout the record. This wider calibration period is more robust and representative of high flow behaviour in the basin, and should be expected (with adequate model performance) to better extrapolate to extreme PMF conditions. A more robust calibration is particularly important for a complex model like WATFLOOD, which is more highly parameterized with wetland processes that are more sensitive to wet/dry cycles. With this approach to model calibration, HEC-HMS and WATFLOOD models may better represent (than SSARR) high flow processes for the extrapolation to PMF conditions and to future climate conditions. However, PMF results from these two models are no longer directly comparable to the SSARR model due to the influence of different calibration periods. This trade-off is deemed acceptable because results from the SSARR model act as a useful baseline, or "historical" value of PMF, and can be indirectly compared to results achieved from the more complex models and wider calibration period.

Five calibration years and five validation years are selected at each of the nine gauges. An analysis of high spring flow years is essential in order to choose the most critical years (based on runoff volume or snowmelt timing for example), while also ensuring that all major flood-generating processes are considered (Debs et al., 1999). In this case, years with the highest

spring peak flows are selected (late April to late June period – the period of interest for Spring PMF), and priority given to years that also include obvious rain-on-snow or heavy spring rainfall events. Years selected for a given sub-basin are then divided into calibration and validation periods so as to include years throughout the record in both groups. In addition, to allow for direct comparison to the SSARR model in the historical period, the validation of a given sub-basin includes the year(s) used to calibrate that basin in the SSARR model.

As an example, Figure 9 provides the hydrometric record (1979-2014) of one tributary gauge in the basin, and shows the selected high flow calibration and validation years for this basin. Note that (a) calibration and validation years are spread throughout the period of record, (b) only years with the highest peak flows in spring are selected (late summer peaks not considered), and (c) the validation years included two years used in calibrating the original SSARR model. Also of note are the much lower peaks exhibited in the two SSARR calibration years relative to the more recent, higher spring peak flows throughout the remainder of the record.

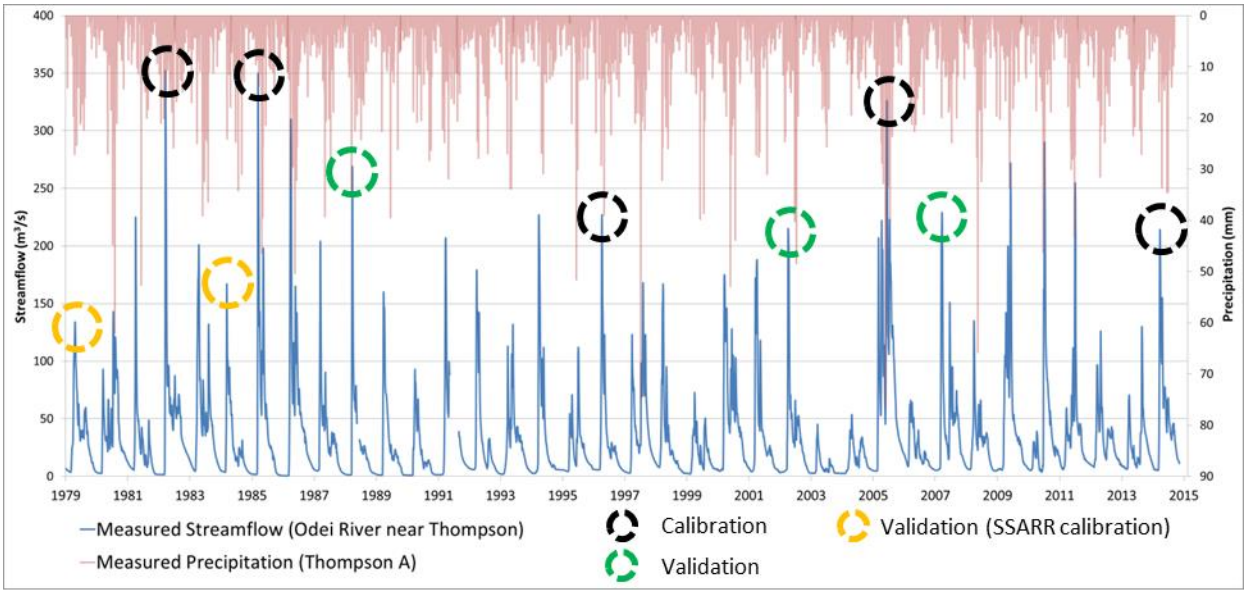

Figure 9: Selected calibration and validation years for the Odei River streamflow gauge

Calibration and validation years are similarly selected for all six hydrometric gauges located on major tributaries plus three downstream gauges located on major river channels. Using this approach, all available long-term hydrometric stations (tributary and downstream) in the basin are used in calibration. Previous studies (e.g. Khakbaz, Imam, Hsu et al., 2012; Xue et al., 2014) have found that considering both interior and downstream gauge locations results in improved model performance at the outlet and reduced error trade-off at upstream gauges.

For two downstream gauges (Thompson and Kelsey G.S.), high flow years are selected based on estimated local inflows only, by subtracting upstream forcing from the discharge record (with allowance for travel time). This prevents the selection of years where high flows were dominated by upstream (regulated) forcing to the model, which would bias the model towards better performance and prevent closer consideration of runoff processes in the ungauged areas. An example of this approach is shown on Figure 10.

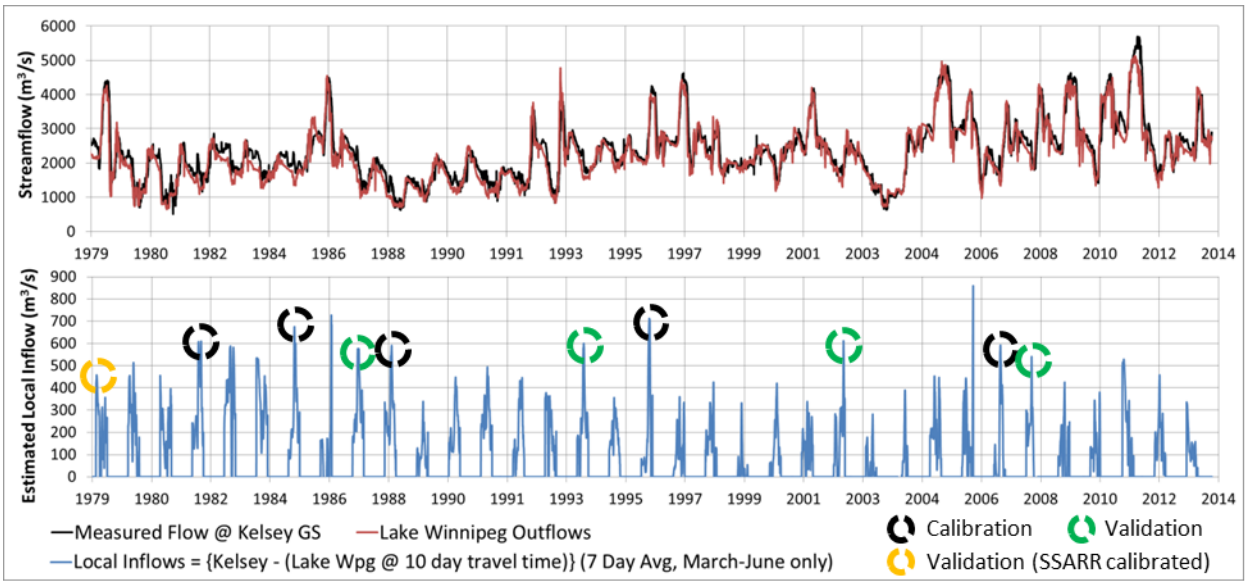

Figure 10: Selected calibration and validation years based on local inflows (blue) to Kelsey G.S.

Note the large proportion of flows at Kelsey G.S. (black) provided by inflows to the LNRB from Lake Winnipeg (red). Also note the estimated isolation of local inflows (blue), using a 7-day moving average to reduce noise in the graph, and the selection of high flow years based on this estimate (which in some cases do not correspond to the years of highest absolute flows observed at Kelsey G.S.).

A similar approach is not applied at Kettle G.S. because measured outflows are heavily influenced by cycling/peaking behaviour of the generating station; therefore, too much error is involved in attempting to isolate local ungauged inflows (the streamflow record was used as is).

Importantly, calibration and validation years are not the same at every gauge; spatial variation in snow accumulation and heavy precipitation can lead to high flow years on some tributaries but not others. This methodology of varied calibration years among gauges follows that originally used for the SSARR PMF model (Crippen Acres Wardrop, 1990), but over a wider period and including more high flow years. The hydrological model is expected to perform similarly over discontinuous periods if they have similar conditions, such as high spring flows in this case (Razavi & Tolson, 2013). As further justification, "unusual events or small data sets" (e.g. the extreme spring freshets here) have even been found to perform sufficiently for validation to average conditions (Haberlandt & Radtke, 2014, p. 363). This approach is therefore not uncommon in literature (see also the case study by Seibert, 2003), and is not necessarily skewed as a result of a discontinuous and selective calibration period.

Table 7 displays years selected for calibration and validation, and their corresponding peak flow and date, for all gauges used in the models. The period of April 10 to September 1 of a given year is used for calibration because this study is only concerned with spring PMF, involving snowmelt in spring and recession of the freshet peak in early to mid-summer. The sub-

year period is large enough to include the processes of interest (the rising and falling limbs of the freshet) without being affected by the fall and winter low flow periods (which are not of concern for PMF). The use of a sub-year calibration is based on the methodology used in the original SSARR PMF model calibration (Crippen Acres Wardrop, 1990); however the approach has also been applied in a summer-fall PMF study by Beauchamp, Leconte, Trudel et al. (2013).

Table 7: Years used for high flow calibration in HEC-HMS and WATFLOOD

Sub-Basin	Calibration Years	Peak Flow (m^3/s)	Peak Flow Date
Grass River	1985	185	July 9
	1986	163	August 16
	1996	183	July 13
	2005	205	August 31
	2007	128	July 2
Gunisao River	1996	146	June 5
	2001	142	May 11
	2005	144	April 17
	2008	85	July 16
	2011	136	May 17
Kettle River	1983	202	June 3
	1986	165	May 18
	1991	110	May 16
	2001	104	May 19
	2007	113	May 8
Limestone River	1982	356	May 3
	1983	438	May 31
	1988	317	May 9
	1991	254	May 13
	2007	244	May 2
Odei River	1982	352	May 3
	1985	350	April 27
	1996	227	May 26
	2005	326	July 31
	2014	214	May 18
Upper Burntwood River	1986	172	May 16
	1996	178	May 22
	1998	151	June 22
	2001	173	May 23
	2014	165	May 14

Downstream Gauge Locations			
Gauge Location	Calibration Years	Peak Inflow (m^3/s) Absolute (Local)	Peak Flow Date Absolute (Local)
Burntwood River at Thompson	1986	1150 (490)	May 19 (May 24)
	1996	860 (366)	June 1 (May 27)
	2001	938 (455)	May 26 (May 27)
	2005	1030 (438)	June 11 (April 23)
	2007	1320 (562)	May 12 (May 12)
Nelson River at Kelsey G.S. (Outflows)	1982	2267 (662)	May 6 (June 7)
	1985	2321 (737)	May 2 (May 2)
	1988	1624 (615)	May 5 (May 14)
	1996	4249 (808)	June 30 (June 4)
	2007	3698 (718)	August 8 (August 21)
Nelson River at Kettle G.S. (Outflows)	1982	3983	May 7
	1986	5897	May 23
	1988	3821	May 15
	1996	5399	June 29
	2007	5280	August 15

Note that significant attenuation within the Grass River (due to lakes) delays the freshet peak until July or August, so calibration years for the basin were selected more based on the speed and timing of the rising limb of the freshet.

4.2.1.2. Calibration Metric

The HEC-HMS and WATFLOOD models are calibrated based on a hybrid objective function that incorporates normalized values of five calibration statistics. The use of multiple statistics aggregated into a single hybrid metric has been applied previously in literature (e.g. (Efstratiadis, Nalbantis, Koukouvinos et al., 2008)), and attempts to avoid biasing the calibration towards only a specific part of the hydrograph that may be emphasized by a single statistic (Boyle et al., 2000; Gupta, Sorooshian, & Yapo, 1998). The weighted sum essentially converts a multiple objectives into a single, descending objective which (a) is better suited for the DDS calibration in WATFLOOD described later and (b) is more comparable to the traditional PMF

modelling approach of achieving a single, local solution. Multi-objective optimization of a PMF model may provide additional benefits to parameter identifiability while requiring greater user input to choose a single solution from a set of non-dominated samples.

The five calibration metrics are selected to evaluate model performance including accurate simulation of volume, timing of rising and falling limbs, and peak flows. Metrics are selected to easily rank simulations relative to each other, while still providing meaningful absolute information about each simulation. In this way, the objective function was designed to be most applicable to this project (i.e. for high flows, and useful in automated and manual calibration settings), as advocated by Wagener et al. (2001).

The normalized calibration metrics and their associated weights (selected by a manual calibration process) are provided in Table 8 and explained below.

Table 8: Performance metrics aggregated into a hybrid calibration statistic

Name	Calculation	Weight
Absolute Average Peak Flow Deviation	$\left\| \frac{\sum_{i=1}^{m} \frac{(Q_{sim\,peak,i} - Q_{obs\,peak,i})}{Q_{obs\,peak,i}}}{m} \right\|$; m = # of years (5)	0.35
Nash-Sutcliffe Efficiency (1 – NSE)	$1 - \sum_{i=1}^{n} \frac{(Q_{sim,i} - Q_{obs,i})^2}{(Q_{obs,i} - \overline{Q_{obs}})^2}$; n = # of days in calibration	0.25
Absolute Bias	$\frac{\sum_{i=1}^{n} \lvert Q_{sim,i} - Q_{obs,i} \rvert}{\sum_{i=1}^{n} Q_{obs,i}}$; n = # of days in calibration	0.15
Percent Bias (here Volume Bias)	$\frac{\sum_{i=1}^{n} (Q_{sim,i} - Q_{obs,i})}{\sum_{i=1}^{n} Q_{obs,i}}$; n = # of days in calibration	0.15
Normalized RMSE	$\sqrt{\frac{\sum_{i=1}^{n} (Q_{sim,i} - Q_{obs,i})^2}{n}}$; n = # of days in calibration	0.1

The most important aspect of a PMF model is simulation of peak flow magnitude; over- or under-estimation are equally problematic. This can be measured using the absolute deviation

of simulated peak flow versus observed peak flow, averaged over all calibration years. The Nash-Sutcliffe Efficiency (NSE) is an important metric of performance in volume and timing (Nash & Sutcliffe, 1970) that will also place more importance on higher flows. To better capture performance across the entire hydrograph (recognizing the importance and difficulty of appropriately modelling non-linear processes on the rising and falling limbs), the percent bias and absolute percent bias are then added as measures of overall volume and timing. Finally, the normalized root mean square error (RMSE), or RMSE-observations standard deviation ratio (RSR; Moriasi et al., 2007), differentiates the skill of the simulation relative to variation in the observed record. A lower RSR value indicates better fit. NSE, percent bias, and RSR also have recognized thresholds of performance that allow for judging the absolute skill of the simulation (Moriasi et al., 2007). Timing of the peak flow is captured primarily by the NSE and absolute bias.

The magnitudes of the five statistics are recognized to be different; however, weights are based on the importance of a change in each statistic. As an example, an improvement of 0.01 (1%) in peak flow deviation is more significant alone than a 0.01 (1%) improvement in volume bias or absolute bias alone. Similarly, a worsening of peak flow deviation by 1% requires significant improvement in the other statistics to maintain the same hybrid metric value. In this way, the primary use of the hybrid objective function is to choose between competing candidate solutions and guide calibration; weights selected (Table 8) achieve this objective.

Weights to scalarize the metrics into a hybrid objective function were chosen by considering theoretical sets of performance statistics and determining the type of performance most ideal as output from the automated calibration routine. There was an expectation that manual calibration would be required after automated runs were complete. Collinearity certainly

exists between the five metrics so that it may be difficult to distinguish the significance of one metric from another; indeed, there may be other sets of weights that produce similar values of the hybrid objective function. However, this set of weights was found to acceptably rank solutions in terms of acceptable simulation of peak flows and the overall hydrograph (i.e. local solutions that could be further exploited).

In the case of calibration in WATFLOOD, optimization runs are conducted on a whole-watershed basis (versus individual gauged sub-basins in HEC-HMS) because the model is distributed. The entire lower Nelson River basin (LNRB) is simulated for the whole calibration period. This requires that all calibration gauges in the LNRB are weighted and aggregated into a single performance measure that could be used to guide an automated calibration routine. This approach is very similar to the Performance Virtue statistic (X. Wang & Melesse, 2005) in that it takes a weighted average of a hybrid objective function at all gauges in the LNRB.

Two methods of weighting are considered here: by upstream local drainage area, and by mean local inflows during the calibration period. Gauge weighting in both cases is provided in Table 9. The term "local" is important in this case – local inflows are estimated at the three downstream locations by removing any upstream gauged contribution. This prevents the calibration from being unfairly biased towards the three downstream gauge sites, which are known to have (a) higher flows, (b) significant contributions from upstream forcing, and therefore (c) naturally better performance in calibration.

Weights by mean local inflows during the calibration period are preferred because of non-proportional runoff behaviour that occurs in certain areas of the LNRB. Specifically, the Grass River basin (15,400 km^2) comprises a larger area than its runoff yield would suggest, resulting from significant wetland and lake storage. This weighting shifts the significance from

lake-dominated areas, such as the local area upstream of Kettle G.S., to more critical response areas such as local areas upstream of Thompson and Kelsey G.S. Weights by mean flows are selected as opposed to peak flows because several smaller basins (e.g. Kettle River) produce high peak flows but lower freshet volume, and so are not as critical for a sustained PMF case.

Table 9: Weighting of calibration sites for single optimization metric in WATFLOOD

Calibration location/gauge	Weights by upstream local drainage area	Weights by mean local inflows in calib. period
Burntwood River above Leaf Rapids	0.08	0.07
Odei River near Thompson	0.08	0.11
Grass River at Standing Stone Falls	0.21	0.14
Kettle River at Gillam	0.03	0.04
Limestone River at Bird	0.04	0.06
Gunisao River at Jam Rapids	0.06	0.06
Burntwood River near Thompson	0.09	0.15
Nelson River at Kelsey G.S.	0.28	0.31
Nelson River at Kettle G.S.	0.12	0.05

The hybrid objective function, and weighting of the hybrid metric at all nine calibration points for WATFLOOD calibration, performed well in pre-calibration testing. The methodology allows for guidance of automated calibration routines and ranking of candidate solutions, and also provides useful information on whether individual simulations could be considered behavioural (an important note for uncertainty analysis described in Section 4.3).

4.2.2. HEC-HMS CALIBRATION

The HEC-HMS model was calibrated in a multiple step process, which is introduced here and explained in detail in the sub-sections to follow:

1. Estimating parameter ranges and selecting decision variables;
2. Calibration at the six gauged sub-basins;
3. Regionalization of parameters;
4. Manual calibration of ungauged areas.

The approach compares very closely to the "multisite cascading" approach advocated by Xue et al. (2014, p. 2), in which parameters at upstream gauges are optimized first, then fixed during optimization of downstream areas. A difference here is that calibration at the downstream gauges was done manually (adjusting based on regionalised values), and not with an automated approach. The approach also represents a "semi-distributed" calibration given the regionalization of parameters. This is less complex than a "distributed" calibration (unique optimization for all basin elements) but has been found to reduce over-fitting and therefore produce better performance in validation (Wi, Yang, Steinschneider et al., 2015).

4.2.2.1. Estimating Parameter Ranges and Selecting Decision Variables

HEC-HMS snowmelt parameters (base melt temperature and a table of cumulative degree-days versus melt rate) were not included in auto-calibration; HEC-HMS was not designed to be automated externally, and there were difficulties at the time in changing those variables via external scripts. Instead, base snowmelt temperature was initially set as per the SSARR model (-4°C) and the snowmelt rate curve was based on the most commonly used snowmelt rate curve in SSARR. The table in SSARR was not directly comparable to HEC-HMS given its basis on snow covered area; however, it provided a useful progression of initial melt rates. Both parameters were tested and adjusted prior to calibration based on visual comparison of the simulated freshet in all gauged sub-basins during the calibration period. Adjustments continued until snowmelt modelling was deemed adequate to hold the parameters constant during auto-calibration. After

auto-calibration was completed, melt rate parameters were revisited and adjusted further if needed. A qualitative comparison to WATFLOOD parameters is discussed in Section 4.2.3.3.

Realistic parameter ranges for each of the six gauged tributaries were required in order to constrain the auto-calibration, however, useful ranges were not available in HEC-HMS documents or from previous models. Parameter ranges were instead estimated from empirical methods, GIS spatial data, and previous knowledge of the basin. GIS data was available from the Soil Landscapes of Canada (SLC) dataset, a 1:1 million data product of the National Soil DataBase based on distributed soil survey data (Agriculture and Agri-Food Canada, 2011). The dataset provided information on major soil formations in terms of vegetation cover, land slope, soil texture, vertical soil horizons, and soil drainage and saturation characteristics.

A detailed explanation is provided in Appendix A of the methodology used to estimate realistic ranges for HEC-HMS parameters in each gauged sub-basin. For brevity, studies by Fleming & Neary (2004), García et al. (2008), and Rawls, Brakensiek, & Saxton (1982), among others, and data from the Soil Landscapes of Canada dataset (Agriculture and Agri-Food Canada, 2011) provided useful guidance on parameter estimation techniques and expected ranges. Different techniques and/or variations in input data (e.g. testing on multiple years) produced a range of values for each decision variable that was then carried forward during calibration.

Parameter ranges in each sub-basin were initially revised based on a sensitivity analysis of 1200 samples over the calibration period. Clear trends in the hybrid metric relative to parameter value were identified, and bounds for parameters were (a) expanded to ensure random samples would not be limited by too narrow of a range, and/or (b) moved inward to reduce the sample space. A list of decision variables and sampling ranges is provided as Table 10.

Table 10: Decision variables and ranges used to constrain HEC-HMS calibration

Parameter	Units	Upper Btwd.	Odei River	Gunisao River	Grass River	Kettle River	Limestone River
Canopy Maximum Storage	mm	2.5	2.2	2.3	2.3	2	2.5
Surface Maximum Storage	mm	8 – 50	10 – 30	15 – 50	10 – 75	20 – 40	15 – 40
Percent Impervious Area	%	15 – 40	7 – 20	5 – 20	11 – 18	7 – 20	15 – 35
Soil Maximum Infiltration	mm/hr	1 – 3.5	1 – 2	1.4 – 3	1.8 – 4	0.8 – 2.2	0.6 – 2
Soil Maximum Storage	mm	180 – 280	230 – 250	160 – 240	180 – 243	160 – 240	195 – 300
Soil Tension Storage	Frac. of max storage	0.5 – 0.75	0.6 – 0.7	0.6 – 0.8	0.4 – 0.6	0.5 – 0.7	0.5 – 0.7
Soil Maximum Percolation	mm/hr	0.4 – 2	0.3 – 1.2	0.5 – 1.25	0.4 – 0.9	0.25 – 0.9	0.25 – 0.7
Groundwater Max. Storage (Upper)	mm	100 – 160	80 – 130	115 – 175	150 – 220	120 – 180	85 – 130
Groundwater Storage Coeff. (Upper)	hr	740 – 1148	556 – 1050	640 – 723	1300 – 2400	411 – 750	495 – 800
Groundwater Max. Percolation (Upper)	Frac. of Soil Perc.	0.6 – 1	0.55 – 0.85	0.6 – 1	0.45 – 0.7	0.5 – 0.8	0.5 – 0.85
Groundwater Max. Storage (Lower)	mm	80 – 120	70 – 130	95 – 140	160 – 230		
Groundwater Storage Coeff. (Lower)	hr	1025 – 1600	854 – 1800	854 – 1655	2608 – 3325		
Groundwater Max. Percolation (Lower)	Frac. of GW1 Perc.	0.6 – 1	0.5 – 0.9	0.55 – 1	0.45 – 0.7		
Time of Concentration	hr	248 – 373	200 – 290	236 – 354	519 – 778	109 – 163	182 – 250
Surface Storage Coefficient	hr	339 – 591	259 – 425	419 – 687	745 – 960	325 – 600	173 – 250

4.2.2.2. Calibration at Gauged Sub-basins

Calibration was conducted separately for each of the six gauged sub-basins; as a semi-lumped model, HEC-HMS allows for basin-specific calibration. The process of calibration at each gauged sub-basin in HEC-HMS is illustrated in Figure 11, alongside the calibration process of WATFLOOD for comparison.

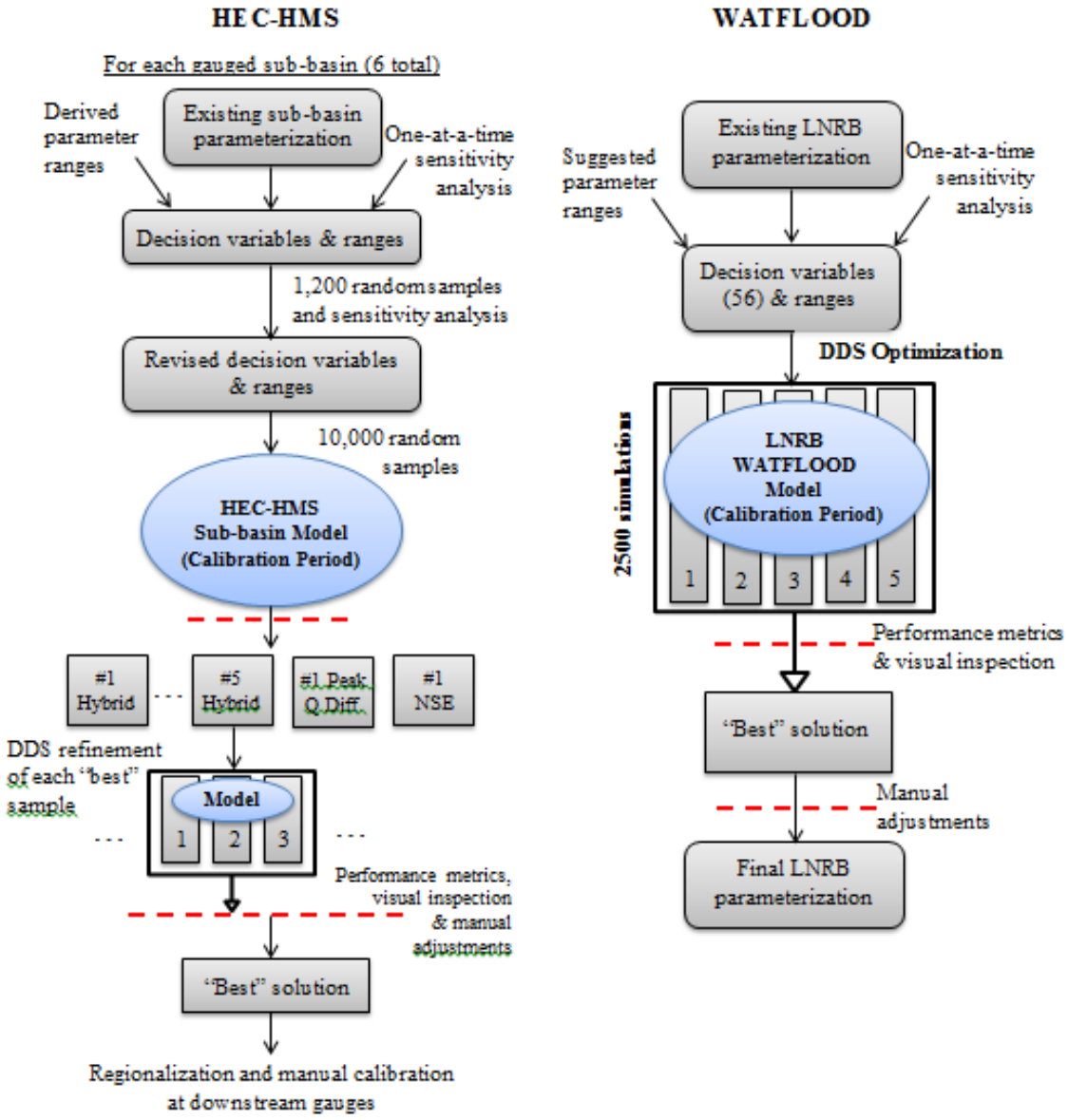

Figure 11: Calibration methodologies in HEC-HMS and WATFLOOD

The calibration routine in HEC-HMS was Monte Carlo-based: for each basin, 10,000 parameter sets were sampled from a uniform random distribution within its respective parameter ranges of that sub-basin. The best performing parameter sets (by hybrid objective function) were extracted for each basin, verified by visual comparison of the hydrographs, and then carried forward for additional adjustments.

Subsequent adjustments of parameters after the Monte Carlo calibration were important for ensuring adequate simulation of peak flow magnitudes. Only one basin (the Kettle River) performed successfully enough after the Monte Carlo simulations to move forward without adjustments. To supervise adjustments and refine performance in the remaining five sub-basins, a DDS algorithm programmed in MATLAB (developed for an unrelated project after calibration) was repurposed for use with the HEC-HMS model. (DDS is described further in Section 4.2.3.2). A short DDS run was used in lieu of extensive manual adjustments, with the following characteristics for each sub-basin: (1) 400-1000 model simulations (depending on the amount of refinement necessary and due to computational constraints), and (2) seven independent trials (initialized by the five best performing parameter sets based on the hybrid objective function and the best performing parameter sets based solely on NSE and peak flow deviation). The best performing sample from among the DDS refinement trials (as determined based on visual inspection and performance metrics) was then selected to use for each of the six gauged sub-basins.

4.2.2.3. Regionalization of Parameters

Design flood guidelines recognize the need for ungauged catchments to be parameterized based on calibration at nearby gauges (e.g. Nathan & Weinmann, 2015). To parameterize the rest of the HEC-HMS model (i.e. areas not directly gauged), the parameter sets from the six

calibrated sub-basins ("index basins") were regionalized to nearby sub-basins. An index basin was related to an ungauged area based on proximity and a qualitative comparison of landcover, drainage characteristics, slope, and base saturation from GIS data (Agriculture and Agri-Food Canada, 2011). This assumes that areas that compare well in the above physiographic characteristics will also exhibit similar runoff behaviour - an approach that Razavi & Coulibaly (2013) note is common among regionalization applications. This "lumped" method was also found by Wallner, Haberlandt, & Dietrich (2012, p. 67) to perform robustly and effectively compared to more sophisticated forms of regionalization (i.e. regression-based or distributed) and was deemed a "promising tool" for use in HEC-HMS climate change impact studies..

Regionalized parameters that were correlated with catchment area (i.e. time of concentration, storage coefficients for surface runoff and baseflow) were not expected to be directly transferable between basins. These values were adjusted as follows:

- Time of concentration (t_c): A value of t_c was estimated for the ungauged basin using an estimate of main channel length from GIS and the Sheridan (1994) equation; for smaller basins, a minimum t_c of 24 hours was required by HEC-HMS.
- Surface storage coefficient (R): Given t_c, the R value from the index basin was adjusted so as to maintain the same $\frac{R}{t_c+R}$ ratio as the index basin. As per FERC (2001), areas of similar hydrologic characteristics should maintain a similar R value.
- Baseflow storage coefficients: Values were adjusted by the same factor as the surface storage coefficient.

The impact of these adjustments was most visible in ungauged local catchments – that is, wide drainage areas with relatively short flowpaths. Time of concentration and storage coefficients in

these basins was greatly decreased as a result of the short flow path. This is intuitive, given the more rapid responses expected from smaller, shorter local catchments.

4.2.2.4. Manual Calibration of Ungauged Areas

A final manual calibration was conducted of ungauged areas by assessing performance at the three downstream gauges (Thompson, Kelsey G.S., and Kettle G.S.). Regionalised values performed well and any minor adjustments were ground-truthed by a comparison of physiography to that of the index basin (e.g., basins with more areas of highly saturated soils were adjusted to increase impervious area and/or decrease maximum infiltration). Muskingum routing times (K) of channel reaches were also adjusted at this stage; often, K was decreased to visually improve timing of the simulated peak flow. After adjustments, the average timing of the freshet was generally accurate at all three downstream gauges. As a final step, snowmelt rates for the HEC-HMS model were revisited and marginally delayed to improve spring melt timing in the majority of basins. Post-calibration adjustment was expected for the snowmelt rate curve.

Calibration in HEC-HMS involved multiple steps that combined the time-savings and search ability of a random, automated calibration with the supervision of manual adjustments before and afterwards. The calibration employed methods that have been reported in literature, but applied here for high flow calibration. The calibration routine successfully produced a local solution that was deemed capable of accurately simulating high flows in the LNRB and thus capable of extrapolation to PMF.

4.2.3. WATFLOOD CALIBRATION

The PMF model in WATFLOOD was calibrated in a similar multi-step process as HEC-HMS, with the following procedures:

1. Pre-Calibration – Sensitivity analysis and decision variable selection;
2. Automated and supervised calibration by DDS;
3. Manual adjustments to refine performance.

This method of combining pre-calibration manual adjustments with subsequent automated calibration is similar to that applied by Bingeman (2001) for a PMF study of the Columbia River Basin in WATFLOOD. A schematic of the WATFLOOD calibration process is provided alongside that of HEC-HMS in Figure 11.

4.2.3.1. Pre-Calibration

Sensitivity analysis and manual adjustments were conducted prior to calibration to reduce the number of decision variables and to more effectively estimate fixed parameters. As Gupta, Sorooshian, & Yapo (1998) and Efstratiadis, Nalbantis, Koukouvinos et al. (2008) note, limiting the number of variables and the parameter space while testing performance at a number of sites and a number of statistics (i.e. the hybrid statistic and nine flow gauges here) is critical for an efficient calibration.

Pre-calibration runs were conducted for the LNRB model (minus the separate Gunisao River model) over the calibration period at all gauges. These runs included one-at-a-time sensitivity analysis of model parameters, using the whole-basin hybrid statistic to measure sensitivity. Subsequent adjustments of fixed parameters were (a) based on visual inspection at individual gauges and (b) were focused on performance at gauge(s) whose upstream areas were dominated by the land/river class of interest. For example, only the Upper Burntwood basin had significant treed rock areas; so, only simulations at that gauge were considered for treed rock parameters. River classes were typically separated by sub-basin, therefore parameters such as baseflow were easily isolated to single calibration points.

Among the river class parameters, in-channel roughness was found to heavily influence simulations and was included in calibration, while the roughness of overbank areas had no effect and was kept at default values. Simulations in the calibration period were also very sensitive to wetland parameters (kcond and theta; lateral conductivity and wetland porosity, respectively). Baseflow parameters had only a moderate effect on the historical high flow hydrographs (perhaps owing to a greater proportion of interflow and surface flow during flood events); given the moderate sensitivity, these parameters were manually adjusted then fixed during calibration.

Simulated flows were most sensitive to land class parameters for infiltration, soil retention, interflow, and recharge/percolation. Given the difficulties in manually adjusting these parameters (non-linear effects on the hydrograph), all were included as decision variables. Parameters for snow-covered processes (under-snow infiltration and recharge) and for surface depressional storage did not significantly impact high flow simulations and were left at their existing values from the original LNRB model. Other parameters associated with evapotranspiration or interception were also not sensitive and were left at existing values. In the cases of fixed parameters such as these, values were checked for realism based on published WATFLOOD parameter ranges (Bingeman, 2001; Kouwen, 2014).

Snow-related parameters (base melt temperature, melt rate, sublimation) were all found to significantly impact performance at all gauges. Melt rate was the most difficult to estimate and so was included in the calibration, while base melt temperature and sublimation rate were more easily estimated and therefore were manually specified. Base snowmelt temperatures for all land classes were specified within a range of -2.5°C to -1°C by fitting the average rising limb of the freshet at each gauge. Base melt temperatures were warmer than specified in HEC-HMS (-4°C); this may be the result of:

- Sublimation in WATFLOOD (i.e. reduced melt volume);
- Invariant routing (time of concentration) in HEC-HMS that responds slower than distributed routing in WATFLOOD;
- Deep groundwater losses in HEC-HMS;

Base melt temperature differences may also be due to the initial parameterization in each model. Sublimation rates in WATFLOOD were derived from MacKay et al. (2006) who found that approximately 16% of observed winter precipitation sublimates in forested regions of Manitoba and Saskatchewan and 9% sublimates in agricultural ("open") areas. Assuming an SWE of between 100-150mm (visual average based on winter precipitation records), this resulted in sublimation rates for canopy-covered and open land classes to be specified between 0.16-0.24 mm/day and 0.1-0.14 mm/day, respectively.

Finally - and distinct between WATFLOOD and the other models – lake/reservoir storage-discharge relationships in WATFLOOD must be specified as power or polynomial relationships, and not in tabular form. Equations were fitted for those lakes with existing storage-discharge tables from the SSARR and HEC-HMS models. Not all twenty lake elements in the model had known data, so the fitted equation from a nearby, similarly-sized and located lake was transferred over in those cases. Model runs were then conducted to ensure an appropriate amount of lake attenuation, and adjustments to the relationships were made at times to achieve more realistic routing and improved performance. The storage-discharge equations were similarly revisited after calibration. This parameterization provided improved skill at downstream gauges when compared to the original LNRB model and lake/reservoir parameters were also grounded in reality given their basis on known storage-discharge tables.

As a final check prior to calibration, internal model processes in the LNRB and Gunisao River models were verified using outputs of surface and soil processes and runoff contributions.

4.2.3.2. Automated Calibration

Automated calibration was conducted in the LNRB model only; the Gunisao River model was manually calibrated afterwards given the LNRB optimized solution. Optimization of the LNRB model was conducted using the Dynamically Dimensioned Search (DDS) algorithm programmed for WATFLOOD. Detailed information on DDS as an efficient search algorithm for computationally demanding models is provided by Tolson & Shoemaker (2007). DDS is not intended to find a global optimum without a robust number of evaluations, but Tolson & Shoemaker (2007) conclude that it is capable of efficiently finding local solutions. The LNRB model was calibrated using a DDS optimization with wide decision variable ranges and initialized at random values. This approach outperformed others (e.g. manual calibration), although manual adjustments provided important information on parameter sensitivity.

After pre-calibration adjustments to moderately sensitive (fixed) parameters, a total of 56 decision variables remained for optimization: eight model parameters, with six to eight land/river classes each. This size of calibration is not uncommon in WATFLOOD; a WATFLOOD PMF study by Bingeman (2001) calibrated 50 decision variables (10 model parameters) using a local search method to fine-tune performance after initial manual adjustments.

The 56 decision variables and their range constraints are provided in Table 11. Ranges were wide to promote searching of the parameter space, and were developed based on (a) ranges suggested in the WATFLOOD manual (Kouwen, 2014), (b) ranges used in previous calibrations of the LNRB model at the University of Manitoba, and (c) ranges provided in Bingeman (2001) for mountainous terrain that were not always directly comparable. The Footprint river class and

impervious land class make up negligible area in the LNRB; their parameters were fixed to reduce the number of decision variables. Also note that some land class parameters are not applicable to connected wetland or water classes due to the WATFLOOD internal structure.

Table 11: Decision variables and ranges in WATFLOOD DDS calibration

Parameter	River Class Parameters								
	Btwd	Nelson	Upper Btwd	Odei	Grass	Minago	Kettle	Lime-stone	Foot-print
Channel Roughness	0.0001 - 0.05	0.0001 - 0.05	0.0001 - 0.05	0.0001 - 0.05	0.0001 - 0.05	0.0001 - 0.05	0.0001 - 0.05	0.0001 - 0.05	
Wetland Porosity	0.1 – 0.75	0.1 – 0.75	0.1 – 0.75	0.1 – 0.75	0.1 – 0.75	0.1 – 0.75	0.1 – 0.75	0.1 – 0.75	
Wetland Lateral Conductivity	0.1 – 0.9	0.1 – 0.9	0.1 – 0.9	0.1 – 0.9	0.1 – 0.9	0.1 – 0.9	0.1 – 0.9	0.1 – 0.9	
	Land Class Parameters								
	Conif. Forest	Mixed Forest	Treed Rock	Shrub	Bogs	Non-Conn. Wetland	Conn. Wetland	Water	Imper -vious
Infiltration Coefficient	0.04 – 50	0.04 – 50	0.04 – 50	0.04 – 50	0.04 – 200	0.04 – 200	N/A	N/A	
Upper Zone Retention (mm)	1 – 200	1 – 200	1 – 200	1 – 200	1 – 200	1 – 200	N/A	N/A	
Interflow Coefficient	0.05 – 10	0.05 – 10	0.05 – 10	0.05 – 10	0.05 – 10	0.05 – 10	N/A	N/A	
Recharge Coefficient	0.001 – 0.2	0.001 – 0.2	0.001 – 0.2	0.001 – 0.2	0.001 – 0.2	0.001 – 0.2	N/A	N/A	
Melt Rate (mm/°C/hr)	0.05 – 0.5	0.05 – 0.5	0.05 – 0.5	0.05 – 0.5	0.05 – 0.5	0.05 – 0.5	0.05 – 0.5	0.05 – 0.5	

The DDS search involved five independent trials each with 2,500 model evaluations. This was based on the computational resources available and the model runtime (~20 minutes) over all calibration years (discontinuous between 1981-2014). The number of model evaluations falls

in between those reported in previous local optimizations of distributed models: 1,000 evaluations for 51 decision variables (Haghnegahdar et al., 2014), and 1,000 – 10,000 evaluations suggested for 30 decision variables (Tolson & Shoemaker, 2007). The scale of the search was considered robust enough to find an acceptable local optimum given that limited hydrological processes and a limited period (freshet) were of concern for this high flow calibration.

The hybrid objective function described in Section 4.2.1.2 was used to calibrate WATFLOOD, with the objective function at each gauge weighted and aggregated into a single performance metric to guide the DDS optimization. Weights by mean local inflow were used (Table 9). Note that only eight gauges were aggregated in the LNRB model optimization (the Gunisao gauge was part of the separate Gunisao River model calibrated afterwards).

Xue et al. (2014) verified that calibration at only downstream gauges may aggregate errors and have poor results at interior gauges, whereas multi-site calibration (such as the approach in this research) generally leads to improved simulation. That study, however, advocated for a "stepwise" approach similar to what was done in HEC-HMS (calibration at upstream gauges first then downstream gauges). The methodology used here instead compares closer to the "pooled" calibration method (all gauges at once, a single optimized parameter set) tested by Wi, Yang, Steinschneider, Khalil, & Brown (2015). This study found that the "pooled" method required less computational time than a "stepwise" method, displayed similar skill in calibration, and improved skill in validation. The "pooled" approach may trade-off error between calibration points, but Wi et al. (2015, p. 866) conclude that "small sacrifices of model performance at certain sites can improve and stabilize basin-wide performance".

4.2.3.3. Refinement of Optimized Solution

From among the five best parameter sets output by DDS (one from each independent trial), one solution was chosen to move forward for manual refinement. The best solution was selected based on visual inspection of calibration statistics and hydrographs at all gauges, as well as the gauge-weighted performance metric, and overall performance of peak flow simulation.

This best parameter set (i.e. local solution) was then manually refined to improve peak flow performance. Land class parameters (those dealing with subsurface behaviour) were primarily left at their optimized values. Manual adjustments were based on visual inspection and engineering judgment that could not be replicated in an automated calibration, including:

- Base snowmelt temperatures (previously fixed) were adjusted towards slightly warmer temperatures (i.e. later melt) to improve overall freshet timing at the majority of gauges.
- River class parameters (channel roughness, wetland characteristics) were adjusted at the sub-basin scale to reduce underestimation and improve timing of peak flows.
- Several lake storage-discharge curves were adjusted further to (a) adjust timing and peak flow performance for the local areas upstream of Thompson and Kelsey G.S., and (b) to fix instability in the initialization of subsequent PMF simulations.

The manual adjustments resulted in a local solution that improved performance in the calibration period compared to the solution from DDS alone. This refined parameter set was then transferred over to the Gunisao River model; performance over its calibration period was acceptable enough that only manual adjustments were required to refine the model.

A direct comparison of the WATFLOOD and HEC-HMS parameter sets (for verification) is difficult given that (a) the models share very few parameters, and (b) many parameters in WATFLOOD are discretized by land class rather than sub-basin. The most comparable

parameters are those related to snowmelt; in comparing those, the melt rates in WATFLOOD (ranging from 1.3-6.5 mm/°C/day) are similar to those from HEC-HMS (stepping from 0.8 – 4.0 mm/°C/day) when considering the proportions of land classes. The base snowmelt temperatures are significantly different (-4°C in HEC-HMS, -1.5°C to 0.2°C in WATFLOOD) although this can be attributed to more rapid intra-basin routing and reduced snowpack due to sublimation in WATFLOOD. Channel roughness in WATFLOOD is also generally positively correlated with time of concentration in WATFLOOD; however, no direct comparison is possible.

A final note is warranted on the use of manual calibration here. Post-optimization adjustments in WATFLOOD and HEC-HMS illustrate the importance of manual calibration for PMF simulations. Peak flow estimation is most important in PMF calibration and, because a local optimization may trade-off skill between peaking and receding flows, visual inspection is vital to ensure acceptable performance. For example, Harlin & Kung (1992) found that manually calibrated solutions tended to produce higher PMF peak flows. Manual adjustments can admittedly trade-off performance between competing metrics and result in worse a hybrid metric. Changes are, however, warranted to improve peak flow performance; this trade-off is not uncommon in literature (e.g. Efstratiadis et al., 2008). The importance of manually refining solutions is also recognized in literature on design flood studies (England et al., 2007; Harlin & Kung, 1992) and PMF guidance documents (Alberta Transportation, 2004).

4.2.4. VALIDATION

The calibrations in HEC-HMS and WATFLOOD were tested on a separate set of high flow years to validate that the local solution performed capably on an independent period. Recall that high flow validation years were selected throughout the period of record at each gauge and included years used to calibrate the existing SSARR model. For the majority of gauges, this

amounted to five validation years (Table 12). The Gunisao River did not display enough sufficiently high flow years, and only three years were deemed applicable for validation.

Table 12: High flow validation years simulated in all three hydrological models

Sub-Basin	Validation Years	Peak Flow (m^3/s)	Peak Flow Date
Grass River	1974	135	July 13
	1979	173	July 17
	1984	148	June 30
	2001	123	July 8
	2014	151	July 22
Gunisao River	1974	84	May 25
	1979	98	May 24
	1983	111	May 25
Kettle River	1974	64	May 13
	1979	59	June 8
	1982	104	May 9
	1988	102	May 15
	2014	77	May 19
Limestone River	1979	113	June 5
	1984	236	May 19
	1986	273	May 15
	1989	324	May 14
	1992	178	May 26
Odei River	1979	134	June 5
	1984	167	April 25
	1988	269	May 11
	2002	215	May 26
	2007	229	May 11
Upper Burntwood River	1979	128	June 2
	1982	188	May 4
	1983	118	May 22
	1991	121	May 14
	1992	176	June 9
Downstream Gauge Locations			
Gauge Location	Calibration Years	Peak Inflow (m^3/s) Absolute (Local)	Peak Flow Date Absolute (Local)
Burntwood River at Thompson	1979	924 (270)	June 5 (June 5)
	1984	1320 (496)	April 29 (April 30)
	1988	1130 (468)	May 11 (May 11)
	1991	1020 (370)	Aug 30 (May 18)
	2009	1100 (392)	May 2 (May 2)

Nelson River at Kelsey G.S. (Outflows)	1979	4409 (1099)	July 18 (Aug 20)
	1987	2492 (651)	April 27 (April 24)
	1994	2398 (687)	May 2 (May 14)
	2002	2615 (650)	Aug 9 (June 20)
	2008	4164 (714)	Aug 25 (April 30)
Nelson River at Kettle G.S. (Outflows)	1979	5785	July 18
	1983	4080	April 15
	1985	4166	May 10
	1991	3735	May 22
	2001	5168	June 24

Note that simulations in SSARR for some of these cases are in fact years that the model was calibrated to. For SSARR then, this does not represent validation, but a comparison to HEC-HMS and WATFLOOD over these periods (as validation of the other models). This will inherently improve the overall performance of SSARR in this period.

4.2.5. SSARR MODEL VALIDATION

The SSARR PMF model was used in its existing form for this study (acting as a baseline model). Some details are available as to the calibration of the model, such as simulated and observed hydrographs for the primary calibration year (1979) and that the model was calibrated manually. Some general techniques for calibration in SSARR are provided by Debs et al. (1999).

As part of this study, the SSARR PMF model was run for all historical years used to calibrate and validate HEC-HMS and WATFLOOD. Given that the model calibration periods differ, this "validation" is an important tool to compare models and to determine what effect, if any, their different calibration periods might have. Any consistent differences can then be related to differences observed in PMF results between the three models.

Therefore, all results of historical simulations shown for HEC-HMS and WATFLOOD (calibration or validation) will also include results from SSARR. The results from SSARR are

designated as “validation” and are expected to have poorer performance, particularly when compared on years that HEC-HMS and WATFLOOD were optimized on. The results from calibration/validation of all three models are shown in Section 5.1.

4.3. Assessment of Parameter Uncertainty

Uncertainty in the calibrations of HEC-HMS and WATFLOOD was explored by assessing a number of additional solutions in each model, testing whether they are behavioural, and applying them in PMF simulations. A consideration of uncertainty was important given both calibrations produced local optima. The goal of the parameter uncertainty assessment was to quantify a range about the baseline PMF in HEC-HMS and WATFLOOD, and to compare the range between models. A sensitivity analysis in SSARR was deemed sufficient to consider uncertainty surrounding the historical parameterization of that model.

The uncertainty assessment sampled a greater number of decision variables than were included during calibration- a result of insight gained after the calibration process. In particular, additional parameters related to snowmelt were included. In the case of WATFLOOD, base snowmelt temperature in all eight land classes was added; although the parameter was easily estimated and fixed pre-calibration, it warranted consideration. In HEC-HMS, the base snowmelt temperature (one variable) and the stepped snow melt rate (six steps) were added. The additions amounted to 64 variables in WATFLOOD and 91 variables in HEC-HMS. The larger number of decision variables in HEC-HMS resulted from the calibration of the model in parts (each gauged sub-basin separately).

Figure 12 below illustrates the process followed to produce a range of plausible scenarios about the baseline PMF, and to also study parameter sensitivity in HEC-HMS and WATFLOOD.

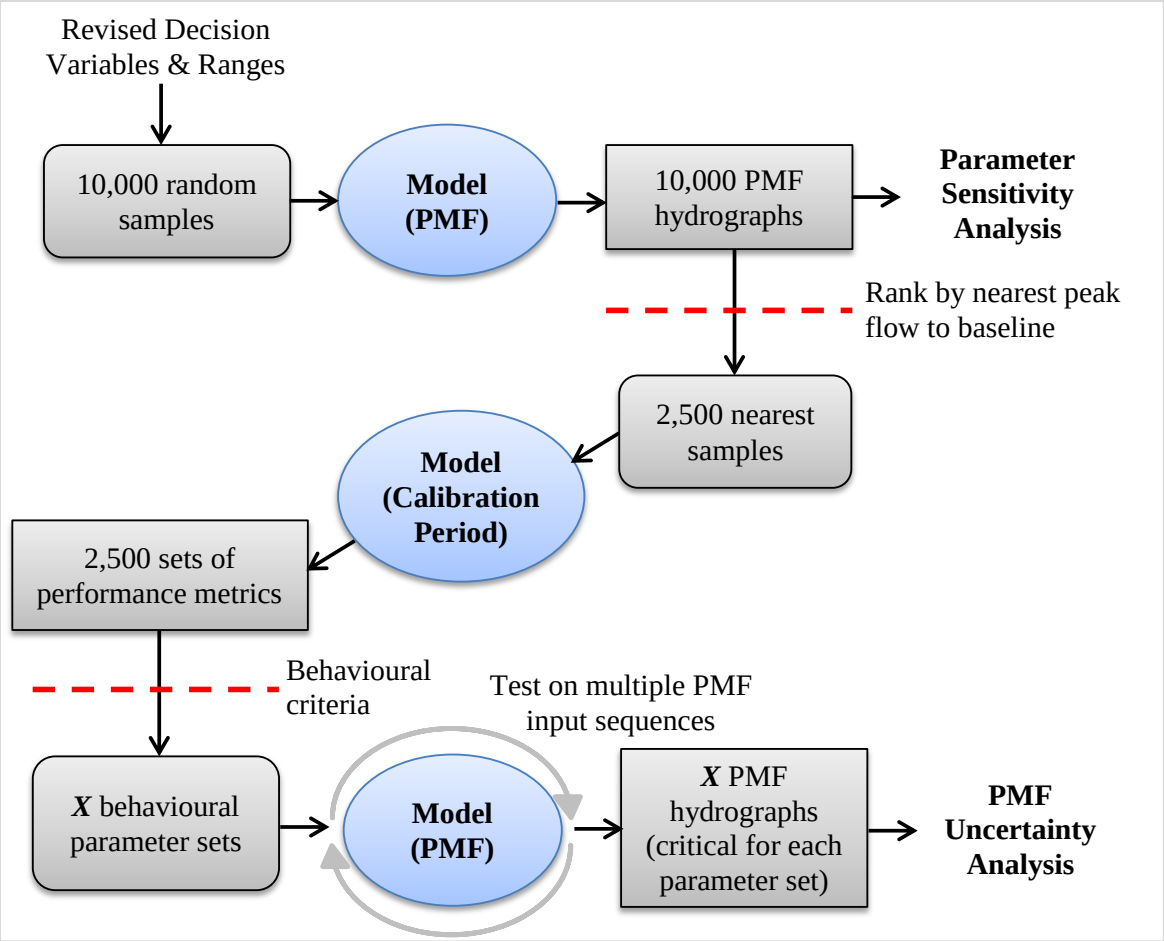

Figure 12: Methodology for PMF uncertainty analysis and parameter sensitivity analysis in HEC-HMS and WATFLOOD

As shown in Figure 12, 10,000 parameter sets in HEC-HMS and in WATFLOOD were sampled by a uniform random distribution. The number of samples was chosen based on (a) the scripts developed for calibration, (b) computational time, and (c) the PMF uncertainty analysis from Bingeman (2001) who cited a general guideline from Crosetto, Tarantola, & Saltelli (2000) of 100 Monte Carlo simulation per variable to produce usable 95% confidence intervals. The choice of random sampling as opposed to Latin Hypercube sampling is recognized as a limitation of the study. Latin Hypercube sampling is understood to be an efficient method to represent the entire parameter space (van Griensven et al., 2006) and produce a more stable estimate (Helton

& Davis, 2003). There is no guarantee that the random sampling adequately sampled the decision space. However, correlation between some model decision variables for high flow simulation (e.g. lower storage times for surface runoff and baseflow runoff) may have posed issues with using Latin Hypercube samples.

The difference in runtimes between the PMF simulation (one minute) and the calibration period (fifteen minutes) prohibited all 10,000 candidate sets from being tested over the historical period. Instead, a modified method was applied whereby each sample was run for the PMF simulation (forced only by the most critical sequence of baseline PMF inputs). PMF results were compared to the baseline PMF and ranked based on the absolute difference of peak flow. The nearest 2,500 parameter sets were then tested in the historical calibration period; behavioural samples (of the 2,500) were used to create a range about the baseline PMF.

The 2,500 samples tested in the calibration period were classified as behavioural based on multiple criteria (Table 13). Behavioural criteria were selected such that, in a calibration setting, those samples could be considered for manual adjustment to improve peak flow performance. This particular threshold was not used during calibration, since time constraints at that time allowed for only the very best solutions to be carried forward. This threshold accepted 20-40% of candidate solutions.

Table 13: Behavioural threshold for candidate solutions in uncertainty assessment

	Metric	Behavioural Threshold	Reasoning
1	Volume Bias	≤ 0.25	Based on recommendations from (Moriasi et al., 2007)
2	Normalized RMSE (RSR)	≤ 0.7	
3	Nash-Sutcliffe Efficiency	≥ 0.5	
4	Absolute Average Peak Flow Deviation	≤ 0.1	Adequate peak flow simulation is most important in PMF calibration.

The parameter uncertainty exploration involved several assumptions and limitations. First, a sample that produced a PMF closer to the baseline was assumed to be more likely to perform adequately in the calibration period (i.e. behavioural). In this way, fewer simulations were conducted of the historical period, while a number of behavioural samples were still obtained. The limitation of testing only the nearest 25% of candidate solutions also limited the uncertainty range; samples that produced very different PMFs were not considered for the final uncertainty bounds, though some may have been behavioural. Finally, as explained throughout Section 4.2, manual refinement was important for adequate peak flow simulation. The candidate solutions tested here were not subject to manual adjustments; therefore they were skewed towards lower PMFs. These limitations were recognized and accepted, as described further with the results in Section 5.5.

A similar uncertainty analysis was not conducted on the SSARR PMF model because it was not calibrated as part of this research and did not have the necessary infrastructure (i.e. estimated parameter ranges, automation scripts) required for an intensive analysis. However, the effect of parameter uncertainty is equally important in SSARR. Therefore, a sensitivity analysis was conducted of the SSARR parameters to assess those contributing the most uncertainty to the PMF simulations. Full results of the uncertainty assessment are provided in Section 5.5.

4.4. PMF INPUTS AND INITIALIZATION

Extreme meteorological and hydrologic inputs are required in order to force the calibrated models to produce PMF conditions. Recall that the most recent Canadian Dam Association guidelines (CDA, 2013) recommend testing two spring PMF scenarios: (1) PMP + 1/100 year snowpack; (2) 1/100 year rainfall + Probable Maximum Snow Accumulation

(PMSA). Additional inputs are common to both scenarios, including a critical temperature sequence, specified upstream contributions, and antecedent conditions. The timing of events also impacts PMF. Timing was varied in this study to test for the most critical PMF scenario.

Baseline PMF inputs were previously derived by Manitoba Hydro or others as part of PMF reviews; these forcing conditions are used here in their existing form. A discussion on the methodology and values for these PMF inputs is available in Appendix B. That discussion also provides justification for the continued use of these historically-derived inputs (and perturbing them for future period simulations).

Combining various input timings is important for PMF simulations. Multiple meteorological sequences are tested to determine the most critical PMF, where a meteorological sequence represents a set of PMF inputs and timings. Meteorological sequences differ based on (a) the onset date of rapid temperature increases to encourage snowmelt, and (b) the date of occurrence of the PMP (5, 10, or 15 days after temperature increase). This methodology is derived from previous Manitoba Hydro PMF studies (Acres Manitoba Ltd., 2006; Hatch Ltd., 2013b), but with a denser framework (adding PMP 10 days after) and with earlier melt sequences (to account for potential earlier snowmelt in a future period). The result is twenty-three different meteorological sequences to test in each baseline and future period, listed in Table 14.

Sequences with temperature increases beginning earlier than April 10th are not considered because (a) the SSARR model run begins on April 10th and changing the start date would require prohibitive changes to the model, and (b) pre-project testing and previous PMF results in the SSARR model found that earlier temperature increases produced lower PMFs. This is likely due to the severe decrease in PMP magnitude that results from seasonality reductions. Similarly, sequences later than June 20th are not considered as snowmelt is completed by this time, and the

scope of this study is only for spring PMF. This set of sequences allows for a dense framework in order to determine the most critical spring PMF in a given baseline or future scenario.

Table 14: Combinations of PMF input timing (meteorological sequences)

Sequence Number	Onset of Rapid Temperature Increase	PMP Date		Sequence Number	Onset of Rapid Temperature Increase	PMP Date
1	April 10	April 15		**13**	April 10	April 15
2	April 10	April 20		**14**	April 10	April 20
3	April 10	April 25		**15**	April 10	April 25
4	April 20	April 25		**16**	April 20	April 25
5	April 20	April 30		**17**	April 20	April 30
6	April 20	May 5		**18**	April 20	May 5
7	April 30	May 5		**19**	April 30	May 5
8	April 30	May 10		**20**	April 30	May 10
9	April 30	May 15		**21**	April 30	May 15
10	May 10	May 15		**22**	May 10	May 15
11	May 10	May 20		**23**	May 10	May 20
12	May 10	May 25				

4.5. INCORPORATING CLIMATE CHANGE

Two ensembles of RCMs (where each RCM is forced at its boundaries by a GCM) were used for climate change projections of PMF inputs: fourth generation Canadian Regional Climate Model (CRCM) simulations, and the North American Regional Climate Change Assessment Program (NARCCAP). These two ensembles, from which a total of fourteen climate model simulations are used for this study, were previously applied as part of the NRCan PMP/PMF study (Clavet-Gaumont et al., 2017). The fourteen RCM-GCM pairs were quality-checked as part of that study, and results from the NRCan PMP/PMF study were based on these simulations only; therefore they were considered the most consistent and appropriate climate model simulations to use in this research.

The Canadian Regional Climate Model (CRCM; currently version 4.2.3 – CRCM4) was developed at the Université du Québec à Montréal with a polar stereographic projection and a 45km grid size (De Elía & Côté, 2010; Music & Caya, 2007). The model includes the Canadian Land Surface Scheme (CLASS), an up-to-date set of processes intended to represent exchanges between known land cover and the atmosphere (Music & Caya, 2007). Most CRCM runs use lateral forcing from the third version of the Canadian Coupled Global Climate Model (CGCM3) (De Elía & Côté, 2010); however, additional runs in this research are driven by the ECHAM5 global climate model (Roeckner et al., 2003). CRCM4 and the newest version of CLASS have been found to balance annual mean runoff internally, and to have reduced annual mean bias in precipitation and better spatial representation of precipitation compared to previous versions (Music & Caya, 2007), and therefore it is useful as a climate model input in this research.

The North American Regional Climate Change Assessment Program (NARCCAP) was developed to provide regional climate change projections for North America and to study uncertainty associated with using different GCMs as boundary conditions and different RCMs for downscaling (Mearns et al., 2012). Four GCMs and six RCMs were selected, where the RCMs have similar resolutions of approximately 50km but provide a variety of physically-based representations of atmospheric processes (Wehner, 2013). To reduce the number of runs by half, each GCM is used as forcing for only three RCMs (Mearns et al., 2012). Skill assessments of the 1980-2004 period show that the RCMs generally represent seasonal temperatures well but less so for seasonal precipitation, and that all six of the NARCCAP RCMs provide useful information and an appropriate spread of uncertainty (Mearns et al., 2012). NARCCAP climate model outputs are publicly available and the dataset is available from Mearns et al. (2007, updated 2014).

In summary then, a total of fourteen climate model simulations are used in this study: eight runs from CRCM4 (five driven by CGCM3, three driven by ECHAM5) and six runs from the NARCCAP project. These fourteen simulations are listed in Table 15. All climate models used in this research are forced by the A2 emissions scenario - the most pessimistic outlook of the Special Report on Emissions Scenarios that projects increasing greenhouse gas emissions to 2100 (Nakicenovic & Swart, 2000). The climate model simulations were only available with this forcing; this prevented the consideration of uncertainty related to selection of an emissions scenario (though the studies noted in Section 2.6 found this form of uncertainty to contribute relatively less than other forms).

Table 15: RCM simulations used for projected climate change impacts

	RCM	Driving GCM	Short Name/ Designation	Grid Points in LNRB
CRCM ENSEMBLE	CRCM4	CGCM3 (member #1)	aey-afb	46
	CRCM4	CGCM3 (member #2)	aez-aec	46
	CRCM4	CGCM3 (member #3)	afa-afd	46
	CRCM4	CGCM3 (member #4)	aet-aet	46
	CRCM4	CGCM3 (member #5)	aev-aev	46
	CRCM4	ECHAM5 (member #1)	agx-agx	46
	CRCM4	ECHAM5 (member #2)	ahi-ahi	46
	CRCM4	ECHAM5 (member #3)	ahj-ahj	46
NARCCAP ENSEMBLE	CRCM4	CCSM3	crcm-ccsm	36
	ECP2	GFDL_CM2.5	ecp2-gfdl	36
	MM5I	CCSM3	mm5i-ccsm	34
	MM5I	HadCM3	mm5i-hadcm3	34
	RCM3	CGCM3	rcm3-cgcm3	38
	RCM3	GFDL_CM2.5	rcm3-gfdl	38

It is important to note here that each RCM, driven by a set of initial conditions, boundary conditions (GCM), emissions scenario, and its own unique structure, represents one physically-based, plausible future climate scenario (Whitfield, 2012). All scenarios are equally likely, and the spread between climate model simulations represents a "potential range of future climate change" (Whitfield, 2012, p. 18).

RCM data were pre-processed and quality-checked prior to use in this research. All RCMs were normalized to remove leap days. In the special case of mm5i-hadcm3, which used a 30 days/month and 360 days/year period, no changes were necessary since both the baseline and future periods of this model used 360 day calendars (i.e. they are compared relative to each other). Two simulations included only 29 years in a period and not 30 (crcm-ccsm in the baseline period, mm5i-ccsm in the baseline and future period). In these cases, any frequency analysis was conducted with only 29 annual values.

4.5.1. PMF Inputs Considered

Climate change impacts were considered on most of the inputs required for spring PMF simulations, namely:

- PMP, and 1/100 year rainfall;
- 1/100 Year SWE, and PMSA;
- Daily temperature sequence to facilitate rapid melt;
- 1/100 year Lake Winnipeg outflows.

The methodologies to derive projected climate change impacts on each input were developed in whole or in part from Ouranos and INRS-ETE as part of the NRCan PMP/PMF study, as detailed by Clavet-Gaumont et al. (2017). In most cases, the climate model projections for the LNRB are used in their original form. An explanation of the methodologies is warranted to provide context

for the results presented here; therefore, those details have been provided in Appendix C. Contributions from Ouranos and projections developed in this research are clearly delineated.

4.5.2. EXCLUSIONS

Several elements of the PMF simulations are not included in the climate change analysis, for varying reasons. First, projected impacts on antecedent conditions (i.e. reservoir levels, soil moisture conditions) are not considered. These conditions are neglected for two reasons: (1) a lack of applicable climate model data to produce such change factors; and (2) typical conservative PMF assumptions of saturated soil moisture conditions and high reservoir levels are assumed not to change in a future period. It is recognized that climate change may have an impact on both soil moisture and reservoir levels, and that initial reservoir levels (Fowler, Hill, Jordan et al., 2010) and soil moisture conditions (Beauchamp et al., 2013) have been found to significantly impact PMF.

Using initial reservoir levels as an example, potential climate change impacts have been incorporated primarily in literature where work was already done to consider how reservoir regulation may change in a future period (e.g. Veijalainen & Vehviläinen, 2008). Without this information, these exclusions are appropriate here.

In addition, climate change impacts on antecedent daily average precipitation are not considered. This decision is based on pre-project sensitivity testing using the SSARR model: a 5% increase in antecedent precipitation had negligible impact on the resulting PMF. Antecedent precipitation would be expected to have an even lesser effect in HEC-HMS and WATFLOOD (based on the earlier critical PMF timing in those two models), and in the future period (due to earlier snowmelt and earlier critical PMF). Thus, it is assumed that sensitivity to antecedent precipitation would not be significant enough to warrant an analysis of climate change effects.

Finally, the hydrological model parameters are assumed to be invariant with climate change. Cunderlik & Simonovic (2005) recognized this limitation of the impact approach but accepted it based on the assumption that the impact of climate change will be much larger on the climate inputs to the model than on the processes governed by the model parameters. This assumption is also inherently made in a number of the studies described in Section 2.5.

Climate change results for PMF conditions/inputs included in the analysis are provided in Section 5.3; the projections are used as forcing for projected future PMF results in Section 5.4.

5.0. RESULTS & DISCUSSION

Three hydrological models were trained on historical high flow years and used to simulate high spring flows in the LNRB. Calibrated models were extrapolated to PMF conditions using historical baseline PMF inputs (i.e., "present climate"). PMF under future climate conditions was estimated using projected climate change impacts on PMF inputs. Finally, an assessment of parameter uncertainty was conducted in HEC-HMS and WATFLOOD (parameter sensitivity in SSARR) in order to provide context to the range of PMFs observed in the preceding sections.

5.1. PMF MODEL CALIBRATION

The PMF models that were developed in HEC-HMS and WATFLOOD were calibrated to historical high flow years in the period of record, and then validated to an additional, independent set of high flow years.

5.1.1. CALIBRATION

Calibration of the HEC-HMS and WATFLOOD PMF models was conducted using a combination of automated and manual methods. The calibration period considered six tributary gauges and three downstream gauges in the basin: each with five extreme high flow years. After calibration and adjustments, both models adequately represented average high flow behaviour throughout the LNRB. The SSARR model, with its existing parameterization from the 1980s, was also validated in these same years to (a) test the transferability of the SSARR calibration to independent higher flow years, and (b) have an additional method of comparing HEC-HMS and WATFLOOD to the "baseline" PMF model in SSARR.

All high flow calibration results compare the observed spring-summer hydrograph (April to August) to calibrated hydrographs from HEC-HMS and WATFLOOD, and to the validation hydrograph from SSARR. It is expected that hydrographs from SSARR should generally perform more poorly compared to the other two models given they were not calibrated to the same high flows.

Appendix D contains comparative hydrographs for every high flow calibration year at each of the nine hydrometric gauges. For the sake of brevity, results here are aggregated into average annual hydrographs at each calibration point (average of five calibration years). Although these graphics do not capture the varying high flow behaviour in different years, they qualitatively show the performance of each model in terms of average peak flow magnitude, timing, and overall flood volume.

Figure 13 shows the average annual hydrographs at each of the six tributary gauges, and Figure 14 shows the average annual hydrographs for the three downstream gauges. Note that Figure 14 also isolates the estimated local inflows to better visualize the simulation of ungauged areas.

From Figure 13, it is generally clear that the existing parameterization in SSARR does not translate well to the additional, more recent high flow years. SSARR overestimates peak flows, freshet volume, and overall spring-summer runoff volume in this wider range of high flow years. This overestimation is especially severe in the Grass River basin and calls into question the calibrated parameters for the basin given the lack of transferability to other years. The rising limb of the freshet in SSARR is also consistently late, suggesting snowmelt processes occur too late in the model. Delayed snowmelt would not only cause freshet timing issues, but would also

produce higher soil moisture conditions persisting later into the summer period (i.e. it would contribute to the greater runoff yield observed in SSARR).

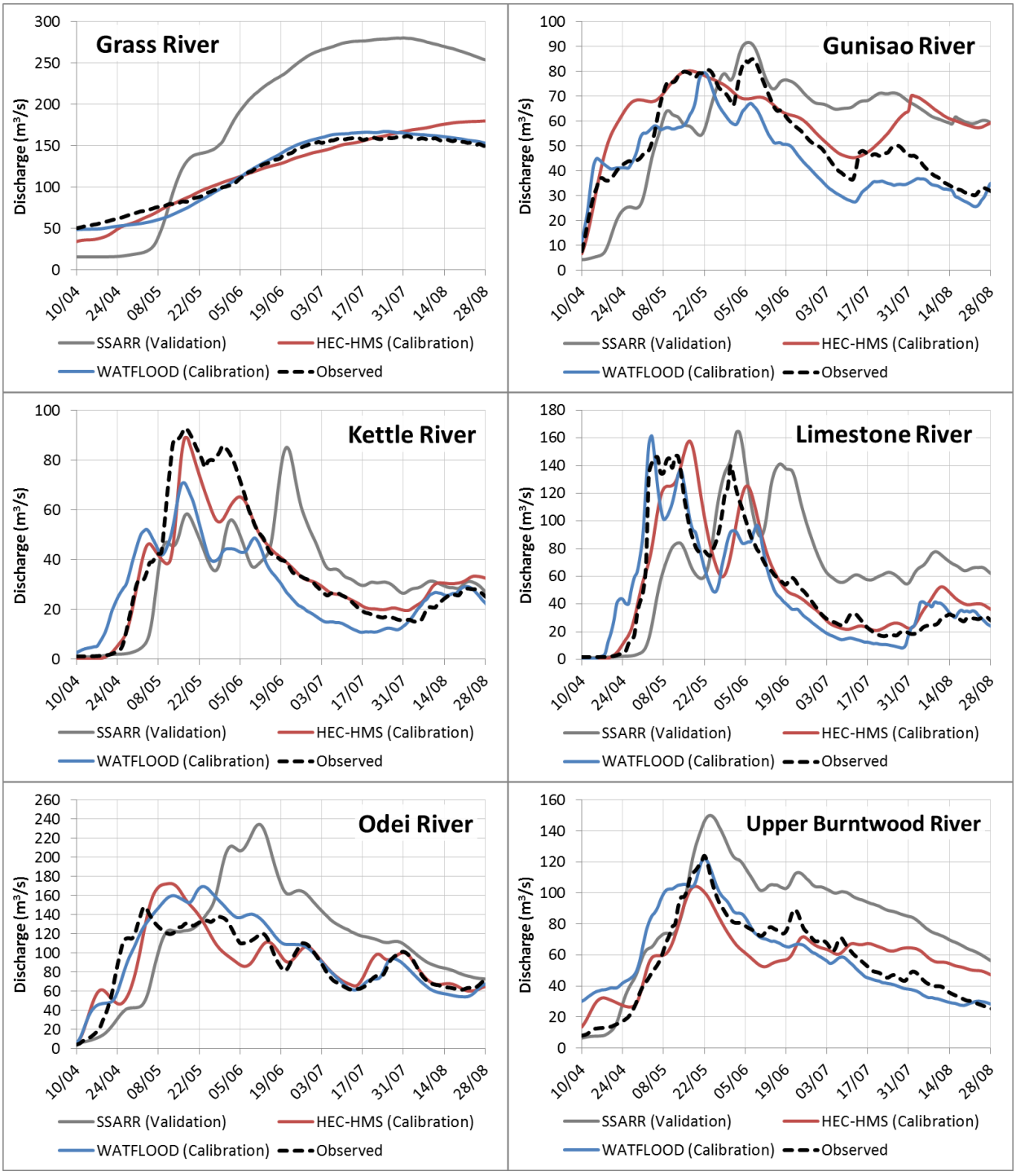

Figure 13: Average annual hydrographs over the calibration period at six tributary gauges in the LNRB

The consistent difference in snowmelt timing between observations and SSARR warranted further analysis. Namely, hydrographs are provided in Appendix F of simulations from the three models for the primary SSARR calibration year (1979). There is clearly a different snowmelt regime in 1979 that SSARR is fitted to, and which HEC-HMS and WATFLOOD are unable to replicate with their current calibrations. A closer examination found that 1979 involved an abnormally gradual snowmelt, resulting from alternating warm and cold spells in April and May. The SSARR model was calibrated to this gradual process using a longer ripening period in its parameterization; because the SSARR calibration was limited to this single year, the model similarly delays snowmelt in other years that do not have such prolonged snowmelt. In contrast, HEC-HMS and WATFLOOD are calibrated to a range of years that consistently exhibit earlier snowmelt - their melt parameterizations reflecting this.

The abnormal snowmelt behaviour in 1979 raises questions as to the use of this year to calibrate the SSARR model and the selection of calibration years for HEC-HMS and WATFLOOD in this research. Delayed snowmelt was recognized during SSARR PMF model development to be a more critical PMF scenario, as it allows for a larger rainfall later in the spring (Crippen Acres Wardrop, 1990); however, 1979 was not selected based on this criterion. Rather, the 1990 project report by Crippen Acres Wardrop (p. 102) states that calibration years were chosen where "runoff volumes were high, resulting from above average snowmelt and spring rainfall events – conditions corresponding to eventual PMF simulation". This is the same methodology used to select recent years for HEC-HMS and WATFLOOD calibration (as described in Section 4.1.2).

HEC-HMS and WATFLOOD perform similarly in the calibration period at all six gauged sub-basins, with some noticeable discrepancies. First, the dedicated wetland model in

WATFLOOD is better able to capture wetland processes, leading to improved simulation in sub-basins with greater wetland area (e.g. the Grass and Gunisao Rivers). HEC-HMS has difficulty capturing the dynamic surface storage response of wetlands, and compensates with higher overall runoff volume to adequately simulate peak flows in those basins. The distributed setup of WATFLOOD also allows improved performance in areas with highly variable physiography, such as the Upper Burntwood, Grass, and Gunisao sub-basins, which have alternating rock outcrop, wetland, and coniferous forest areas. Finally, although only visible in the yearly hydrographs provided in Appendix D, a distributed precipitation forcing also allows WATFLOOD to better simulate some rainfall-induced summer peaks.

The HEC-HMS parameterization is capable of simulating high flow years in northern basins (Kettle and Limestone river basins, Figure 13). These areas are dominated by coniferous forest and shrubland, and are underlain with less clay material than the rest of the basin. This suggests that the semi-lumped calibration of HEC-HMS (where gauged basins have unique parameter sets) allowed for closer representation of the dominant processes in these northern basins. In contrast, these two sub-basins had the smallest weights in the distributed WATFLOOD calibration (as a result of their lower mean flows in the historical period) and were less influential in guiding the DDS calibration.

In general, both HEC-HMS and WATFLOOD achieve similar performance and are visually and statistically (Moriasi et al., 2007) adequate in their simulation of peak flows, runoff volume, and runoff timing of the highest flow years on each gauged tributary.
Results at the three downstream calibration points (Figure 14) show similar performance to that shown at the six tributary gauges. Overestimation of total runoff volume is clear in SSARR, with

a late freshet peak at both Kelsey G.S. and Kettle G.S. This increased runoff yield would be expected to have an impact on subsequent PMF simulations as well.

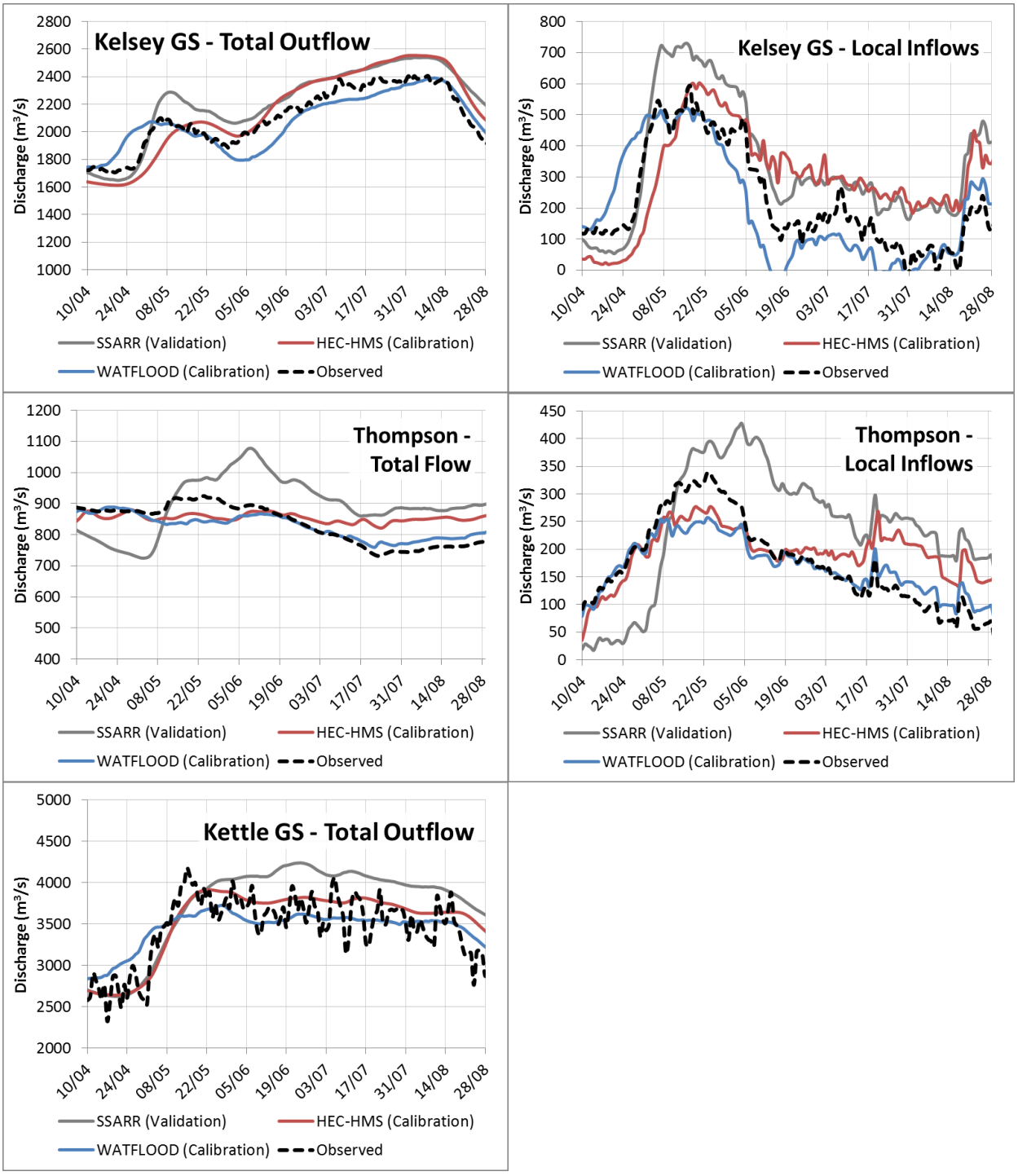

Figure 14: Average annual hydrographs over calibration period at three downstream gauges in the LNRB

HEC-HMS and WATFLOOD both underestimate peak flows on the Burntwood River at Thompson. Several freshet peaks (2006-2008) measured by the hydrometric gauge at Thompson have been previously identified by Manitoba Hydro to be potentially overstated, particularly as compared to prorated gauged local inflows; the suspected cause being an early switch from the ice-covered to open water rating curve (P. Slota, personal communication, May 10, 2016). Given that overestimates have been identified in some years by end users (i.e. Manitoba Hydro), it is possible that additional freshet peaks in the record may be similarly overstated.

Otherwise, HEC-HMS produces slightly higher peak flows than WATFLOOD at the downstream gauges, though primarily the result of overestimating total runoff volume (i.e. overestimation in the summer recession period). These higher peaks in the historical period were found to not necessarily translate into a higher PMF (discussed further in Section 5.2). In general, as on the gauged tributaries, both HEC-HMS and WATFLOOD capably simulate peak flows and total runoff.

Average metrics over the calibration period at all nine calibration points are provided in Table 16 to quantify the performance of all three models. A weighted value is also provided to summarize each metric, based on the weighting of calibration points described in Section 4.2.1.2. Note again that statistics from SSARR represent those from a validation with no parameter adjustments and that statistics for the Kelsey G.S. and Thompson gauges were calculated based on total streamflow. Estimated local inflows were found to be a useful visual tool for selecting high flow years and during manual calibration, but were too volatile to calculate metrics.

Table 16: PMF model performance metrics averaged over the calibration period

Calibration Point	Upper Burntwood River	Odei River	Grass River	Kettle River	Limestone River	Gunisao River	Burntwood R. @ Thompson	Kelsey G.S. Outflow	Kettle G.S. Outflow	Weighted Average
SSARR (Validation)										
$\frac{RMSE}{\sigma_{obs}}$	1.12	1.09	2.03	1.06	1.28	0.88	1.01	0.22	0.49	0.91
D_v (%)	47.6	25.4	54.6	-5.8	35.7	12.9	7.8	5.7	8.3	20.0
APB (%)	60.7	63.6	71.9	70.6	105.9	46.1	15.6	8.1	14.2	39.3
NSE	-0.26	-0.18	-3.11	-0.13	-0.65	0.23	-0.02	0.95	0.76	-0.19
Peak Q Diff (%)	8.4	-3.1	66.7	13.6	-4.7	2.7	17.2	7.7	-2.7	15.3
Hybrid	0.618	0.548	1.654	0.553	0.769	0.378	0.452	0.082	0.152	0.537
HEC-HMS (Calibration)										
$\frac{RMSE}{\sigma_{obs}}$	0.74	0.62	0.67	0.44	0.64	0.75	0.54	0.20	0.38	0.48
D_v (%)	5.1	1.2	1.4	-3.2	4.7	15.6	2.5	3.0	2.6	3.2
APB (%)	35.4	28.7	19.8	31.6	43.5	38.0	7.9	6.6	10.1	18.5
NSE	0.45	0.62	0.55	0.80	0.59	0.44	0.70	0.96	0.85	0.72
Peak Q Diff (%)	-10.6	3.6	8.0	5.2	7.8	-14.4	-4.1	0.4	-4.0	-0.1
Hybrid	0.311	0.216	0.241	0.164	0.265	0.346	0.159	0.049	0.118	0.169
WATFLOOD (Calibration)										
$\frac{RMSE}{\sigma_{obs}}$	0.72	0.60	0.49	0.64	0.65	0.66	0.43	0.20	0.42	0.44
D_v (%)	4.9	6.7	0.0	-19.5	-6.8	-14.7	-0.7	-1.0	0.2	-1.5
APB (%)	33.1	31.7	12.9	47.7	49.5	30.8	5.6	6.2	11.3	17.8
NSE	0.49	0.64	0.75	0.59	0.58	0.57	0.82	0.96	0.82	0.77
Peak Q Diff (%)	-15.6	2.3	3.1	-1.7	5.6	-5.6	-7.6	-0.1	-11.0	-2.2
Hybrid	0.311	0.215	0.141	0.272	0.274	0.261	0.124	0.040	0.143	0.148

The calibration metrics quantify the performance observed in the average annual hydrographs. Both HEC-HMS and WATFLOOD meet thresholds of acceptable performance (Moriasi et al., 2007) at all nine calibration gauges, with WATFLOOD displaying slightly better performance of both overall timing and volume of high flow simulations. Not surprisingly, the statistics also reinforce the poor performance of the SSARR model when validated against a wider period of higher flow years. The overestimation of volume and runoff is particularly clear, especially overestimated runoff volume in the Grass River basin.

Comparing HEC-HMS and WATFLOOD, error trade-off between gauges during the distributed calibration makes WATFLOOD less capable of simulating peak flows as closely as HEC-HMS (Table 16). This was particularly true during manual adjustment to improve peak flow performance – it was difficult to isolate an improvement at a single gauge in WATFLOOD. WATFLOOD is otherwise more capable of capturing the spring-summer high flow behaviour in the LNRB. Differences at the sub-basin scale were previously noted; HEC-HMS and WATFLOOD display varying skill in simulations at individual tributary gauges.

Both HEC-HMS and WATFLOOD appear to represent local inflows at the downstream calibration points. Although performance metrics are skewed based on upstream forcing, the simulation of both volume and peak flows is sufficient given that there is dual uncertainty associated with both the measured upstream forcing and hydrometric gauge. It is important to note that Kettle G.S. is a peaking hydroelectric generation station – as such, its outflows are difficult to replicate in a model and volume is a more important indicator of performance.

5.1.2. VALIDATION

The three PMF models were applied to an additional set of high flow years at each gauge to validate the calibration on an independent period. As explained in Section 4.2.1, three to five

high flow years were selected at each gauge, including years that were used to calibrate the existing SSARR model. Therefore, performance metrics for SSARR may be skewed towards improved performance since SSARR was calibrated to some years within this period. Table 17 shows statistics from the validation of each model at all nine hydrometric gauges.

The performance of SSARR is noticeably better in the validation period as a result of the model having been calibrated to several of the years within this period (primarily 1979). However, SSARR was overall not transferable to the independent set of high flow years, as it continued to overestimate peak flows and runoff volume when considering the entire validation period.

HEC-HMS and WATFLOOD displayed strong transferability to the validation period (both absolutely and relative to SSARR). However, the majority of statistics at both a sub-basin and basin-averaged scale (i.e. RSR, APB, NSE, hybrid metric) indicate that HEC-HMS simulated flows slightly better than WATFLOOD. A difference in performance is not unexpected given HEC-HMS was parameterized at the sub-basin scale, allowing it to more closely represent behaviour in each sub-basin. The scale of calibration was also greater in HEC-HMS - calibrating small groups of decision variables at individual gauges allows for more extensive searching of the parameter space than the simultaneous distributed calibration in WATFLOOD. The result in HEC-HMS is a set of local solutions at the sub-basin scale that are more transferable to this validation period compared to the local solution in WATFLOOD that may trade-off error between calibration points. A similar comparison of behaviour in validation between WATFLOOD and a lumped model was found by Dibike & Coulibaly (2007).

Table 17: PMF model performance metrics over the validation period

Calibration Point	Upper Burntwood River	Odei River	Grass River	Kettle River	Limestone River	Gunisao River	Burntwood R. @ Thompson	Kelsey G.S. Total Outflow	Kettle G.S. Total Outflow	Weighted Average
SSARR										
$\frac{RMSE}{\sigma_{obs}}$	1.21	0.67	1.64	1.09	0.96	0.92	0.80	0.22	0.66	0.78
D_v (%)	45.6	24.6	45.8	18.2	34.2	6.0	3.8	3.3	9.6	17.7
APB (%)	63.7	46.3	58.2	71.1	75.8	59.4	11.6	6.1	15.1	33.5
NSE	-0.47	0.55	-1.79	-0.27	0.08	0.14	0.33	0.95	0.57	0.15
Peak Q Diff (%)	31.1	-3.2	52.1	53.7	-3.0	12.2	-4.3	4.5	0.9	13.0
Hybrid	0.763	0.296	1.201	0.748	0.502	1.977	0.287	0.063	0.214	0.518
HEC-HMS										
$\frac{RMSE}{\sigma_{obs}}$	0.66	0.67	0.65	0.58	0.70	0.90	0.48	0.22	0.41	0.50
D_v (%)	-5.2	6.8	-3.9	11.4	0.8	39.2	-0.1	2.8	2.4	3.8
APB (%)	34.4	36.8	19.3	39.2	46.3	52.9	7.2	6.6	8.9	20.5
NSE	0.57	0.55	0.58	0.64	0.52	0.18	0.77	0.95	0.83	0.71
Peak Q Diff (%)	-2.1	12.9	-12.3	17.2	14.4	12.7	-5.1	0.9	-6.9	1.0
Hybrid	0.241	0.289	0.249	0.284	0.312	0.373	0.135	0.054	0.134	0.182
WATFLOOD										
$\frac{RMSE}{\sigma_{obs}}$	0.84	0.67	0.67	0.75	0.86	0.84	0.47	0.22	0.48	0.53
D_v (%)	11.6	2.5	-8.1	-20.5	-9.4	24.8	-2.4	-0.8	-0.2	-0.6
APB (%)	38.5	40.7	21.4	53.0	69.3	47.4	6.8	6.7	11.0	23.2
NSE	0.29	0.56	0.54	0.43	0.27	0.29	0.78	0.95	0.77	0.66
Peak Q Diff (%)	5.9	-3.5	-10.2	17.4	-2.4	15.5	-7.4	4.0	-7.1	-0.1
Hybrid	0.358	0.255	0.262	0.389	0.395	0.423	0.143	0.059	0.148	0.204

HEC-HMS and WATFLOOD successfully represent the average high flow behaviour in the LNRB during the independent period, since the basin weighted-average statistics are well above typically acceptable thresholds (Moriasi et al., 2007). Performance did, however, fall below these thresholds in several tributary basins, most notably those that were previously identified as difficult to calibrate due to computational or physiographic complications (i.e. the Upper Burntwood and Gunisao Rivers). Due to the overall acceptable performance of the model parameterizations, and to maintain the independence of the validation, no further adjustments were undertaken to the parameter sets to attempt to improve validation statistics.

The performance of both HEC-HMS and WATFLOOD was noticeably limited by extremely poor representation of spring-summer 1979. Comparative hydrographs at all gauges in 1979 can be found in Appendix D. HEC-HMS and WATFLOOD simulate snowmelt and the freshet much earlier than was observed in reality, resulting in extremely poor performance statistics that hamper the overall validation performance. Since this year was the primary calibration year for SSARR, it was included here in the validation as a further comparison between the "baseline" model and the two newly developed PMF models. Given the relatively low peak flows in 1979 compared to other years in the period of record it would not otherwise have been selected as part of the analysis. It is therefore acknowledged that the inclusion of 1979 reduces the validation performance in HEC-HMS and WATFLOOD.

5.1.3. Summary of Historical High Flow Simulations

The methodology for calibration was based on existing PMF guidelines and the methodology originally used for SSARR. High flow years were selected by similar criteria as for SSARR, and a combination of techniques led to an efficient and successful local optimization of the new PMF models. The resulting solutions in HEC-HMS and WATFLOOD sufficiently

represent the observed flow response throughout the LNRB over a robust range of the highest flow years, and were therefore considered appropriate to extrapolate to PMF conditions. This reinforces the finding from PMF guidance documents (e.g. Alberta Transportation, 2004) that a more robust calibration can be transferred to independent high flow years and extrapolated to PMF with greater confidence.

In contrast, the existing calibration of the SSARR PMF model did not validate as well to the same robust period; the parameterization was not similarly transferable to more recent years with higher and earlier freshet peaks. There is thus less confidence in extrapolating SSARR to PMF conditions. However, SSARR continued to be used for PMF simulations in this research to allow for comparison to the "baseline" PMF model.

Finally, it is important to note that varying the calibration period (that is, between SSARR and HEC-HMS/WATFLOOD) had a significant effect on model parameterization. Calibration to high flow years including the more recent hydrometric record produced an earlier and more rapid snowmelt regime (in both HEC-HMS and WATFLOOD). This warrants further investigation outside of this thesis, but qualitatively suggests that snowmelt may be occurring earlier in more recent years. This also suggests that the snowmelt regime during the earlier SSARR calibration period may no longer be representative of that generally observed in the highest flow years in the basin. The shift in snowmelt timing has an important effect on the critical PMF that will be expanded upon in the following section.

5.2. MULTI-MODEL COMPARISON – BASELINE PMF

The three PMF models were first extrapolated to baseline PMF conditions using historically-derived baseline PMF inputs (Section 4.8). Figure 15 presents the most critical PMF

at Keeyask G.S. from each model forced by the first PMF scenario (PMP + 1/100 year SWE). Recall that the critical PMF is defined as the hydrograph with the highest peak flow based on testing twenty-three different meteorological sequences (PMP timing and daily temperature time series). Details on the critical set of inputs for each model are also provided in Table 18. The PMF hydrograph from SSARR matches that from the most recent PMF update study conducted for Manitoba Hydro in 2013.

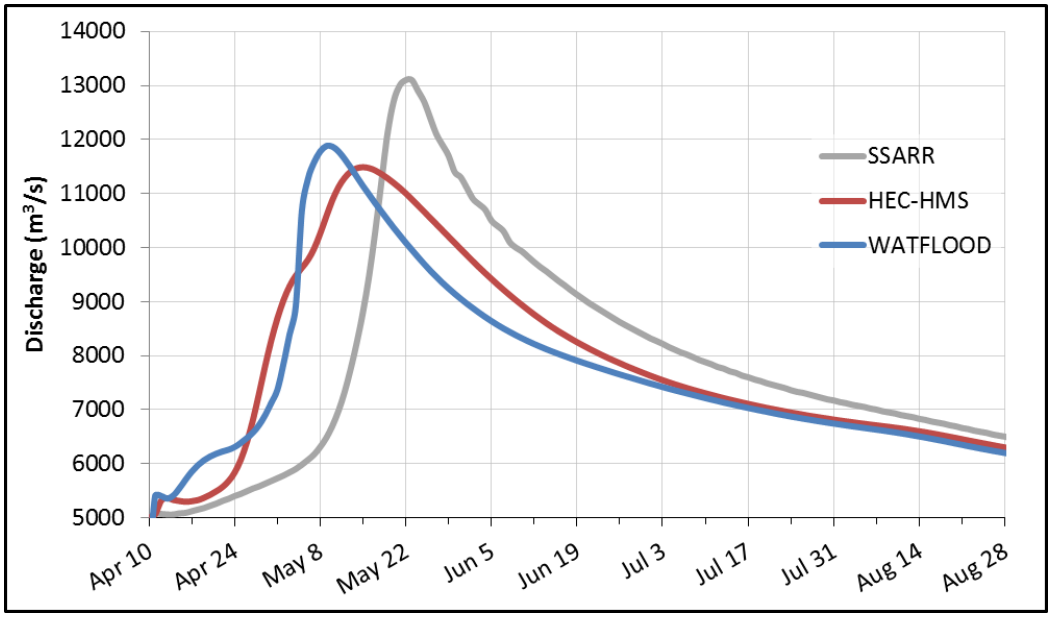

Figure 15: Baseline PMF (PMP) at Keeyask G.S.

Table 18: Baseline PMF (PMP) and Critical Meteorological Sequences at Keeyask G.S.

	Critical Meteorological Sequence	Rapid Melt Onset	Start of 48-hour PMP	PMF Peak Flow (m^3/s)	PMF Peak Flow Date
SSARR	10	May 10	May 15	13100	May 22
HEC-HMS	6	April 20	May 5	11488	May 15
WATFLOOD	7	May 1	May 5	11880	May 9

The limited and different calibration period (and more gradual snowmelt) used to parameterize the SSARR model results in a later critical PMF than the other models. The lingering snowpack maintains saturated soil moisture conditions later into the spring, which allows for the PMP to also be delayed. Due to seasonality, a later PMP will also be larger. This greater total moisture input results in a more critical PMF hydrograph (1220 m^3/s greater than WATFLOOD). Such a large difference between the PMF from SSARR and the two newer models is also a product of the performance observed over the historical period; overestimation in SSARR of peak flows in the majority of high flow years has clearly and not surprisingly extrapolated to a much higher PMF peak flow.

In contrast, HEC-HMS and WATFLOOD (with a common calibration period) produce relatively similar PMFs at Keeyask. The critical PMF in both models occurs earlier in the spring due to an earlier melt of the 1/100 year snowpack, and both earlier PMFs peak at a lower value than the PMF from SSARR. There are, however, differences of note between the PMF responses of HEC-HMS and WATFLOOD:

- Although the critical PMP occurs on the same date in both models, flows at Keeyask peak more rapidly in WATFLOOD. This illustrates the impact of varying routing schemes. In the distributed representation of WATFLOOD, flows are routed between grid cells using a storage routing method parameterized with Manning's roughness values for channel and overbank regions (Kouwen, 2014; Kouwen et al., 2005). This method will respond quicker and route flows with less attenuation under a larger rainfall. In contrast, HEC-HMS uses a time of concentration parameter for in-basin runoff routing that will not decrease under larger moisture input (i.e. it is assumed to be a function of the watershed only). However, Meyersohn (2016) found that time of concentration also

varies with precipitation intensity. That study concluded that an invariant method of intra-basin routing (e.g. time of concentration) may lead to a more attenuated hydrograph (e.g. a wider PMF hydrograph) that could underestimate peak flows.

- HEC-HMS does not simulate evapotranspiration on days with precipitation (every day prior to the PMP based on the assumption of daily average antecedent precipitation), while WATFLOOD simulates evapotranspiration throughout the period. This results in greater moisture loss in WATFLOOD and also contributes to a narrower PMF hydrograph that has 2.2% less volume than HEC-HMS.

An examination of PMF results from the same timing of inputs is also useful to qualify differences between the models. PMF hydrographs for the critical meteorological sequences of HEC-HMS (sequence 6) and WATFLOOD (sequence 7) are provided on Figure 16. The gap between SSARR and the other models is narrower in these earlier scenarios, because the snowmelt rate in SSARR has not yet allowed for sufficient melt volume. Even without the full snowmelt volume, the consistent overestimation of runoff volume by SSARR during the historical period manifests itself in higher PMF hydrographs here. However, a coincident timing of snowmelt and PMP in WATFLOOD (Sequence 7) results in a higher simulated PMF at Keeyask G.S. than SSARR. This can again be attributed to the routing scheme in WATFLOOD (because SSARR, too, uses an invariant routing scheme based on time of storage). This also illustrates that WATFLOOD (calibrated over the whole period, thus presumably also HEC-HMS) is likely capable of simulated the full range of flows predicted among the three models.

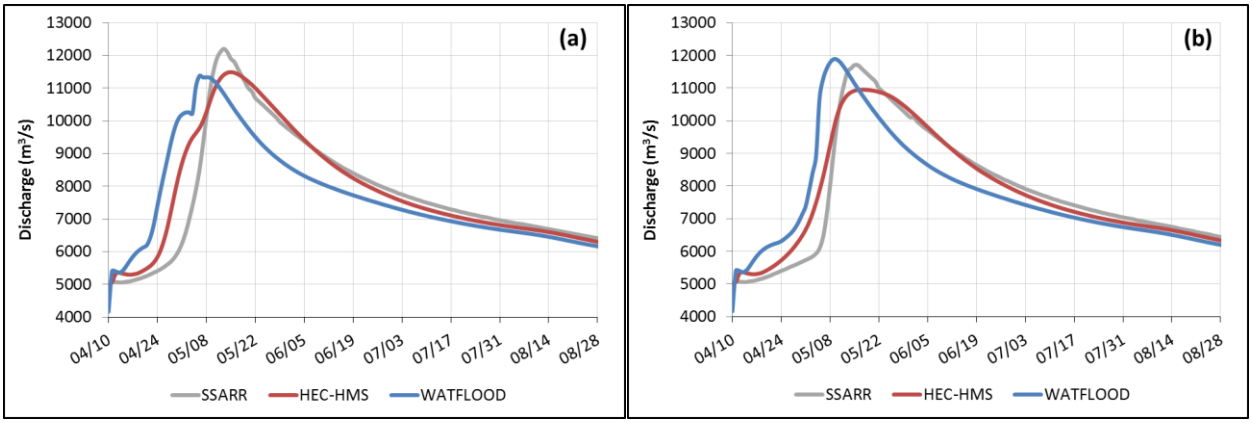

Figure 16: Baseline PMF at Keeyask G.S. for meteorological sequences (a) 6, and (b) 7.

While keeping inputs constant, differences in PMF volume between SSARR, HEC-HMS (0.5% smaller than SSARR in Sequence 7), and WATFLOOD (1.4% smaller than SSARR) can also be attributed to differences in runoff processes in each model (Figure 4). Specifically:

- Both HEC-HMS and WATFLOOD account for canopy interception and surface depressional storage, as well as evapotranspiration from these storages. SSARR does not account for these and would therefore have lower moisture losses. In particular, depressional storage can hold excess precipitation for future infiltration, which would reduce the direct runoff potential in HEC-HMS and WATFLOOD;
- HEC-HMS is the only model to account for percolation losses from the deepest baseflow reservoir. Although this was a calibrated parameter (i.e. adjusted for extreme high flow years), this process results in greater losses from HEC-HMS.
- WATFLOOD simulates the greatest amount of evapotranspiration during the critical rising limb period of the PMF simulation (April 10 to mid-May). By May 10th, approximate basin average evapotranspiration amounts in each model are:
    - SSARR: 18 mm (specified values of 0 mm/day in April; 2 mm/day in May)
    - HEC-HMS: 0 mm (evapotranspiration is restricted when precipitation > 0.5 mm)

- WATFLOOD: 30 mm.

The greater early evaporative loss in WATFLOOD represents more than half of the difference in total runoff volume compared to SSARR, and exceeds the difference in volume compared to HEC-HMS (countered by percolation losses in HEC-HMS). An added effect of this greater loss will be reduced storage in lakes/reservoirs that further attenuates peak flows in WATFLOOD.

The simulated PMFs at generating stations downstream of Keeyask are also important to consider. Table 19 lists the critical PMF peak flow at all stations in the Lower Nelson River Complex, and Figure 58 in Appendix F compares the PMF hydrographs at each station. In the majority of cases, critical PMFs at these stations result from the same sequence of PMF inputs, which were critical for Keeyask G.S. Some different responses do occur; particularly downstream of Kettle G.S.

Table 19: Baseline PMF (PMP) at all stations in Lower Nelson River Complex

PMF (m^3/s)	Keeyask G.S.	Kettle G.S. Inflow	Kettle G.S. Outflow	Long Spruce G.S.	Limestone G.S.	Conawapa G.S.
SSARR	13100	13700	12800	13100	13200	13700
HEC-HMS	11488	11777	11497	11731	11803	12040
WATFLOOD	11880	12489	12000	12691	12810	14040

The higher, later PMF at Keeyask in SSARR similarly leads to larger peak flows at the majority of downstream generating stations. The only significant attenuation is provided from the reservoir of Kettle G.S. (Stephens Lake), therefore both simulated inflows and outflows are important to consider there. Immediately downstream of Kettle G.S., the range between the three models narrows as a result of this attenuation.

Differences between HEC-HMS and WATFLOOD are larger at the downstream stations. In particular, the local inflows to Long Spruce G.S. and to Conawapa G.S. are much higher in WATFLOOD (730 m^3/s and 1230 m^3/s higher, respectively; 2.5 times greater than SSARR and 3-4 times greater than HEC-HMS). Both cases can be attributed to contributions from local tributaries (the 1969 km^2 Kettle River upstream of Long Spruce G.S. and the 3210 km^2 Limestone River upstream of Conawapa G.S.).

Figure 17 isolates the PMF hydrograph at each station and the local inflows from the major gauged tributary. In both SSARR and HEC-HMS, the freshet on the gauged tributary peaks lower than WATFLOOD and peaks earlier than the freshet at the generating station (i.e. they do not coincide). This response is due to (a) earlier and rapid melt in HEC-HMS, and (b) a later PMP and longer preceding melt period in SSARR. Meanwhile, the timing of local snowmelt runoff and PMP nearly coincide in WATFLOOD, as well as the timing between local and upstream freshet. This leads to more critical conditions and larger peak flows at the downstream stations in WATFLOOD.

The difference in routing between the distributed setup in WATFLOOD and time of concentration in HEC-HMS is especially significant when considering local inflows between generating stations on the Nelson River. Despite attempts to reduce time of concentration in HEC-HMS for local basins with short flow paths, these areas respond more rapidly in WATFLOOD. The grid size in WATFLOOD (approximately 11 km) will in particular respond with more volatility compared to a lumping of local areas into a sub-basin element in HEC-HMS. This is clear in the more rapid, higher peak local inflows in WATFLOOD (Figure 17).

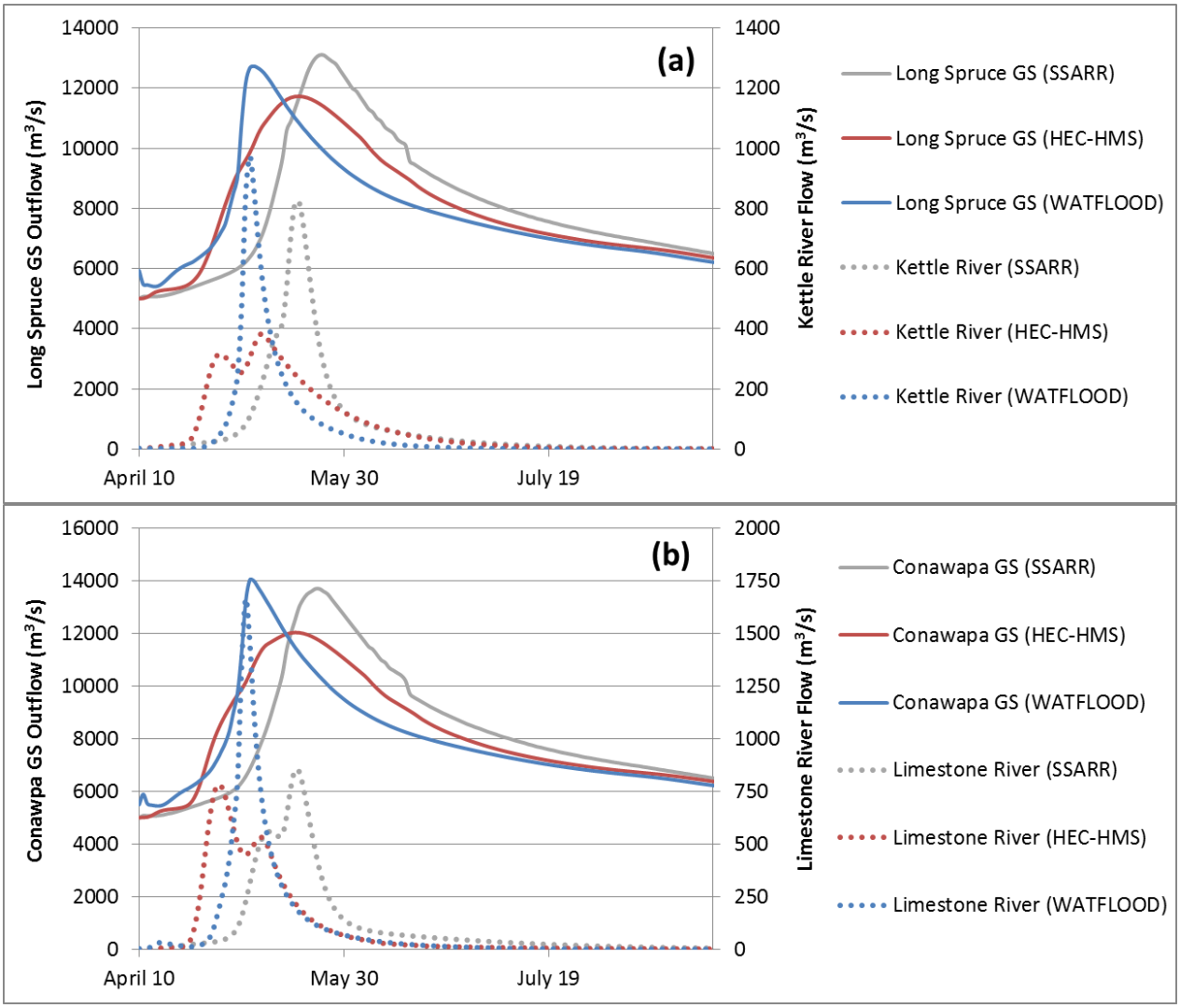

Figure 17: Total and major local PMF inflows to (a) Long Spruce G.S. and (b) Conawapa G.S.

The baseline PMF produced by the second scenario recommended by the CDA Dam Safety Guidelines (1/100 year rainfall + PMSA) was also simulated to compare the two PMF scenarios in each model. Table 20 lists the peak flows from the PMSA scenario and the critical timing of inputs in each model, and Figure 59 shows the PMF (PMSA) hydrographs at all downstream stations in the Lower Nelson River Complex.

Table 20: Baseline PMF (PMSA) and Critical Meteorological Sequences

	Rapid Temp. Increase Start	48-hour 1/100 Year Rainfall	PMF Peak Flow (m^3/s)	PMF Peak Flow Date
SSARR	May 10	May 20	12300	May 26
HEC-HMS	April 20	May 5	11188	May 16
WATFLOOD	May 1	May 5	11450	May 9

As with the PMF (PMP) scenario, the SSARR model simulates the largest PMF as a result of a later critical sequence of inputs and the general overestimation of runoff observed in the historical period. The critical sequence of PMF inputs in SSARR shifts slightly, with the 1/100 year rainfall occurring 5 days later than in the PMP scenario. This shift is the result of the larger snowpack, which allows for a later and larger rainstorm. The critical PMF sequences in the other two models remained the same as in the PMP scenario.

HEC-HMS and WATFLOOD continue to simulate lower overall PMFs in the PMSA scenario when compared to SSARR; however, the reduction in peak flow from the PMP to PMSA scenario is half of the reduction in SSARR. This results from the larger snowpack, earlier snowmelt and earlier critical timing of PMF in HEC-HMS and WATFLOOD, which places greater importance on snowpack. This point is corroborated in Section 5.4.2 – HEC-HMS and WATFLOOD are shown to have greater sensitivity to snowpack inputs than SSARR. Therefore, one effect of the wider calibration period of HEC-HMS and WATFLOOD was earlier snowmelt, which resulted in more similar magnitudes of PMF between the PMP and PMSA scenarios.

As further consideration for the areas in the downstream end of the LNRB, Table 21 shows the PMF peak flow magnitudes at all generating stations in the Lower Nelson River Complex.

Table 21: Baseline PMF (PMSA) at all stations in Lower Nelson River Complex

PMF (m^3/s)	Keeyask G.S.	Kettle G.S. Inflow	Kettle G.S. Outflow	Long Spruce G.S.	Limestone G.S.	Conawapa G.S.
SSARR	12300	12700	12200	12400	12500	12900
HEC-HMS	11188	11408	11257	11438	11492	11676
WATFLOOD	11450	11806	11580	12188	12310	13410

All generating stations continue to follow the trend that the PMF is largest as a result of the PMP scenario rather than from the PMSA scenario. WATFLOOD continues to display the same behaviour as observed in the PMP scenario, whereby a more rapid response in local inflow and reduced travel time of upstream flow result in larger peak flows than HEC-HMS. Once again, this behaviour illustrates a more critical (and, importantly, plausible) combination of upstream runoff and local runoff simulated by WATFLOOD at the downstream generating stations.

5.3. PROJECTED CLIMATE CHANGE IMPACTS ON PMF INPUTS

Projected changes in PMF inputs were assessed via analysis of data from regional climate model simulations. Recall that fourteen RCM simulations were used, and that results are quantified in terms of relative change factors of PMF inputs between the baseline period (1971-2000) and the future period (2041-2070).

Climate model data, analysis methodologies, and most PMF input projections were provided by Ouranos. The projections that were provided match, in part, those that were used for the LNRB as part of the NRCan PMP/PMF study and presented by Clavet-Gaumont et al. (2017). The analyses and projected changes to each PMF input, as well as a discussion on

impacts of various sources of uncertainty, are provided in Appendix E. Projected changes to all PMF inputs are also summarized in Table 35 in Appendix F.

5.4. Multi-Model Comparison – Projected Future PMF and Input Sensitivity

This section details the impact of projected changes to PMF inputs in the LNRB on PMF hydrographs from each model. These results are important in terms of both (a) estimating climate change impacts on PMF, and (b) qualifying the sensitivity of the hydrological models to each PMF input. To consider both characteristics at once, changes to PMF inputs are incorporated in a stepwise fashion. Specifically, the progression of simulations was as follows:

- Changes to rainfall inputs (PMP and 1/100 year rainfall);
- Changes to rainfall and snowpack (1/100 year SWE and PMSA) inputs;
- Changes to rainfall and snowpack inputs, and the daily temperature time series;
- Changes to rainfall and snowpack inputs, temperature, and 1/100 year outflows from Lake Winnipeg.

Note that the final set of simulations is considered to be the most complete picture of projected climate change impacts on PMF.

Both PMF scenarios (PMP + 1/100 year SWE, 1/100 year rainfall + PMSA) are considered in the following analysis, in case of a potential shift in the critical PMF scenario. For input sensitivity, only the PMF (PMP) scenario is considered (because the relative sensitivity in each model should be similar in the PMF (PMSA) case). Each of the fourteen sets of projections from the climate models (future climate scenarios) were used individually to perturb the PMF models; this is appropriate given that (a) each model is an equally plausible representation of

climate processes, and (b) a greater number of future scenarios allowed for more guidance on sensitivity. Note that because there were fourteen future climate scenarios, the "median" future PMF shown in the ensuing figures is considered to be the scenario producing the larger of the two middle PMFs (eighth out of the fourteen scenarios). The maximum and minimum are taken as those scenarios producing the highest and lowest peak flows, respectively.

5.4.1. CHANGES TO RAINFALL INPUTS

The following simulations depict the range of future PMFs that occur in each hydrological model as a result of projected climate change impacts to only rainfall inputs (PMP or 1/100 year rainfall). Table 22 and Figure 18 show the range in peak flows and PMF hydrographs at Keeyask G.S., respectively, that result from the fourteen future climate scenarios. Similar results for the other generating stations are provided in Appendix F.2.

The projected future hydrographs in Figure 18 show the scenarios that produce the maximum, median, and minimum peak flows at Keeyask G.S. These graphs better illustrate the range about the baseline PMF hydrograph.

Table 22: Changes in PMF at Keeyask G.S. after incorporating climate change impacts to rainfall inputs

	SSARR	HEC-HMS	WATFLOOD
PMF (PMP) – Changes in Peak Flow at Keeyask G.S. (%)			
Maximum	6.1	4.7	4.2
Median	-1.5	-1.4	-1.4
Minimum	-6.9	-5.0	-4.9
PMF (PMSA) – Changes in Peak Flow at Keeyask G.S. (%)			
Maximum	6.5	4.1	4.3
Median	2.4	1.2	1.2
Minimum	-0.8	-0.8	-1.0

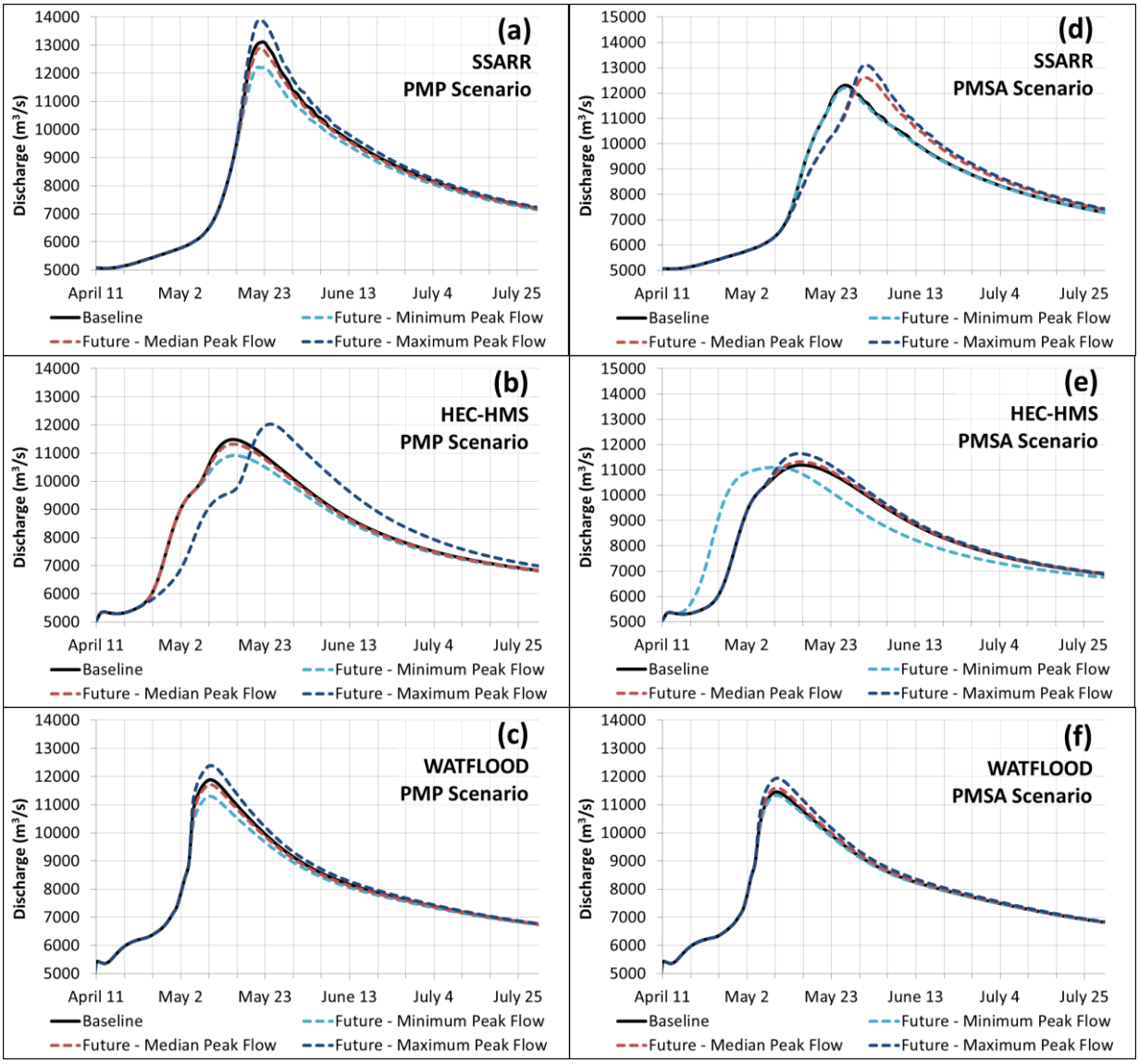

Figure 18: Range of future PMF hydrographs at Keeyask G.S. produced by incorporating climate change impacts on rainfall inputs (PMP or 1/100 year rainfall).

All three median hydrographs from the PMP scenario (Figure 18a, b, c) peak slightly below the baseline; this corresponds to the median PMP projection of approximately -10%. However, the lack of consensus among PMP projections results in the range of future hydrographs being approximately equal on either side of the baseline. This range shows that there can be significant sensitivity to larger projected PMP changes (increases or decreases).

Considering the PMF (PMSA) scenario (Figure 18 d, e, f), although the projected changes in 1/100 year rainfall are larger than those for PMP, the range about the baseline PMF is not proportionately larger. This is due to the 1/100 year rainfall making up a less significant portion of the total runoff in the PMSA scenario. The clear direction of projections towards increased 1/100 year rainfall does lead to an upwards shift of both the median future hydrograph and the total range of the future hydrographs. However, the median future PMF (PMSA) hydrograph continues to remain less critical than the median future hydrograph from the PMF (PMP) scenario in all three models.

Larger peak flow changes in SSARR show that the model is the most sensitive to changes in PMP. This results from a later critical sequence of inputs in SSARR that puts more weight on the PMP relative to snowpack and allows for a larger baseline PMP. HEC-HMS and WATFLOOD display nearly identical sensitivity in contrast, suggesting that the calibration period (which led to similar critical timing of inputs) has a greater impact than hydrological model selection, in this case. However, Figure 18(b) and (e) show that the PMF timing can be more sensitive in HEC-HMS.

Another method of comparing the sensitivity of each model to individual PMP changes, and to further analyze PMF processes in general, is a scatterplot of the correlation between changes in PMP and corresponding changes in peak flow, given in Figure 19. Figure 19 illustrates a near-perfect linear relationship in each model between changes in PMP forcing and changes in the peak flow at Keeyask G.S. Specifically, this amounts to a 1:5 (PMF:PMP % change) slope from SSARR results and a 1:7 slope from HEC-HMS and WATFLOOD.

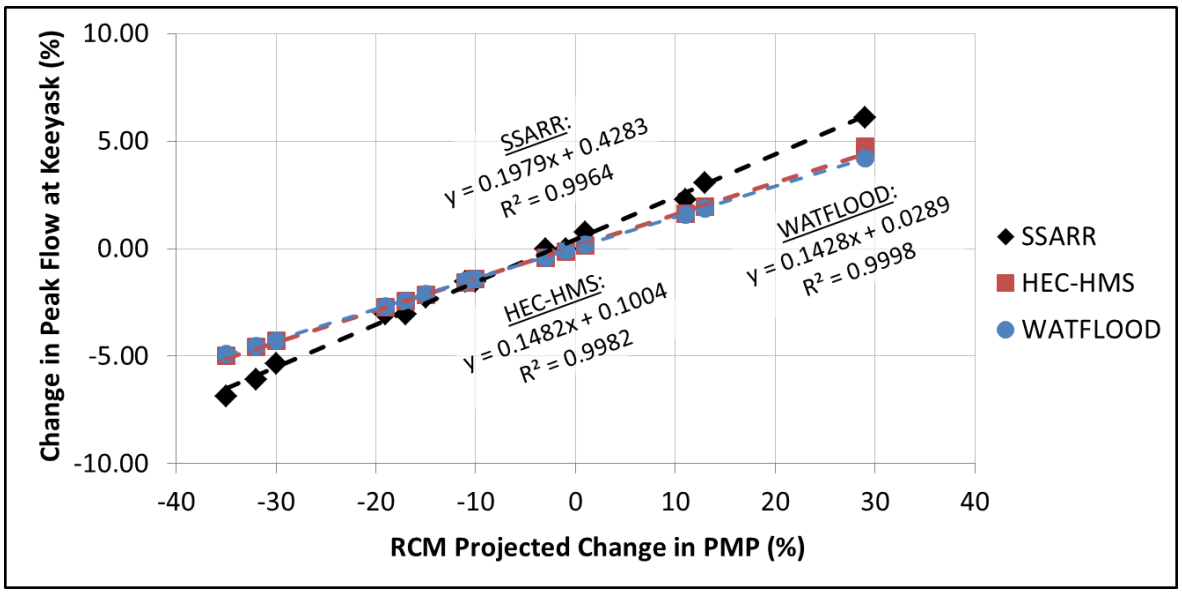

Figure 19: Correlation between PMP changes and corresponding PMF changes at Keeyask G.S.

The linearity here is not necessarily surprising. Saturated conditions at the time of the PMP will lead to less contribution of precipitation to non-linear soil/sub-surface processes and an increased direct translation to excess precipitation. A linear relationship between excess rainfall and runoff is an expansion of the unit hydrograph concept and is common in lumped, conceptual watershed models (by extension, semi-lumped models) and, in conjunction with a non-linear loss module, can be a "good predictor of streamflow" (Jakeman & Hornberger, 1993).

5.4.2. Changes to Rainfall and Snowpack Inputs

The following simulations depict the range of future PMFs that occur as a result of projected climate change impacts to both rainfall (PMP or 1/100 year rainfall) and snowpack (1/100 year or PMSA) inputs. Table 23 and Figure 20 show the range in peak flows and PMF hydrographs, respectively, at Keeyask G.S. that result from the fourteen future climate scenarios. Similar results for the other generating stations are provided in Appendix F.2.

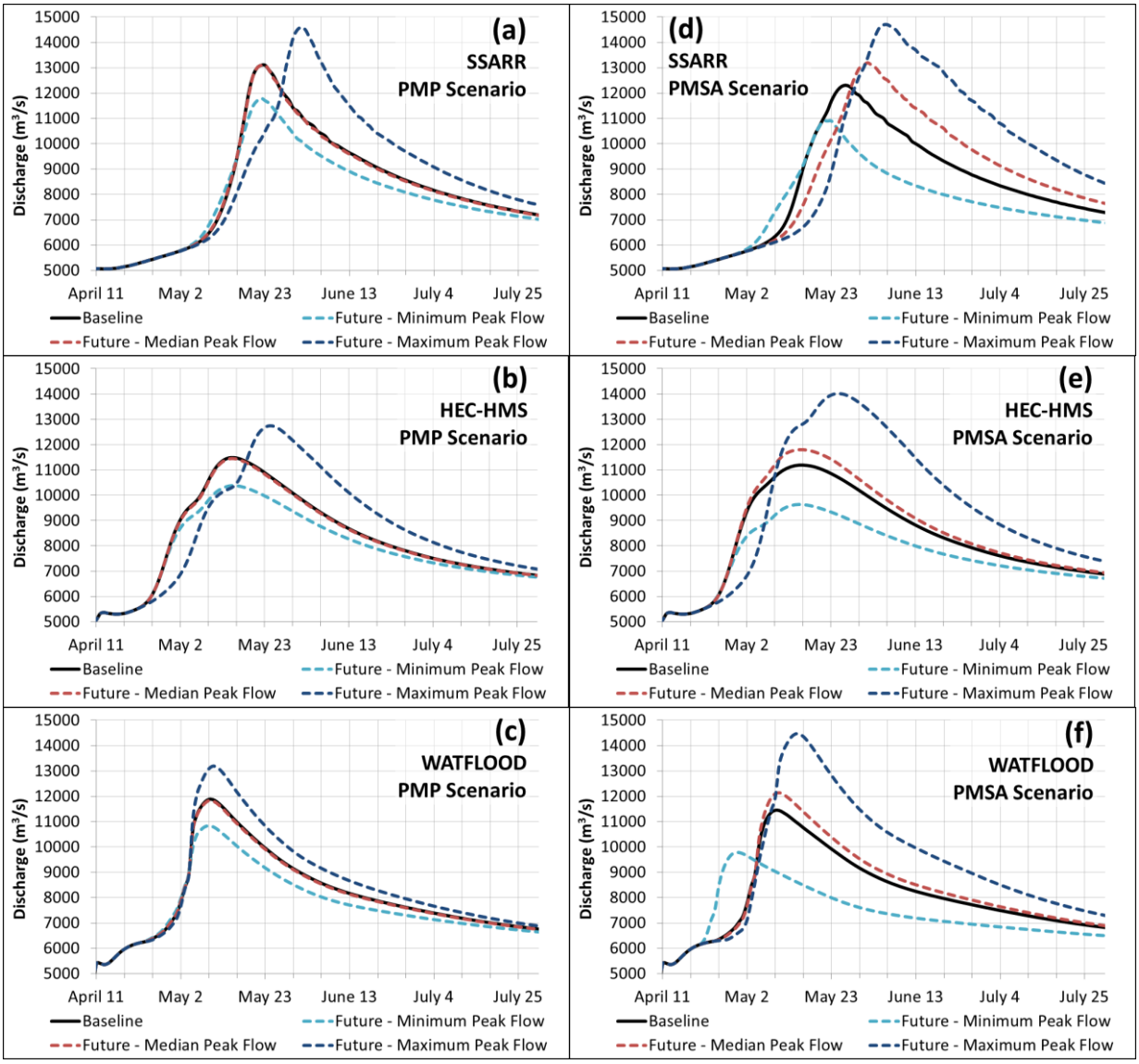

Figure 20: Range of future PMF hydrographs at Keeyask G.S. produced by incorporating climate change impacts on rainfall and snowpack inputs.

With the addition of projected changes to 1/100 year snowpack (which, on average, projected increased snowpack), the median of the future PMF (PMP) hydrographs rises slightly and is now nearly identical to the baseline in all three models (Figure 20a, b, c). This offsets a projected decrease, on average, of PMP magnitude. The range of future PMF hydrographs nearly doubles in all three models as a result of RCMs that project PMP and snowpack changes in the same direction.

Table 23: Changes in PMF at Keeyask G.S. after incorporating climate change impacts on rainfall and snowpack inputs

	SSARR	HEC-HMS	WATFLOOD
PMF (PMP) – Changes in Peak Flow at Keeyask G.S. (%)			
Maximum	11.5	10.9	11.0
Median	0.0	-0.3	-0.4
Minimum	-9.9	-9.6	-8.8
PMF (PMSA) – Changes in Peak Flow at Keeyask G.S. (%)			
Maximum	19.5	25.3	26.3
Median	7.3	5.5	6.0
Minimum	-11.4	-13.9	-14.6

Larger increases in snowpack also result in a later critical PMF timing in SSARR (Figure 20a) and HEC-HMS (Figure 20b), as a larger snowpack allows for a later and larger PMP event. The critical sequence of PMF inputs in WATFLOOD (Figure 20c) was not sensitive to even the largest projected increase in 1/100 year snowpack (i.e. a later, larger PMP was not achieved).

The addition of PMSA changes in the second PMF scenario (which, on average, projected increased snowpack in addition to increased rainfall) result in a median future PMF hydrograph that is well further above the baseline (Figure 20d, e, f). The range of future PMF (PMSA) hydrographs also increases by three to eight times compared to the range associated only with incorporated changes to 1/100 year rainfall (Figure 18d, e, f). This wider range is the result of more extreme projected changes than in the PMP scenario. Finally, the median future peak flows also increased sufficiently to be equivalent to peak flows from the PMP scenario (comparing Figure 20a-d, b-e, and c-f). This suggests that both scenarios are important to consider in future PMF reviews in the LNRB; the PMSA scenario cannot be assumed to be significantly less critical than the PMP scenario.

Table 38 and Table 39 in Appendix F.2 illustrate additional sensitivity at the downstream generating stations. The range of peak flows in all three models initially decreases downstream of Kettle G.S. due to attenuation from Stephens Lake, and increases closer to the mouth of the LNRB (Conawapa G.S.) due to a greater contribution from local inflows. This behaviour is more pronounced in HEC-HMS and WATFLOOD because of lower PMFs and subsequently greater attenuation; in the maximum future scenario in SSARR, flows at Kettle G.S. are sufficient to exceed the maximum outflow capacity, resulting in little to no attenuation from the reservoir.

The three models can again be compared in terms of their sensitivity to each of the fourteen future climate scenarios. This information is provided in the combined column and scatter plot in Figure 21, where changes in peak flows at Keeyask are depicted as columns and climate change impacts on PMF (PMP) inputs are provided as scatter points. This is useful to isolate the sensitivity of each model to changes in SWE.

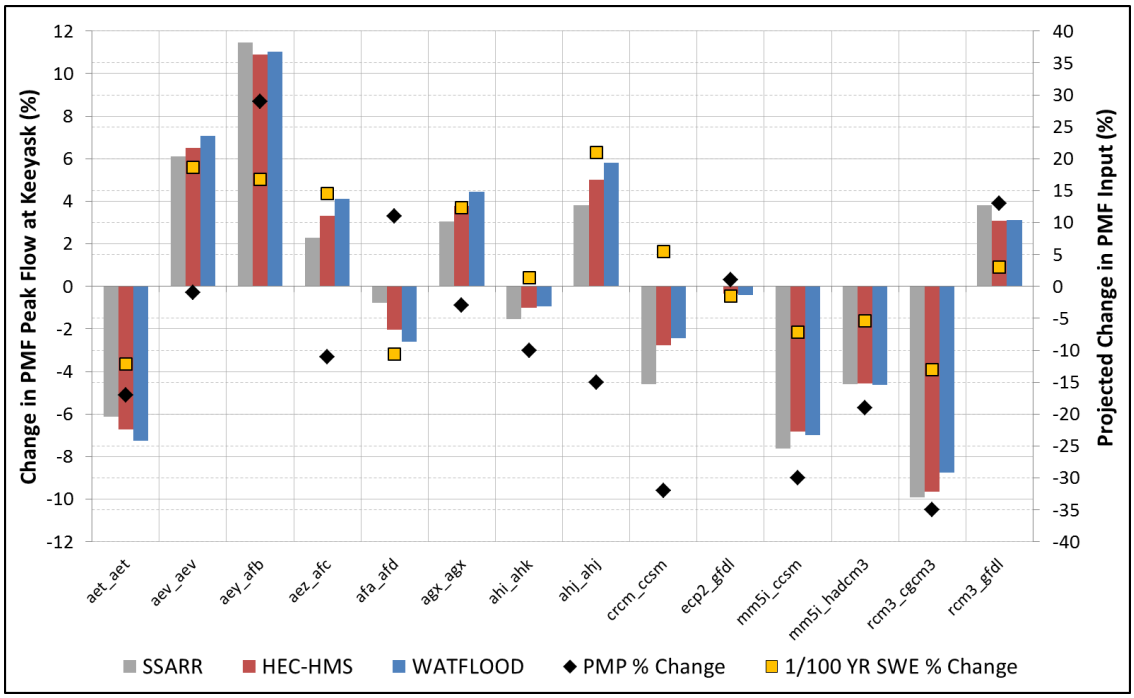

Figure 21: Changes to PMF peak flows among hydrologic models and PMP inputs at Keeyask G.S. for each RCM simulation

Both HEC-HMS and WATFLOOD are more sensitive to changes in snowpack than SSARR, as a result of the earlier critical timing of inputs in both models. The earlier critical timing puts more emphasis on snowmelt volume and involves a smaller PMP (because of seasonality). Of the two models, WATFLOOD displays greater sensitivity to snowpack changes. As the baseline PMF simulations illustrated, the timing of snowmelt and PMP in WATFLOOD coincide more critically in lower parts of the LNRB compared to in the other two models; this would be expected to produce greater sensitivity in WATFLOOD.

It can also be observed from Figure 21 that all three models are more sensitive to changes in 1/100 year snowpack than to changes in PMP. For example, similar but opposing magnitudes of changes to PMP and SWE in the *aez_afc* and *afa_afd* simulations both result in significant peak flow changes in the direction of SWE. Greater sensitivity is not surprising given snowpack has a dual effect in the PMF simulation: snowpack contributes volume to the runoff hydrograph, and also contributes to soil moisture that impacts the proportion of the PMP converted into runoff. Considering those two simulations, SSARR, HEC-HMS, and WATFLOOD display approximately 1.5, 2.0, and 2.5 times more sensitivity to 1/100 year SWE than PMP, respectively. Clearly then, calibration period also impacts the significance of the snowpack input; earlier snowmelt and an earlier critical PMF timing puts more weight on 1/100 year snowpack. This differential sensitivity should be inflated in the PMSA scenario, as a result of the larger relative magnitude of probable maximum snowpack compared to the 1/100 year rainfall.

5.4.3. CHANGES TO RAINFALL, SNOWPACK, AND TEMPERATURE INPUTS

The following simulations depict the range of future PMFs that occur as a result of projected climate change impacts to rainfall (PMP or 1/100 year rainfall) and snowpack (1/100 year or PMSA) inputs, as well as the critical temperature sequence (daily time series). Table 24

and Figure 22 show the range in peak flows and PMF hydrographs, respectively, that result out of the fourteen future climate scenarios. Similar results for the other generating stations are provided in Appendix F.2. Note that absolute changes to the daily temperature time series were common to all fourteen future climate scenarios.

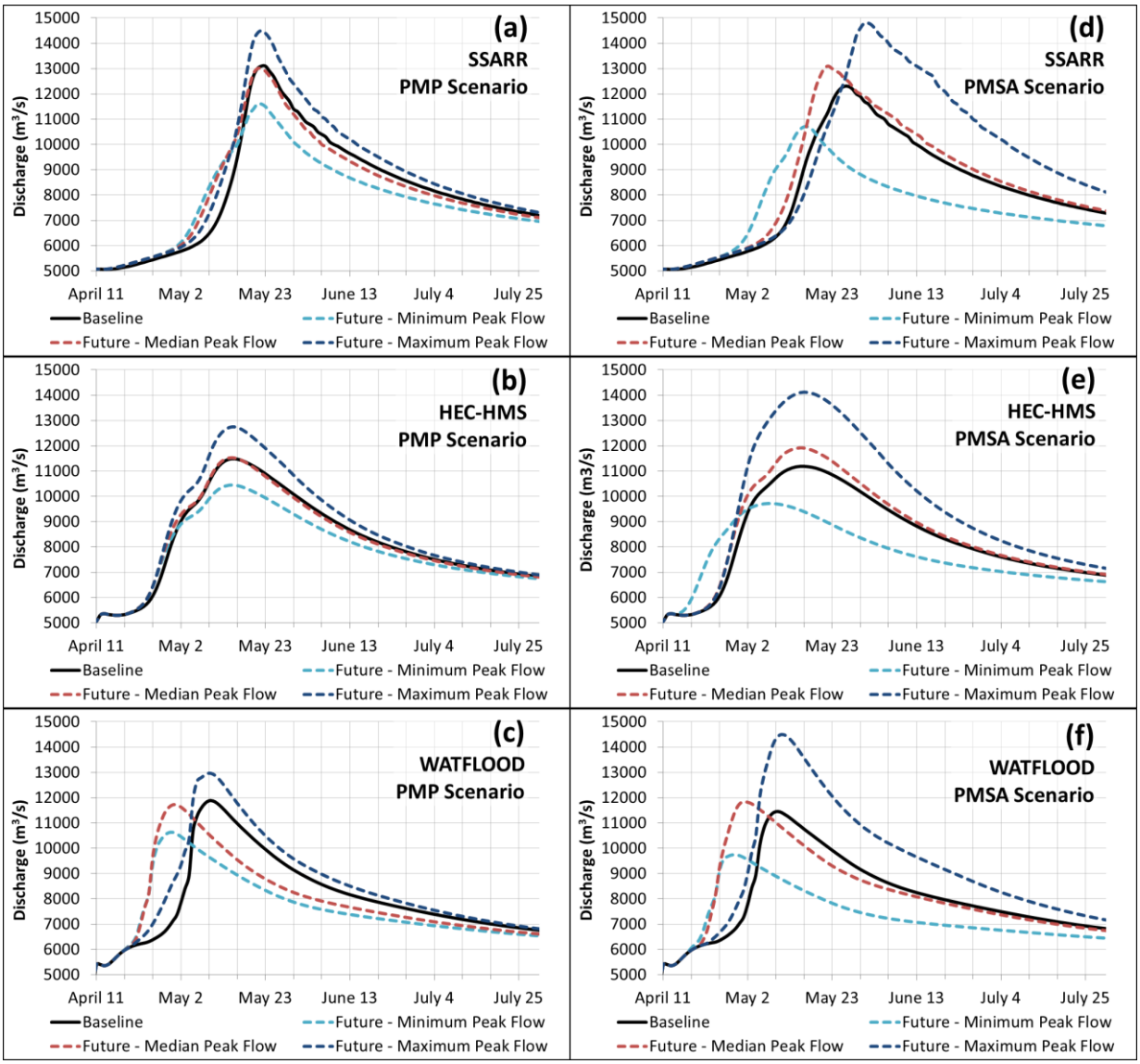

Figure 22: Range of future PMF hydrographs at Keeyask G.S. produced by incorporating climate change impacts on rainfall, snowpack, and temperature inputs.

Table 24: Changes to PMF at Keeyask G.S. after incorporating climate change impacts on rainfall, snowpack, and temperature inputs

	SSARR	HEC-HMS	WATFLOOD
PMF (PMP) – Changes in Peak Flow at Keeyask G.S. (%)			
Maximum	10.7	10.9	9.2
Median	-0.8	-0.3	-1.3
Minimum	-11.5	-9.6	-10.5
PMF (PMSA) – Changes in Peak Flow at Keeyask G.S. (%)			
Maximum	20.3	26.2	26.6
Median	6.5	6.5	3.4
Minimum	-13.0	-13.1	-17.0

Table 24 illustrates that the projected increase in daily temperature has a negligible effect on PMF magnitude (PMP and PMSA scenarios) in all three models; however, the effect on the PMF hydrographs in Figure 22 cannot be overlooked. Higher daily temperatures lead to earlier snowmelt and an earlier passage of snowmelt runoff through the watershed. The critical PMF timing is therefore shifted earlier for some of the PMF hydrographs, particularly those that are above the baseline. In the PMF (PMP) case, this brings the median, minimum, and maximum PMF hydrographs in SSARR (Figure 22a) and HEC-HMS (Figure 22b) back to the same critical timing as in the baseline (negates the timing changes observed in Figure 20). In WATFLOOD (Figure 22c), the median and minimum future hydrographs also shift to an earlier timing. There are similar earlier shifts in the PMF (PMSA) scenario (Figure 22d, e, f), and peak flows of the shifted hydrographs are no more critical than previous results (i.e. Figure 20d, e, f). However, the median future hydrograph in the PMSA scenario continues to peak well above the baseline in all three models.

Higher temperature and earlier melt of snow generally leads to reduced PMFs in SSARR and WATFLOOD (always lower in the PMP scenario, often lower in the PMSA scenario).

However, a more critical PMF occurs in HEC-HMS in every future climate simulation and both scenarios. This can be attributed to two factors. First, HEC-HMS does not account for evapotranspiration prior to the PMP, whereas the other two models will simulate marginally higher evaporative losses as a result of higher temperatures. Second, the critical PMF sequence (snowmelt and PMP) occurs earlier in HEC-HMS than the other two models (temperatures rapidly increasing on April 20th). Snowmelt is already early and rapid enough that higher temperatures do not cause a shift in timing; rather, this contributes to more rapid snowmelt runoff. In contrast, in SSARR and WATFLOOD, higher temperatures cause snowmelt volume to move through the system earlier, resulting in decreased PMF as a result of (a) more volume loss prior to the PMP, and/or (b) an earlier (smaller) PMP to coincide with the earlier snowmelt peak.

Table 40 and Table 41 in Appendix F.2 for other generating stations in the Lower Nelson River Complex show a similar relationship as that at Keeyask, in terms of the effect on PMF and differences between models. Peak flows at the downstream of the LNRB (Conawapa G.S.) were more sensitive to the temperature increase, particularly in WATFLOOD. This stems from earlier snowmelt in the local basins (e.g. the Kettle River and Limestone River). The result is a local runoff hydrograph that shifts more drastically than that from upstream and thus reduces the peak flow at the furthest downstream generating stations.

5.4.4. CHANGES TO ALL PMF INPUTS

The following simulations depict the range of future PMFs that occur as a result of projected climate change impacts to all four PMF inputs considered in this study: rainfall (PMP or 1/100 year rainfall) and snowpack (1/100 year or PMSA) inputs, the critical temperature sequence (daily time series), and the 1/100 year monthly outflow time series from Lake Winnipeg into the LNRB. Table 25 and Figure 23 show the range in peak flows and PMF

hydrographs, respectively, that result out of the fourteen future climate scenarios. Similar results for the other generating stations are provided in Appendix F.2.

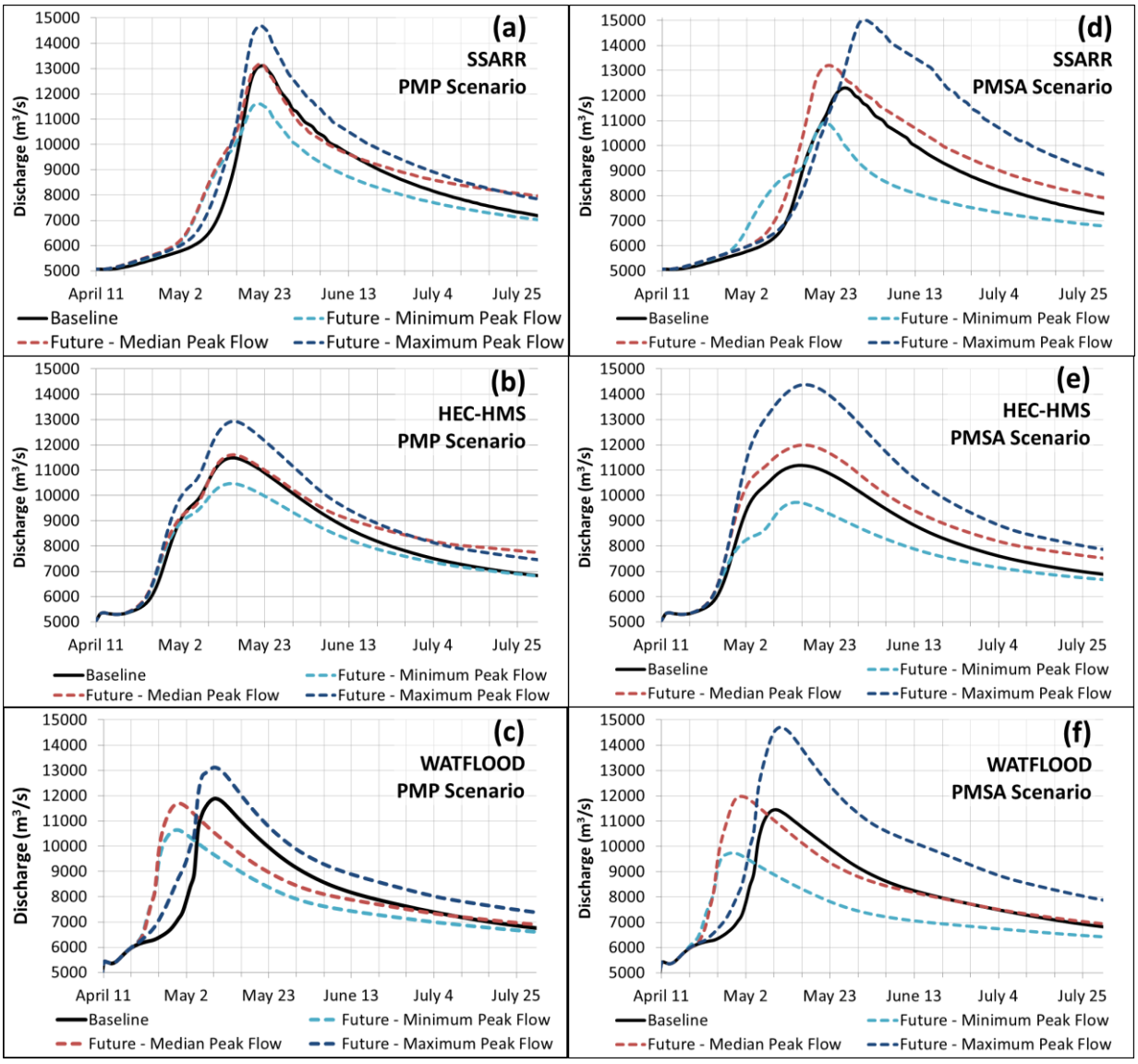

Figure 23: Range of future PMF hydrographs at Keeyask G.S. produced by incorporating climate change impacts on all four PMF inputs

Table 25: Changes to PMF at Keeyask G.S. after incorporating climate change impacts on rainfall, snowpack, and temperature inputs, and inflows from Lake Winnipeg

	SSARR	HEC-HMS	WATFLOOD
PMF (PMP) – Changes in Peak Flow at Keeyask G.S. (%)			
Maximum	12.2	12.5	10.4
Median	0.8	1.0	-1.5
Minimum	-11.5	-8.8	-10.4
PMF (PMSA) – Changes in Peak Flow at Keeyask G.S. (%)			
Maximum	22.0	28.6	28.5
Median	7.3	7.2	4.6
Minimum	-11.4	-13.1	-14.9

Projected changes to Lake Winnipeg outflows had the least effect on PMF of the four tested inputs; however, this was caused primarily by small projected changes in the climate scenarios at the extremes of the range. When considering individual future scenarios, the sensitivity of PMF to Lake Winnipeg outflow changes was similar in magnitude to the sensitivity to PMP changes.

PMF changes at Keeyask in Table 25 and at the downstream generating stations in Appendix F suggest that generally increased flows from Lake Winnipeg are least impactful in the WATFLOOD model. The reduced impact in WATFLOOD is caused by the following:

a) The majority of simulations have an earlier critical timing due to the projected temperature increase (earlier PMFs will be less impacted by flows from upstream); and
b) Slight differences exist in the storage-discharge relationship at Kelsey G.S. between the tables in SSARR/HEC-HMS and the fitted polynomial required in WATFLOOD.

In contrast, PMF results from SSARR (Figure 23a, d) were generally the most sensitive to changes in upstream contributions as a result of the later critical PMF timing, which (a) places

greater importance on upstream flows to maintain high reservoir levels, and (b) allows more time for higher upstream flows to route through the system.

Changes to Lake Winnipeg outflows can also have an impact on PMF volume. The median future hydrographs in all six graphs in Figure 23 show that the falling limb of the PMF hydrograph can be drawn out significantly. This is a result of the assumption that the monthly change factor was proportional to outflows from the highest outflow year on record; this leads to larger changes moving into summer. The change does not impact the PMF peak flow or timing; however, the PMF simulation assumes no rainfall after the PMP. If this were not the case, then the combination of continued rainfall and increased upstream contributions could draw out the peak of the PMF hydrograph and maintaining high reservoir levels for a longer period of time.

5.4.5. SUMMARY

Given the number of results presented in this section, it is worthwhile to synthesize the most significant findings:

- PMFs in all three models were most sensitive to changes to initial snowpack. This sensitivity was greatest in HEC-HMS and WATFLOOD due to an earlier critical PMF timing (result of a wider calibration period).
- There was also significant sensitivity to changes to rainfall inputs. Sensitivity was greatest in SSARR due to its later PMF timing (again a result of its calibration), which placed greater importance on the rainfall input.
- Sensitivity to temperature was limited to changes in PMF timing; a number of PMF hydrographs were shifted earlier. In most cases, this negated a shift to later PMFs that previously occurred due to increased snowpack.

- There is sensitivity of PMF to generally increased Lake Winnipeg outflows but this did not have an impact on the range of projected future PMFs. The change was primarily limited to changes in PMF volume on the falling limb of the hydrograph.
- Sensitivity to PMF input changes is reduced at generating stations immediately downstream of Kettle G.S. due to attenuation from Stephens Lake; however, sensitivity was greatest at Conawapa G.S.

5.5. EXPLORATION OF PARAMETER UNCERTAINTY

Uncertainty associated with model parameterization was important to consider in terms of its effect on PMF simulations relative to climate change or hydrological model choice. An exhaustive analysis, however, was not practical given the scope of this study. Additionally, the user interface in the SSARR model was not conducive to automating a large number of solutions. Analysis of parameter uncertainty in the SSARR model was therefore limited to a local sensitivity analysis of the most significant model parameters, while uncertainty analysis in HEC-HMS and WATFLOOD involved a limited number of solutions.

The limited sampling of the parameter uncertainty range in HEC-HMS and WATFLOOD identified a number of behavioural local solutions to generate a range about the baseline PMF. Similar to the climate change impact analysis, this uncertainty band only captures a range of plausible PMF hydrographs associated with some behavioural samples; the uncertainty band does not quantify the entire range of parameter uncertainty that may exist. The limited uncertainty band provided sufficient information to compare the two models, and to compare the magnitude of parameter uncertainty with that from model structural and climate scenario uncertainty.

5.5.1. SSARR – SENSITIVITY ANALYSIS

The SSARR legacy model interface and parameters (tables versus single values) does not lend itself well to an automated setup; programming an uncertainty analysis similar to the other models was therefore prohibitive. This necessitated that a local, one-at-a-time sensitivity analysis be used to assess (a) local parameter sensitivity around the existing solution, and (b) a limited range of uncertainty about the baseline PMF hydrograph.

Each parameter in the PMF model was independently perturbed by +/-20% from its calibrated value, based on a sensitivity analysis conducted by Cunderlik & Simonovic (2005). Parameters represented by tables were adjusted by perturbing every table value by +/-20%. Because the SSARR model is semi-lumped, parameter values were adjusted from their respective values in every sub-basin of the model. The model was then run over the baseline PMF period, for all twenty-three sequences of PMF inputs, to determine the new critical PMF at Keeyask and Conawapa. Table 26 details the change in PMF peak flow and timing at each location in the model for each parameter change. Note that the SSARR model rounds flows of this magnitude to the nearest hundred (e.g. 0.76% change equates to a change of 100 m^3/s at Keeyask).

The most significant conclusion from Table 26 is that the PMF peak flows at both Keeyask G.S. and Conawapa G.S. are relatively insensitive to most of the parameter perturbations (relative to changes resulting from climate change impacts). Many of the changes are no more than 100 m^3/s (<1% change in peak flow), or just above the range of rounding for the model. This insensitivity is a result of the one-at-a-time analysis being limited to a search immediately around the existing model parameterization – a parameterization that is sufficiently critical that much of the LNRB reaches saturation during the simulation (i.e. 100% runoff

generation). As an example, Figure 24 shows the time series of runoff generation (as percent of moisture input) in the Upper Burntwood Basin. Initial saturated conditions are assumed as part of PMF, and then maintained by snowmelt and then the PMP. Runoff generation remains above 90% for the first two months of the simulation.

Table 26: Changes in PMF peak flow at Keeyask G.S. and Conawapa G.S. from local parameter sensitivity analysis in SSARR model

Parameter	Adj.	PMF Change – Keeyask G.S. (% of Baseline)	PMF Change – Conawapa G.S. (% of Baseline)
Base Melt Temperature (°C)	+20%	0.76	0.73
	-20%	0.76	0.00
Snow Melt Rate	+20%	0.76	0.73
	-20%	0.76	0.00
Soil Moisture Index – Percent Runoff	+20%	0.76	0.00
	-20%	-3.82	-3.65
Baseflow Infiltration Index – Baseflow Runoff Percent	+20%	-3.05	-2.19
	-20%	3.05	3.65
Surface vs Subsurface Runoff Ratio	+20%	0.76	0.00
	-20%	0.00	0.00
Basin Linear Reservoir Storage Times (hours)	+20%	-3.05	-2.19
	-20%	4.58	4.38
BII Storage Time for Rising Discharge (hours)	+20%	0.00	0.00
	-20%	0.76	0.00

The result is that the LNRB is in a critical state such that any single parameter change has little effect on the PMF (that is, any single parameter change has little effect on the runoff generation behaviour in Figure 24). Specifically, one-at-a-time perturbations (a) cannot significantly increase the runoff generation in the basin, and (b) cannot significantly reduce the effects of the near 100% runoff generation. The PMF at Conawapa G.S. is especially insensitive in Table 26, as a result of attenuation from additional upstream reservoirs (i.e. Stephens Lake).

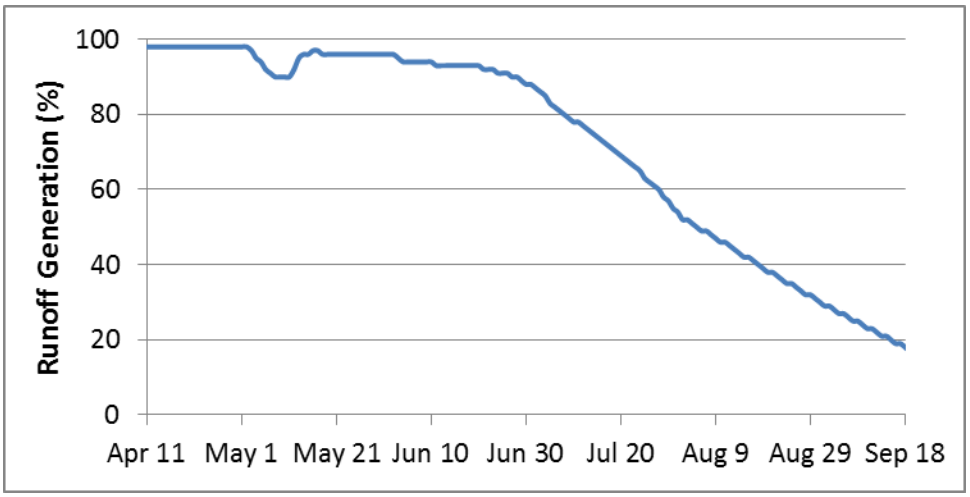

Figure 24: Runoff generation (as percent of moisture input) in the Upper Burntwood Basin during PMF simulation

There is, however, sensitivity at both sites to changes in the relationship between Baseflow Infiltration Index and percentage of runoff as baseflow (BII-BFLOW), and to changes in the storage times of linear reservoirs representing surface, subsurface, and baseflow. BII-BFLOW is the first partition from the runoff volume and thus has an impact on all three forms of runoff (i.e. runoff timing). Sensitivity to storage times continues to illustrate the significance of in-basin routing in PMF simulations (all three models). The difficulty in estimating storage time parameters, particularly for the invariant routing schemes in SSARR and HEC-HMS, makes this sensitivity even more significant.

5.5.2. HEC-HMS – Uncertainty Analysis

Parameter sets were randomly sampled from a uniform distribution with relatively wide ranges. Parameter ranges were similar to those used in the baseline Monte Carlo calibration outlined in Section 4.2.2 (that is, grounded in previous literature). However, the final calibrated solution in HEC-HMS included some values that were very close to the edge of their respective

parameter range. Therefore, in those cases, the sample ranges were widened for this analysis to allow for sampling parameter values that may not have been included in the initial calibration.

Re-sampling was conducted at the six gauged sub-basins, and new parameter values were then regionalized similar to the baseline PMF calibration. The global snowmelt rate table (six parameters controlling melt rate) and the base snowmelt temperature (one parameter) were also re-sampled to consider snowmelt uncertainty in the analysis. This amounted to a total of 91 decision variables (provided along with the ranges sampled within for each gauged sub-basin in Table 27.

Ten thousand parameter sets were run in the PMF period (given its shorter computation time as a single spring-summer period compared to the historical period). Ten thousand samples were initially used; however, given the number of decision variables, the sensitivity analysis was inconclusive and necessitated additional samples. Then, 2,500 samples with peak flows nearest to the baseline PMF were validated in the historical period (i.e., to test whether they were behavioural). The nearest samples were selected given that they had a higher chance of being representative of the calibration period. After running this subset through the historical period, 1,097 samples were found to be behavioural (i.e. adequately simulate peak flows in historical high flow years based on the criteria described in Section 4.3).

The ranges of PMF produced by (a) the 10,000 randomly sampled parameter sets, (b) the 2,500 nearest samples simulated in the calibration period, and (c) the 1,097 identified behavioural samples, are shown in Figure 25 at Keeyask G.S. and Conawapa G.S. Note that both figures are limited to only the set of PMF inputs/timing found to be critical in the baseline scenario (April 20th rapid temperature increase, May 5th PMP).

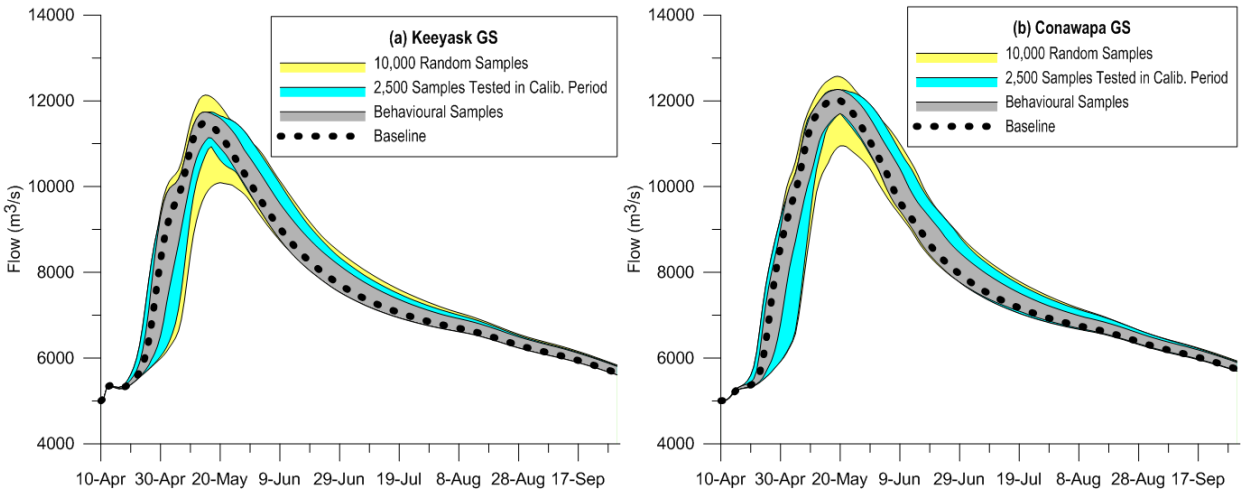

Figure 25: Progression of the HEC-HMS uncertainty envelope during each step of the analysis, at (a) Keeyask G.S., and (b) Conawapa G.S.

Random samples tested directly in the PMF case resulted in a band (yellow shaded) about the baseline PMF. The range of PMFs from samples tested in the calibration period (blue shaded) is representative of much of the original uncertainty band, with less representation at the peak.

The population subset was selected based on the hypothesis that samples with peak flows similar to the baseline were more likely to be behavioural. A large majority of random samples produced PMFs below the baseline, and the purpose of this analysis was to consider the samples expected to be most likely, not necessarily the samples that are most catastrophic. Therefore, selection criteria that fully represents the original uncertainty band (yellow shaded) above the baseline peak flow (a) would require a much larger subset to equally represent above and below the baseline (80-95% of the population), or (b) would bias the selection of random samples, and potentially the resulting parameter uncertainty envelope, towards those samples with PMFs above the baseline.

Table 27: Decision variables and ranges sampled for exploration of parameter uncertainty in HEC-HMS

Parameter	Units	Upper Btwd.	Odei River	Gunisao River	Grass River	Kettle River	Limestone River
Canopy Maximum Storage	mm	2.5	2.2	2.3	2.3	2	2.5
Surface Maximum Storage	mm	8 – 50	10 – 30	15 – 50	10 – 75	20 – 40	15 – 40
Percent Impervious Area	%	15 – 40	7 – 20	5 – 20	11 – 18	7 – 20	15 – 35
Soil Maximum Infiltration	mm/hr	1 – 3.5	1 – 2	1.4 – 3	1.8 – 4	0.8 – 2.2	0.6 – 2
Soil Maximum Storage	mm	180 – 280	230 – 350	160 – 240	180 – 243	160 – 240	195 – 300
Soil Tension Storage	Frac. of max storage	0.5 – 0.75	0.6 – 0.7	0.6 – 0.8	0.4 – 0.6	0.5 – 0.7	0.5 – 0.7
Soil Maximum Percolation	mm/hr	0.4 – 2	0.3 – 1.2	0.5 – 1.25	0.4 – 0.9	0.25 – 0.9	0.25 – 0.7
Groundwater Max. Storage (Upper)	mm	100 – 160	80 – 130	115 – 175	150 – 220	120 – 180	85 – 130
Groundwater Storage Coeff. (Upper)	hr	740 – 1148	556 – 1050	640 – 723	1300 – 2400	411 – 750	495 – 800
Groundwater Max. Percolation (Upper)	Frac. of Soil Perc.	0.6 – 1	0.55 – 0.85	0.6 – 1	0.45 – 0.7	0.5 – 0.8	0.5 – 0.85
Groundwater Max. Storage (Lower)	mm	80 – 120	70 – 130	95 – 140	160 – 230		
Groundwater Storage Coeff. (Lower)	hr	1025 – 1600	854 – 1800	854 – 1655	2608 – 3325		
Groundwater Max. Percolation (Lower)	Frac. of GW1 Perc.	0.6 – 1	0.5 – 0.9	0.55 – 1	0.45 – 0.7		
Time of Concentration	hr	248 – 373	200 – 290	236 – 354	519 – 778	109 – 163	182 – 250
Surface Storage Coefficient	hr	339 – 591	259 – 425	419 – 687	745 – 960	325 – 600	173 – 250
Global Parameters							
Snowmelt Rate	mm/°C/ day	0.01 - 6	0.05 - 6	0.1- 6	0.5 - 6	1 - 6	2 - 6
Base Snowmelt Temperature	°C	-5 - 0					

After filtering to only include samples that met the behavioural threshold over the calibration period (gray shaded), the uncertainty band was nearly unchanged on the rising limb, peak, or early falling limb at both stations. This result suggests two findings. First, given that no further narrowing of the uncertainty band was observed when only considering behavioural parameter sets, it was considered acceptable to move forward with the uncertainty band from the behavioural samples only. Second, samples at the edges of the tested band were behavioural; this suggests that there are likely additional behavioural samples outside of this range (i.e. samples producing higher or lower PMFs than those tested). The scope and time available for this study prohibited testing a wider range of samples. However, such an analysis would be advantageous to identify additional behavioural samples and more fully explore the PMF uncertainty band.

Samples identified as behavioural were further tested in the PMF period for a wider range of meteorological sequences (sequences 4-13 from Table 14), with the hypothesis that varying parameter sets may lead to PMFs with different critical inputs. Figure 27 shows the frequency of critical input timings when tested with each behavioural sample, and Figure 26 displays the uncertainty bands at Keeyask G.S. and Conawapa G.S. after ensuring that all behavioural samples produced their most critical PMF hydrograph. This uncertainty band is the most complete of any shown in this section, being mindful that the bands may be (a) narrowed given a subset of the nearest samples were tested in the calibration period, and (b) biased towards lower values due to the lack of manual adjustments compared to the baseline PMF hydrograph.

Figure 26 illustrates that the PMF hydrographs (peak flow and timing) are sensitive to plausible changes to the HEC-HMS model parameter set. Samples deemed to be behavioural resulted in simulations with higher peak flows and either the same or later critical timing,

suggesting that different combinations of parameters can lead to comparable representation in the historical period but variable PMFs.

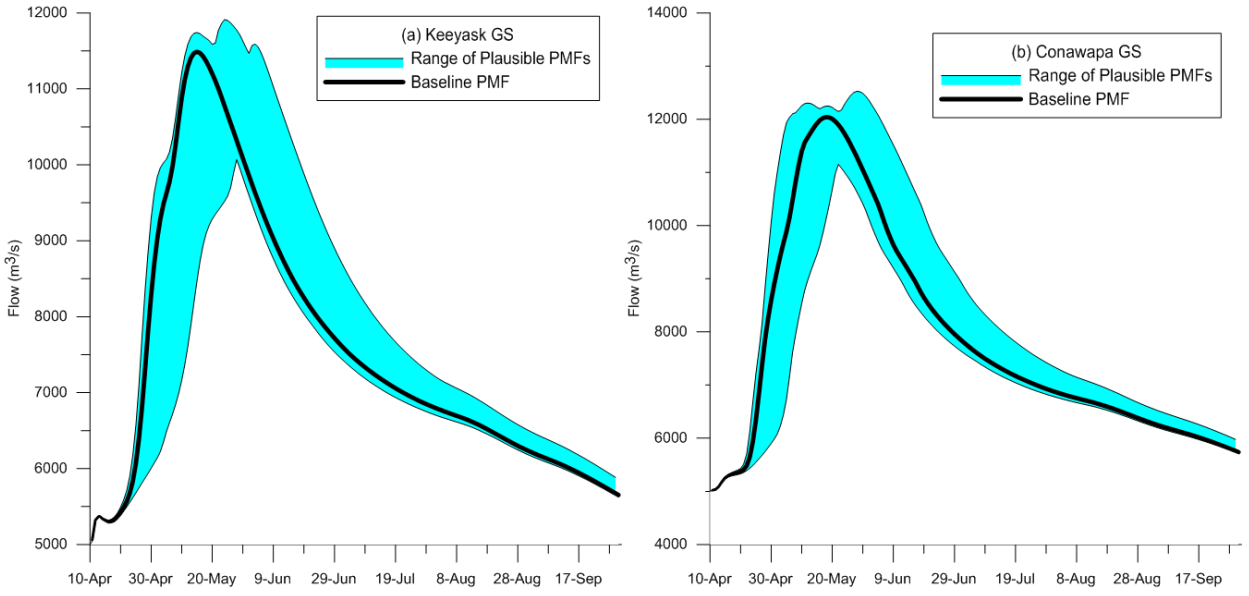

Figure 26: Envelope of plausible PMF hydrographs from behavioural HEC-HMS parameter sets at (a) Keeyask G.S., and (b) Conawapa G.S.

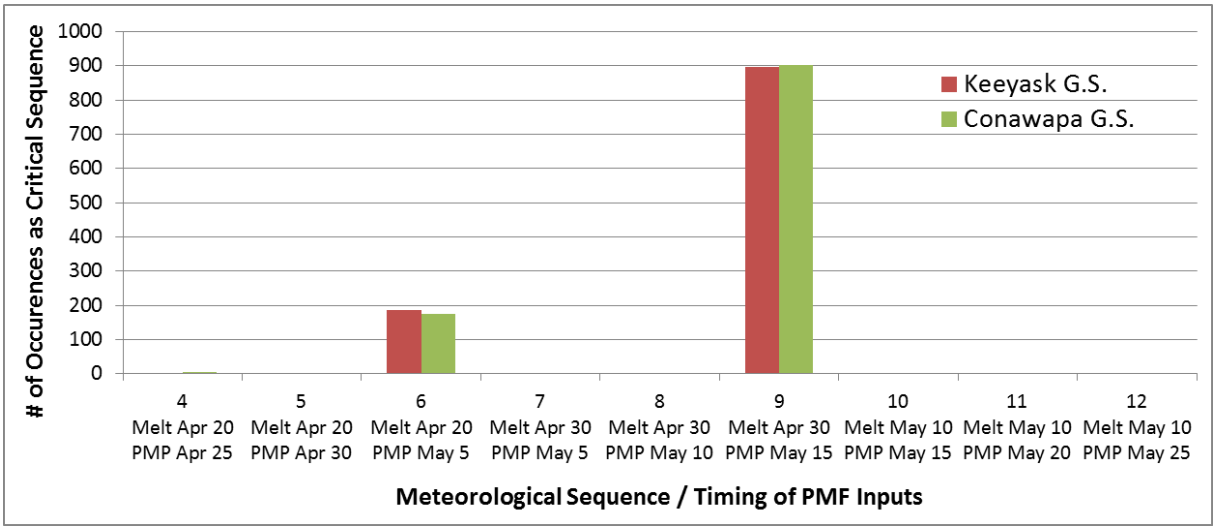

Figure 27: Histogram of critical PMF input sequence for behavioural HEC-HMS samples

The range of hydrographs varied between Keeyask G.S. and Conawapa G.S. (upstream and downstream ends of the Lower Nelson River Complex, respectively). At Keeyask, the set of peak flows encountered ranged from +3.7% to -2.2% of the baseline, while at Conawapa the

range of peak flows was +4.0% to -2.6%. The baseline PMF thus falls around the 60th percentile of the uncertainty band in both cases. Importantly, when a stricter behavioural threshold was tested (accepting 5% of samples), the change in the uncertainty range at the peak flow at Keeyask was negligible (5% range, versus 6% in Figure 26).

Figure 27 also corroborates that a later critical timing can result in a higher PMF. A ten-day shift of the timing of rapid snowmelt and PMP more often produces the most critical PMF, among the samples tested. Such a later shift, which allows for a later and larger PMP, could be produced by more gradual snowmelt or a higher base snowmelt temperature (e.g., as in the SSARR results shown previously). In general, from Figure 27, the PMF in HEC-HMS at both Keeyask and Conawapa is most critical when the PMP occurs fifteen days after temperatures increase to drive snowmelt (i.e. sequences 6 and 9). This behaviour is also limited to snowmelt occurring in the latter half of April. This finding may assist in narrowing the scope of future PMF review studies of the LNRB using HEC-HMS.

A final step of the analysis was to identify decision variables in HEC-HMS that were particularly impactful on PMF. The Monte Carlo Analysis Toolbox (MCAT) in MATLAB was utilized for ease of analysis (Wagener, Wheater, & Lees, 2004); specifically, a regional sensitivity analysis tool in MCAT was used to visually assess parameter sensitivity. As an example, Figure 28 below displays the regional sensitivity analysis results for the time of concentration (t_c) parameter. Note that the analysis considers changes to peak flows at Keeyask G.S. and time of concentration, as with other HEC-HMS parameters, is parameterized at the six gauged sub-basins (and regionalized from there).

The regional sensitivity analysis ranks the data by magnitude of peak flow at Keeyask G.S., separates the data into ten groups, then plots the cumulative distribution of each group with

respect to the decision variable of interest; greater separation among the CDFs denotes greater sensitivity (Wagener et al., 2004). Figure 28 illustrates, as an example, that the larger basins with outflows further downstream (Odei and Grass rivers) are more sensitive to t_c changes.

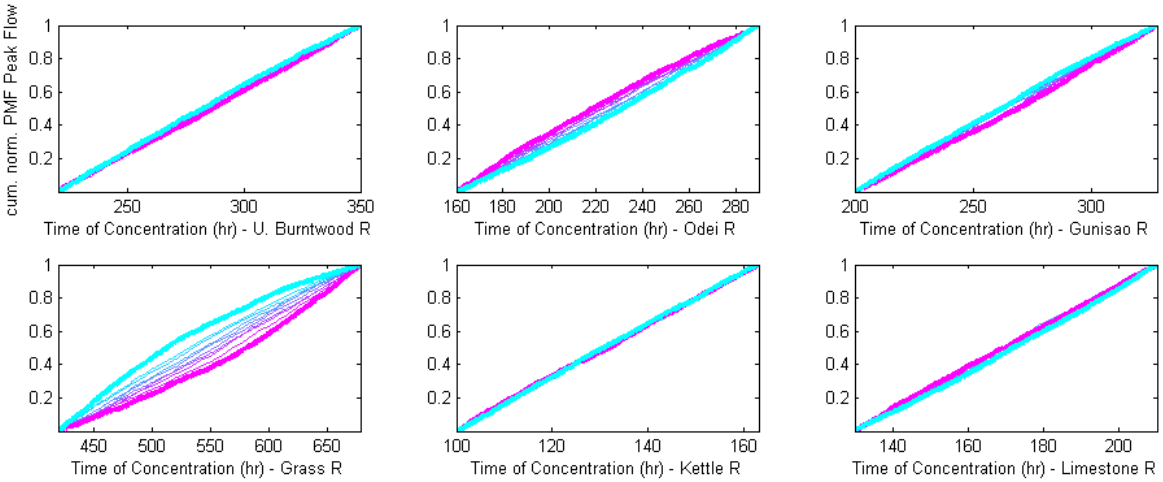

Figure 28: Regional sensitivity analysis results for the time of concentration parameter in HEC-HMS (unique to each gauged sub-basin)

Initial sensitivity results were largely inconclusive – this was assumed to be a result of the number of decision variables (91 in HEC-HMS). To provide meaningful results, an additional 10,000 parameter sets were randomly sampled and simulated in the PMF period. The regional sensitivity analysis (e.g. Figure 28) was then based on all 20,000 total parameter sets and produced non-negligible results. (Importantly, only the initial 10,000 samples were used in the uncertainty analysis above, to maintain comparability with WATFLOOD). The qualitative sensitivity analysis, comparing between basins and between parameters, had the following findings:

- The effect of catchment-specific parameters in HEC-HMS is apparent. Greater sensitivity was observed in parameters associated with the Grass and Odei river basins (i.e. larger basins further downstream with less distance between the outlet and the point of interest).

- There is negligible sensitivity to surface parameters (surface storage and percent impervious area). The insensitivity to impervious area contradicts observations during manual calibration, and may be the result of discretizing the parameter range too widely.
- There is significant sensitivity to subsurface percolation values (i.e. from the soil layer, upper baseflow and lower baseflow layers). Percolation from the lower baseflow layer represents a permanent "deep groundwater" loss; sensitivity to percolation values throughout the subsurface is associated with increases or decreases in this loss. In contrast, soil and baseflow storage parameters showed negligible sensitivity.
- There was also significant sensitivity to storage coefficients. This is not surprising given that these empirical parameters influence the amount of attenuation in the runoff hydrograph. Sensitivity was highest for surface runoff, and decreased with depth.
- Time of concentration was sensitive in larger basins with outlets further downstream (the Odei and Grass rivers). The sensitivity was less than that of the other Clark Unit Hydrograph parameter (surface storage coefficient), particularly for local basins directly upstream of Keeyask G.S. (dependent on Kettle River and Limestone River parameters).
- Base snowmelt temperature is one of the most sensitive parameters tested; namely, higher PMFs generally have lower (colder) base melt temperature. The higher and later peak flows observed in the uncertainty bands at Keeyask and Conawapa (Figure 26) are thus likely not attributable to a higher base melt temperature compared to the calibrated solution. This is also intuitive given the attenuation within HEC-HMS routing noted in Chapter 5.2 (i.e. melt runoff takes longer to reach the point of interest).
- There is also significant sensitivity to the stepped melt rate values in the temperature-index snowmelt function. Specifically, higher PMFs are generally associated with higher

melt rates. The later and more critical PMFs at the top of the uncertainty bands in Figure 26 may, in part, be attributed to higher snowmelt rates.

- Finally, the analysis illustrates very low sensitivity to parameters associated with the Limestone River basin. This is accurate, given that this basin is downstream of Keeyask G.S. (save for minor local areas with regionalised parameters from the Limestone River), and increases confidence in the results from this approach.

The parameter sensitivity analysis emphasized snowmelt, processes that affect the magnitude of deep groundwater losses (a unique feature in HEC-HMS among the models in this study), and empirical parameters that directly impact the amount of runoff attenuation. Parameters representing "bucket" storage had negligible effects on peak flows at Keeyask G.S. Figures from the regional sensitivity analysis are provided in Appendix G.1.

5.5.3. WATFLOOD – UNCERTAINTY ANALYSIS

The analysis conducted in WATFLOOD followed a similar methodology as that for HEC-HMS, save for the number of decision variables tested. Table 28 displays the decision variables and ranges sampled for each land cover/river class type. The ranges are very similar to those used in the DDS model calibration, save for the following: (a) ranges were slightly narrowed here for channel roughness, recharge coefficient, and melt rate based on knowledge gained during calibration related to realistic values of parameters, and (b) base snow melt temperature was included in the uncertainty analysis based on its significance during manual adjustments. As in the calibration, values for the Footprint River class and impervious land class were not included due to their relatively small areas in the LNRB. The result was 64 decision variables considered in the WATFLOOD parameter uncertainty exploration.

Table 28: Decision variables and ranges sampled for exploration of parameter uncertainty in WATFLOOD

Parameter	River Class Parameters								
	Btwd	Nelson	Upper Btwd	Odei	Grass	Minago	Kettle	Lime-stone	Foot-print
Channel Roughness	0.001-0.02	0.001-0.02	0.001-0.02	0.001-0.02	0.001-0.02	0.001-0.02	0.001-0.02	0.001-0.02	
Wetland Porosity	0.1 – 0.75	0.1 – 0.75	0.1 – 0.75	0.1 – 0.75	0.1 – 0.75	0.1 – 0.75	0.1 – 0.75	0.1 – 0.75	
Wetland Lateral Conductivity	0.1 – 0.9	0.1 – 0.9	0.1 – 0.9	0.1 – 0.9	0.1 – 0.9	0.1 – 0.9	0.1 – 0.9	0.1 – 0.9	
	Land Class Parameters								
	Conif. Forest	Mixed Forest	Treed Rock	Shrub	Bogs	Non-Conn. Wetland	Conn. Wetland	Water	Imper-vious
Infiltration Coefficient	0.04 – 50	0.04 – 50	0.04 – 50	0.04 – 50	0.04 – 200	0.04 – 200	N/A	N/A	
Upper Zone Retention (mm)	1 – 200	1 – 200	1 – 200	1 – 200	1 – 200	1 – 200	N/A	N/A	
Interflow Coefficient	0.05 – 10	0.05 – 10	0.05 – 10	0.05 – 10	0.05 – 10	0.05 – 10	N/A	N/A	
Recharge Coefficient	0.01 – 0.2	0.01 – 0.2	0.01 – 0.2	0.01 – 0.2	0.01 – 0.2	0.01 – 0.2	N/A	N/A	
Melt Rate (mm/°C/hr)	0.05 – 0.4	0.05 – 0.4	0.05 – 0.4	0.05 – 0.4	0.05 – 0.4	0.05 – 0.4	0.05 – 0.4	0.05 – 0.4	
Base Melt Temp.(°C)	-3 – 2	-3 – 2	-3 – 2	-3 – 2	-3 – 2	-3 – 2	-3 – 2	-3 – 2	

Ten thousand randomly sampled parameter sets were run for the PMF period; given the lower number of decision variables, a smaller number of simulations were needed to sufficiently qualify parameter sensitivities (as compared to HEC-HMS). Then, 2,500 samples with peak flows nearest in magnitude to the baseline PMF were validated in the historical period (i.e., to

test whether they were behavioural). The nearest samples were selected given that they had a higher chance of being representative of the calibration period, and time was limited (approximately 40 days to simulate all 2,500 samples in the calibration period). A total of 638 solutions were identified as behavioural from among the 2,500 validated sets.

The ranges of PMF produced by (a) the 10,000 randomly sampled parameter sets, (b) the 2,500 nearest samples simulated in the calibration period, and (c) the 638 identified behavioural samples, are shown in Figure 29 at Keeyask G.S. and Conawapa G.S. Note that both figures are limited to only the set of PMF inputs/timing found to be critical in the baseline scenario (May 1st rapid temperature increase, May 5th PMP). Instability in approximately 5% of the automated simulations at Keeyask and 10% of the automated solutions at Conawapa (of the 10,000 samples run on the PMF period) caused errors which led to missing volume from upstream contributions (Notigi, Jenpeg); these simulations resulted in abnormally low PMFs and were removed from the analysis.

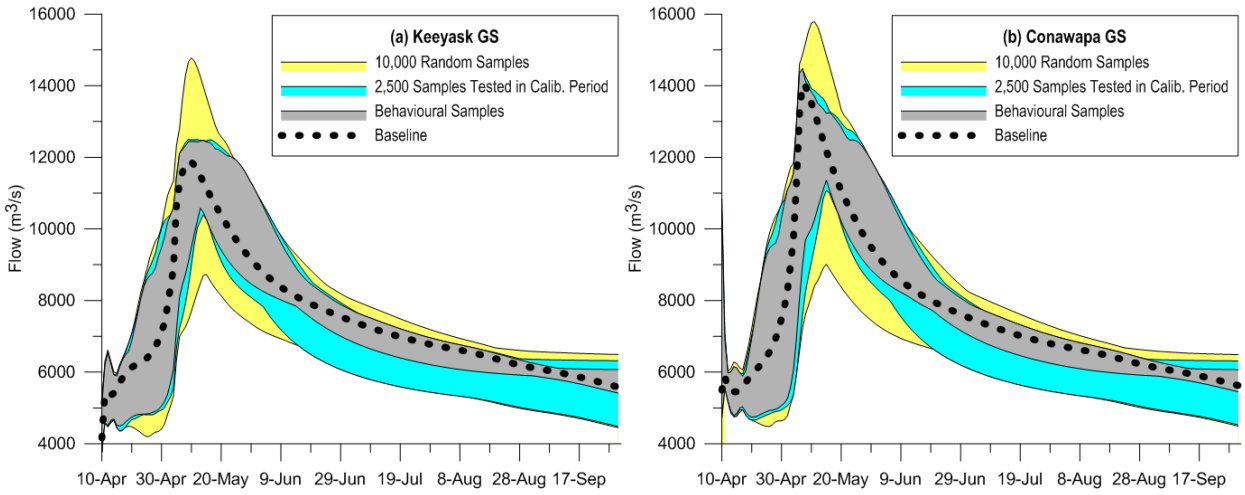

Figure 29: Progression of the WATFLOOD uncertainty envelope during each step of the analysis, at (a) Keeyask G.S., and (b) Conawapa G.S.

The random samples tested directly on the PMF case resulted in a wide band (yellow shaded) about the baseline PMF at both generating stations, particularly at the peak flow. This is

not unexpected given that wide parameter ranges were used to maintain the independence of every sample. The band is also wider in WATFLOOD than HEC-HMS (Figure 25).

Other findings from Figure 29 are similar to those reported for HEC-HMS, namely:

- The range of PMFs based on samples tested in the calibration period (blue shading) captured the majority of the original uncertainty band, except at the peak flow. This is once again a result of bias in the selection criteria, and a larger band of uncertainty encountered in WATFLOOD. An explanation is further provided in Section 5.5.2.
- Restricting to only behavioural samples resulted in no further narrowing of the uncertainty band at the critical areas of the hydrograph, at both Keeyask and Conawapa.

Similar to the finding for HEC-HMS, analysis of a wider range of samples over the calibration period would lead to further exploration of the PMF uncertainty band. This is particularly true for WATFLOOD, given the significant uncertainty at higher peak flows that was not tested.

As a final step, samples identified as behavioural were tested in the PMF period for a wider range of meteorological sequences (specifically, sequences 4-13 from Table 14). Figure 31 shows the frequency of critical input timings when tested with each behavioural solution, and Figure 30 displays the uncertainty bands at Keeyask G.S. and Conawapa G.S. after ensuring that all behavioural samples produced their most critical PMF hydrograph. This uncertainty band is the most complete of any shown in this section, although the bands may be (a) narrowed based on the subset of samples tested in the calibration period, and (b) biased towards lower values due to the lack of manual adjustments compared to the baseline PMF hydrograph.

Figure 30 illustrates that the PMF hydrographs (peak flow and timing) are sensitive to plausible changes to the WATFLOOD model parameter set. Samples deemed to be behavioural resulted in both earlier and later critical timings with higher peak flows, suggesting that different

combinations of parameters can lead to comparable representation in the historical period but variable PMFs.

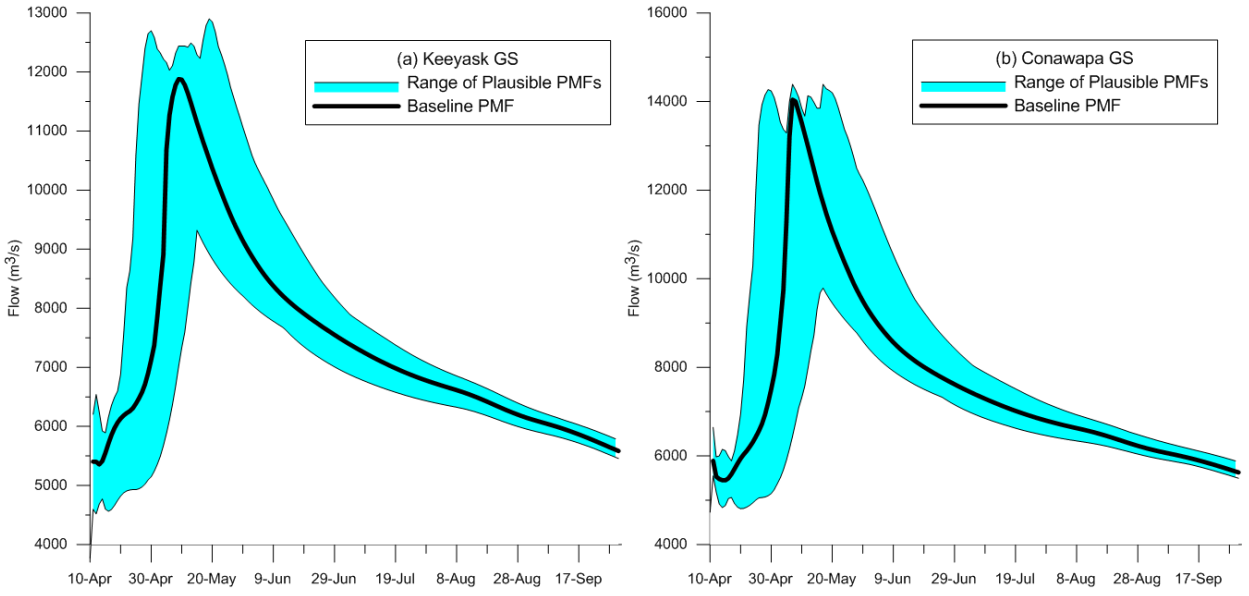

Figure 30: Envelope of plausible PMF hydrographs from behavioural WATFLOOD parameter sets at (a) Keeyask G.S., and (b) Conawapa G.S.

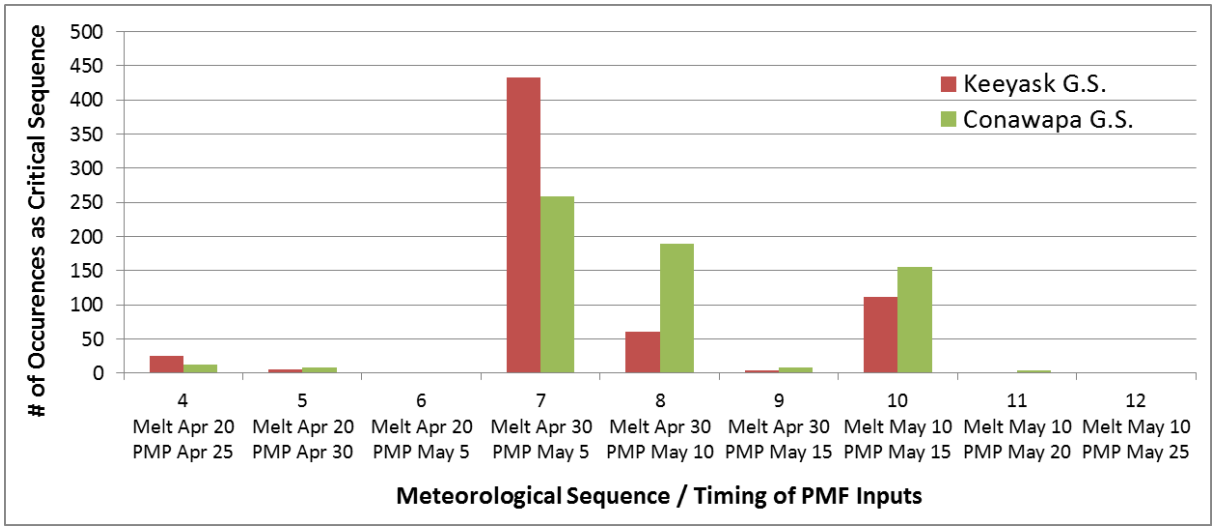

Figure 31: Histogram of critical PMF input sequence for behavioural WATFLOOD samples

The envelope of uncertainty around the hydrograph peak varied between Keeyask G.S. and Conawapa G.S. (upstream and downstream ends of the Lower Nelson River Complex,

respectively). At Keeyask G.S., the set of peak flows encountered ranged from +8.6% to -5.2% of the baseline, suggesting that when accounting for varying timing, the PMF at Keeyask G.S. could be significantly larger as a result of varying parameters within the model. In contrast, at Conawapa G.S., the baseline hydrograph peaked near the top of the envelope, and the peak flows encountered ranged from +2.5% to -14.9%. This further supports the previous finding that the baseline calibration in WATFLOOD produces an aggregation of local and upstream runoff at Conawapa G.S. that is very extreme; the behavioural re-samples were rarely able to produce a higher peak flow. Finally, as with HEC-HMS, when a stricter behavioural threshold was tested (accepting 2% of solutions for WATFLOOD), the range at the peak flow at Keeyask decreased to 12% from 14% in Figure 30.

Figure 31 again shows that some parameter sets led to different critical timings of PMF inputs. The PMF at both Keeyask G.S. and Conawapa G.S. was most often produced by the same timing of inputs as that for the baseline PMF calibration. However, there was sensitivity to later shifts, particularly at Conawapa. In general, from Figure 31, the PMF in WATFLOOD at Keeyask is most critical when the PMP occurs five days after temperatures increase to drive snowmelt (i.e. sequences 4, 7, 10), while there is more flexibility of the critical PMF timing at Conawapa. This finding may assist in narrowing or shifting the scope of future PMF review studies of the LNRB using WATFLOOD (i.e. it may be unnecessary to test sequences where PMP occurs ten or fifteen days after rapid melt begins).

The regional sensitivity analysis tool in MCAT (Wagener, Wheater, & Lees, 2004) in MATLAB was once again utilized to identify the relative sensitivity of decision variables in WATFLOOD. As an example, Figure 32 displays regional sensitivity analysis results for the six parameters associated with the coniferous forest land class (the most significant landcover type

in the LNRB), and Figure 33 displays the results for the three parameters associated with the Odei river class. Both analyses consider impacts to peak flows downstream at Keeyask G.S.

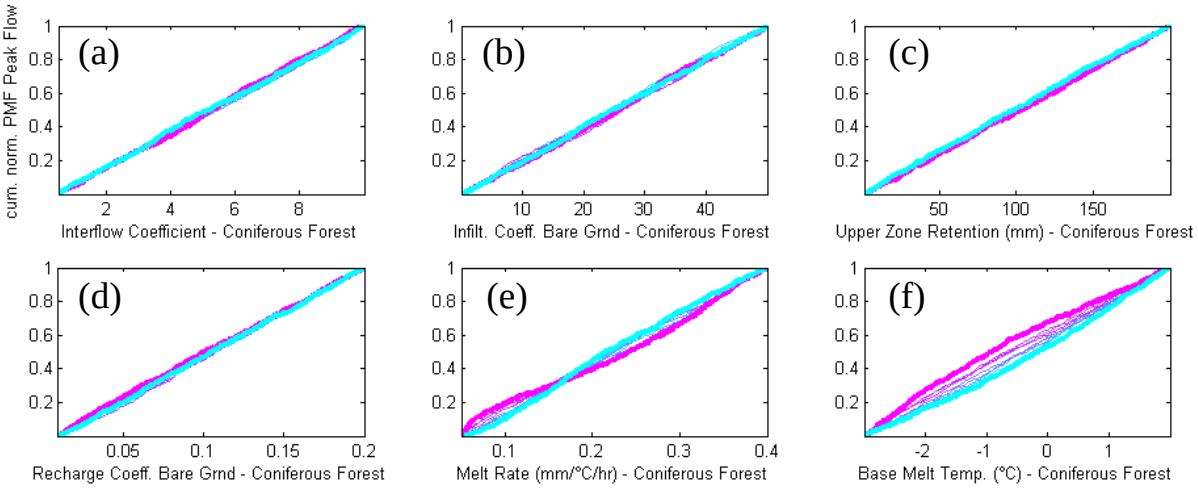

Figure 32: Regional sensitivity analysis of peak flow at Keeyask G.S. for coniferous forest land class parameters of (a) interflow coefficient, (b) infiltration coefficient, (c) upper zone retention, (d) recharge coefficient, (e) base snowmelt temperature, (f) snow melt rate

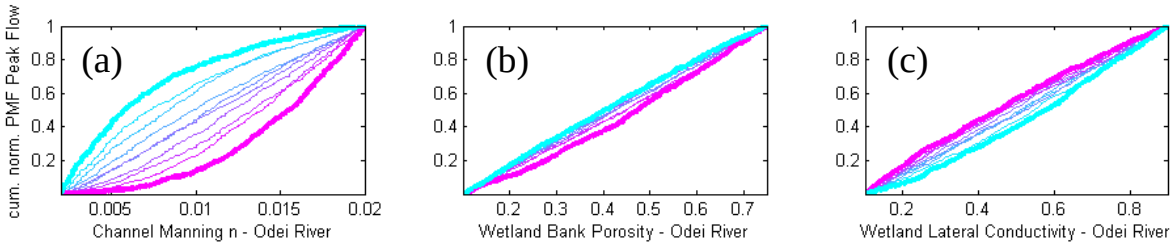

Figure 33: Regional sensitivity analysis of peak flow at Keeyask G.S. for Odei river class parameters of (a) channel roughness, (b) wetland/bank porosity, and (c) wetland/bank lateral conductivity

From Figure 32, the greatest sensitivity of PMF produced by WATFLOOD was to the snowmelt parameters, with very little sensitivity to subsurface parameters. Similarly, Figure 33 shows that there is significant sensitivity to routing parameters, including channel roughness for the Odei river class, with moderate sensitivity to the wetland parameters. This visual analysis was applied for all 64-decision variables with the following findings:

- The most sensitive parameter is channel roughness (r2n) for all river classes; in general, the sensitivity was proportional to the relative size of the area covered by that river class.
- PMF was also generally sensitive to wetland parameterization (porosity and lateral conductivity) and snowmelt parameters (base melt temperature and melt rate). Of these, base melt temperature and melt rate were equally significant across all eight land classes. Lateral conductivity (kcond) was more impactful than bank porosity (theta) across all eight river classes but particularly in classes with greater areas of surface water (Grass River, Minago River).
- Wetland parameters in river classes with a greater percent area of wetlands and with outlets lower in the LNRB were more sensitive (i.e. the Grass River and Odei River).
- Snowmelt parameters were more sensitive in land classes that make up a larger portion of the LNRB area (i.e. coniferous forest and surface water), and generally showed that higher PMF is associated with a warmer base melt temperature and moderate melt rate. In contrast, snowmelt parameters for land classes concentrated further upstream (e.g. treed rock) or associated with slower travel time (e.g. bogs and non-connected wetlands) were more critical with an earlier base melt temperature and faster melt rate.
- There was negligible sensitivity to the tested soil/subsurface parameters. Of the four parameters, upper zone retention was the most important.
- There was no relationship between sensitivity of soil/subsurface parameters and land class areas or locations in the basin. Additional model runs would be required to determine with confidence whether PMF is insensitive to soil/subsurface parameters or if this is caused by interaction between parameters.

- As a quality check, the sensitivity analysis correctly showed that PMF at Keeyask G.S. was not sensitive to river class parameters downstream of the station (i.e. for Kettle River and Limestone River).

The sensitivity analysis thus emphasized the importance of snowmelt parameters for land classes/GRUs and channel roughness and wetland lateral conductivity for river classes. Meanwhile, the results suggested that PMF scenarios modelled in WATFLOOD are less sensitive to soil and subsurface parameters. Figures output from the regional sensitivity analysis are separated by parameter and presented in Appendix G.2.

5.5.4. Summary & Comparison of Ranges

To synthesize the analyses in this research, this section quantifies the range of PMF scenarios encountered as a result of (a) baseline PMF runs in multiple models (HEC-HMS and WATFLOOD), (b) parameter uncertainty testing, and (c) projected climate change impacts, at both Keeyask G.S. and Conawapa G.S. The ranges are defined by their maximum, minimum, and median, relative to the baseline, in each model. Model uncertainty is defined by the difference in baseline PMF from HEC-HMS and WATFLOOD. Table 29 shows results at Keeyask (also generally representative for Kettle G.S. inflows), while Table 30 shows results at Conawapa G.S. (also generally representative for Long Spruce G.S. and Limestone G.S.).

Table 29: Ranges of PMF at Keeyask G.S. caused by varied sources of change (% change relative to baseline PMF)

	Multi-Model Baseline PMF (%)	Parameter Uncertainty (%)			Proj. Climate Change Impacts (%)		
		MIN	MED	MAX	MIN	MED	MAX
SSARR	N/A	-3.8	0.8	4.6	-11.5	0.8	12.2
HEC-HMS	3.3	-2.2	0.5	3.7	-8.8	1.0	12.5
WATFLOOD		-5.2	-1.7	8.6	-10.4	-1.5	10.4

Table 29 illustrates a number of relationships between the sources of uncertainty of the PMF models at Keeyask, in particular:

- The range of parameter uncertainty from WATFLOOD is comparable to the range of uncertainty from projected climate change impacts. HEC-HMS displays a much narrower parameter uncertainty range, especially when compared relative to climate change impacts (and despite having a greater number of decision variables). SSARR displayed a similarly reduced parameter uncertainty envelope (though from a limited one-at-a-time sensitivity analysis). Therefore, parameter uncertainty was greatest in the more complex (and distributed) WATFLOOD model, while HEC-HMS was less sensitive in both analyses. In contrast, Bastola, Murphy, & Sweeney (2011) found the parameter uncertainty envelope was largest in the model with the most decision variables (HEC-HMS in this research).
- The degree of uncertainty related to climate change impacts was not clearly dependent on model type; rather, uncertainty was larger from the model (SSARR) that was calibrated to a more limited period and that consistently overestimated historical peak flows.
- Previous literature on uncertainty in hydrological model simulations at high flows consistently found that projected climate change impacts are the largest source of uncertainty (e.g. Chen, Brissette, Poulin et al., 2011; Kay & Jones, 2012; Najafi, Moradkhani, & Jung, 2011). This multi-model study on PMF had a similar finding.
- However, the literature does not so closely agree on the relationship between model and parameter uncertainty; the results above are similarly unclear. Recall Butts, Payne, Kristensen, & Madsen (2004) found model uncertainty to be larger than parameter uncertainty, while Steinschneider, Wi, & Brown (2015) found the two to be of similar

magnitude. This research found differences due to model structure to be smaller than those from parameterization, albeit only two models calibrated over the same period were considered.

- Given that only the nearest 25% of candidate samples were tested on the historical period, parameter uncertainty of PMF at Keeyask G.S. should be treated as equally significant as uncertainty from climate change impacts. This is in contrast to findings from previous studies (Chen, Brissette, Poulin, et al., 2011; Exbrayat et al., 2014).
- Considering the median from each range of PMFs, no source of uncertainty displays a clear direction in any of the three models.

Similarly, Table 30 shows the range of plausible PMFs at Conawapa resulting from the parameter uncertainty and climate change analyses, and the difference between baseline PMF peak flows from HEC-HMS and WATFLOOD.

Table 30: Ranges of PMF at Conawapa G.S. caused by varied sources of change (% change relative to baseline PMF)

	Multi-Model Baseline PMF (%)	Parameter Uncertainty (%)			Proj. Climate Change Impacts (%)		
		MIN	MED	MAX	MIN	MED	MAX
SSARR	N/A	-3.7	0.0	4.4	-11.7	0.0	19.7
HEC-HMS	15.3	-2.6	0.3	4.0	-9.3	0.6	12.2
WATFLOOD		-14.9	-2.6	2.5	-14.4	-3.2	13.0

Similar to the results at Keeyask G.S., projected climate change impacts remain the largest source of uncertainty, with relatively similar ranges between the three models (neglecting upstream overtopping effects in SSARR). Parameter uncertainty is similar in the two semi-distributed models (SSARR and HEC-HMS) and larger in the more complex, distributed model

(WATFLOOD). However, a number of differences from Table 29 become apparent when considering Conawapa G.S. (i.e. the most downstream generating station). Namely:

- Model uncertainty in baseline PMF grows to be larger than or equal to parameter uncertainty. This growth in model uncertainty is primarily due to a significantly higher baseline PMF in WATFLOOD (evidenced by the larger parameter uncertainty range). The results illustrate the greater impact of model differences on local inflows; this also falls closer to conclusions found in the literature.
- Uncertainty in WATFLOOD is skewed towards decreased PMF at Conawapa G.S. relative to the baseline; both parameter changes and input changes generally caused more significant decreases in the PMF relative to the other models. This reinforces that a critical combination of upstream and local inflow timing at Conawapa G.S. was achieved in the baseline calibration of WATFLOOD. SSARR and HEC-HMS, in contrast, simulate approximately equal uncertainty in both directions.

The rank of different sources of uncertainty is expected to be similar at the two generating stations directly upstream of Conawapa G.S. (Long Spruce G.S., Limestone G.S.). However, the Limestone River, which had a significant impact at Conawapa G.S., is downstream of both sites.

The comparison of uncertainty sources at both generating stations illustrates similarities to past uncertainty literature, with the exception of greater impacts from parameterization as the models are extrapolated to extreme PMF conditions. In general, the results do not provide guidance on a clear direction of PMF estimates relative to the baseline; however, the relative size of uncertainty envelopes provide important information to guide future hydrological modelling and PMF review studies in the LNRB, and future studies of uncertainty surrounding PMF estimates.

6.0. CONCLUSIONS AND RECOMMENDATIONS

The sensitivity, and in some cases uncertainty, of Probable Maximum Flood (PMF) estimates in the Lower Nelson River Basin (LNRB) to choice of hydrological model, parameter uncertainty, and projected climate change impacts on PMF inputs, was explored in this research. Two modern hydrological models with existing user support (HEC-HMS, WATFLOOD) were calibrated for extrapolation to PMF conditions and compared to an existing calibrated PMF model for the LNRB (SSARR). Performance in historical high flow years in HEC-HMS and WATFLOOD differed greatly from that of the SSARR model. Differences between the models due to calibration period and model structure were also evident in the baseline PMF results.

Climate change impacts on PMF inputs were provided using fourteen Regional Climate Model (RCM) simulations analyzed by Ouranos as part of an NRCan study on PMP/PMF under changing climate conditions (Ouranos, 2015). The range of projections was wide for all four PMF inputs, a result of uncertainties inherent in the RCM simulations and data analysis process. Finally, a limited parameter uncertainty analysis was conducted in each hydrological model. In SSARR, only local sensitivity around the existing parameterization was considered. In HEC-HMS and WATFLOOD, a randomly sampled group of parameter sets was simulated for PMF conditions and used to assess both parameter sensitivity and uncertainty.

6.1. CONCLUSIONS

Findings from this research, detailed here, are separated by the major analyses, namely: (1) the application of calibration methodologies to HEC-HMS and WATFLOOD for PMF calibration and comparison of the models over historical high flow years, (2) the effect of hydrological model choice and calibration period on PMF simulations, (3) the incorporation of

climate change impacts on PMF inputs and sensitivity of PMF estimates to these projections, (4) parameter sensitivity and/or uncertainty in all three models, and (5) a comparison of the sources of uncertainty analyzed in this research.

The following conclusions relate to the development and calibration of HEC-HMS and WATFLOOD models for PMF simulation, and comparing the performance of those models for historical high flow years to an existing PMF model in SSARR:

- Calibration of HEC-HMS and WATFLOOD to a set of the highest flow years in the LNRB in the period of record led to different snowmelt parameterization than the earlier calibration period in SSARR. Namely, snowmelt generally occurred earlier in more recent high flow years.
- HEC-HMS and WATFLOOD achieved comparable and acceptable performance, on average, during the calibration and validation periods. A validation of the existing SSARR model to the same periods found that it generally overestimated peak flows and runoff volume, and failed to satisfy several basin-average performance metrics.

The following conclusions focus on the impact of hydrological model choice and calibration period on PMF simulations:

- Traditional PMF assumptions are difficult to incorporate into more complex models (i.e. HEC-HMS and WATFLOOD). Both models have additional vertical storage reservoirs and more complex parameterizations that prevent exact replication of historical PMF assumptions. This reduced the comparability to the existing SSARR PMF model.
- Earlier snowmelt in HEC-HMS and WATFLOOD led to an earlier critical PMF, characterized by earlier rapid melt and an earlier PMP. The earlier PMFs were less

critical than the PMF simulated by SSARR at upstream generating stations in the Lower Nelson River Complex (Keeyask G.S., Kettle G.S.). However, WATFLOOD simulated a more critical PMF at Conawapa G.S. as a result of local inflows and upstream inflows closely coinciding.

- HEC-HMS and WATFLOOD (calibrated to the same period) produced relatively similar baseline PMFs at Keeyask G.S. SSARR (calibrated to a limited period with distinctively later snowmelt) simulated a significantly higher PMF at most stations (e.g. 12% higher at Keeyask G.S.). Hence, an updated calibration period had a greater effect on PMF results than the choice or complexity of hydrological model.
- The semi-distributed models (SSARR and HEC-HMS) and distributed model (WATFLOOD) differed most notably in routing within sub-basin elements. Physically-based routing in WATFLOOD responded more rapidly than routing schemes such as time of concentration which do not vary with rainfall volume. This finding supports results from a previous study using time of concentration (Meyersohn, 2016).
- The earlier critical PMF in HEC-HMS and WATFLOOD place greater emphasis on snowmelt runoff, resulting in the baseline PMSA scenario being more comparable to the baseline PMP scenario. In contrast, the PMSA scenario is much less critical in SSARR.

The following conclusions relate to the incorporation of projected climate change impacts on PMF inputs and sensitivity of the hydrological models to PMF inputs:

- Significant uncertainty existed in the projected future changes to extreme PMF inputs, even when using RCMs. Uncertainty stemmed from model structure, natural climate

variability, and sampling uncertainty. This was manifested in relatively wide ranges of projections.

- Projected changes to initial snowpack had the most significant impact on all three PMF models. For example, a 1/100 year SWE change had 1.5-2.5 times more impact on peak flow magnitude than a similar PMP change. Sensitivity was greatest in WATFLOOD, then HEC-HMS, due to an earlier critical PMF.
- Sensitivity to the rainfall input was greatest in the SSARR model due to its later PMF timing that allows for a larger event (seasonality).
- Sensitivity to increased temperature was limited to changes in PMF timing: a number of critical PMF hydrographs were shifted earlier. In most cases, this negated a shift to later PMFs that occurred due to increased snowpack.
- Sensitivity to Lake Winnipeg outflows was similar in magnitude as sensitivity to PMP when considering individual future scenarios. However, outflow changes did not result in a change in the range of future projected PMFs.
- There is reduced sensitivity to PMF input changes at generating stations immediately downstream of Kettle G.S. due to attenuation from Stephens Lake. Conawapa G.S. has the greatest range of sensitivity of any generating station in the basin as a result of local inflows (5% of the total basin area) that are more volatile due to reduced attenuation.
- Projected increases in PMSA result in the median future PMF (PMSA) hydrograph being equivalent to the median future PMF (PMP) hydrograph in HEC-HMS and WATFLOOD. Therefore, the PMSA scenario cannot be assumed to be significantly less critical than the PMP scenario, especially when considering more robustly calibrated

models (more sensitive to snowpack) and projected effects of climate change. It is necessary to continue to test both scenarios in future PMF review studies.

- The sequence of inputs (PMP timing, date of temperature increase) that produces the critical PMF is not necessarily the same at each generating station. After projected impacts of climate change are accounted for, there is further variation in critical input sequences between the stations. Each generating station in the Lower Nelson River Complex may have a unique set of critical conditions that must be considered.

The following conclusions relate to the study of parameter sensitivity in all three models and the limited uncertainty analysis conducted in HEC-HMS and WATFLOOD:

- The parameter uncertainty envelope was largest in the distributed (i.e. more complex) WATFLOOD model. The WATFLOOD model had fewer decision variables than HEC-HMS, but was calibrated as a whole as opposed to the calibration of gauged sub-basin units separately in HEC-HMS. Despite differences in calibration period, the semi-lumped models (SSARR and HEC-HMS) yielded similar ranges of parameter sensitivity.
- The SSARR model in its current parameterization was insensitive to nearly all single parameter changes that were attempted. There was sensitivity observed to changes in the distribution of runoff as baseflow and changes in linear reservoir routing storage times.
- The HEC-HMS PMF model was most sensitive to parameters associated with snowmelt and processes that affected deep groundwater losses, as well as empirical parameters with a direct impact on runoff attenuation.
- The WATFLOOD PMF model was most sensitive to channel roughness, wetland and snowmelt parameters. These findings were consistent with those from HEC-HMS,

illustrating the significance of routing a large input volume (roughness and wetland effects) and the earlier critical PMF (snowmelt).

Finally, the following conclusions relate to the comparison of uncertainty from model selection, model parameterization, and PMF input changes. In all three cases, uncertainty is taken as the range in PMF that develops as a result of plausible/projected changes, and does not represent an exhaustive uncertainty band.

- Projected climate change impacts on PMF inputs were found here to be the largest source of uncertainty affecting the range of plausible PMFs. The climate change projections in this study incorporated uncertainty from both GCMs and RCMs (downscaling).
- Model parameterization was the next largest source of uncertainty followed by hydrological model choice (taken as the difference between HEC-HMS and WATFLOOD). The model uncertainty envelope may be limited by the use of only two hydrological models and the similarity of the models in some processes (e.g. snowmelt). The parameter uncertainty envelopes may be impacted by a limited sampling of parameter sets (for parameter uncertainty).

The conclusions stated here, framed in the context of the study objectives and findings from previous literature, illustrate advancement in the study of PMF simulations.

6.2. CONTRIBUTION TO CURRENT KNOWLEDGE AND STATE OF PRACTICE

PMF is a significant factor in dam design and dam safety reviews, yet uncertainties around estimated PMFs have not previously been thoroughly examined. The need for exploration has been recognized, including of the potential sensitivity to climate change effects (Chernet et

al., 2014), additional hydrometric data available for calibration (Environment Canada, 2004; Watt & Marsalek, 2013), and the development of new hydrological models (FEMA, 2012). However, many of the same studies acknowledge that this uncertainty is rarely explored (Alberta Transportation, 2004; Chernet et al., 2014), and the CDA suggest in their Technical Bulletin on Hydrotechnical Considerations for Dam Safety only that conservatism be employed in the absence of a recognized methodology for incorporating climate change (CDA, 2007).

This research was founded on existing PMF inputs for the LNRB and traditional PMF assumptions and methodologies used in practice. Its analysis then expanded beyond the typical scope of PMF studies to explore the knowledge gaps above. The results showed that the effects of climate change, hydrological model selection, model calibration period, and uncertainty around model parameterization can have significant impacts on PMF estimates.

It is intended that this study's contribution to the state of practice for PMF estimation may include, but not be limited to, the following:

- The currency and length of calibration period for a PMF model were found to be important, particularly in the context of a changing climate. PMF models calibrated to earlier historical periods may need to be considered more carefully by dam owners now that additional hydrometric data is available. A prescribed frequency of re-calibration may be a consideration for guidance documents.
- The impact of a change in calibration period had, in this case, a more significant impact than a change in hydrological model. A first experiment for dam owners may therefore be re-calibration instead of developing new models, particularly where there is internal expertise and confidence in a given hydrological model platform.

- The climate models applied in this study project a wide range of future impacts on PMF inputs, resulting in a large uncertainty band about the baseline PMF. Uncertainty was caused primarily by natural climate variability and sampling uncertainty. Further advancements in model data period lengths and super-ensembles of model runs are needed to have greater confidence in projections of PMF inputs and to confidently select a single index PMF value within the uncertainty band.
- This study produced a range of plausible PMFs around a baseline estimate but could not recommend a value to choose from within that range; that selection would be subjective to a dam owner's respective risk tolerance. However, the study concluded that the plausible range can be significant and should be considered in practice.
- The study also quantified the relative significance of each PMF input for the LNRB, which may be transposed to other similar basins of interest. In particular, changes in temperature and upstream flows were less significant; this may narrow the scope of future PMF studies. A linear relationship between PMP change and PMF change was found that may also be employed for initial calculations.
- The study utilized several hydrological models commonly applied in North America and qualified sensitive parameters in each model during high flow simulations. This can narrow the scope of calibration or re-calibration of PMF models.

At a local scale, these findings may guide future PMF studies in northern Manitoba. At a broader scale, the improved understanding of sensitivity in PMF simulations should promote expanded research into PMF uncertainty and, ideally, contribute to a standardized methodology for incorporating and quantifying sources of uncertainty into PMF estimation in Canada.

6.3. RECOMMENDATIONS FOR FUTURE RESEARCH

This research has advanced the science of PMF estimation and uncertainty for the Lower Nelson River Basin. There remain a number of issues, however, that are unresolved by this study, and would benefit hydropower utilities in Canada to consider. Among those areas that warrant further consideration are the following:

- For a complete multi-model study involving the existing PMF model in SSARR (for the LNRB and for other utilities that employ SSARR models for PMF), the SSARR model would need to be re-calibrated using high flow years from the period of record (e.g. to the same period as HEC-HMS and WATFLOOD in this study). The effect of calibration period on PMF results was found to be significant. The addition of a recalibrated SSARR model could widen the model uncertainty ranges reported in this research.
- It would be advantageous to have similar multi-model studies conducted on other basins of interest to dam owners, employing the period of record for calibration and models of varying complexity. This would be an ideal way to test the findings of this research (e.g. the significance of calibration period and effects of model structure), while also furthering the goals of promoting and standardizing uncertainty assessment of PMF across Canada.
- With additional computational time and resources, a "next-step" methodology for PMSA estimation such as that of Klein, Rousseau, Frigon, Freudiger, & Gagnon (2016) could be employed. This method would be preferred to a frequency analysis of a 1/10,000 event as was used here. Super-ensembles of GCMs to drive RCMs would allow for a closer examination of natural climate variability and could be strung together into longer time periods from which to sample extreme events.

- A reassessment of the baseline PMF inputs is another source of uncertainty not considered in this research. The analysis would be time-intensive; however, it would be necessary to consider how additional meteorological data and already-observed changes in climate may affect the existing values of PMF inputs. It would be more appropriate to apply climate change factors to those re-analyzed PMF inputs.
- The parameter uncertainty analysis only considered a narrow range of behavioural samples; the full range of uncertainty about the baseline PMF hydrograph could not be quantified due to time and computational restraints. With additional resources, parameter uncertainty (and the comparison to other sources of uncertainty) could be more accurately quantified.
- A method of simulating manual adjustments by a hydrologist to improve peak flow performance (e.g. through a modified calibration statistic) would improve the study of parameter uncertainty. Namely, this would reduce the underestimation bias of randomly sampled behavioural solutions compared to a baseline manually adjusted parameterization.

REFERENCES

Abbs, D. J. (1999). A numerical modeling study to investigate the assumptions used in the Calculation of Probable Maximum Precipitation. *Water Resources Research*, *35*(3), 785–796. http://doi.org/10.1029/1998WR900013

Acres International Ltd. (1999). *Churchill River Complex PMF Review and Development Study Volume 1 - Main Report*. Report prepared for Newfoundland and Labrador Hydro, Acres International Ltd. P12858.00.02, January 1999.

Acres Manitoba Ltd. (2006). *Update of Probable Maximum Flood Studies for the Lower Nelson River*. Winnipeg, MB. Report Prepared for Manitoba Hydro, Acres Manitoba Limited, P14058.11, July 2006.

Agriculture and Agri-Food Canada. (2011). Soil Landscapes of Canada (SLC). Retrieved from http://sis.agr.gc.ca/cansis/nsdb/slc/index.html

Agriculture and Agri-Food Canada. (2013a). A National Ecological Framework for Canada. National Ecological Framework. Retrieved from http://sis.agr.gc.ca/cansis/nsdb/ecostrat/index.html

Agriculture and Agri-Food Canada. (2013b). PFRA Sub-basins of the AAFC Watersheds Project - 2013. Retrieved from http://open.canada.ca/data/en/dataset/4f3c7d6d-e018-4a69-a6cf-a4c327572b24

Ajami, N. K., Gupta, H., Wagener, T., & Sorooshian, S. (2004). Calibration of a semi-distributed hydrologic model for streamflow estimation along a river system. *Journal of Hydrology*, *298*, 112–135. http://doi.org/10.1016/j.jhydrol.2004.03.033

Alberta Transportation. (2004). *Guidelines on Extreme Flood Analysis*. Alberta Transporation - Transportation and Civil Engineering Division, Civil Projects Branch. Retrieved from

http://www.transportation.alberta.ca/Content/doctype125/Production/gdlnextrmfld.pdf

Alberta Transportation. (2007). *Uncertainty in Hydrologic Modelling for PMF Estimation*. Retrieved from http://www.transportation.alberta.ca/Content/doctype30/Production/unhydmodel.pdf

Andreadis, K. M., Schumann, G. J. P., & Pavelsky, T. (2013). A simple global river bankfull width and depth database. *Water Resources Research, 49*(10), 7164–7168. http://doi.org/10.1002/wrcr.20440

Aral, M. M., & Gunduz, O. (2005). Large-Scale Hybrid Watershed Modeling. In V. P. Singh & D. K. Frevert (Eds.), *Watershed Models*. Boca Raton, FL: CRC Press.

Arnell, N. W., & Gosling, S. N. (2013). The impacts of climate change on river flow regimes at the global scale. *Journal of Hydrology, 486*, 351–364. http://doi.org/10.1016/j.jhydrol.2013.02.010

B.C. Hydro. (1994). *PMP/PMF Study Guidelines*. Report no. H2748, Hydroelectric Engineering Division.

Bae, D.-H., Jung, I., & Lettenmaier, D. P. (2011). Hydrologic uncertainties in climate change from IPCC AR4 GCM simulations of the Chungju Basin, Korea. *Journal of Hydrology*, *401*, 90–105. http://doi.org/10.1016/j.jhydrol.2011.02.012

Barker, B., Schaefer, M. G., Mumford, J., & Swain, R. (1997). *A Monte Carlo approach to determine the variability of PMF estimates. Final Report on Bumping Lake Dam for USBR Dam Safety Office.*

Bastola, S., Murphy, C., & Sweeney, J. (2011). The role of hydrological modelling uncertainties in climate change impact assessments of Irish river catchments. *Advances in Water Resources*, *34*, 562–576. http://doi.org/10.1016/j.advwatres.2011.01.008

Beauchamp, J., Leconte, R., Trudel, M., & Brissette, F. (2013). Estimation of the summer-fall PMP and PMF of a northern watershed under a changed climate. *Water Resources Research*, *49*(6), 3852–3862. http://doi.org/10.1002/wrcr.20336

Beke, G. J., Veldhuis, H., & Thie, J. (1973). *Bio-Physical Land Inventory of the Churchill-Nelson Rivers Sutdy Area, North-Central Manitoba*. Retrieved from http://sis.agr.gc.ca/cansis/publications/surveys/mb/index.html

Bennett, T. H., & Peters, J. C. (2000). Continuous soil moisture accounting in the Hydrologic Engineering Center Hydrologic Modeling System (HEC-HMS). In *Proceedings of the 2000 Joint Conference on Water Resources Engineering and the Water Resources Planning and Management*. Minneapolis: ASCE. http://doi.org/10.1017/CBO9781107415324.004

Beven, K., & Freer, J. (2001). Equifinality, data assimilation, and uncertainty estimation in mechanistic modelling of complex environmental systems using the GLUE methodology. *Journal of Hydrology*, *249*, 11–29.

Beven, K. J. (2001). *Rainfall-Runoff Modeling - The Primer* (1st ed.). Chichester, UK: Wiley.

Beven, K. J., Buytaert, W., & Smith, L. A. (2012). On virtual observatories and modelled realities (or why discharge must be treated as a virtual variable). *Hydrological Processes*, *26*, 1905–1908. http://doi.org/10.1002/hyp.9261.

Beven, K. J., & Young, P. (2013). A guide to good practice in modeling semantics for authors and referees. *Water Resources Research*, *49*, 5092–5098. http://doi.org/10.1002/wrcr.20393

Bingeman, A. K. (2001). *Improving Dam Safety Analysis by Using Physically-Based Techniques to Derive Estimates of Atmospherically Maximum Precipitation* (Doctoral dissertation). Retrieved from http://www.civil.uwaterloo.ca/watflood/downloads/bingeman.pdf

Boyle, D. P., Gupta, H. V., & Sorooshian, S. (2000). Toward improved calibration of hydrologic

models: Combining the strengths of manual and automatic methods. *Water Resources Research*, *36*(12), 3663–3674. http://doi.org/10.1029/2000WR900207

Boyle, D. P., Gupta, H. V, Sorooshian, S., Koren, V., Zhang, Z., & Smith, M. (2001). Toward improved streamflow forecasts: Value of semidistributed modeling. *Water Resources Research*, *37*(11), 2749–2759.

Butts, M. B., Payne, J. T., Kristensen, M., & Madsen, H. (2004). An evaluation of the impact of model structure on hydrological modelling uncertainty for streamflow simulation. *Journal of Hydrology*, *298*, 242–266. http://doi.org/10.1016/j.jhydrol.2004.03.042

CDA. (2007). *Hydrotechnical Considerations for Dam Safety*. Canadian Dam Association.

CDA. (2013). *Dam Safety Guidelines 2007, revised 2013*. Canadian Dam Association.

Charrier, R., & Li, Y. (2012). Assessing resolution and source effects of digital elevation models on automated floodplain delineation: A case study from the Camp Creek Watershed, Missouri. *Applied Geography*, *34*, 38–46. http://doi.org/10.1016/j.apgeog.2011.10.012

Chen, J., Brissette, F. P., & Leconte, R. (2011). Uncertainty of downscaling method in quantifying the impact of climate change on hydrology. *Journal of Hydrology*, *401*, 190–202. http://doi.org/10.1016/j.jhydrol.2011.02.020

Chen, J., Brissette, F. P., Poulin, A., & Leconte, R. (2011). Overall uncertainty study of the hydrological impacts of climate change for a Canadian watershed. *Water Resources Research*, *47*(12), 1–16. http://doi.org/10.1029/2011WR010602

Chernet, H. H., Alfredsen, K., & Midttømme, G. H. (2014). Safety of Hydropower Dams in a Changing Climate. *Journal of Hydrologic Engineering*, *19*, 569–582. http://doi.org/10.1061/(ASCE)HE.1943-5584.0000836.

Chow, K. C. A., & Jones, S. B. (1994). *Probable Maximum Floods in Boreal Regions - Volume*

I: Main Report. Report for the Canadian Electrical Association. Atria Engineering Hydraulics Inc., CEA No. 9111 G 839, January 1994.

Clavet-Gaumont, J., Huard, D., Frigon, A., Koenig, K., Slota, P., Rousseau, A., … Larouche, B. (2017). Probable maximum flood in a changing climate: An overview for Canadian basins. *Journal of Hydrology: Regional Studies*, *13*, 11–25. http://doi.org/10.1016/j.ejrh.2017.07.003

Coulibaly, P., & Dibike, Y. B. (2004). *Downscaling of Global Climate Model Outputs for Flood Frequency Analysis in the Saguenay River System* (Project no. S02-15-01). Hamilton, ON: McMaster University.

Coulibaly, P., Samuel, J., Pietroniro, A., & Harvey, D. (2013). Evaluation of Canadian National Hydrometric Network density based on WMO 2008 standards. *Canadian Water Resources Journal*, *38*(2), 159–167. http://doi.org/10.1080/07011784.2013.787181

Crippen Acres Wardrop. (1987). *Nelson River Flood Study Phase I* (Report No. G&TP 87-14). Winnipeg, MB. Prepared for Manitoba Hydro, June 1987.

Crippen Acres Wardrop. (1990). *Nelson River Flood Study Phase II*. Winnipeg, MB. Prepared for Manitoba Hydro, January 1990.

Crosetto, M., Tarantola, S., & Saltelli, A. (2000). Sensitivity and uncertainty analysis in spatial modelling based on GIS. *Agriculture Ecosystems & Environment*, *81*, 71–79.

Cubasch, U., Wuebbles, D., Chen, D., Facchini, M. C., Frame, D., Mahowald, N., & Winther, J.-G. (2013). Introduction. In T. F. Stocker, D. Qin, G.-K. Plattner, M. Tignor, S. K. Allen, J. Boschung, … P. M. Midgley (Eds.), *Climate Change 2013: The Physical Science Basis. Contribution of Working Group I to the Fifth Assessment Report of the Intergovernmental Panel on Climate Change* (pp. 119–158). Cambridge, United Kingdom and New York, NY,

USA: Cambridge University Press. http://doi.org/10.1017/CBO9781107415324.007

Cunderlik, J. M., & Simonovic, S. P. (2005). Hydrological extremes in a southwestern Ontario river basin under future climate conditions. *Hydrological Sciences Journal*, *50*(4), 631–654. http://doi.org/10.1623/hysj.2005.50.4.631

Dankers, R., & Feyen, L. (2009). Flood hazard in Europe in an ensemble of regional climate scenarios. *Journal of Geophysical Research Atmospheres*, *114*(16), 1–16. http://doi.org/10.1029/2008JD011523

De Elía, R., & Côté, H. (2010). Climate and climate change sensitivity to model configuration in the Canadian RCM over North America. *Meteorologische Zeitschrift*, *19*(4), 325–339. http://doi.org/10.1127/0941-2948/2010/0469

Debs, I., Sparks, D., & Birikundavyi, J. R. S. (1999). Évaluation Des Méthodes Utilisées Pour L'Estimation De La Crue Maximale Probable En Régions Nordiques. *Canadian Journal of Civil Engineering*, *26*, 355–367. http://doi.org/10.1139/l98-071

Déqué, M., Rowell, D. P., Lüthi, D., Giorgi, F., Christensen, J. H., Rockel, B., … van den Hurk, B. (2007). An intercomparison of regional climate simulations for Europe: assessing uncertainties in model projections. *Climatic Change*, *81*, 53–70. http://doi.org/10.1007/s10584-006-9228-x

Deser, C., Knutti, R., Solomon, S., & Phillips, A. S. (2012). Communication of the role of natural variability in future North American climate. *Nature Climate Change*, *2*(11), 775–779. http://doi.org/10.1038/nclimate1562

Dibike, Y. B., & Coulibaly, P. (2007). Validation of hydrological models for climate scenario simulation: the case of Saguenay watershed in Quebec. *Hydrological Processes*, *21*, 3123–3135. http://doi.org/10.1002/hyp.6534

Doherty, S. J., Bojinski, S., Henderson-Sellers, A., Noone, K., Goodrich, D., Bindoff, N. L., … Zwiers, F. W. (2009). Lessons Learned from IPCC AR4: Scientific Developments Needed to Understand, Predict, and Respond to Climate Change. *Bulletin of the American Meteorological Society*, 497–513. http://doi.org/10.1175/2008BAMS2643.1

Duan, Q. (2003). Global Optimization for Watershed Model Calibration. In Q. Duan, H. V. Gupta, S. Sorooshian, A. N. Rousseau, & R. Turcotte (Eds.), *Calibration of Watershed Models* (pp. 89–104). American Geophysical Union.

Efstratiadis, A., Nalbantis, I., Koukouvinos, A., Rozos, E., & Koutsoyiannis, D. (2008). HYDROGEIOS: a semi-distributed GIS-based hydrological model for modified river basins. *Hydrology and Earth System Sciences*, *12*(4), 989–1006. http://doi.org/10.5194/hess-12-989-2008

Ehrlich, W. A., Pratt, L. E., Barr, J. A., & Leclaire, F. P. (1959). *Soil Survey of a Cross-Section Through the Upper Nelson River Basin along the Hudson Bay Railway in Northern Manitoba*. Manitoba Department of Agriculture and Conservation. Retrieved from http://sis.agr.gc.ca/cansis/publications/surveys/mb/index.html

England, J. F. (2011). Flood frequency and design fl ood estimation procedures in the United States: Progress and challenges. *Australian Journal of Water Resources*, *15*(1), 33–47. http://doi.org/10.1080/13241583.2011.11465388

England, J. F., Velleux, M. L., & Julien, P. Y. (2007). Two-dimensional simulations of extreme floods on a large watershed. *Journal of Hydrology*, *347*, 229–241. http://doi.org/10.1016/j.jhydrol.2007.09.034

Environment Canada. (2004). *Threats to Water Availability in Canada*. National Water Research Institute, Burlington, Ontario. NWRI Scientific Assessment Report Series No. 3 and ACSD

Science Assessment Series No. 1. Retrieved from http://www.ec.gc.ca/inre-nwri/default.asp?lang=En&n=0CD66675-1&offset=6&toc=show

Environment Canada. (2015). Historical Climate Data - Climate - Environment Canada. Retrieved July 15, 2015, from http://climate.weather.gc.ca/

Exbrayat, J. F., Buytaert, W., Timbe, E., Windhorst, D., & Breuer, L. (2014). Addressing sources of uncertainty in runoff projections for a data scarce catchment in the Ecuadorian Andes. *Climatic Change*, *125*, 221–235. http://doi.org/10.1007/s10584-014-1160-x

Feldman, A. D. (2000). *Hydrologic Modeling System HEC-HMS: Technical Reference Manual*. Davis, CA. United States Army Corps of Engineers - Hydrologic Engineering Center. Retrieved from http://www.hec.usace.army.mil/software/hec-hms/documentation.aspx

FEMA. (2012). *Summary of Existing Guidelines for Hydrologic Safety of Dams* (FEMA P-919). US Federal Energy Management Agency. Retrieved from https://www.fema.gov/media-library/assets/documents/28555

FERC. (2001). *Determination of the Probable Maximum Flood. In Engineering Guidelines for the Evaluation of Hydropower Projects*. Federal Energy Regulatory Commission. Retrieved from https://www.ferc.gov/industries/hydropower/safety/guidelines/eng-guide/chap8.pdf

Feser, F., Rockel, B., von Storch, H., Winterfeldt, J., & Zahn, M. (2011). Regional Climate Models add value to global model data. *Bulletin of the American Meteorological Society*, 1181–1192. http://doi.org/10.1175/2011BAMS3061.1

Flato, G., Marotzke, J., Abiodun, B., Braconnot, P., Chou, S. C., Collins, W., … Rummukainen, M. (2013). Evaluation of Climate Models. In T. F. Stocker, D. Qin, G.-K. Plattner, M. Tignor, S. K. Allen, J. Boschung, … P. M. Midgley (Eds.), *Climate Change 2013: The Physical Science Basis. Contribution of Working Group I to the Fifth Assessment Report of*

the Intergovernmental Panel on Climate Change (pp. 741–866). Cambridge, United Kingdom and New York, NY, USA. http://doi.org/10.1017/CBO9781107415324

Fleming, M., & Neary, V. (2004). Continuous Hydrologic Modeling Study with the Hydrologic Modeling System. *Journal of Hydrologic Engineering*, *9*(3), 175–183. http://doi.org/10.1061/(ASCE)1084-0699(2004)9:3(175)

Fowler, K., Hill, P., Jordan, P., Nathan, R. J., & Sih, K. (2010). Application of Available Climate Science to Assess the Impact of Climate Change on Spillway Adequacy. In *ANCOLD Proceedings of Technical Groups*. Hobart, Australia.

García, A., Sainz, A., Revilla, J. A., Álvarez, C., Juanes, J. A., & Puente, A. (2008). Surface water resources assessment in scarcely gauged basins in the north of Spain. *Journal of Hydrology*, *356*, 312–326. http://doi.org/10.1016/j.jhydrol.2008.04.019

Gupta, H. V., Sorooshian, S., & Yapo, P. O. (1998). Toward improved calibration of hydrologic models: Multiple and noncommensurable measures of information. *Water Resources Research*, *34*(4), 751–763. http://doi.org/10.1029/97WR03495

Haberlandt, U., & Radtke, I. (2014). Hydrological model calibration for derived flood frequency analysis using stochastic rainfall and probability distributions of peak flows. *Hydrology and Earth System Sciences*, *18*, 353–365. http://doi.org/10.5194/hess-18-353-2014

Haghnegahdar, A., Tolson, B. A., Craig, J. R., & Paya, K. T. (2015). Assessing the performance of a semi-distributed hydrological model under various watershed discretization schemes. *Hydrological Processes*, *29*, 4018–4031. http://doi.org/10.1002/hyp.10550

Haghnegahdar, A., Tolson, B. A., Davison, B., Seglenieks, F. R., Klyszejko, E., Soulis, E. D., … Matott, L. S. (2014). Calibrating Environment Canada's MESH Modelling System over the Great Lakes Basin. *Atmosphere-Ocean*, *52*(4), 281–293.

http://doi.org/10.1080/07055900.2014.939131

Harlin, J., & Kung, C. S. (1992). Parameter uncertainty and simulation of design floods in Sweden. *Journal of Hydrology, 137*, 209–230. http://doi.org/10.1016/0022-1694(92)90057-3

Hatch Ltd. (2013a). *Manitoba Hydro Climate Change Sensitivity Study - Nelson River PMF Estimates*. Winnipeg, MB. Report H345128, Rev.A. Draft Report Prepared for Manitoba Hydro.

Hatch Ltd. (2013b). *Review of Probable Maximum Flood*. Winnipeg, MB. Report H341433. Report Prepared for Manitoba Hydro.

Hawkins, E., & Sutton, R. (2011). The potential to narrow uncertainty in projections of regional precipitation change. *Climate Dynamics, 37*, 407–418. http://doi.org/10.1007/s00382-010-0810-6

Helton, J. C., & Davis, F. J. (2003). Latin hypercube sampling and the propagation of uncertainty in analyses of complex systems. *Reliability Engineering and System Safety, 81*, 23–69. http://doi.org/10.1016/S0951-8320(03)00058-9

IPCC. (2007). *Climate Change 2007: Synthesis Report. Contribution of Working Groups I, II, and III to the Fourth Assessment Report of the Intergovernmental Panel on Climate Change*. (Core Writing Team, R. K. Pachauri, & A. Reisinger, Eds.). Geneva, Switzerland: IPCC.

IPCC. (2014). *Climate Change 2014: Synthesis Report. Contribution of Working Groups I, II, and III to the Fifth Assessment Report of the Intergovernmental Panel on Climate Change*. (Core Writing Team, R. K. Pachauri, & L. A. Meyer, Eds.). Geneva, Switzerland: IPCC.

Jakeman, A. J., & Hornberger, G. M. (1993). How much complexity is warranted in a rainfall-

runoff model? *Water Resources Research*, *29*(8), 2637–2649.

Jiang, T., Chen, Y. D., Xu, C., Chen, X., Chen, X., & Singh, V. P. (2007). Comparison of hydrological impacts of climate change simulated by six hydrological models in the Dongiang Basin, South China. *Journal of Hydrology*, *336*, 316–333. http://doi.org/10.1016/j.jhydrol.2007.01.010

Kang, B., & Ramírez, J. A. (2007). Response of Streamflow to Weather Variability under Climate Change in the Colorado Rockies. *Journal of Hydrologic Engineering*, *12*(1), 63–72. http://doi.org/10.1061/(ASCE)1084-0699(2007)12:1(63)

Kawazoe, S., & Gutowski Jr., W. J. (2013). Regional, Very Heavy Daily Precipitation in NARCCAP Simulations. *Journal of Hydrometeorology*, *14*, 1212–1227. http://doi.org/10.1175/JHM-D-12-068.1

Kay, A. L., & Jones, D. A. (2012). Transient changes in flood frequency and timing in Britain under potential projections of climate change. *International Journal of Climatology*, *32*, 489–502. http://doi.org/10.1002/joc.2288

KGS Acres Ltd. (2010). *Hazard Classification and Selection of Inflow Design Flood*. Manitoba Hydro - Keeyask Generating Station Stage IV Studies - Axis GR-4: Design Memorandum GN-2.7.

Khakbaz, B., Imam, B., Hsu, K., & Sorooshian, S. (2012). From lumped to distributed via semi-distributed: Calibration strategies for semi-distributed hydrologic models. *Journal of Hydrology*, *418-419*, 61–77. http://doi.org/10.1016/j.jhydrol.2009.02.021

Khaliq, M. N., Sushama, L., Monette, A., & Wheater, H. (2015). Seasonal and extreme precipitation characteristics for the watersheds of the Canadian Prairie Provinces as simulated by the NARCCAP multi-RCM ensemble. *Climate Dynamics*, *44*, 255–277.

http://doi.org/10.1007/s00382-014-2235-0

Kirchner, J. W. (2006). Getting the right answers for the right reasons: Linking measurements , analyses , and models to advance the science of hydrology. *Water Resources Research, 42*, 1–5. http://doi.org/10.1029/2005WR004362

Klein, I. M., Rousseau, A. N., Frigon, A., Freudiger, D., & Gagnon, P. (2016). Evaluation of probable maximum snow accumulation: Development of a methodology for climate change studies. *Journal of Hydrology, 537*, 74–85. http://doi.org/10.1016/j.jhydrol.2016.03.031

Knutti, R., Abramowitz, G., Collins, M., Eyring, V., Glecker, P. J., Hewitson, B., & Mearns, L. (2010). Good Practice Guidance Paper on Assessing and Combining Multi Model Climate Projections. In T. Stocker, Q. Dahe, G. Plattner, M. Tignor, & P. Midgley (Eds.), *Meeting Report of the Intergovernmental Panel on Climate Change Expert Meeting on Assessing and Combining Multi Model Climate Projections*. IPCC Working Group I Technical Support Unit, University of Bern, Bern, Switzerland.

Knutti, R., & Sedláček, J. (2012). Robustness and uncertainties in the new CMIP5 climate model projections. *Nature Climate Change, 3*, 1–5. http://doi.org/10.1038/nclimate1716

Koirala, S., Hirabayashi, Y., Mahendran, R., & Kanae, S. (2014). Global assessment of agreement among streamflow projections using CMIP5 model outputs. *Environmental Research Letters, 9*, 1–11. http://doi.org/10.1088/1748-9326/9/6/064017

Kouwen, N. (2014). *WATFLOOD^{TM} / WATROUTE Hydrological Model Routing & Flow Forecasting System. University of Waterloo*. Waterloo, Ontario, Canada. Retrieved from http://www.civil.uwaterloo.ca/watflood/

Kouwen, N., Danard, M., Bingeman, A., Luo, W., Seglenieks, F. R., & Soulis, E. D. (2005). Case study: Watershed modeling with distribued weather model data. *Journal of Hydrologic*

Engineering, *10*(1), 23–38.

Kuczera, G., & Parent, E. (1998). Monte Carlo assessment of parameter uncertainty in conceptual catchment models: the Metropolis algorithm. *Journal of Hydrology*, *211*, 69–85.

Kulkarni, B. D., Nandargi, S., & Mulye, S. S. (2010). Zonal estimation of probable maximum precipitation rain depths over the Krishna basin in peninsular India. *Hydrological Sciences Journal*, *55*(1), 93–103. Retrieved from http://www.tandfonline.com.uml.idm.oclc.org/doi/full/10.1080/02626660903529015

Kundzewicz, Z. W., & Robson, A. J. (2004). Change detection in hydrological records - a review of the methodology. *Hydrological Sciences Journal*, *49*(1), 7–19. http://doi.org/10.1623/hysj.49.1.7.53993

Kunkel, K. E., Karl, T. R., Brooks, H., Kossin, J., Lawrimore, J. H., Arndt, D., … Wuebbles, D. (2013). Monitoring and understanding trends in extreme storms: State of knowledge. *Bulletin of the American Meteorological Society*, *94*(4), 499–514. http://doi.org/10.1175/BAMS-D-11-00262.1

Kunkel, K. E., Karl, T. R., Easterling, D. R., Redmond, K., Young, J., Yin, X., & Hennon, P. (2013). Probable maximum precipitation and climate change. *Geophysical Research Letters*, *40*(7), 1402–1408. http://doi.org/10.1002/grl.50334

Lamb, R. (1999). Calibration of a conceptual rainfall-runoff model for flood frequency estimation by continuous simulation. *Water Resources Research*, *35*(10), 3103–3114.

Le Clerc, S., & Garros-Berthet, H. (2011). Global warming and design flood: The case study of Bagatelle dam, Mauritius. In A. J. Schleiss & R. M. Boes (Eds.), *Dams and Reservoirs under Changing Challenges* (pp. 533–539). London: Taylor & Francis. Retrieved from https://books.google.com/books?id=c8PLBQAAQBAJ&pgis=1

Ludwig, R., May, I., Turcotte, R., Vescovi, L., Braun, M., Cyr, J.-F., … Mauser, W. (2009). The role of hydrological model complexity and uncertainty in climate change impact assessment. *Advances in Geosciences*, *21*, 63–71.

MacKay, M. D., Bartlett, P. A., Chan, E., Derksen, C., Guo, S., & Leighton, H. (2006). On the simulation of regional scale sublimation over boreal and agricultural landscapes in a climate model. *Atmosphere-Ocean*, *44*(3), 289–304. http://doi.org/10.3137/ao.440306

Mailhot, A., Beauregard, I., Talbot, G., Caya, D., & Biner, S. (2012). Future changes in intense precipitation over Canada assessed from multi-model NARCCAP ensemble simulations. *International Journal of Climatology*, *32*(8), 1151–1163. http://doi.org/10.1002/joc.2343

Manitoba Hydro. (2013). *Future Climate Scenarios for Sensitivity Analysis of Lower Nelson River Probable Maximum Flood*. Winnipeg, MB. Water Resources Engineering Department, Power Planning Division. Internal Draft Report.

Manitoba Hydro. (2016a). Churchill River Diversion. Retrieved June 27, 2016, from https://www.hydro.mb.ca/corporate/water_regimes/churchill_river_diversion.shtml

Manitoba Hydro. (2016b). Generating stations. Retrieved June 27, 2016, from https://www.hydro.mb.ca/corporate/facilities/generating_stations.shtml

Mearns, L. O., McGinnis, S., Arritt, R., Biner, S., Duffy, P., Gutowski, W., … Zoellick, C. (2007, updated 2014). The North American Regional Climate Change Assessment Program dataset. National Center for Atmospheric Research Earth System Grid data portal, Boulder, CO. doi:10.5065/D6RN35ST

Mearns, L. O., Arritt, R., Biner, S., Bukovsky, M. S., McGinnis, S., Sain, S., … Snyder, M. (2012). The North American Regional Climate Change Assessment Program: Overview of Phase I Results. *Bulletin of the American Meteorological Society*, *93*(9), 1337–1362.

http://doi.org/10.1175/BAMS-D-11-00223.1

Meehl, G. A., Covey, C., Delworth, T., Latif, M., McAvaney, B., Mitchell, J. F. B., … Taylor, K. E. (2007). The WCRP CMIP3 multimodel dataset - A new era in climate change research. *Bulletin of the American Meteorological Society*, *88*(9), 1383–1394. http://doi.org/10.1175/BAMS-88-9-1383

Mekis, É., & Vincent, L. A. (2011). An Overview of the Second Generation Adjusted Daily Precipitation Dataset for Trend Analysis in Canada. *Atmosphere-Ocean*, *49*(2), 163–177. http://doi.org/10.1080/07055900.2011.583910

Meyersohn, W. D. (2016). Runoff prediction for dam safety evaluations based on variable time of concentration. *Journal of Hydrologic Engineering*, *21*(10). http://doi.org/10.1061/(ASCE)HE.1943-5584.0001406

Mills, G. F., Veldhuis, H., & Forrester, D. B. (1976). *A Guide To Biophysical Land Classification Kettle Rapids , 54D Manitoba*. Canada-Manitoba Soil Survey for Province of Manitoba Dept. of Renewable Resources and Transportation Services.

Mladjic, B., Sushama, L., Khaliq, M. N., Laprise, R., Caya, D., & Roy, R. (2011). Canadian RCM projected changes to extreme precipitation characteristics over Canada. *Journal of Climate*, *24*(10), 2565–2584. http://doi.org/10.1175/2010JCLI3937.1

Monette, A., Sushama, L., Khaliq, M. N., Laprise, R., & Roy, R. (2012). Projected changes to precipitation extremes for northeast Canadian watersheds using a multi-RCM ensemble. *Journal of Geophysical Research*, *117*, 1–15. http://doi.org/10.1029/2012JD017543,2012

Moore, R. D., Hamilton, A. S., & Scibek, J. (2002). Winter streamflow variability, Yukon Territory, Canada. *Hydrological Processes*, *16*, 763–778. http://doi.org/10.1002/hyp.372

Moradkhani, H., & Sorooshian, S. (2009). General Review of Rainfall-Runoff Modeling: Model

Calibration, Data Assimilation, and Uncertainty Analysis. In S. Sorooshian, K.-L. Hsu, E. Coppola, B. Tomassetti, M. Verdecchia, & G. Visconti (Eds.), *Hydrological Modelling and the Water Cycle: Coupling the Atmospheric and Hydrological Models* (pp. 1–24). Springer Science+Business Media.

Moriasi, D. N., Arnold, J. G., Van Liew, M. W., Bingner, R. L., Harmel, R. D., & Veith, T. L. (2007). Model evaluation guidelines for systematic quantification of accuracy in watershed simulations. *Transactions of the ASABE*, *50*(3), 885–900.

Morris, M.D. (1991). Factorial sampling plans for preliminary computational experiments. *Technometrics*, *33*(2), 161-174.

Musgrave, G. W. (1955). How much of the rain enters the soil? *In Water Yearbook of Agriculture* (pp. 151–159). Washington D.C.: U.S. Department of Agriculture.

Music, B., & Caya, D. (2007). Evaluation of the hydrological cycle over the Mississippi River Basin as simulated by the Canadian Regional Climate Model (CRCM). *Journal of Hydrometeorology*, *8*, 969–988. http://doi.org/10.1175/JHM627.1

Najafi, M. R., Moradkhani, H., & Jung, I. W. (2011). Assessing the uncertainties of hydrologic model selection in climate change impact studies. *Hydrological Processes*, *25*, 2814–2826. http://doi.org/10.1002/hyp.8043

Nakicenovic, N., & Swart, R. (2000). *IPCC Special Report on Emissions Scenarios: A special report of Working Group III of the Intergovernmental Panel on Climate Change*. Emissions Scenarios. Intergovernmental Panel on Climate Change: Cambridge University Press.

Nash, J. E., & Sutcliffe, J. V. (1970). River flow forecasting through conceptual models. Part 1: A discussion of principles. *Journal of Hydrology*, *10*(3), 282–290.

Nathan, R., & Weinmann, E. (2015). Book 8: Very to Extreme Flood Estimation. In J. Ball (Ed.),

Australian Rainfall and Runoff: A Guide to Flood Estimation - Draft for Industry Comment 151205. Retrieved from http://book.arr.org.au/

Natural Resources Canada. (2000a). *GeoBase - Canadian Digital Elevation Data*. Natural Resources Canada, Earth Sciences Sector, Canada Centre for Mapping and Earth Observation. Retrieved from http://geogratis.gc.ca/api/en/nrcan-rncan/ess-sst/3A537B2D-7058-FCED-8D0B-76452EC9D01F.html

Natural Resources Canada. (2000b). *GeoBase - Land Cover, circa 2000-Vector (LCC2000-V).* Natural Resources Canada, Earth Sciences Sector, Canada Centre for Mapping and Earth Observation. Retrieved from http://geogratis.gc.ca/api/en/nrcan-rncan/ess-sst/643c4911-475b-4765-b730-2dde9be50d5b.html

Natural Resources Canada. (2015). GeoBase - National Hydro Network (NHN). Retrieved from http://geogratis.gc.ca/api/en/nrcan-rncan/ess-sst/87066e9a-94ee-680a-b1ba-591f4688db7d.html

NRCS. (2007). Chapter 7: Hydrologic Soil Groups. In *Part 630 National Engineering Handbook*. Natural Resources Conservation Service, United States Department of Agriculture.

Ohara, N., Kavvas, M. L., Kure, S., Chen, Z. Q., Jang, S., & Tan, E. (2011). Physically based estimation of maximum precipitation over American River Watershed, California. *Journal of Hydrologic Engineering*, *16*(4), 351–361. http://doi.org/10.1061/(ASCE)HE.1943-5584.0000324

Ouranos. (2015). *Probable Maximum Floods and Dam Safety in the 21st Century Climate.* Report submitted to Climate Change Impacts and Adaptation Division, Natural Resources Canada, 39 p. Retrieved from https://www.ouranos.ca/en/publications/

Pietroniro, A., & Soulis, E. D. (2003). A hydrology modelling framework for the Mackenzie GEWEX programme. *Hydrological Processes*, *17*(3), 673–676. http://doi.org/10.1002/hyp.5104

Poitras, V., Sushama, L., Seglenieks, F., Khaliq, M. N., & Soulis, E. (2011). Projected changes to streamflow characteristics over Western Canada as simulated by the Canadian RCM. *Journal of Hydrometeorology*, *12*(6), 1395–1413. http://doi.org/10.1175/JHM-D-10-05002.1

Randall, D. A., Wood, R. A., Bony, S., Colman, R., Fichefet, T., Fyfe, J., … Taylor, K. E. (2007). Climate Models and Their Evaluation. In S. Solomon, D. Qin, M. Manning, Z. Chen, M. Marquis, K. B. Averyt, … H. L. Miller (Eds.), *Climate Change 2007: The Physical Science Basis. Contribution of Working Group I to the Fourth Assessment Report of the Intergovernmental Panel on Climate Change*. Cambridge, United Kingdom and New York, NY, USA: Cambridge.

Rawls, W. J., Brakensiek, D. L., & Miller, N. (1983). Green-Ampt infiltration parameters from soils data. *Journal of Hydraulic Engineering*, *109*(1), 62–70. http://doi.org/10.1061/(ASCE)0733-9429(1983)109:1(62)

Rawls, W. J., Brakensiek, D. L., & Saxton, K. E. (1982). Estimation of soil water properties. *Transactions of the ASAE*, *25*(5), 1316–1320 & 1328. http://doi.org/10.13031/2013.33720

Razavi, S., & Tolson, B. A. (2013). An efficient framework for hydrologic model calibration on long data periods. *Water Resources Research*, *49*(12), 8418–8431. http://doi.org/10.1002/2012WR013442

Razavi, T., & Coulibaly, P. (2013). Streamflow prediction in ungauged basins: Review of regionalization methods. *Journal of Hydrologic Engineering*, *18*(8), 958–975.

http://doi.org/10.1061/(ASCE)HE.1943-5584.0000690

Refsgaard, J. C., & Knudsen, J. (1996). Operational validation and intercomparison of different types of hydrological models. *Water Resources Research*, *32*(7), 2189–2202. http://doi.org/10.1029/96WR00896

Renard, B., Kavetski, D., Kuczera, G., Thyer, M., & Franks, S. W. (2010). Understanding predictive uncertainty in hydrologic modeling: The challenge of identifying input and structural errors. *Water Resources Research*, *46*, 1–22. http://doi.org/10.1029/2009WR008328

Roberts, J., Pryse-Phillips, A., & Snelgrove, K. (2012). Modeling the potential impacts of climate change on a small watershed in Labrador, Canada. *Canadian Water Resources Journal*, *37*(3), 231–251. http://doi.org/10.4296/cwrj2011-923

Roeckner, G., Baeuml, G., Bonaventura, L., Brokopf, R., Esch, M., Giorgetta, M., … Tompkins, A. (2003). *The atmospheric general circulation model ECHAM 5. PART I: Model description*. Hamburg. Max Planck Institute for Meteorology Rep. 349, 127p. Retrieved from https://www.researchgate.net/publication/258437837_The_atmospheric_general_circulation_model_ECHAM_5_PART_I_model_description

Rousseau, A. N., Klein, I. M., Freudiger, D., Gagnon, P., Frigon, A., & Ratt??-Fortin, C. (2014). Development of a methodology to evaluate probable maximum precipitation (PMP) under changing climate conditions: Application to southern Quebec, Canada. *Journal of Hydrology*, *519*, 3094–3109. http://doi.org/10.1016/j.jhydrol.2014.10.053

Sagan, K. A. B. (2014). *Evaluation of Probable Maximum Flood scenarios for the Lower Nelson River system* (Undergraduate thesis). University of Manitoba.

Salas, J. D., Gavilán, G., Salas, F. R., Julien, P. Y., & Abdullah, J. (2014). Uncertainty of the PMP and PMF. In S. Eslamian (Ed.), *Handbook of Engineering Hydrology: Modeling Climate Change, and Variability* (pp. 575–603). CRC Press. http://doi.org/doi:10.1201/b16683-29

Seibert, J. (2003). Reliability of Model Predictions Outside Calibration Conditions. *Nordic Hydrology*, *34*(5), 477–492. http://doi.org/10.2166/nh.2003.028

Sheridan, J. M. (1994). Hydrograph time parameters for flatland watersheds. *Transactions of the ASAE*, *37*(1), 103–113.

Singh, V. P., & Frevert, D. K. (2005). Introduction. In V. P. Singh & D. K. Frevert (Eds.), *Watershed Models*. Boca Raton, FL: CRC Press. Retrieved from https://books.google.ca/books

SNC-Shawinigan Inc. (1993). *Complexe Saint-Maurice: crues maximales probables*. Montréal: Avant-projet, phase I, préparé pour Hydro- Québec.

Stadnyk-Falcone, T. A. (2008). *Mesoscale Hydrological Model Validation and Verification using Stable Water Isotopes: The isoWATFLOOD Model* (Doctoral dissertation). Retrieved from https://uwspace.uwaterloo.ca/handle/10012/3970

Steinschneider, S., Wi, S., & Brown, C. (2014). The integrated effects of climate and hydrologic uncertainty on future flood risk assessments. *Hydrological Processes*. http://doi.org/10.1002/hyp.10409

Stratz, S. A., & Hossain, F. (2014). Probable Maximum Precipitation in a changing climate: Implications for dam design. *Journal of Hydrologic Engineering*, *19*(12), 06014006. http://doi.org/10.1061/(ASCE)HE.1943-5584.0001021

Sushama, L., Laprise, R., Caya, D., Frigon, A., & Slivitzky, M. (2006). Canadian RCM projected

climate-change signal and its sensitivity to model errors. *International Journal of Climatology*, *26*, 2141–2159. http://doi.org/10.1002/joc

Taylor, K. E., Stouffer, R. J., & Meehl, G. A. (2012). An overview of CMIP5 and the experiment design. *Bulletin of the American Meteorological Society*, *93*(4), 485–498. http://doi.org/10.1175/BAMS-D-11-00094.1

Tebaldi, C., & Knutti, R. (2007). The use of the multi-model ensemble in probabilistic climate projections. *Philosophical Transactions of the Royal Society A: Mathematical, Physical and Engineering Sciences*, *365*(1857), 2053–2075. http://doi.org/10.1098/rsta.2007.2076

Tolson, B. A., & Shoemaker, C. A. (2007). Dynamically dimensioned search algorithm for computationally efficient watershed model calibration. *Water Resources Research*, *43*, 1–16. http://doi.org/10.1029/2005WR004723

Trenberth, K. E., Dai, A., Rasmussen, R. M., & Parsons, D. B. (2003). The changing character of precipitation. *Bulletin of the American Meteorological Society*, *84*(9), 1205–1217. http://doi.org/10.1175/BAMS-84-9-1205

USACE. (1991). *User Manual: SSARR Model - Streamflow Synthesis and Reservoir Regulation*. Portland, OR: United States Army Corps of Engineers - North Pacific Division.

van Griensven, A., Meixner, T., Grunwald, S., Bishop, T., Diluzio, M., & Srinivasan, R. (2006). A global sensitivity analysis tool for the parameters of multi-variable catchment models. *Journal of Hydrology*, *324*, 10–23. http://doi.org/10.1016/j.jhydrol.2005.09.008

Van Steenbergen, N., & Willems, P. (2012). Method for testing the accuracy of rainfall–runoff models in predicting peak flow changes due to rainfall changes, in a climate changing context. *Journal of Hydrology*, *414-415*, 425–434. http://doi.org/10.1016/j.jhydrol.2011.11.017

Van Vuuren, D. P., Edmonds, J., Kainuma, M., Riahi, K., Thomson, A., Hibbard, K., … Rose, S. K. (2011). The representative concentration pathways : an overview. *Climatic Change, 109*, 5–31. http://doi.org/10.1007/s10584-011-0148-z

Vansteenkiste, T., Tavakoli, M., Ntegeka, V., De Smedt, F., Batelaan, O., Pereira, F., & Willems, P. (2014). Intercomparison of hydrological model structures and calibration approaches in climate scenario impact projections. *Journal of Hydrology*, *519*, 743–755. http://doi.org/10.1016/j.jhydrol.2014.07.062

Vansteenkiste, T., Tavakoli, M., Van Steenbergen, N., De Smedt, F., Batelaan, O., Pereira, F., & Willems, P. (2014). Intercomparison of five lumped and distributed models for catchment runoff and extreme flow simulation. *Journal of Hydrology*, *511*, 335–349. http://doi.org/10.1016/j.jhydrol.2014.01.050

Vaze, J., Post, D. A., Chiew, F. H. S., Perraud, J., Viney, N. R., & Teng, J. (2010). Climate non-stationarity – Validity of calibrated rainfall–runoff models for use in climate change studies. *Journal of Hydrology*, *394*, 447–457. http://doi.org/10.1016/j.jhydrol.2010.09.018

Veijalainen, N., & Vehviläinen, B. (2008). The effect of climate change on design floods of high hazard dams in Finland. *Hydrology Research*, *39*(5–6), 465. http://doi.org/10.2166/nh.2008.202

Veldhuis, H., Mills, G. F., & Forrester, D. B. (1979). *A Guide to Biophysical Land Classification - Sipiwesk, 63P and S.E. 1/4 of Split Lake 64A- Manitoba* (Technical Report No. 79-2). Canada-Manitoba Soil Survey and Department of Mines, Natural Resources and Environment.

Vieira, M. J. F. (2016). *738 years of global climate model simulated streamflow in the Nelson-Churchill River Basin* (Master's thesis). Retrieved from

https://mspace.lib.umanitoba.ca/handle/1993/31124

Vrugt, J. A., Gupta, H. V, Bouten, W., & Sorooshian, S. (2003). A Shuffled Complex Evolution Metropolis algorithm for optimization and uncertainty assessment of hydrologic model parameters. *Water Resources Research*, *39*(8). http://doi.org/10.1029/2002WR001642

Wagener, T., Boyle, D. P., Lees, M. J., Wheater, H. S., Gupta, H. V, Wagener, T., … Hoshin, V. (2001). A framework for development and application of hydrological models. *Hydrology and Earth System Sciences*, *5*(1), 13–26.

Wagener, T., Wheater, H. S., & Lees, M. J. (2004). *Monte-Carlo Analysis Toolbox User Manual - Version 5*. Penn State University. Retrieved from http://www.imperial.ac.uk/environmental-and-water-resource-engineering/research/software/

Wallner, M., Haberlandt, U., & Dietrich, J. (2012). Evaluation of different calibration strategies for large scale continuous hydrological modelling. *Advances in Geosciences*, *31*, 67–74. http://doi.org/10.5194/adgeo-31-67-2012

Wang, X., & Melesse, A. (2005). Evaluation of the SWAT model's snowmelt hydrology in a northwestern Minnesota watershed. *Transactions of the ASAE*, *48*(4), 1–18. http://doi.org/10.1002/hyp.7457

Water Survey of Canada. (2014). Environment and Climate Change Canada - Water - Water Survey of Canada Homepage. Retrieved March 15, 2015, from http://www.ec.gc.ca/rhc-wsc/

Watt, E., & Marsalek, J. (2013). Critical review of the evolution of the design storm event concept. *Canadian Journal of Civil Engineering*, *40*(2), 105–113. http://doi.org/10.1139/cjce-2011-0594

Watt, W. E. (1989). *Hydrology of Floods in Canada: A Guide to Planning and Design*. National Research Council Canada, Associate Committee on Hydrology.

Wehner, M. F. (2013). Very extreme seasonal precipitation in the NARCCAP ensemble: Model performance and projections. *Climate Dynamics*, *40*, 59–80. http://doi.org/10.1007/s00382-012-1393-1

Wehner, M. F., Smith, R. L., Bala, G., & Duffy, P. (2009). The effect of horizontal resolution on simulation of very extreme US precipitation events in a global atmosphere model. *Climate Dynamics*, *34*, 241–247. http://doi.org/10.1007/s00382-009-0656-y

Whitfield, P. H. (2012). Floods in future climates: A review. *Journal of Flood Risk Management*, *5*(4), 336–365. http://doi.org/10.1111/j.1753-318X.2012.01150.x

Wi, S., Yang, Y. C. E., Steinschneider, S., Khalil, A., & Brown, C. M. (2015). Calibration approaches for distributed hydrologic models in poorly gaged basins: Implication for streamflow projections under climate change. *Hydrology and Earth System Sciences*, *19*(2), 857–876. http://doi.org/10.5194/hess-19-857-2015

Wilby, R. L., & Harris, I. (2006). A framework for assessing uncertainties in climate change impacts: Low-flow scenarios for the River Thames, UK. *Water Resources Research*, *42*, 1–10. http://doi.org/10.1029/2005WR004065

WMO. (2009). *Manual on Estimation of Probable Maximum Precipitation (PMP)* (WMO-No. 1045). Geneva, Switzerland: World Meteorological Organization.

Wulder, M., & Nelson, T. (2003). *EOSD Land Cover Classification Legend Report Version 2. Victoria, B.C. Natural Resources Canada and TNT Geoservices*. Retrieved from http://ftp.geogratis.gc.ca/pub/nrcan_rncan/vector/geobase_lcc_csc/doc/EOSD_Legend_Report.pdf

Xue, X., Zhang, K., Hong, Y., Gourley, J. J., Kellogg, W., Mcpherson, R. A., … Austin, B. N. (2014). New multisite cascading calibration approach for hydrological models : Case study in the Red River Basin using the VIC model. *Journal of Hydrologic Engineering*, *21*(2), 1–9. http://doi.org/10.1061/(ASCE)HE.1943-5584.0001282.

Yang, J., Reichert, P., Abbaspour, K. C., Xia, J., & Yang, H. (2008). Comparing uncertainty analysis techniques for a SWAT application to the Chaohe Basin in China. *Journal of Hydrology*, *358*, 1–23. http://doi.org/10.1016/j.jhydrol.2008.05.012

Yang, J. (2011). Convergence and uncertainty analyses in Monte-Carlo based sensitivity analysis. *Environmental Modelling and Software*, *26*(4), 444–457. http://doi.org/10.1016/j.envsoft.2010.10.007

APPENDIX A: METHODS OF HYDROLOGICAL MODEL PARAMETERIZATION

Appendix A provides more detail on the estimation of initial hydrological model parameter values and sampling ranges for calibration. Guidance was available from the WATFLOOD manual (Kouwen, 2014) and previous modelling of the LNRB to aid in developing WATFLOOD parameter ranges. Generalized ranges (not basin-specific) suggested by the manual, in particular, formed the basis for wide sampling ranges.

Similar guidance was not available for HEC-HMS, in part because previous HEC-HMS models of the basin were limited to manual calibration (and thus did not include explicit parameter ranges). Instead, several published studies correlated HEC-HMS parameters to available physiographic (GIS) or hydrometric data, or empirical methods. In this case, GIS data was available from the Soil Landscapes of Canada (SLC) dataset, a 1:1 million data product of the National Soil DataBase based on distributed soil survey data (Agriculture and Agri-Food Canada, 2011). The dataset provided information on major soil formations in terms of vegetation cover, land slope, soil texture, vertical soil horizons, and soil drainage and saturation characteristics. Hydrometric data was available as per Table 4.

The synthesis below therefore describes the estimation of realistic ranges for each HEC-HMS parameter after initial sensitivity testing. The list works downwards through the Soil Moisture Accounting process.

- Maximum canopy storage (mm) – This parameter was relatively insignificant in pre-calibration testing. There was a small range in published values for varying canopy types and densities (Fleming & Neary, 2004; García et al., 2008); a realistic value was selected for each basin based on dominant forest type.

- Maximum surface depression storage (mm) – The range of land slopes in each sub-basin (based on SLC data) was correlated to storage amounts suggested in Fleming & Neary (2004). Given the significant wetland areas in most sub-basins, surface storages were estimated to be slightly higher than those suggested in the published table.
- Maximum soil infiltration (mm/hr) – The predominant soil type in each sub-basin was identified from SLC data, in terms of general soil texture and NRCS soil type (A-D) (Natural Resources Conservation Service, 2007). Published values of saturated hydraulic conductivity (Musgrave, 1955; Rawls, Brakensiek, & Miller, 1983; Rawls et al., 1982) and maximum soil infiltration (García et al., 2008) were then used to estimate lower and upper bounds, respectively.
- Impervious area (%) – Impervious area was estimated based on treed rock and bedrock landcover from GIS data. Given that highly saturated soils may also be more susceptible to frozen soil effects in the spring, soil types identified as very poorly drained were also used to increase estimates of impervious area.
- Soil tension storage (mm) and maximum storage (mm) – Published estimates of these parameters could not be used as they were often site-specific; instead two methods were averaged:
    1. SLC data on soil contents and drainage was used to estimate soil texture, which was then correlated to water retention characteristics from Rawls et al. (1982).
    2. Water retention characteristics included in the SLC dataset were used to estimate storage in each soil horizon, and a weighted average of horizons was taken.

  Both methods were conducted for all major soil formations in each sub-basin and then averaged. Unitless water retention estimates were then converted to depths of storage

based on the approximate depth of soil recorded in SLC data. A range of +/-20% about the estimate was used to produce each parameter range. For calibration, tension storage was defined as a fraction of maximum storage to ensure it was always equal to or less than maximum storage.

- Maximum soil percolation rate (mm/hr) – A similar estimate was conducted as for soil infiltration, as per the recommendation of Fleming & Neary (2004), but for the lowest soil layers identified in the SLC dataset.
- Maximum baseflow storages (upper and lower) (mm) – SLC data was used to estimate baseflow storage depths based on soil horizons below the water table but above underlying bedrock. Assuming soil at this depth was primarily clay, the difference between average soil porosity and average wilting point for clay (Rawls et al., 1982) was used to convert total soil depth into an available depth of baseflow storage. This depth was then separated into upper and lower storage where necessary. Given the uncertainty around this parameter, a ± 30% about the estimate was used.
- Maximum baseflow percolation rate (upper and lower) (mm/hr) – Percolation rates were estimated as a fraction (0.5-1) of the percolation rate immediately above. This method is based on that used by García et al. (2008) due to lack of additional data.
- Time of concentration (t_c; hours) – An empirical equation from Sheridan (1994), which was developed to estimate t_c for moderately sized flatland areas, was used. The only input required was the length of the main channel in a sub-basin. Main channel length was estimated using a global GIS dataset of remotely sensed hydrography, bankfull width and depth (Andreadis, Schumann, & Pavelsky, 2013).

- Storage coefficients (surface, upper and lower baseflow) (hours) – As per Fleming & Neary (2004), these quantities were estimated based on recession analysis. The recession limb of the spring peak in each calibration year was separated into the upper (steepest), middle, and lower (shallowest) portions. Each portion was then plotted in log-scale and an exponential decay rate (linear in log-scale) was fitted. The range in decay rates among the five calibration years defined the subsequent range for each parameter.

Decision variables and ranges are provided in Table 10, and were used to constrain HEC-HMS calibration as described in Section 4.2.2.

APPENDIX B: PMF MODELLING IN THE LNRB - INPUTS & INITIALIZATION

Extreme meteorological and hydrologic inputs are used to produce PMF conditions in the hydrological models. Two different spring PMF scenarios are simulated in this study: a PMP + 1/100 year SWE, and a 1/100 year rainfall and PMSA. Both scenarios also require common inputs of temperature, upstream inflows, and antecedent conditions.

The baseline PMF inputs described here were derived by Manitoba Hydro or external consultants as part of previous dam safety reviews; they are used here in their existing values and are not original to this study. Most of the inputs were developed as part of the first comprehensive PMF study by Crippen Acres Wardrop (1990) which applied best practice guidelines at the time. The inputs were then updated in an Acres Manitoba Ltd. (2006) study based on new data and dam safety guidelines from the Canadian Dam Association, and finally reviewed as part of a PMF update study by Hatch Ltd. (2013b).

This appendix represents a background on the most current methodology and value(s) for each PMF input, and justification for their continued use here as baseline inputs.

B.1. PROBABLE MAXIMUM PRECIPITATION (PMP)

A review of historical storms in locations transferable to the LNRB was conducted as part of the initial PMF model development by Crippen Acres Wardrop (1990). Storm magnitudes were maximized by comparing the precipitable water content during each storm to the maximum precipitable water possible at that time and location, as per WMO guidelines at the time. That study selected a 48 hour storm from Alberta as the most severe maximized event to represent the PMP. The storm was then oriented over the LNRB to produce a maximum effect, given as a

basin average magnitude in Table 31. The temporal distribution of rainfall over the 48 hours (at a daily scale) was not changed. The magnitude of the PMP event is at its maximum in July and August, and decreases in magnitude towards April as a result of reduced moisture carrying capacity in the atmosphere. A seasonality factor such as this has since been recommended and used elsewhere (CDA, 2007; Veijalainen & Vehviläinen, 2008).

Table 31: Baseline PMP – Basin Average, 100% of Seasonal Depth (Crippen Acres Wardrop, 1990)

Time Period	Depth of Rainfall (mm)
0-24 Hours	92
24-48 Hours	34
Total	126

The PMP is distributed to sub-basins in the model using a weighting factor based on the critical storm position over Split Lake. Weighting factors are provided at the centroids of the National Hydro Network (NHN) delineated sub-basins (Natural Resources Canada, 2015).

The PMP, along with its temporal and spatial distribution, and seasonality, was reviewed most recently by Hatch Ltd. (2013b), and is used again in this study. CDA (2007) recommends the use of previously estimated PMP values or published estimates before conducting project-specific PMP analysis. Similarly, WMO (2009) notes that there are no standard methods for estimating PMP, and methods are often basin specific and dependent on available data. Use of the historically estimated PMP in this research as a baseline value is therefore justified as there may be more uncertainty associated with re-analyzing the PMP.

B.2. 1/100 YEAR RAINFALL

Estimates of the 1/100 year rainfall event were conducted by Acres Manitoba Ltd. (2006). That study compared the 1/100 year event derived from (a) frequency analysis at several stations, and (b) from the non-maximized magnitude of the PMP candidate storm. The estimates were found to be similar but the study concluded that the estimate based on the PMP candidate storm was more conservative. This estimate was used for the basin average 1/100 year spring rainfall event (Table 32). The 1/100 rainfall event was also assumed to follow the same spatial orientation, temporal distribution, and seasonality of the PMP storm.

Table 32: Baseline 1/100 Year Rainfall – Basin Avg, 100% of Seasonal Depth (Acres Manitoba Ltd., 2006)

Time Period	Depth of Rainfall (mm)
0-24 Hours	48.2
24-48 Hours	17.8
Total	66

A recent review of 1/100 year rainfall at several gauges in the basin conducted by Hatch Ltd. (2013b) provided confidence in continuing to use the same values.

B.3. 1/100 YEAR SNOW WATER EQUIVALENT

Snow water equivalent (SWE) estimates were also completed as part of the 2006 PMF update study by Acres Manitoba Ltd., using measured SWE data from the Canadian Snow Data CD for several snow courses in the basin. For 1/100 year snowpack, a lognormal distribution was fit to snowpack depth on a weekly scale and a 1/100 year value was extracted. The 1/100 year point values were then distributed to produce estimates at the sub-basin scale. Estimates by sub-

basin are provided in Table 33. Note that on a whole watershed scale, this snowpack should be slightly more conservative than a 1/100 year event, as it assumes a 1/100 year snowpack at every sub-basin (Acres Manitoba Ltd., 2006).

Table 33: Initial snow water equivalent for April 10th start date (Acres Manitoba Ltd., 2006)

Sub-basin	Description	1/100 Yr SWE (mm)	PMSA (mm)
05TA	Upper Grass River	300	382
05TB	Middle Grass River	299	346
05TC	Middle Grass River	294	317
05TD	Lower Grass River	294	317
05TE	Upper Burntwood River	293	376
05TF	Burntwood River upstream of Thompson	289	378
05TG	Odei River and lower Burntwood River	290	342
05UA	Gunisao River	310	300
05UB	Nelson River East Channel	304	303
05UC	Minago River	306	325
05UD	Cross Lake Local Basin	302	299
05UE	Upper Nelson River	294	309
05UF	Split Lake, Stephens Lake basins, Kettle River	280	321
05UG	Limestone River	274	328
05UH	Lower Nelson River around Conawapa	276	319

B.4. PROBABLE MAXIMUM SNOW ACCUMULATION (PMSA)

There are multiple methods recognized for the estimation of PMSA: snowstorm maximization, partial season, and statistical analysis. The partial season method, which combines the largest observed snowfalls regardless of year (e.g. largest monthly snowfalls) into a single seasonal maximum snowpack, is highly uncertain because estimates are too dependent on the partial season length (Chow & Jones, 1994). The statistical method noted by the Canadian

Electrical Association (1994) to be the most commonly applied and preferred over the partial season method is dependent on snow course data and requires extrapolation to extreme return periods based on short observed records. Snowstorm maximization was therefore recommended for PMSA studies. This method involves maximizing all of the largest recorded synoptic snowfall events, by comparing event precipitable water to maximum available precipitable water, over a high-snowfall winter period (Chow & Jones, 1994).

The Acres Manitoba Ltd. (2006) estimated PMSA by snowstorm maximization. Two high snowfall winters were identified from meteorological stations in the basin. Upper air measurements during large synoptic snowfall events in each winter were used to estimate the moisture available during each storm. Estimates of monthly maximum precipitation water, as per maps published by Chow & Jones (1994), were then used to maximize snowfall in each large event. The most critical year in terms of total snowpack on April 10th was selected, with measured SWE values again interpolated to the sub-basin scale and provided in Table 33. Note that the PMSA for several basins in the south of the watershed is smaller than the 1/100 year SWE as a result of the two values being calculated using different methods.

B.5. CRITICAL TEMPERATURE SEQUENCE

PMF scenarios with snowmelt contributions also require a specified temperature sequence in order to produce more critical snowmelt. These critical temperature sequences are often based on frequency analysis of observed temperature records (Alberta Transportation, 2004; CDA, 2007; FERC, 2001). Some guidelines also suggest testing sensitivity to multiple temperature sequences (FERC, 2001).

Critical temperature sequences for the LNRB were first developed in 1990 by Crippen Acres Wardrop, and then updated by the Acres Manitoba Ltd. (2006) study. The sequences were derived based on limiting temperature curves at the Thompson A. meteorological gauge for 1, 3, 7, 31-day average maximum temperatures, as well as 1/100 year dewpoint temperature. A critical temperature sequence, based on the methodology of Acres Manitoba Ltd. (2006), consisted of:

1. Daily mean temperatures up to the specified day of rapid temperature increase; then
2. Three days at the historical 3-day moving average maximum temperature; then
3. Two days at the historical daily 1:100 year dewpoint; then
4. A two to three week plateau period of temperatures between the 1:100 year dewpoint and mean temperature, before returning to daily mean temperatures.

Multiple temperature sequences were derived, where sequences differ by the start date of rapidly increasing temperatures (which facilitates rapid snowmelt). Various temperature sequences (by rapid temperature increase date) are provided as part of Table 14.

B.6. UPSTREAM CONTRIBUTIONS

Recall that there are two sources of upstream contribution to the LNRB: the Churchill River Diversion (CRD) through the Notigi Control Structure, and the outlet of Lake Winnipeg. At the CRD, contributions in the PMF scenario have historically been assumed to be 1,000 m^3/s based on licensing agreements, with this assumption continued here. Outflows from Lake Winnipeg are assumed to be at a 1/100 year magnitude, based on recommendations from a Crippen Acres Wardrop (1987) study and in accordance with CDA (2007) recommendations for upstream contributions.

A 1/100 year outflow event from Lake Winnipeg is defined based on 1/100 year annual inflows into the lake. This methodology and estimates have been updated regularly as part of previous PMF update studies. Frequency analysis was conducted on the "inflow volume available for outflow" historical record for Lake Winnipeg and a 1/100 year annual inflow volume was extracted. The annual inflows were then distributed to monthly values based on the inflow hydrograph of the highest inflow year on record. Finally, storage routing and an outflow rating curve were used to convert inflows to monthly average outflows, which are given in Table 34. To produce an outflow time series, monthly average values were placed at the center of each month and linearly interpolated between them.

Table 34: Baseline monthly average Lake Winnipeg outflows (Hatch Ltd., 2013b)

Month	1/100 Year Outflow (m^3/s)
April	4715
May	5002
June	5225
July	5210
August	4923
September	4434

B.7. ANTECEDENT CONDITIONS

Antecedent inputs include initial conditions at the start of the PMF simulation (April 10th) and conditions up to the PMP/rainfall occurrence that are intended to produce more critical conditions. The extreme snowpack input (1/100 year or PMSA) is assumed to be on the ground at the start of the model run, with 100% snow covered area in the basin. Soil storages are initially assumed to be saturated; this assumption is common among PMF literature (Alberta Transportation, 2004; CDA, 2007; Chernet et al., 2014). To achieve this soil storage assumption,

and in an attempt to mimic other PMF assumptions in the existing SSARR model, each model has its own specific initial conditions that will be discussed further in Appendix B.8.

Precipitation occurring between April 10th and the PMP event has historically been assumed to occur at daily average amounts and uniformly over the LNRB. Daily average precipitation was calculated as part of the initial PMF study by Crippen Acres Wardrop (1990) and has remained unchanged since those estimates. The same daily normal antecedent precipitation is similarly used in this project, as opposed to a more updated calculation with more recent meteorological records, for the following reasons:

- The normal daily average precipitation used historically is more conservative than more recent calculations. For the April 10-June 30 period, the currently used antecedent rainfall is 18% larger than that estimated based on 1981-2010 climate normals at the Thompson A gauge.
- Pre-project sensitivity analysis found that small changes in antecedent precipitation have no effect on the resulting PMF hydrograph. Additionally, testing with antecedent rainfall based on 1981-2010 climate normals led to insignificant changes in the critical PMF.
- Use of the currently used antecedent rainfall time series was most closely comparable to previous PMF update studies at Manitoba Hydro.

An important note on the antecedent rainfall is that the use of daily normal amounts creates a “drizzle everyday” time series. This is recognized to be not wholly realistic, as opposed to a precipitation time series including both wet and dry days. Indeed, some previous PMF studies (Beauchamp et al., 2013) have randomly inserted the PMP into a more realistic measured or projected precipitation time series. Drizzling antecedent precipitation was selected here because it is better suited for testing various PMP dates (as described in Section 4.4.7). If

inserted into an observed rainfall time series, PMPs may occur after abnormally wet or dry periods, leading to the various PMFs being wrongfully impacted by the antecedent rainfall (which should not be the case in a theoretical PMF simulation). Instead, a "drizzle everyday" time series weights all PMPs equally, places less sensitivity on the antecedent rainfall input, and is used primarily then to maintain high soil moisture conditions.

In addition, no precipitation is assumed to occur from four days before the PMP until the PMP date. This assumption is based on the recommendation by an expert with knowledge of PMF modelling and of the Manitoba Hydro PMF model, who noted that a four to five day dry period preceding the PMP is common practice to prevent overly-conservative estimates (J. Groeneveld, personal communication, January 30, 2015). A four day dry period preceding the PMP is slightly more conservative than the five day period recommended by Alberta Transportation (2004).

Finally, initial reservoir levels at the start of the PMF simulation were specified to be consistent with those in the SSARR model (Crippen Acres Wardrop, 1990). Regulated reservoirs were initialized at summer full supply levels, while unregulated reservoirs were initialized so that initial natural outflows were consistent with contributions coming from upstream (i.e. 1,000 m^3/s from Notigi through the Burntwood River, 4,000 m^3/s from Lake Winnipeg through the Upper Nelson River, summing to 5,000 m^3/s on the Lower Nelson River). Based on a comparison to long term average levels, the unregulated reservoir levels correspond to above-average conditions. Note that initial conditions were more difficult to specify in WATFLOOD, as a result of instability in the model's internal initialization. Initial reservoir levels in WATFLOOD were specified instead so as to stably simulate a high magnitude of initial outflows comparable to those from the other two models.

The magnitude of initial reservoir levels used in SSARR and continued here are consistent with or more conservative than those recommended or used in other PMF literature. CDA (2007, p. 14) guidelines recommend levels at "the higher bracket of the range of reservoir level that may be expected at the time of the beginning of the PMF", while Chernet et al. (2014, p. 574) initialize reservoir levels for a PMF study in Norway "to be as unfavorable as possible with respect to minimization of flood magnitudes". In contrast, some U.S. state guidelines specify initial water levels at normal conditions (FEMA, 2012) and Veijalainen & Vehviläinen (2008, p. 467) initialize spring water levels "near the average water levels during that time of year".

B.8. SPECIFIC MODEL INITIALIZATION

As stated previously, PMF simulations require conservative initial soil and subsurface conditions, often assumed to be at saturation, in order to produce a more critical response. Each hydrological model has a different representation of surface and subsurface processes, and therefore critical antecedent conditions took on different forms in each model. Given that the SSARR model was being used as a baseline, the initial conditions from SSARR were mimicked as closely as possible in HEC-HMS and WATFLOOD for consistency. The following sections describe the baseline PMF initialization in SSARR and the attempt to transfer those initial conditions to HEC-HMS and WATFLOOD. Note that PMF simulations in all models are assumed to begin on April 10th (i.e. that is when initial soil moisture and snowpack conditions are set).

B.8.1. SSARR

Antecedent soil conditions in the SSARR PMF model were developed by Crippen Acres Wardrop (1990), reviewed in previous PMF update studies (Acres Manitoba Ltd, 2006; Hatch Ltd., 2013b), and used in their original form in this study.

To represent saturated soil conditions, the Soil Moisture Index (SMI) was assumed to be at its maximum value in all basin elements at the start of the model run – April 10th. At maximum SMI, all moisture input is converted into runoff with no losses. The SMI fluctuates during the simulation (drops from the maximum initially then rises again with snowmelt moisture input), but this assumption maintains soil moisture at very high levels throughout the critical PMF period.

In addition, the Baseflow Infiltration Index (BII) was also initially set to a very high value in all basin elements. This high value means that the majority of runoff would occur as surface or subsurface flow, and not as slower baseflow. This conditions leads to a more critical response with reduced attenuation of runoff.

B.8.2. HEC-HMS

The HEC-HMS representation uses five vertical reservoirs – a greater complexity than the SSARR representation.

Canopy storage was assumed in all basins to be initially saturated. This assumption has a negligible effect on PMF, given the small size of the canopy storage reservoir (2-3mm). Surface storage was also assumed to be 100% filled at the start of the model run, representing high saturation levels during freezing in the previous fall, with all surface depressions filled. There is little guidance on initializing depressional storage in PMF models (because less complex models have generally been used for PMF), and no comparable condition from the SSARR model.

Therefore, this assumption was considered conservative and in accordance with the general PMF conditions of probable worst-case basin conditions.

Initial soil moisture saturation was assumed to be at 100%, in accordance with the SSARR condition for SMI.

The greatest difficulty came in determining appropriate initial saturation conditions for upper and lower baseflow reservoirs. No guidance was available from PMF literature, and the BII condition used in the SSARR model (of baseflow making up a smaller proportion of runoff) was not comparable to baseflow storage in HEC-HMS. Complete saturation of the baseflow reservoirs may have provided a similar effect as the extreme initial BII; however, this was deemed unrealistic given the large volume of initial moisture this would add into the watershed and given that over-winter baseflow recession would be expected to have occurred. Therefore, the initial condition in SSARR could not be represented in HEC-HMS. Instead, baseflow reservoir saturation was initialized for a specific return period, as opposed to complete saturation, based on a recommendation of B.C. Hydro (1994) and based indirectly on the recommendation of Haberlandt & Radtke (2014) that average values be used for antecedent conditions in design flood runs.

For each of the gauged sub-basins in the HEC-HMS model, simulated daily baseflow saturation was extracted from the calibration period (1981-2014). Saturation data was then condensed to only include points (a) in March and April, (b) when the daily hydrograph rise is at least 2% (to avoid over-winter storage amounts), and (c) when daily streamflow was less than 5-10% of the freshet peak (to avoid significant input from snowmelt recharge). This criteria isolated baseflow saturation on days at the beginning of the freshet (most comparable to initialization for PMF) and often ensured that at least one point per year was extracted. Multiple

data points from a given year were averaged to produce a single value in each year. The following steps were then followed with the annual time series for each basin:

1. Years where baseflow storage was empty were removed from the time series (for ease of distribution fitting later) and the probability of baseflow storage being non-zero was recorded.
2. A distribution was fitted to non-zero annual baseflow storage values. The method of maximum likelihood within the MATLAB Distribution Fitting Toolbox was used, often resulting in the GEV distribution being used. Significant variation between basins, and between upper and lower baseflow storage data, required several other distributions to be sporadically used.
3. A return period was estimated from the distribution, such that the combined probabilities of a non-zero storage and the return period of the value summed to a 1/100 year event. It was deemed too conservative to ignore the prevalence of years where baseflow storage was zero prior to the freshet, so the combined probability was applied to reduce the return period extracted from the distribution. More clearly, the combined probability took the form:

$$\frac{1}{100} = P(GW\ Storage\ > 0) * \frac{1}{Return\ Period}$$

This therefore represents a 1/100 year pre-freshet baseflow saturation, for each gauged sub-basin and both upper and lower baseflow reservoirs. These initial values were then regionalised by the same methodology as other basin parameters. Lacking any guiding literature on baseflow initialization for PMF, the 1/100 year saturation was deemed to be appropriately conservative based on the use of a 1/100 return period for initial snowpack in the PMP case, or a

1/100 year rainfall in the PMSA case. The selection also allows for more consistency and repeatability for future PMF studies in the LNRB.

B.8.3. WATFLOOD

Initial soil moisture in WATFLOOD is specified as a value for each land class. In this case, in keeping with the assumptions in SSARR and HEC-HMS, all land classes were assumed to have saturated soil reservoirs. The remainder of initial conditions in WATFLOOD are calculated internally based on initial values of other model data. As such, there was less control on the values of these initial conditions, and several iterations were required in order to get high but realistic initial conditions.

Initial lower zone storage (similar to the baseflow saturations in HEC-HMS) at a given location is computed in WATFLOOD based on the lower zone model parameters and the initial flow occurring from each grid cell. In turn, this initial flow is based on initial observed streamflow values at each gauge in the basin. Because there was no observed streamflow available for a PMF simulation, the first few days of simulated streamflow from the SSARR and HEC-HMS PMF models were used as initial observed discharge data in WATFLOOD. This reduced numerical instability that occurred in initial flows, however instability is still visible at the beginning of the PMF runs in WATFLOOD (Section 5.2).

Finally, an additional note on the parameterization of reservoir storage-discharge relationships in WATFLOOD is required here: as stated previously, an assumption in PMF modelling is that dams act as free overflow weirs once the maximum outflow is reached. This results in a large jump at the high end of the storage-discharge curve (no longer conforming to the shape) that is very difficult to fit with a single polynomial equation. As such, it was difficult to replicate this assumption in WATFLOOD (i.e. WATFLOOD is less flexible in its reservoir

routing scheme). The final polynomial regressions attempt to simulate this assumed free overflow behaviour (with subsequent error trade-off at lower flows), but WATFLOOD is recognized as having less ability than the other models in accurately simulating the PMF response of generating stations in the lower Nelson River complex.

APPENDIX C: METHODS OF PROJECTING CLIMATE CHANGE IMPACTS ON PMF INPUTS

The following sections provide background on the calculation of projected changes in a number of PMF inputs, for each climate model simulation between the baseline and the future period ("deltas" or "change factors"). The background differentiates between methodologies and data provided directly by Ouranos, and those applied as part of this project in consultation with Ouranos and Manitoba Hydro.

C.1. PROBABLE MAXIMUM PRECIPITATION (PMP)

Projected changes to 48-hour spring PMP over the Nelson River Basin were provided by Ouranos (developed with INRS-ETE as part of the NRCan PMP/PMF study) and were used in their original form. A summary is provided here; however, a more complete methodology can be found in Clavet-Gaumont et al. (2017). Several previous works (Beauchamp et al., 2013; Rousseau et al., 2014) were recognized as the foundation for the methodology, which attempted to follow the traditional form of PMP estimation (e.g. WMO, 2009) via storm maximization by precipitable water content. Rainfall events considered for maximization to spring PMP were limited to those where a snowpack of at least 10mm is on the ground. The methodology followed three steps:

1) Extract 30 year output data series from RCM simulations: rainfall (p), snowpack (SWE), and precipitable water (pw). Extract 48-hour events from the rainfall time series (in accordance with the baseline PMP for the LNRB).

2) For each 48-hour rainfall event, maximize the event by: $r = \frac{pw_{100}}{pw_{event}}$, where pw_{100} is the 1/100 year monthly maximum precipitable water (from RCM data) and pw_{event} is the largest precipitable water value during the event.
3) Where SWE > 10mm (assumed spring event), 48-hour rainfall events were maximized by $p_{max} = p_{event} * r$. The PMP was selected as the largest maximized event within a 30 year reference period.

The methodology was conducted by Ouranos for areas of 1-25 RCM grid cells over an extended area around the LNRB to represent storms of various sizes. Given that the baseline PMP used for the LNRB covers much of the basin, this research only applied results from the largest area of consideration (25 grid cells; approximately 50,000 km^2). The PMP then was the maximum storm estimated from all possible elliptical combinations of 25 grid cell areas in the extended basin area. The maximum 48-hour event was extracted from each year to produce a 30 year time series of annual maximum events – the largest assumed to be representative of the PMP. A change factor of PMP was then calculated between the baseline and future period. Complete details of the PMP change factor methodology can be found in Clavet-Gaumont et al. (2017).

C.2. 1/100 YEAR RAINFALL

Projected changes to the 48-hour 1/100 year spring rainfall in the LNRB were not calculated as part of the NRCan PMP/PMF study (only PMP-driven events were considered in that study). Instead these projections were estimated as part of this project; a methodology used by Ouranos for projecting changes to 72-hour storms was re-applied here for analysis of the 48-hour storm.

Using raw RCM output provided by Ouranos, rainfall at each time step was extracted at the grid point scale by (a) the liquid precipitation variable in the eight CRCM runs, and (b) any precipitation occurring when temperature ≥ 0°C in the six NARCCAP runs. Annual maximum 48-hour rainfall occurring between March 1 and July 31 was then calculated for each year in the baseline and future period. This wider period was selected by Ouranos, and used again here, in order to remove potential seasonality effects (i.e. it is unknown when spring may occur in a future scenario). A GEV distribution was used to estimate 1/100 year spring rainfall at the grid point scale, which was then averaged over all grid points in the basin to achieve 1/100 year rainfall values in the baseline and future period (and the resulting change factor). The GEV distribution was previously applied by Ouranos and was verified to adequately fit the majority of 30-year climate model periods tested in this study.

C.3. 1/100 YEAR SNOW WATER EQUIVALENT

Projected changes to basin average 1/100 year SWE were provided by Ouranos as part of the NRCan PMP/PMF study, and were used in their original form here. The methodology, intended to closely follow the traditional method of basin 1/100 year SWE estimation (e.g. Appendix B.3), is described below (Clavet-Gaumont et al., 2017).

Annual maximum SWE was extracted at the grid point scale for each year in the baseline and future period. A GEV distribution (as chosen based on maximum likelihood estimation testing) was fit to the 30 year time series of annual maximum SWE at each grid point, and used to estimate a 1/100 year value. The 1/100 year estimates were then averaged for all grid points in the basin to estimate basin average 1/100 year SWE in the baseline and in the future period.

C.4. PROBABLE MAXIMUM SNOW ACCUMULATION

As with 1/100 year spring rainfall, analysis of changes to PMSA was not included in the NRCan PMP/PMF study. Projected changes to probable maximum snow accumulation (PMSA) are estimated here, based on data and a suggested methodology provided by Ouranos.

Following a similar initial approach to 1/100 year snowpack, annual maximum SWE was extracted at the grid point scale for each year in the 30 year baseline and future periods. A GEV distribution was then used to estimate a 1/10,000 year annual maximum SWE at the grid point scale, which was then averaged at all grid points for basin values of PMSA in the baseline and future periods.

The methodology mimics the "Statistical" approach that has historically been one option for estimating PMSA. Two points regarding this approach must be recognized. First, there is lower confidence in PMSA estimates using frequency analysis compared to a snowstorm maximization approach (Chow & Jones, 1994). This was particularly true here given the uncertainty associated with estimating a 10,000 year event on 30 years of data; however, snowstorm maximization has historically required detailed analysis of individual snowstorms (e.g. see Appendix B.4). Second, a recent study by Klein, Rousseau, Frigon et al. (2016) has reported on a method to conduct the snowstorm maximization approach on climate model data (i.e. automatically, to avoid a tedious process of manual storm maximization). Given computational and time constraints (that study was published in spring 2016), this method could not be applied here. The snowstorm maximization method of Klein et al. (2016) is likely an improvement in estimating PMSA based on climate model data; however, since only relative changes in PMSA were necessary for this project, the statistical method was deemed sufficient.

A final note on this methodology is the selection of a 10,000 year return period to estimate PMSA, and the decision to estimate this value based on a distribution fitted to only 30 data points. This methodology applied to a relatively short data period has previously been applied by Manitoba Hydro for an internal study of climate change impacts on PMF using GCM projections (Manitoba Hydro, 2013) and by consultants for Newfoundland and Labrador Hydro, as a reasonable comparison to PMSA via snowstorm maximization in a PMF study of the Churchill River complex (Acres International Ltd., 1999). Other return periods for extreme SWE were also considered here, including recommendations of 1/1,000 year (W. E. Watt, 1989) and 1/500 year (Chow & Jones, 1994). However, both of these works were published prior to the development of the PMSA concept and, in the case of the 1/500 year event, were found to underestimate PMSA from snowstorm maximization (Chow & Jones, 1994). Therefore, the 1/10,000 year event estimated from a 30 year period (despite uncertainties described in Appendix E.3) was deemed most appropriate.

C.5. TEMPERATURE SEQUENCE

Projected changes to daily average temperatures over the LNRB were provided by Ouranos as part of the NRCan PMP/PMF study (Ouranos, 2015). Ensemble average values of 25th, 50th, and 75th percentile changes for each day from April 1 to June 30 were provided (i.e. a single set of projections from the ensemble of fourteen model simulations).

Temperature changes were additionally required for July through September in the PMF simulation. The temperature delta for June 30th was assumed to hold constant through that period. This assumption is expected to have no effect on peak flows in future PMF simulations, as the latest occurrence of a spring PMF is in early July (that is, if driven by a PMP on June 30th).

If a similar study on summer PMF were to be conducted, this assumption would need to be revisited.

C.6. UPSTREAM CONTRIBUTIONS

Projected changes to upstream contributions were also required given the two sources of inflow to the LNRB. No change was assumed in maximum inflows from the CRD based on recommendation from Manitoba Hydro. Changes in 1/100 year outflows from Lake Winnipeg were estimated as per below, based on recommendations from Ouranos and Manitoba Hydro.

For each of the fourteen simulations, the runoff variable was provided by Ouranos and extracted at the grid point scale for all grids within the Lake Winnipeg watershed. This data was then basin-averaged and summed into annual inflow volumes to Lake Winnipeg, resulting in 30 year inflow time series in the baseline and future periods. A lognormal distribution was fit to each 30 year period, and a 1/100 year annual inflow volume to Lake Winnipeg was estimated for each period. The use of a lognormal distribution was consistent with previous Manitoba Hydro studies of projected changes to Lake Winnipeg inflow volumes (Manitoba Hydro, 2013); a chi-squared goodness of fit test was used to validate the choice of a lognormal distribution.

The 1/100 year inflow volume was then converted into a resulting 1/100 year outflow based on the method previously described in Section 4.5.6. Recall that this involved using this annual volume to scale the monthly average inflow pattern from the largest historical annual inflow, and then using lake storage routing and an outflow rating curve to produce resulting 1/100 year monthly outflows. Final projected climate change factors were then determine by comparing 1/100 year monthly outflows between each baseline and future period.

APPENDIX D: MODEL CALIBRATION RESULTS

Appendix D includes hydrographs from historical simulations (calibration and validation) from all three hydrological models, separated by sub-basin. The results are best considered in the context of the performance metrics and average annual hydrographs in Section 5.1.

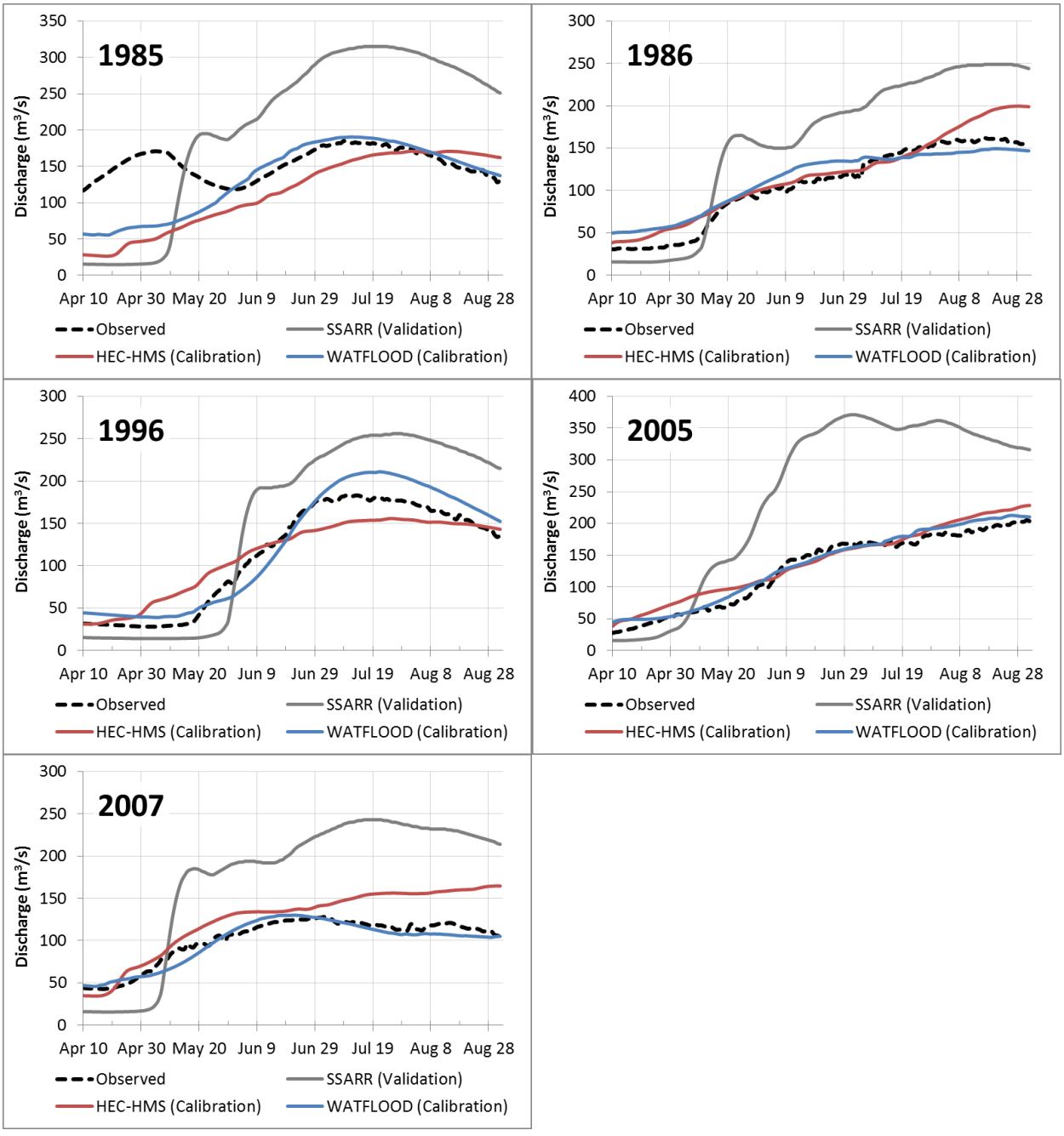

Figure 34: Comparative hydrographs of historical high flow years (SSARR- validation; HEC-HMS and WATFLOOD - calibration) in the Grass River basin

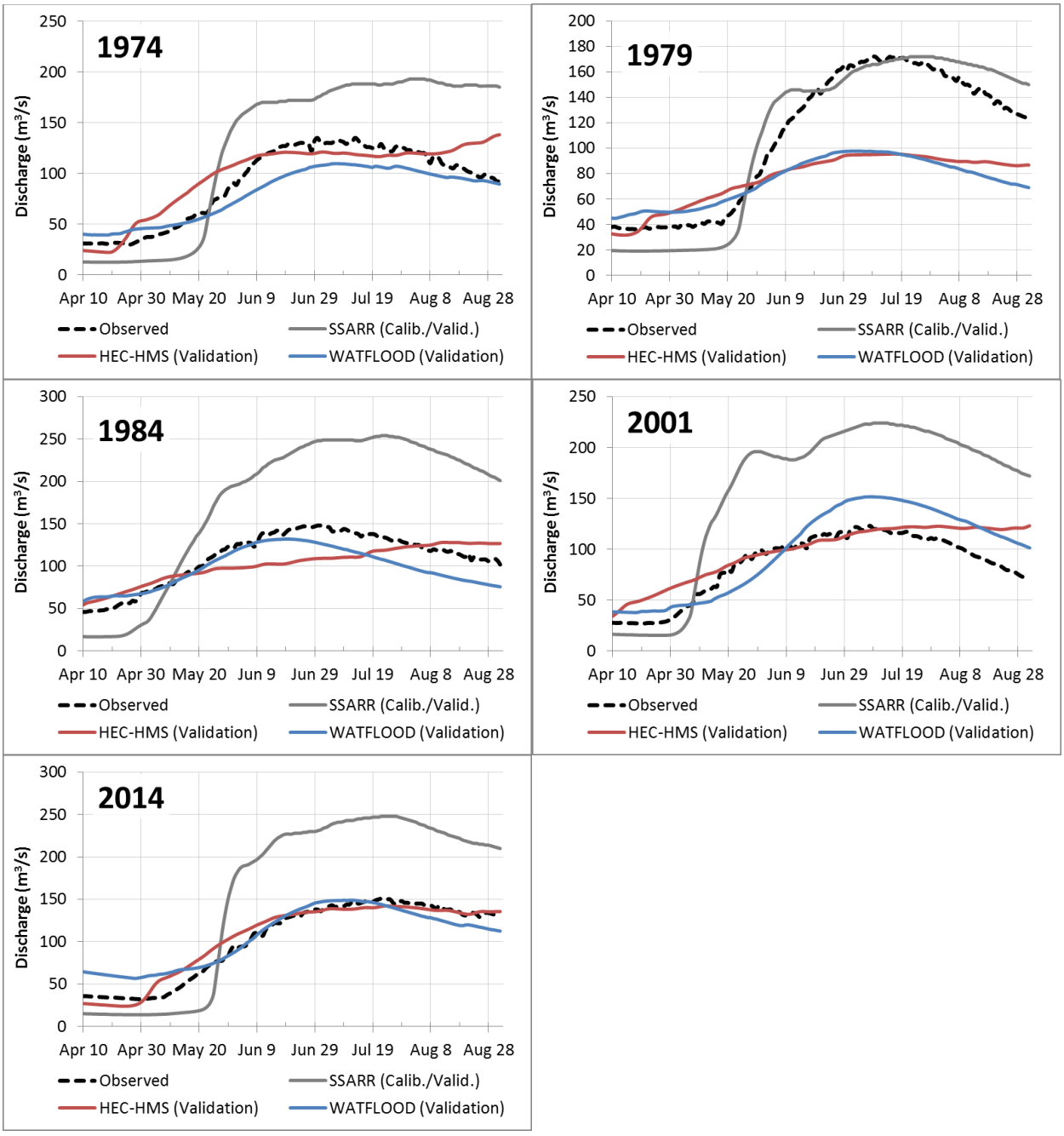

Figure 35: Comparative hydrographs of historical high flow years (SSARR- calibration & validation; HEC-HMS and WATFLOOD - validation) in the Grass River basin

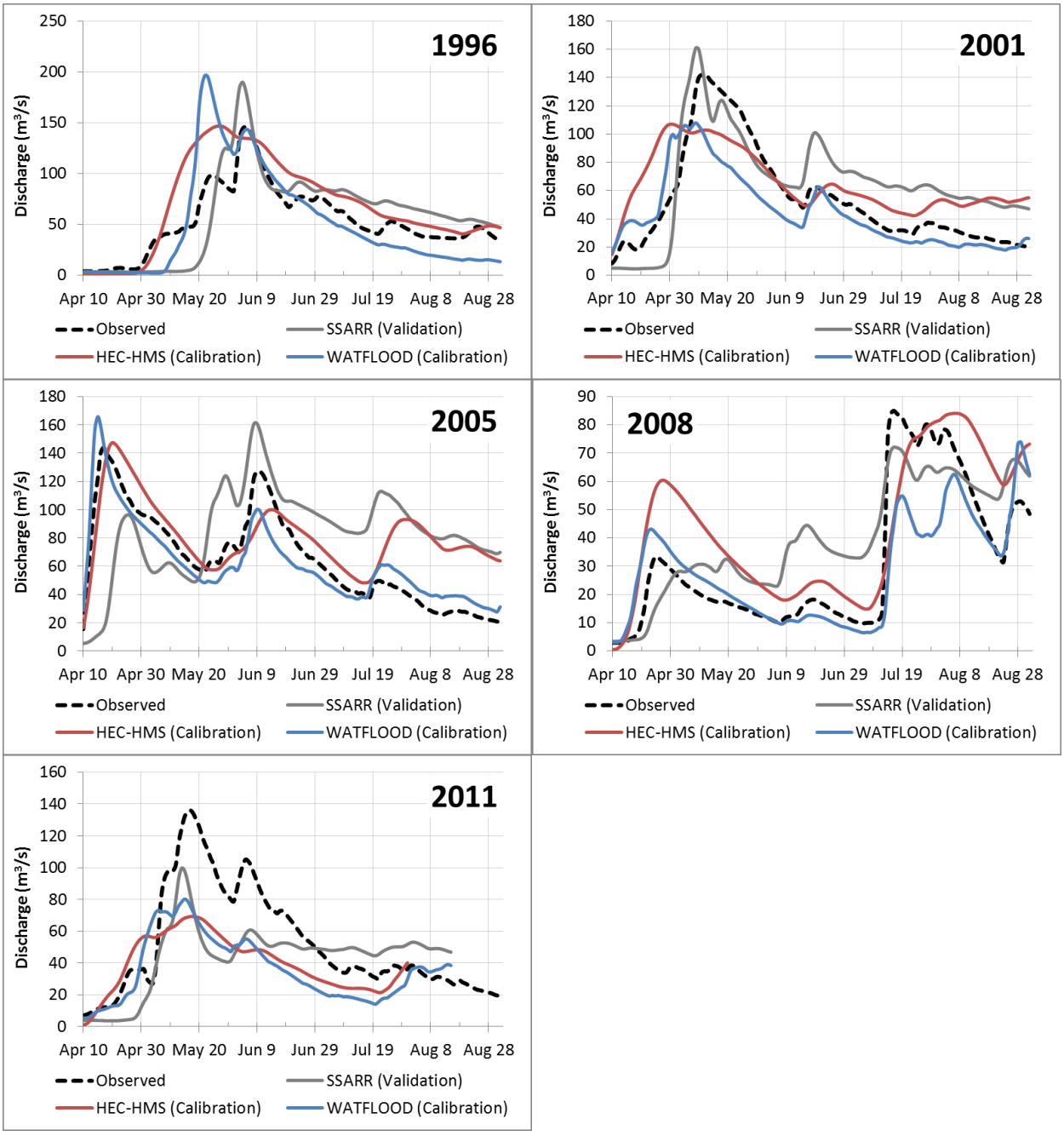

Figure 36: Comparative hydrographs of historical high flow years (SSARR- validation; HEC-HMS and WATFLOOD - calibration) in the Gunisao River basin

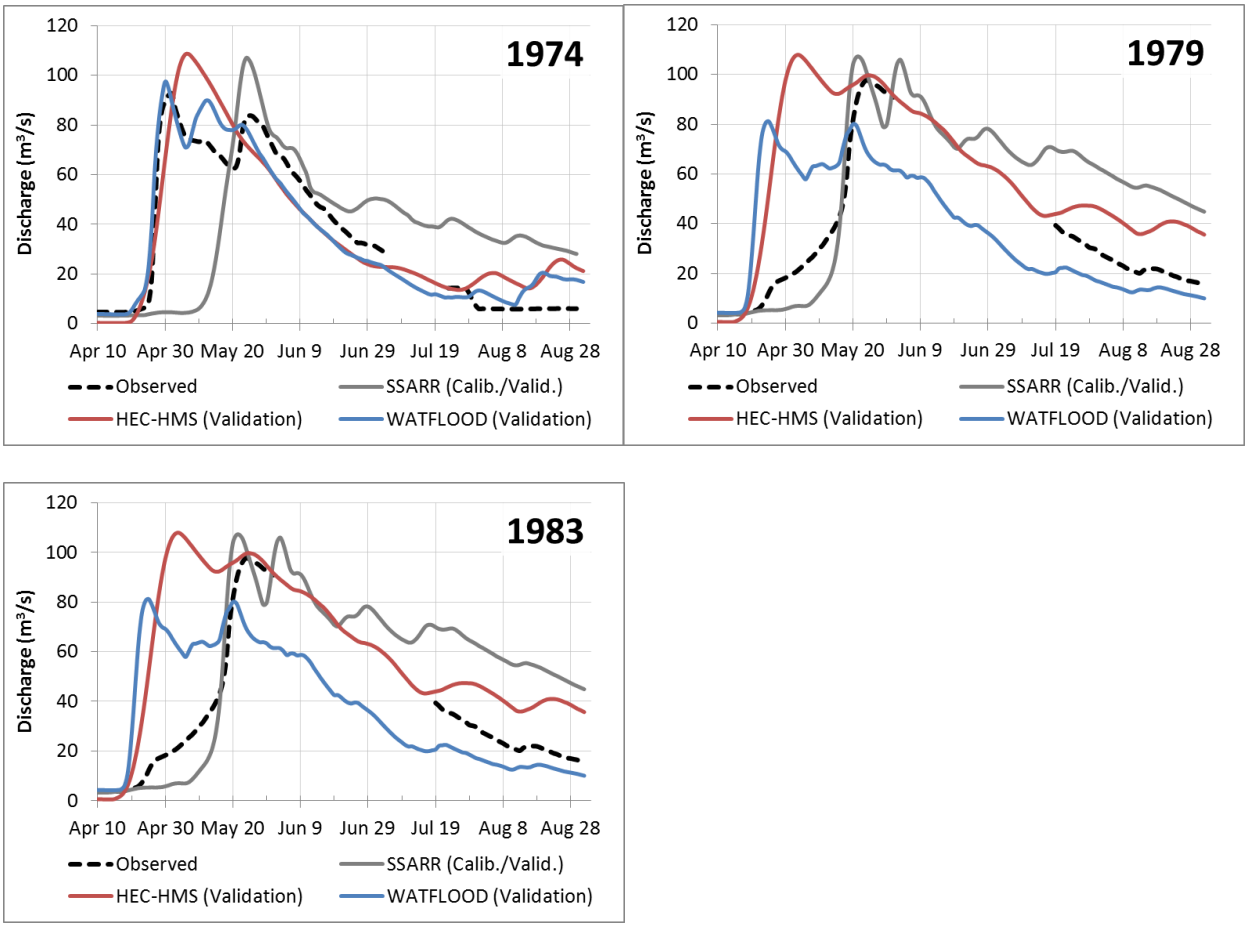

Figure 37: Comparative hydrographs of historical high flow years (SSARR- calibration & validation; HEC-HMS and WATFLOOD - validation) in the Gunisao River basin

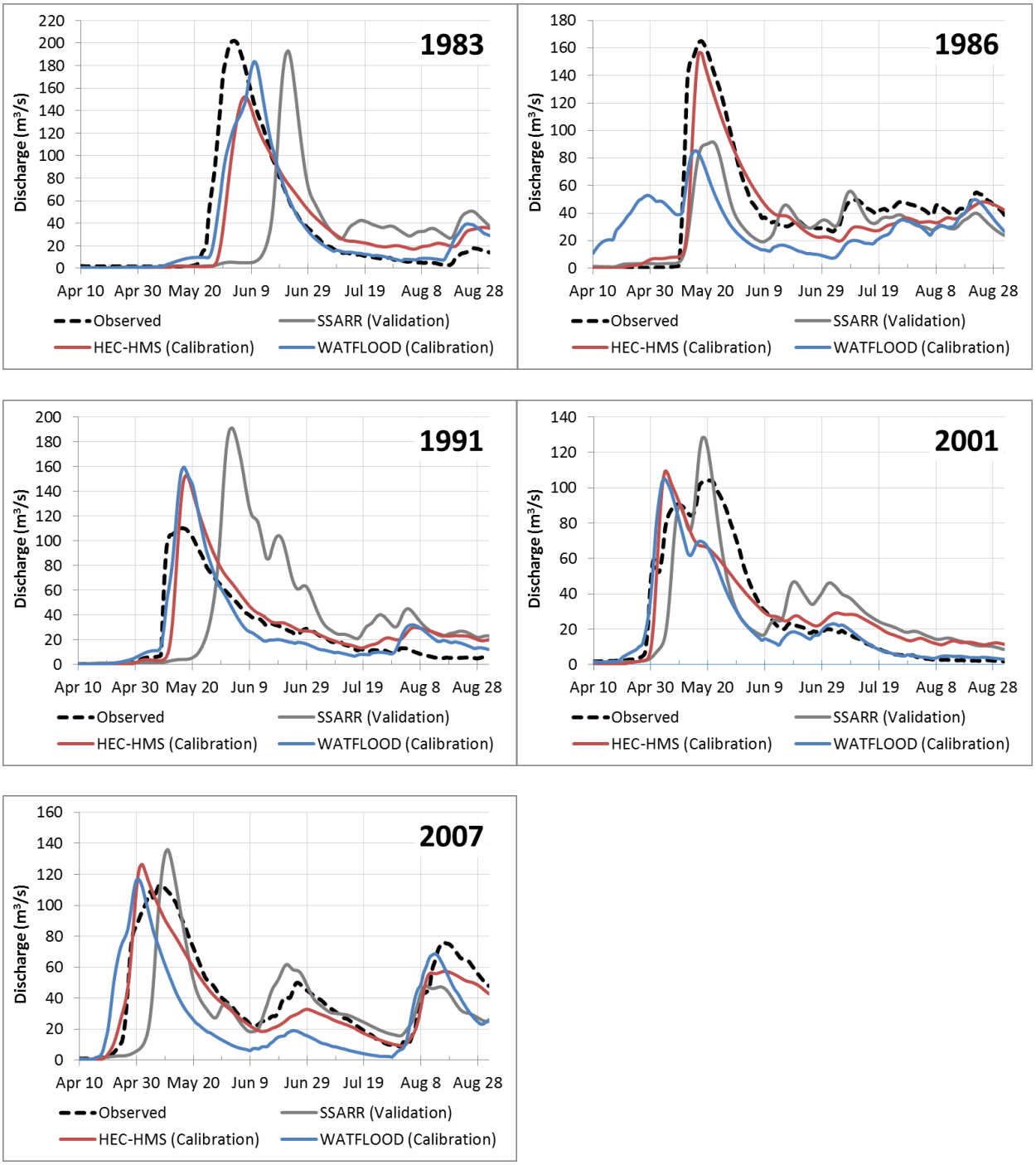

Figure 38: Comparative hydrographs of historical high flow years (SSARR- validation; HEC-HMS and WATFLOOD - calibration) in the Kettle River basin

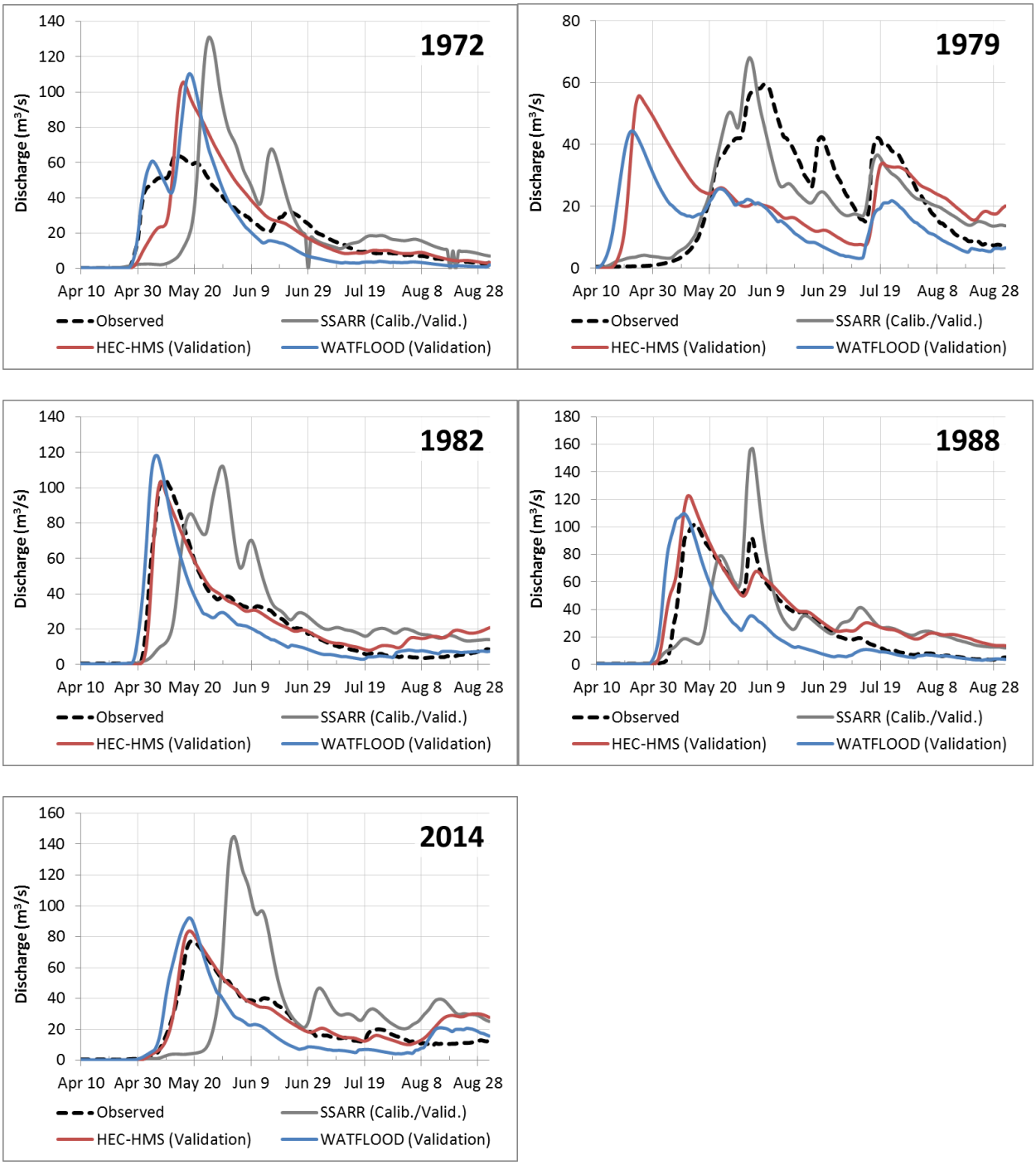

Figure 39: Comparative hydrographs of historical high flow years (SSARR- calibration & validation; HEC-HMS and WATFLOOD - validation) in the Kettle River basin

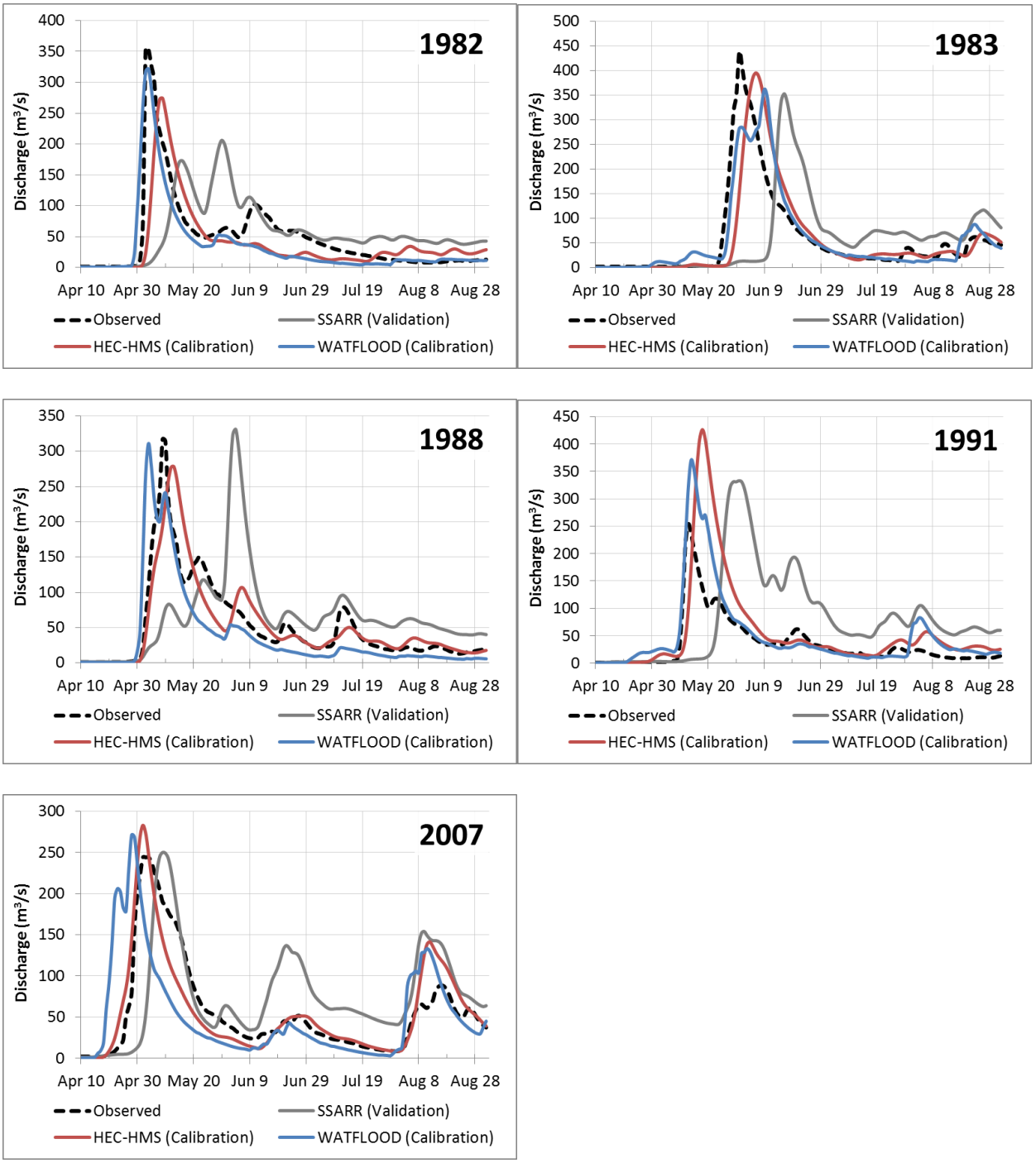

Figure 40: Comparative hydrographs of historical high flow years (SSARR- validation; HEC-HMS and WATFLOOD - calibration) in the Limestone River basin

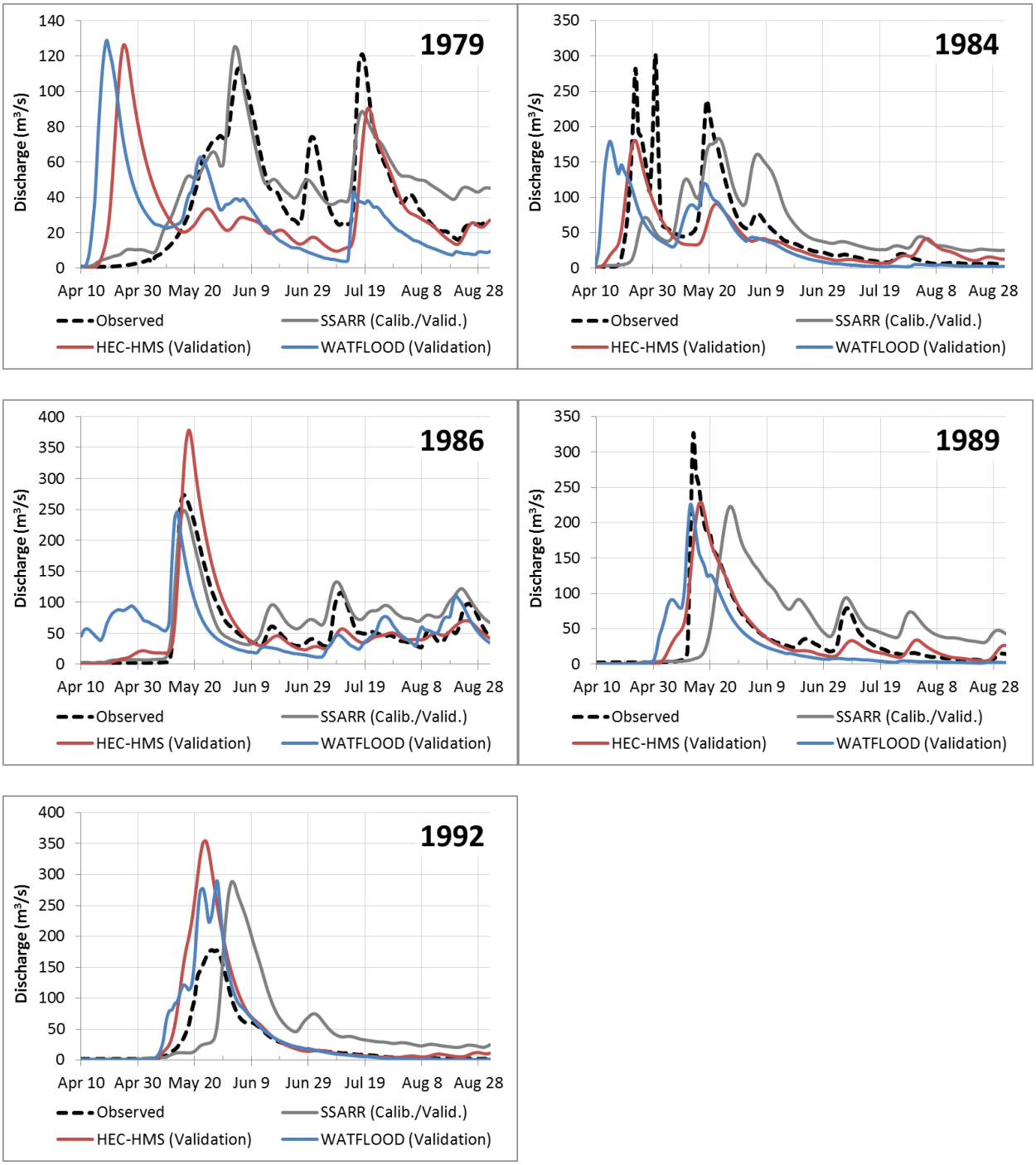

Figure 41: Comparative hydrographs of historical high flow years (SSARR- calibration & validation; HEC-HMS and WATFLOOD - validation) in the Limestone River basin

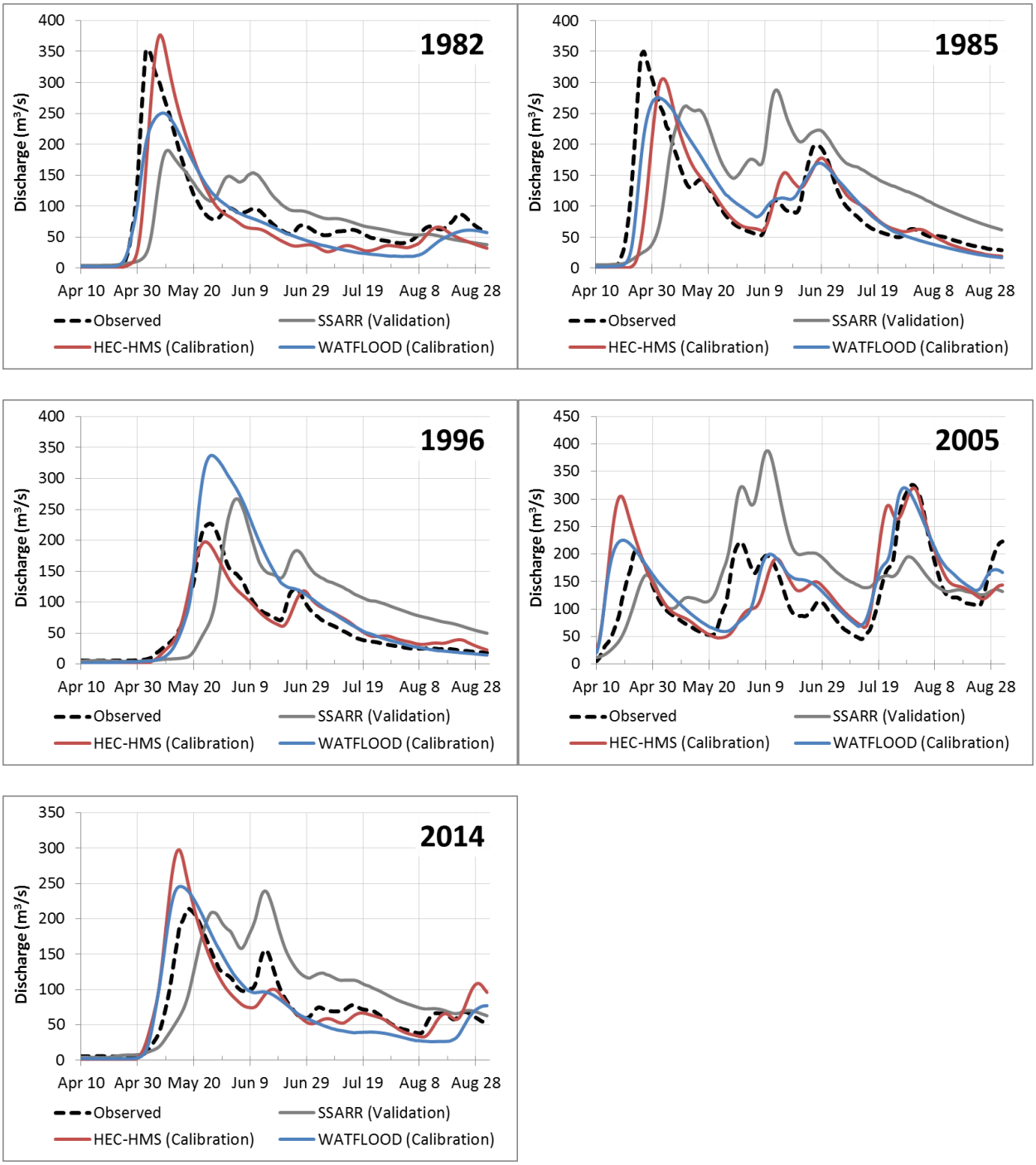

Figure 42: Comparative hydrographs of historical high flow years (SSARR- validation; HEC-HMS and WATFLOOD - calibration) in the Odei River basin

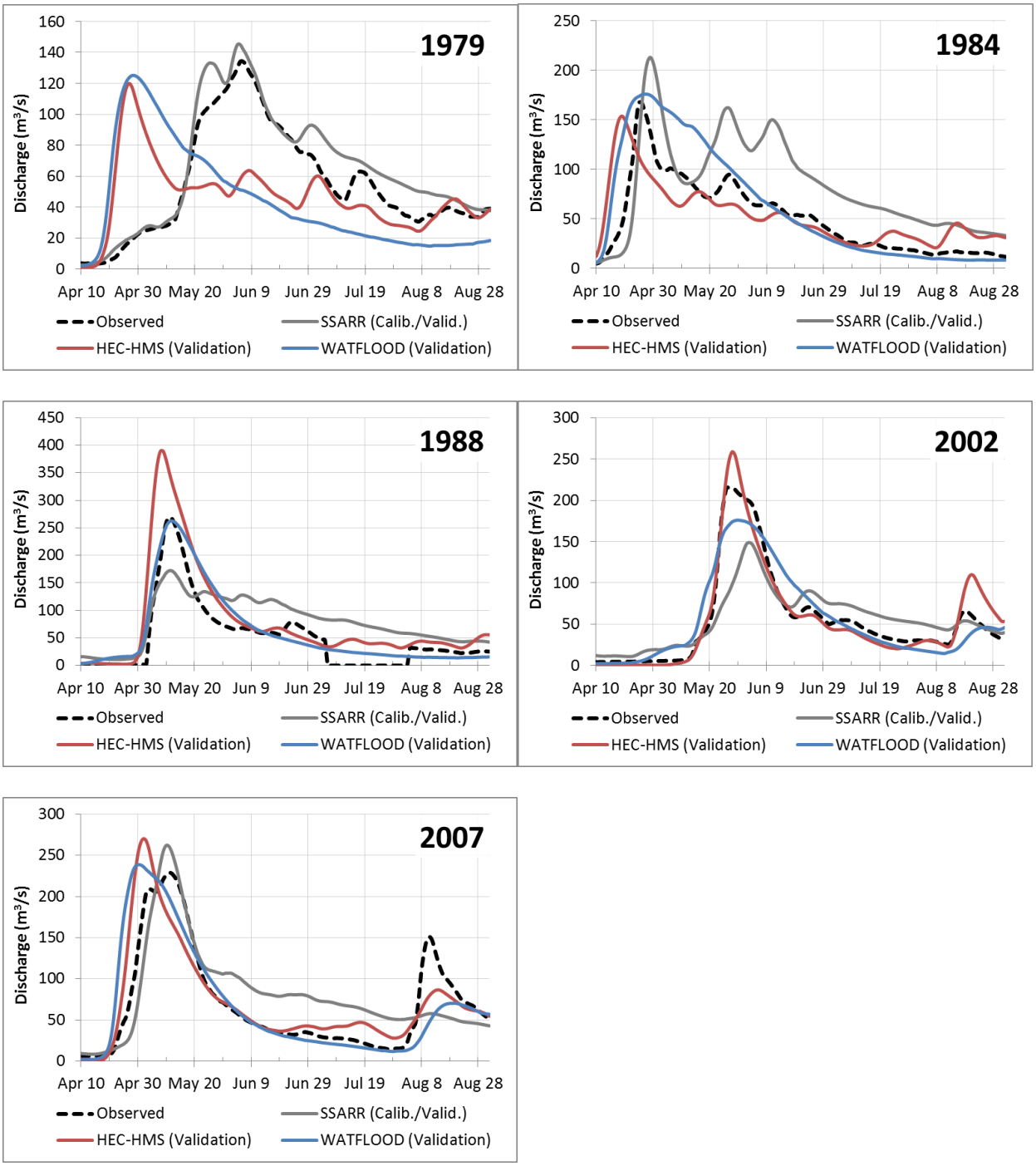

Figure 43: Comparative hydrographs of historical high flow years (SSARR- calibration & validation; HEC-HMS and WATFLOOD - validation) in the Odei River basin

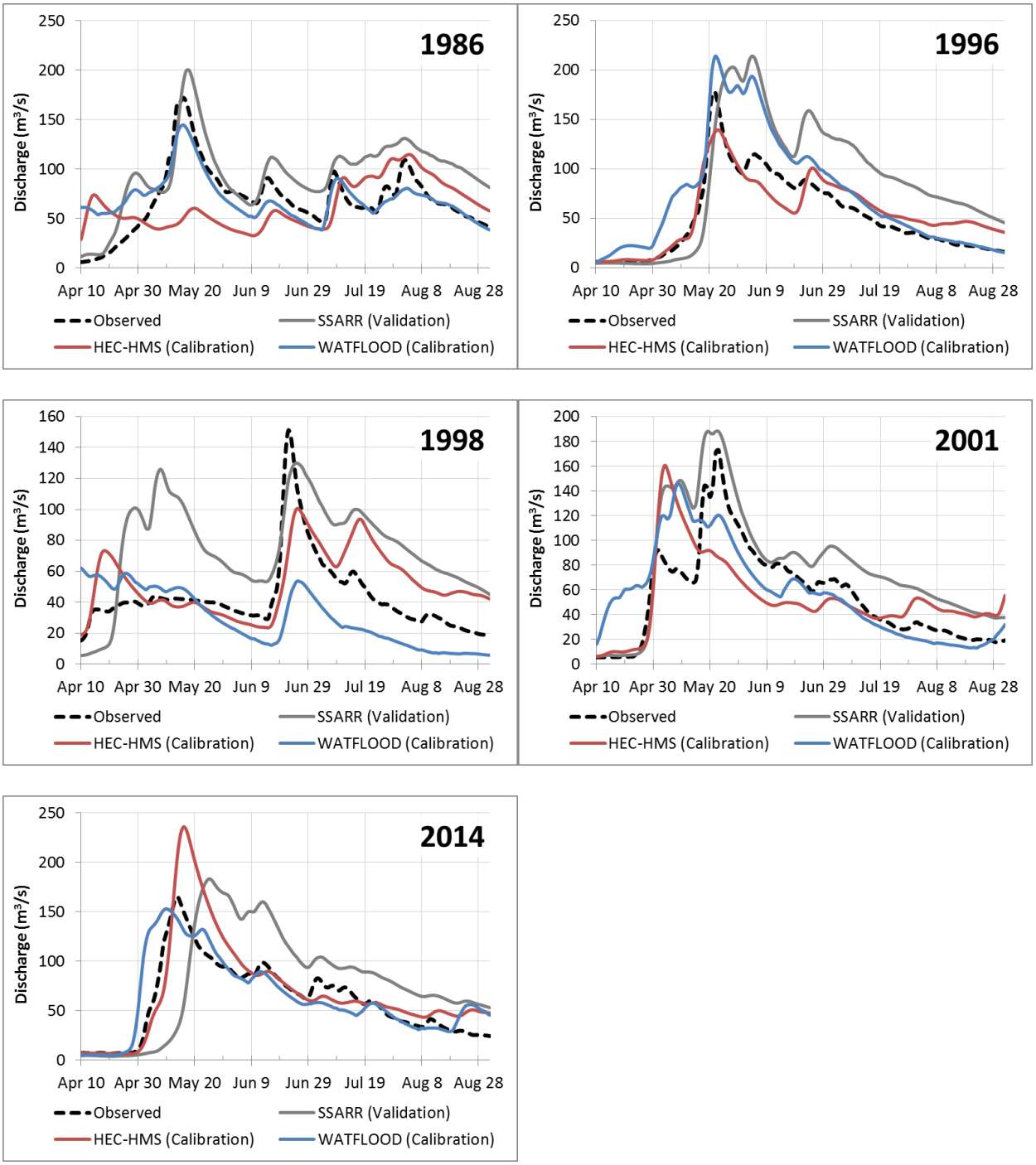

Figure 44: Comparative hydrographs of historical high flow years (SSARR- validation; HEC-HMS and WATFLOOD - calibration) in the Upper Burntwood River basin

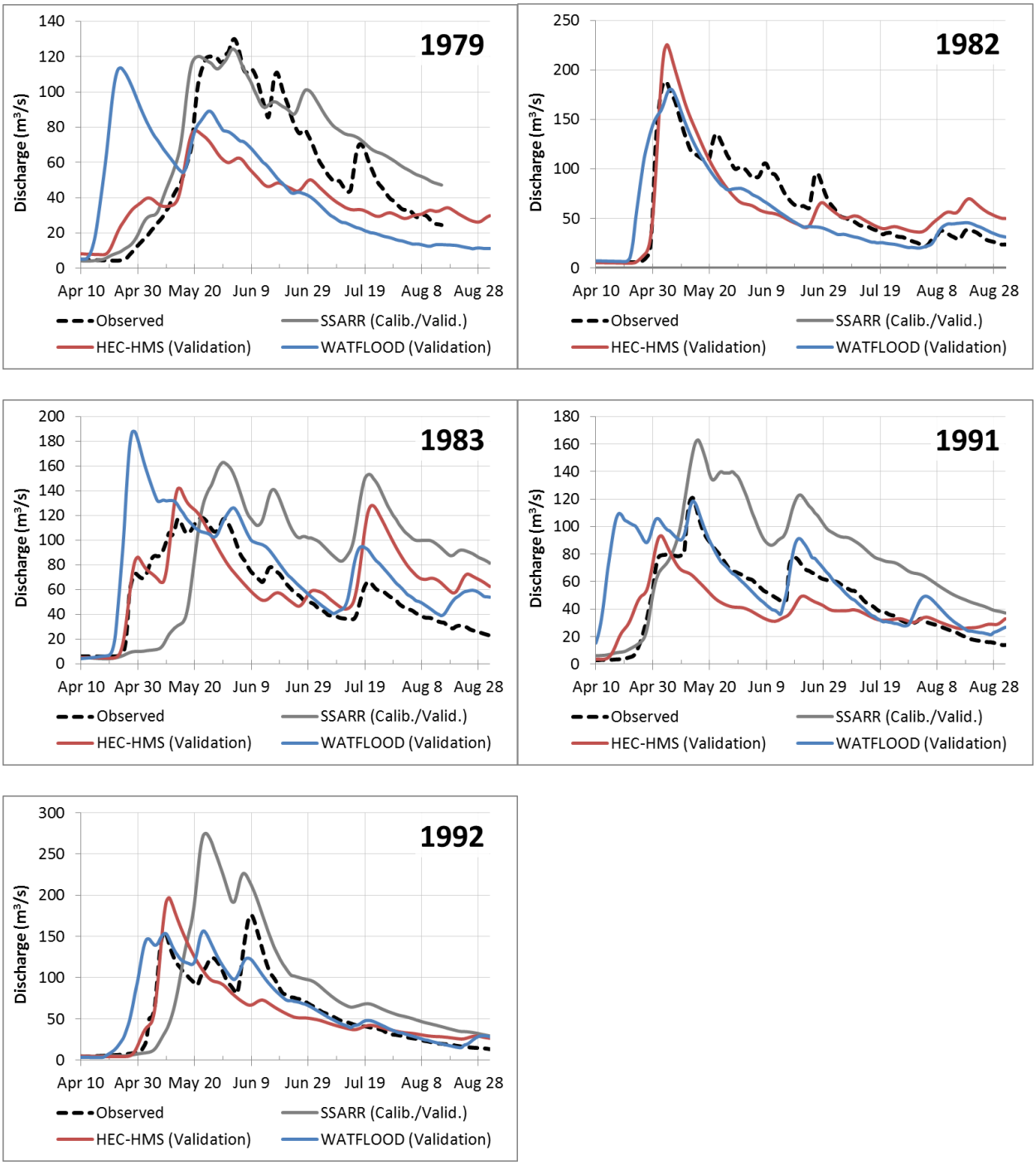

Figure 45: Comparative hydrographs of historical high flow years (SSARR- calibration & validation; HEC-HMS and WATFLOOD - validation) in the Upper Burntwood River basin

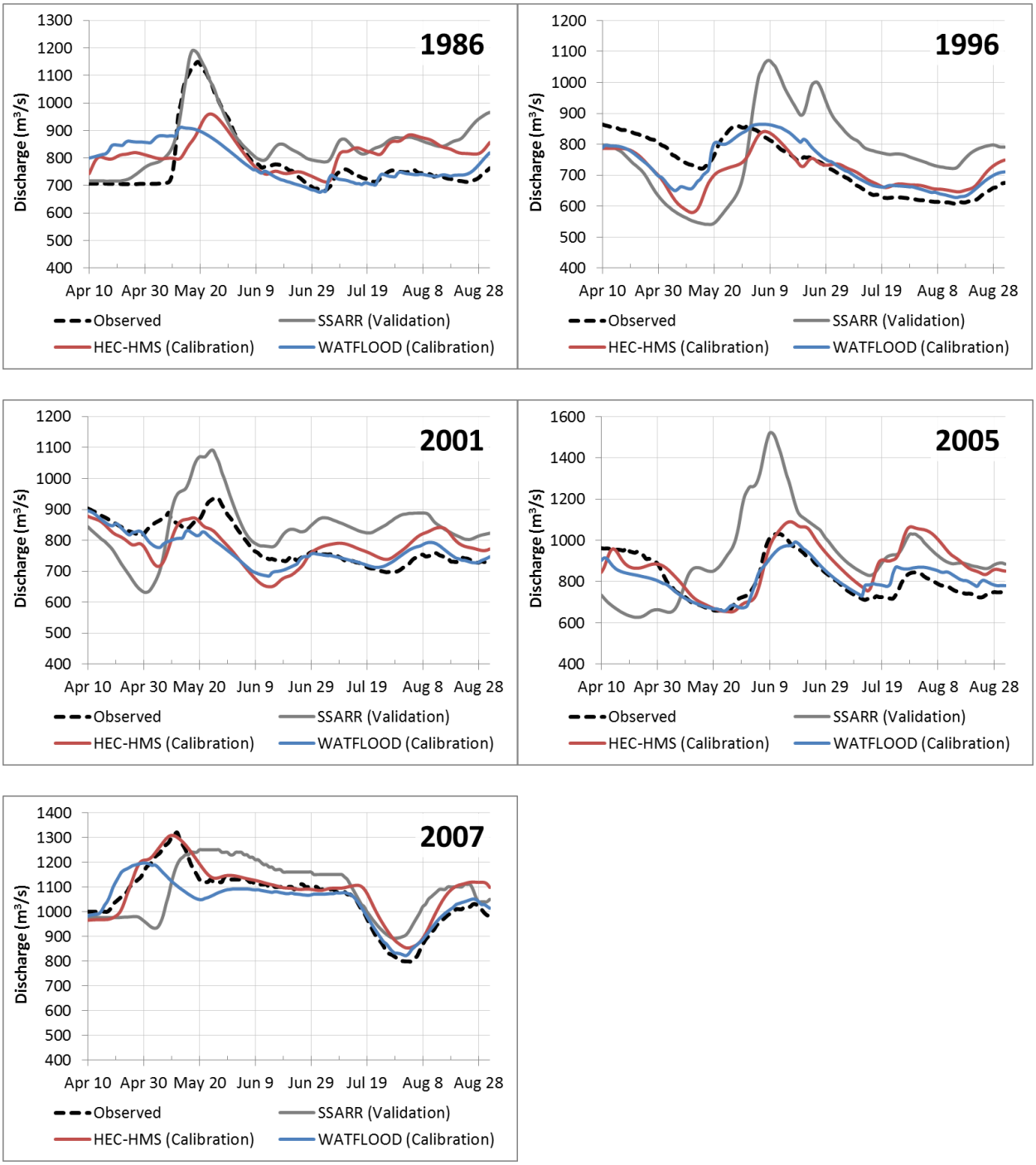

Figure 46: Comparative hydrographs of historical high flow years (SSARR- validation; HEC-HMS and WATFLOOD – calibration) at the Burntwood River at Thompson.

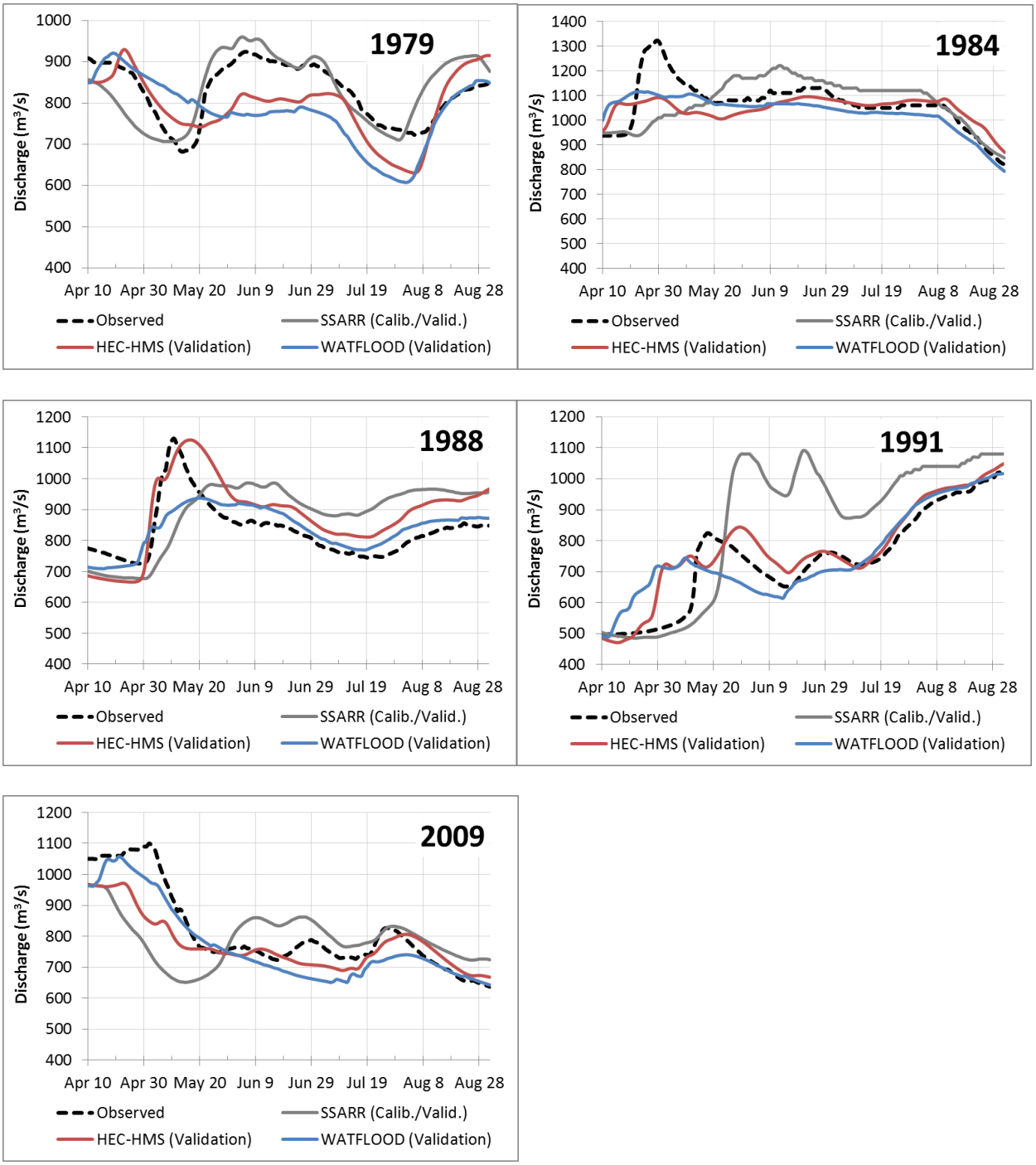

Figure 47: Comparative hydrographs of historical high flow years (SSARR- calibration & validation; HEC-HMS and WATFLOOD - validation) at the Burntwood River at Thompson

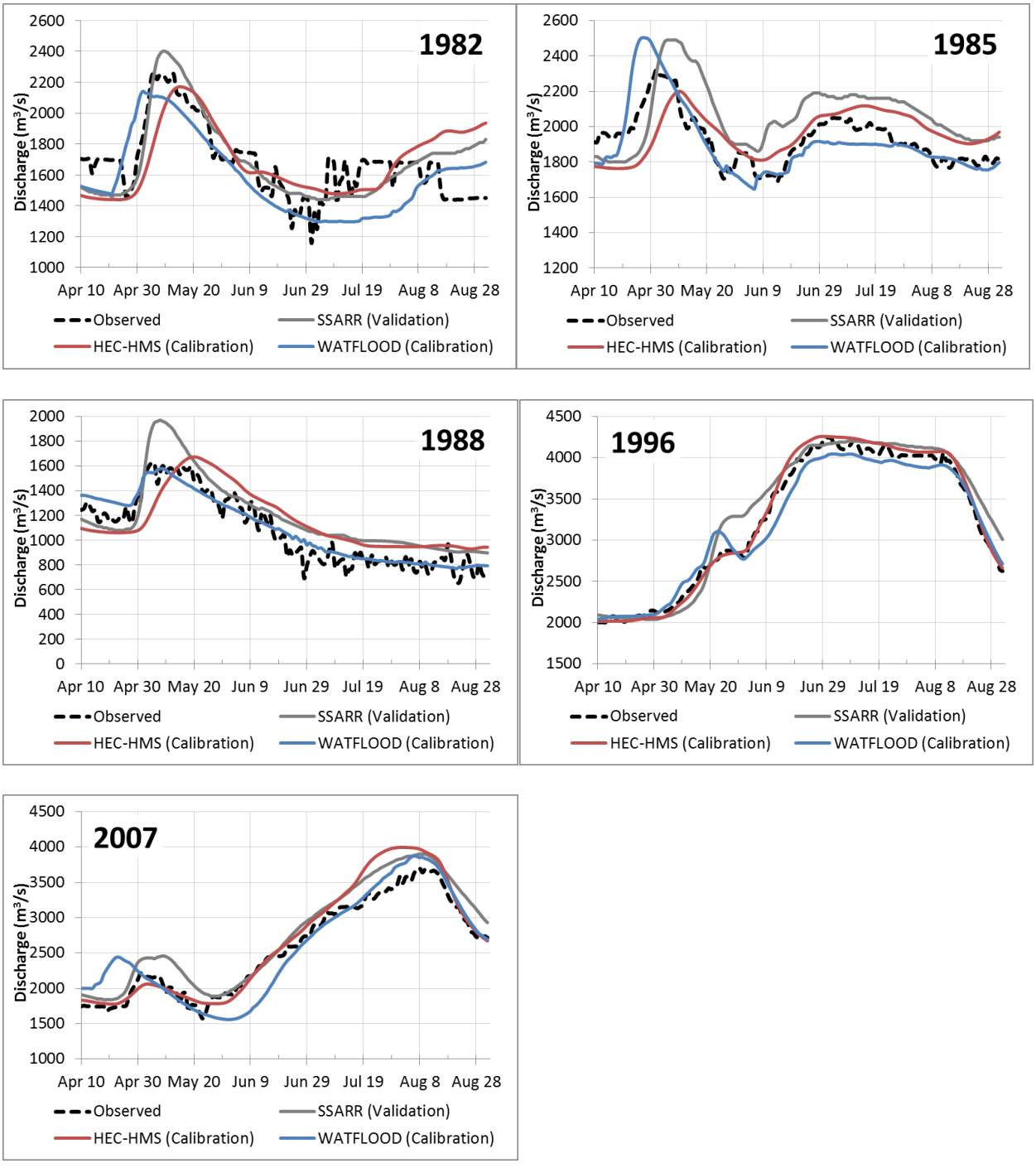

Figure 48: Comparative hydrographs of historical high flow years (SSARR- validation; HEC-HMS and WATFLOOD – calibration) at Kelsey G.S.

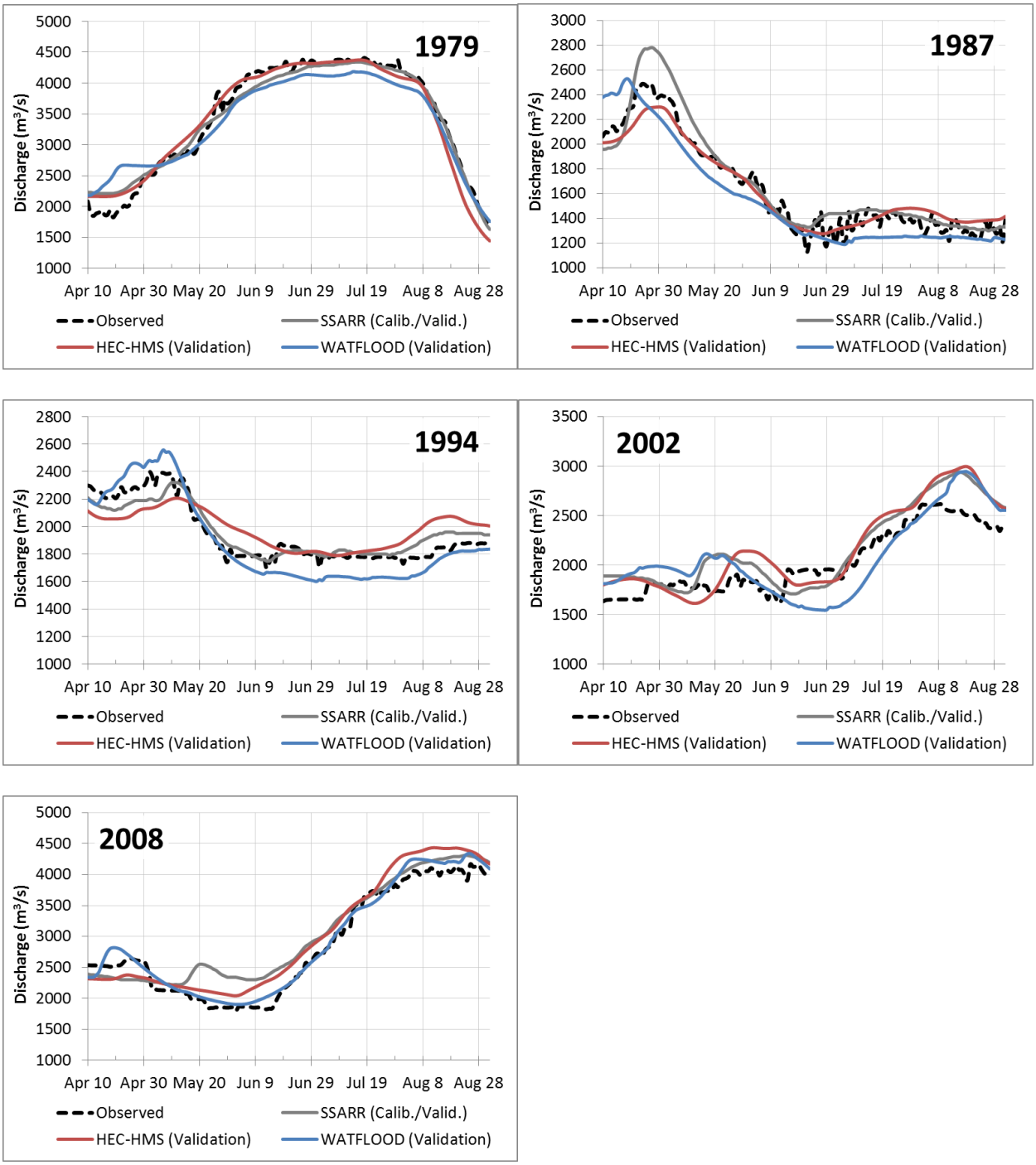

Figure 49: Comparative hydrographs of historical high flow years (SSARR- calibration & validation; HEC-HMS and WATFLOOD - validation) at Kettle G.S.

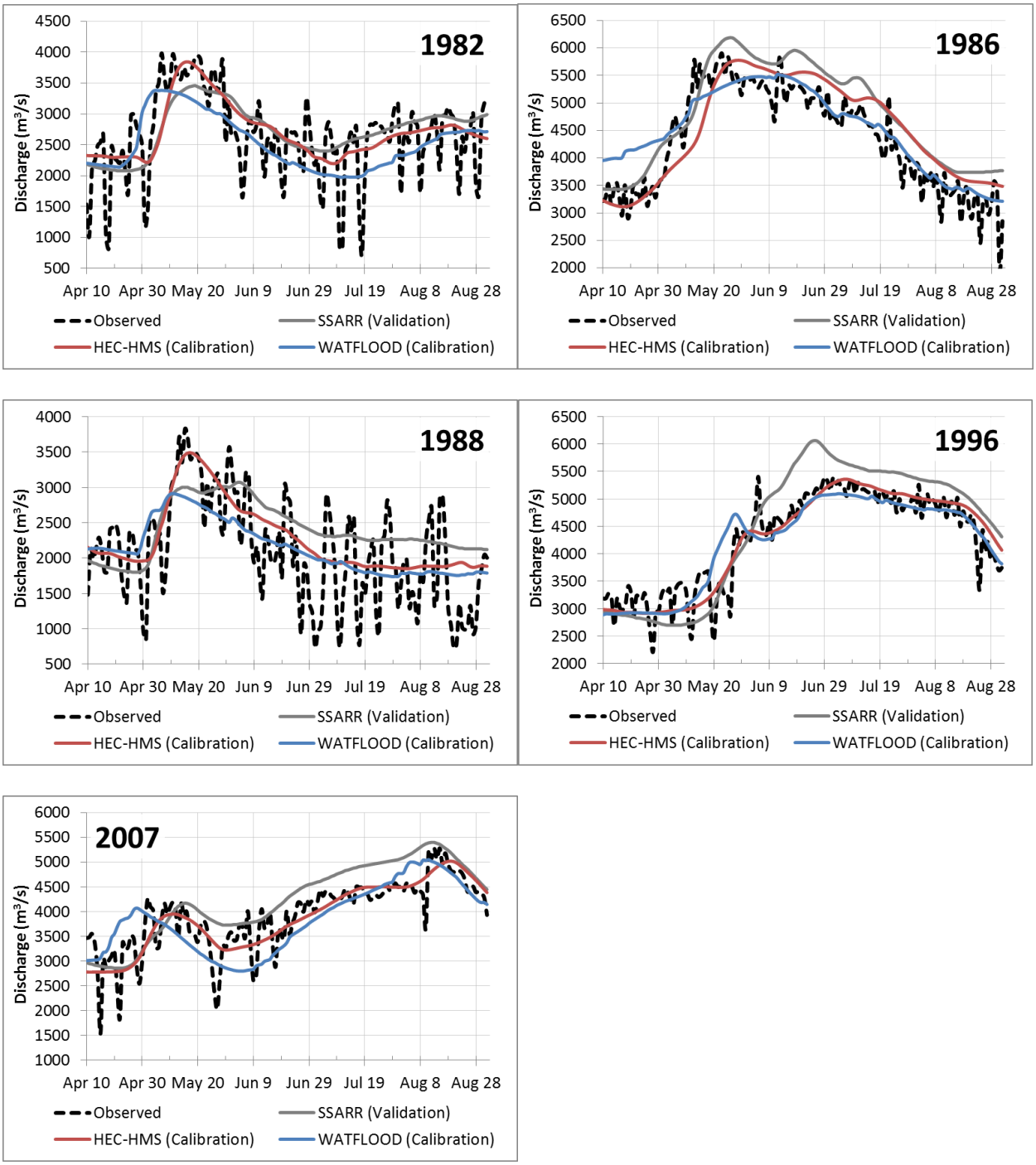

Figure 50: Comparative hydrographs of historical high flow years (SSARR- validation; HEC-HMS and WATFLOOD – calibration) at Kettle G.S.

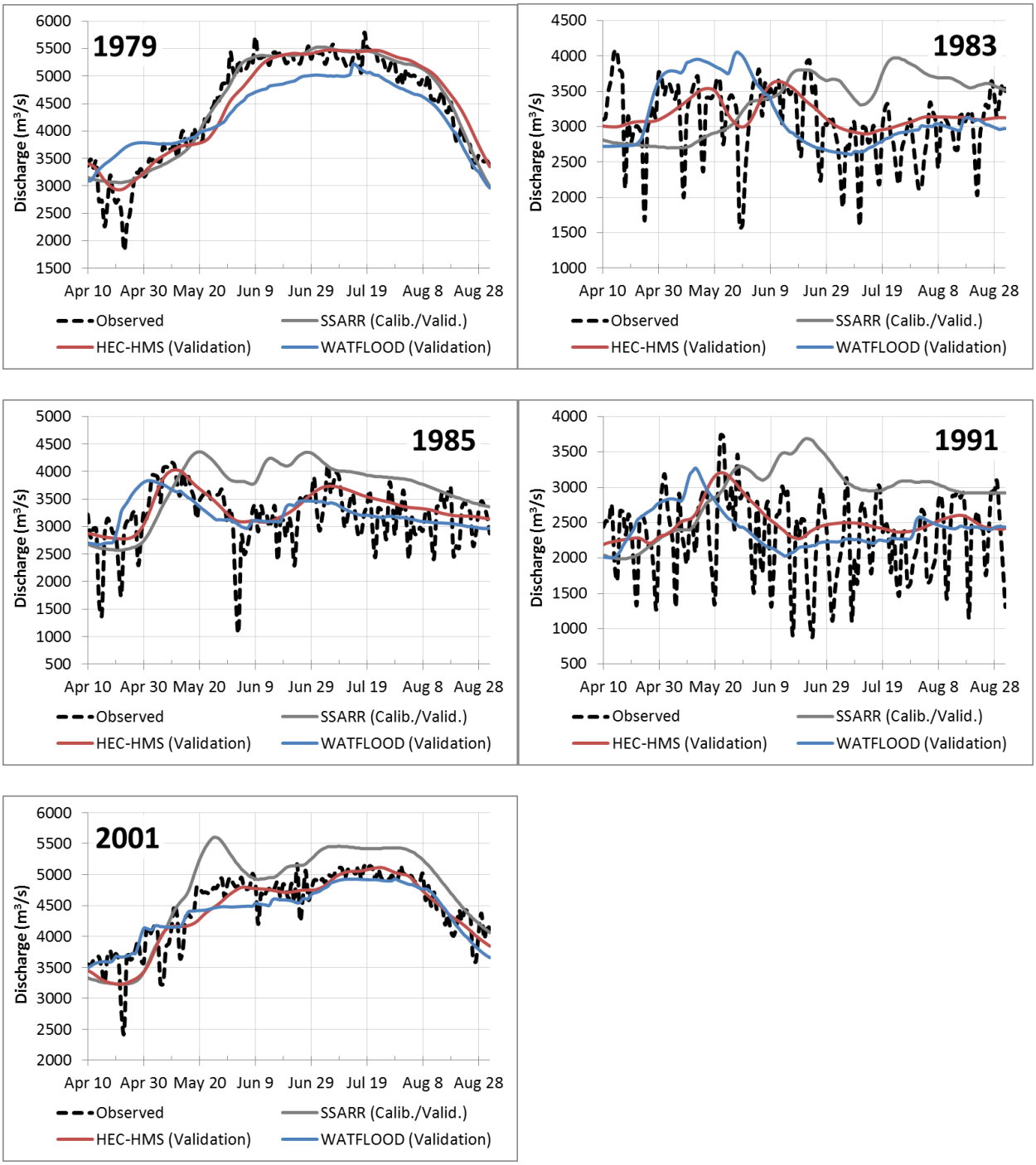

Figure 51: Comparative hydrographs of historical high flow years (SSARR- calibration & validation; HEC-HMS and WATFLOOD - validation) at Kettle G.S.

APPENDIX E – PROJECTED CLIMATE CHANGE IMPACTS ON PMF INPUTS

Appendix E reports the projections from the fourteen future climate scenarios simulated in this research. These projections were derived based on the methodologies in Appendix C, and their impact on PMF simulations is illustrated in Section 5.4 and Appendix F.

E.1. PRECIPITATION AND SNOWPACK

Changes were projected for PMF inputs related to precipitation (PMP or 1/100 year spring rainfall) and initial snowpack (1/100 year or PMSA). Figure 52 illustrates the spread of RCM projected changes to baseline PMP and baseline 1/100 year snowpack, as well as the median change from the fourteen RCMs. These projections were developed by Ouranos and INRS-ETE for the NRCan PMP/PMF study and are used here in their original form.

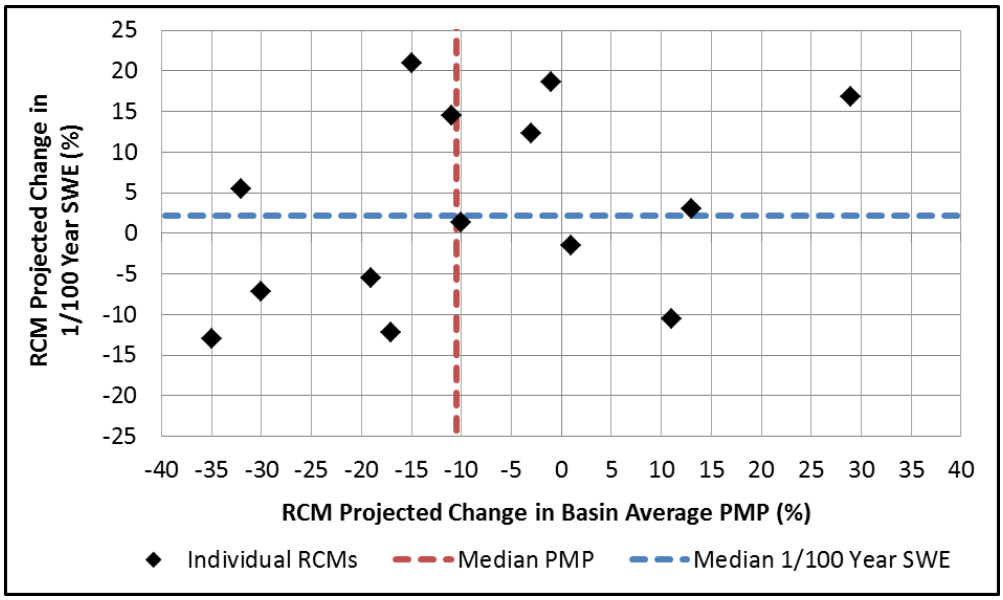

Figure 52: RCM projected changes to baseline PMF inputs (PMP scenario); data provided by Ouranos from NRCan study (Clavet-Gaumont et al., 2017; Ouranos, 2015)

The range of projected changes to PMP (65% of the baseline value) is nearly twice as large as the range for 1/100 year SWE (34%). The median projected change in each input also differs in both magnitude and direction: -10.8% (PMP) and +2.2% (SWE). The wide range, particularly of PMP projections, resulted from a number of forms of uncertainty discussed in detail in Appendix E.3.

A level of confidence in the directions of medians can be estimated based on the spread of model projections, as per the IPCC's 5th Assessment Report; for more details see Cubasch et al. (2013, ch. 1, pp. 139,142). Given that both variables have approximately equal number of projections on each side of the origin, there is "no consensus" in terms of the direction of change in PMP or 1/100 year SWE. Having said that, of importance to this research is the range of possible future scenarios.

Figure 53 shows similar projections for the PMSA scenario; these projected changes were developed as part of this research by extending existing methodologies used by Ouranos.

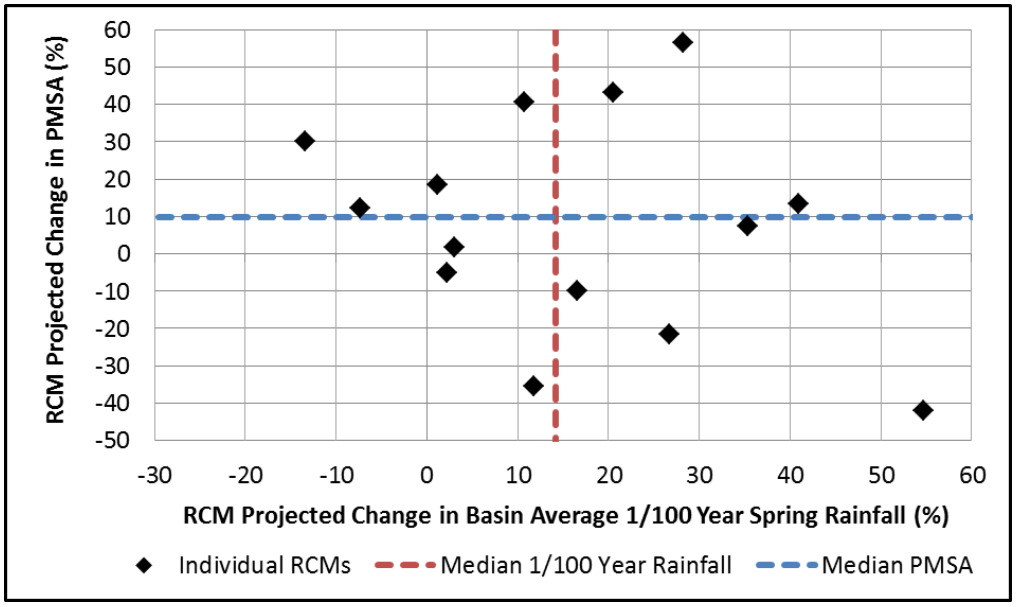

Figure 53: RCM projected changes to baseline PMF inputs (PMSA scenario)

The range of projected changes to inputs in the PMSA scenario is much larger than those for the PMP scenario. There is a 71% range about the baseline for 1/100 year 48-hour spring rainfall and a 99% range about the baseline for projected PMSA changes. The median projections for each input both agree on increased amounts: a 14.2% increase in 1/100 year rainfall and a 9.9% increase in PMSA. Using a similar assessment of confidence as described earlier from Cubasch et al. (2013), there is no consensus in the direction of PMSA change but there is a "likely" increase in 1/100 year spring rainfall (12/14 projections agree on the direction). This agreement among scenarios manifests itself in the future PMF (PMSA) hydrographs presented in Section 5.4,

Note that the range and median of projected changes for 1/100 year spring rainfall are very different from those for spring PMP, sometimes in opposing directions even from the same climate model. Such large differences between the two quantities are not unexpected for a number of reasons:

- Given the lack of consensus in the PMP projections, there is little confidence in the sign or magnitude of the median of the projected PMP changes. As such, the opposing direction of the PMP and 1/100 year spring rainfall median changes is not significant.
- The 48-hour PMP and 48-hour 1/100 year spring rainfall represent entirely different precipitation events. The PMP incorporates an additional variable, precipitable water, in order to maximize the simulated storm. The two precipitation events thus may not necessarily change by the same magnitude or direction given that PMP also depends on modelled precipitable water and an estimate of the 1/100 year maximum precipitable water.

- Significant uncertainty (under-sampling, model uncertainty, and natural climate variability to be discussed further in Appendix E.3) led to highly variable projections. However, an important note to make is that the size of projected change should not necessarily be proportional to the magnitude of the variable of interest. In particular, the more extreme event (PMP) may not necessarily have more extreme delta values, or more or less confidence in the ensemble median, compared to results for the 1/100 year storm.

The relatively large range of projected changes to PMSA (~100% of the baseline value) warranted additional analysis given the potentially significant impact this could have on PMF (PMSA) simulations. As a test of uncertainty surrounding the PMSA projections, 95% confidence intervals were estimated for each RCM by bootstrap resampling. A detailed explanation of bootstrap resampling methodology can be found in Kundzewicz & Robson (2004). The method was ideal for this case (and generally is recommended for hydrological data) as it does not assume a statistical distribution for the observed data – it merely resamples values from the observed time series (Kundzewicz & Robson, 2004). The *bootci()* function in MATLAB was utilized for bootstrap resampling analysis. In this application, the 30 year time series of simulated annual maximum snowpack (for both baseline and the future period) at each grid point in the LNRB were resampled with replacement. The baseline and future 1/10,000 year event was then estimated at each grid point (same as in the original projections), and a basin average change factor was developed. The process was repeated for 1,000 resamples and 95% confidence intervals were developed for each RCM. Figure 54 provides the original projected PMSA deltas and the 95% confidence intervals around each projection.

Figure 54 illustrates the confidence intervals that develop when sampling a 1/10,000 year event from a series of 30 data points, then basin-averaging those quantities. The confidence intervals are noticeably wide, with the narrowest interval still having a range of 60% of the baseline value. However, the wide intervals also lead to significant overlapping among the climate models; this shows that even the most extreme projections cannot be discounted given that they fall within the confidence interval of other RCMs.

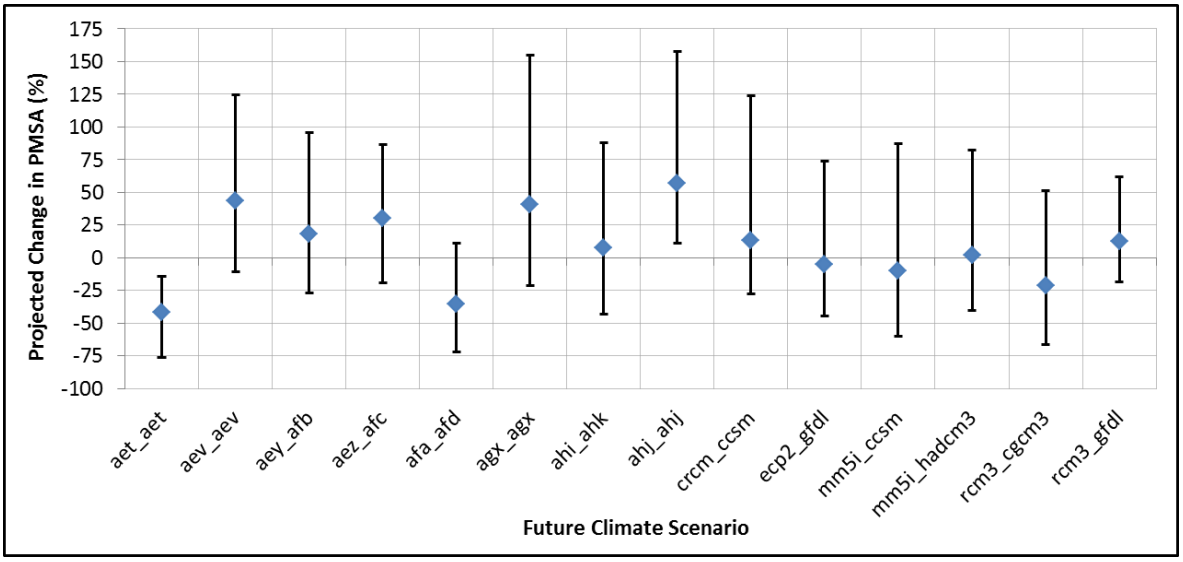

Figure 54: Confidence intervals (95%) of PMSA projections by bootstrap resampling

In fact, confidence intervals from twelve of the fourteen models include between -5% to +5% of the baseline, suggesting that the direction of change is also uncertain in a majority of the future climate projections. Having made this uncertainty clear, the main conclusion of this extended analysis is that the wide range of PMSA results is not erroneous; rather, the range signals a great deal of uncertainty inherent in the climate modelling and frequency analysis of this extreme event.

E.2. TEMPERATURE AND INFLOW PROJECTIONS

Daily temperature deltas were based on the absolute change in mean temperature over centred 30-day moving windows for the critical PMF simulation period (April to June). Individual temperature projections from each RCM were not used in this study, as described further below. Instead, a common sequence of temperature deltas (median of the ensemble) was applied to each future climate scenario. Figure 55 shows the time series of median daily temperature deltas. This time series of change factors was also applied commonly to all future PMF simulations regardless of meteorological sequence in each PMF simulation (i.e., the delta values do not change based on the date of rapid temperature increase).

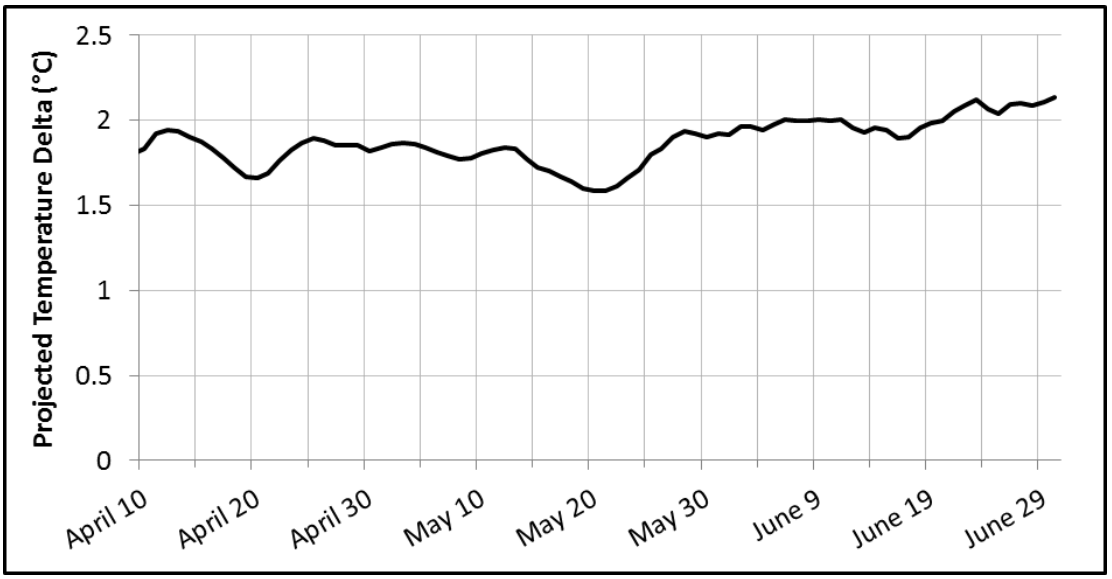

Figure 55: Projected change to baseline daily mean temperature (median of RCM projections); data provided by Ouranos as part of NRCan study (Clavet-Gaumont et al., 2017; Ouranos, 2015)

The deltas fluctuate between +1.5°C to +2°C for the majority of the snowmelt period. The increased temperatures would be expected to lead to earlier snowmelt and increased evapotranspiration in the future PMF simulations. Note that the projected temperature delta for June 30th was carried forward for July and August in the PMF simulations – this assumption was

expected to have a negligible effect on PMF results as the critical peak flow timing in the Lower Nelson River Complex is much earlier in the simulation period (often in May).

The median temperature sequence was used, as opposed to temperature deltas from each individual future climate scenario, for several reasons. First, the ensemble median temperature sequence for the LNRB, developed by Ouranos, was available and easily transferable. Second, preliminary SSARR PMF simulations completed in conjunction with Manitoba Hydro for the NRCan PMP/PMF study determined that temperature changes had a limited effect on peak flows. Given the low sensitivity, the results in Section 5.4.3 are not expected to change significantly with the incorporation of individual RCM temperature change projections. Clavet-Gaumont et al. (2017) similarly noted the insensitivity (resulting from the negligible projected change to the baseline temperature sequences) and did not present PMF results with temperature changes included.

Finally, changes to Lake Winnipeg outflows were estimated based on the change in 1/100 year annual runoff from the Lake Winnipeg watershed. Recall that the relative change factor for 1/100 year inflows to the lake was then applied to the monthly inflow sequence from the largest year of recorded inflows, and converted to outflows using a lake routing model. Figure 56 shows the resulting monthly delta values from each of the fourteen future climate scenarios.

Delta values are adjusted to a previously recorded sequence of inflows, so all fourteen future climate scenarios follow the same shape with varying magnitudes of change. The monthly change factors are such that changes get larger moving from spring to summer (following the shape of the historical sequence of inflows). The median of the ensemble shows a moderate increase in outflows. Given that 11/14 simulations project increasing contributions from Lake

Winnipeg (and only 2/14 project a noticeable decrease), there is confidence in a "likely increase" in Lake Winnipeg outflows, although the magnitude of change remains uncertain.

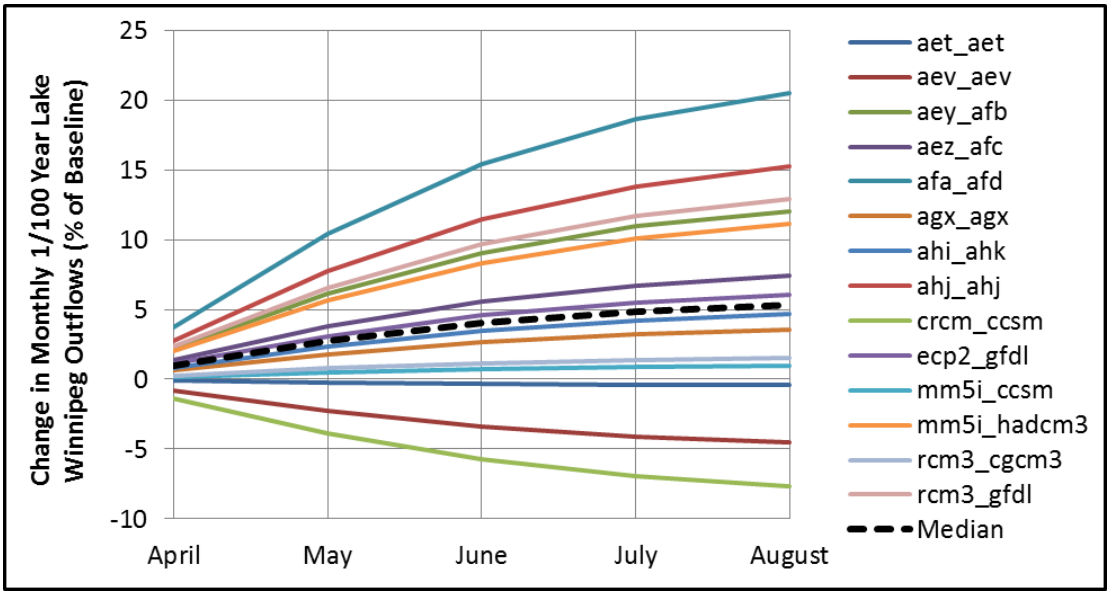

Figure 56: Projected change to baseline monthly average 1/100 year Lake Winnipeg outflows

The range of projections most important to consider are those from April through May that, accounting for travel time, will have the most impact on a spring PMF peak flow. The range in outflows in this period is smaller compared to those of other PMF inputs, with approximately a -4% to +10% change in mid-May (the median below +5% change throughout this period). The smaller range of projections can be attributed to dampening associated with routing 1/100 year inflows through Lake Winnipeg. Having said this, Lake Winnipeg outflows provide a significant portion of flow in the PMF scenario; minor changes can lead to a large change in total volume reaching the generating stations in the Lower Nelson River Complex.

E.3. JUSTIFICATION AND DISCUSSION OF UNCERTAINTY

The wide spread of projected changes to extreme rainfall and snowpack PMF inputs warranted further explanation and justification as to their use in the PMF simulations to follow. The range and uncertainty can be attributed, at least in part, to several limitations or forms of uncertainty in climate modelling

One notable form of uncertainty which does not apply here is the selection of a future emissions scenario to force the climate model. A number of future "outlooks" exist, and in several forms; this study, however, is conservatively isolated only to the "worst-case" A2 scenario from Nakicenovic & Swart (2000).

There is, however, uncertainty related to the choice of climate model ("model uncertainty"). Each model includes different approximations of physical processes, and will respond differently to the same radiative forcing (Hawkins & Sutton, 2011). To quantify this uncertainty, multiple models are used. A greater number of climate models is generally preferred; however, the selection is typically limited to those available and previously quality-checked, as was the case for this study. Statistics related to the ensemble (i.e., the median and range) are often used to describe the spread of projections, as this has generally been found to outperform projections from single models alone (Tebaldi & Knutti, 2007).

Ensemble statistics are reported in this research, but model projections are applied individually to the hydrological model for future PMF scenarios. This methodology was chosen for two reasons. First, the lack of consensus in the model spread did not provide any more confidence in the ensemble mean/median compared to any single model. Second, a more robust sensitivity analysis (of PMF and of each hydrological model) required a number of future climate scenarios to be tested; hence, each model's projections were used as plausible future scenarios.

In addition, there is uncertainty related to natural climate variability that stems from random fluctuations in atmospheric processes. A lack of accurate and complete initial conditions results in drastically different unfolding of atmospheric processes even from small adjustments to conditions at the start of a global climate model run. This is considered "irreducible uncertainty" (Deser et al., 2012, p. 775), because two members of a "perfect" model with an exhaustive period of data will still produce different results. One method to quantify this uncertainty is to include multiple members of the same GCM (each member having a different set of initial conditions; e.g. Deser et al., 2012). Of the fourteen RCM-GCM pairs used in this study, five members of CGCM3 (aet_aet, aev_aev, aey_afc, aez_afc, and afa_afd) and three members of ECHAM5 (agx_agx, ahi_ahk, ahj_ahj) were used to force CRCM4. The five-member ensemble from CGCM3 is explored below in an attempt to estimate the impact of irreducible uncertainty.

Figure 57 isolates only those projections associated with the five member ensemble of CGCM3 that were used to force CRCM4, thus removing model uncertainty. There are significantly varying magnitudes and even opposing directions of change among the 5 scenarios, despite changes only to GCM initial conditions. The differences suggest that, even if the climate model were a perfect representation of physical processes, uncertainty associated with natural climate variability (and with under-sampling here) still leads to a large spread of projections (Hawkins & Sutton, 2011). Considering 1/100 year SWE, where under-sampling should have the least effect (given the shorter return period), there is still a 30% range relative to the baseline and opposing directions of change. This further suggests that even when limiting under-sampling, irreducible uncertainty still widens the spread of projections when considering extreme events.

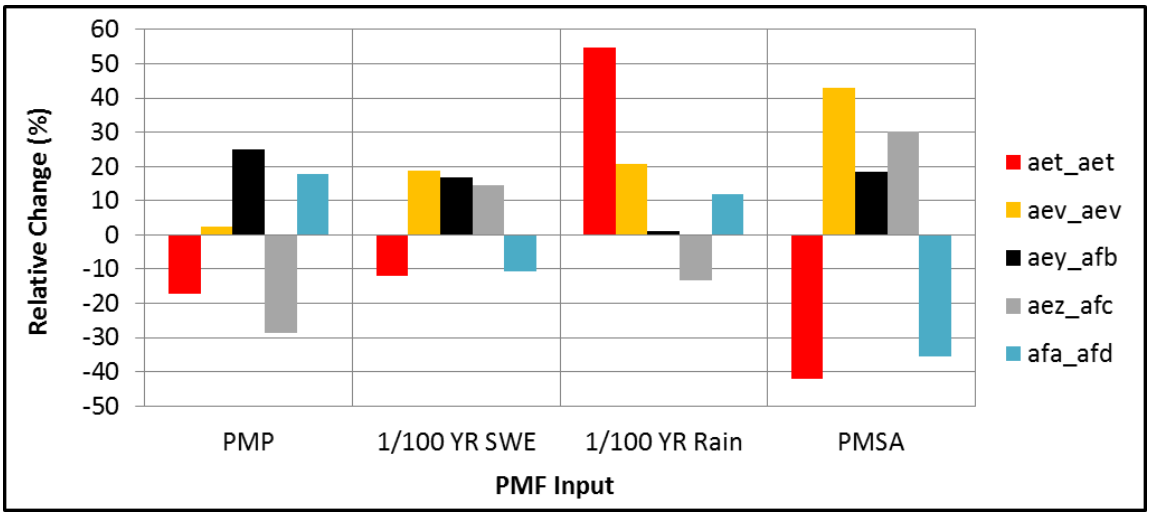

Figure 57: Projected changes to PMF inputs from CRCM4 forced by 5 members of CGCM3

Significant impacts from natural climate fluctuations have also been found in other published studies that considered precipitation variables at a regional scale for a mid-range period such as 2041-2070 (Deser et al., 2012; Hawkins & Sutton, 2011). In addition, keeping in mind that the GCMs used in this study were part of the CMIP3 ensemble of 2005-2006 (since superseded by the CMIP5 ensemble of climate models from 2013), both Deser et al. (2012) and Knutti & Sedláček (2012) concluded that natural climate variability would not reduce significantly through the use of newer, more complex models. In fact, Knutti & Sedláček (2012) found that the more complex models from CMIP5 displayed a slightly increased sensitivity of precipitation projections to natural climate fluctuations. These findings illustrate that, in terms of irreducible uncertainty, the use of GCMs from the CMIP3 ensemble is not a limitation.

In addition to these sources, under-sampling during frequency analysis of extreme events is a significant source of uncertainty in the climate model projections, particularly given the use of 30-year time periods which may mask a shift in the distribution of extreme events (Veijalainen & Vehviläinen, 2008). This is especially important for PMP and would require an

extremely large number of samples in order to adequately estimate that upper bound in a given period. Given the short data periods, it is a virtual certainty that the most extreme events are not sampled in any 30 year period.

Flato et al. (2013) acknowledge that, even in AR5, there are few RCMs with long simulation periods. A potential solution to this issue would be the use of "super-ensembles" (Tebaldi & Knutti, 2007, p. 2056), whereby each RCM would be forced by many members from the same GCM (a "member" meaning a run with slightly perturbed initial conditions, all equally likely). Since each GCM member represents a plausible representation of historical conditions, the 30-year time series simulated by each RCM-GCM member pair could be combined to create a longer series from which to sample from. Super-ensembles have been applied in previous climate model studies (e.g. Deser et al., 2012 for estimating natural climate variability) and the importance of large ensembles was recognized by Doherty et al. (2009) for adequate modelling of extreme events. Large member ensembles for the driving GCMs used here were not readily available at the time of this study; however, Clavet-Gaumont et al. (2017) note that large ensembles for GCMs and RCMs have been developed and published more recently.

Having made clear the uncertainty surrounding this methodology for projecting extreme events from RCM data, it is important to validate that the methodology is not predisposed to the relatively large spread observed in the LNRB projections. As part of the NRCan PMP/PMF study, Ouranos provided PMP and 1/100 year SWE projections for five study basins in Canada, including the LNRB. Three of the five basins showed a "likely increase" in 48-hour PMP (the LNRB showed no consensus), while four basins had projected increased PMP magnitudes (only the LNRB showed a decrease) (Clavet-Gaumont et al., 2017). Thus, the lack of consensus of LNRB projections is the exception rather than the norm, and the methodology was considered

viable for projecting changes to extremes for impact modelling and producing a plausible range of PMF scenarios.

APPENDIX F: PMF RESULTS

F.1. BASELINE PERIOD

PMF hydrographs at all generating stations in the Lower Nelson River Complex are provided for both the spring PMF scenarios (see next page).

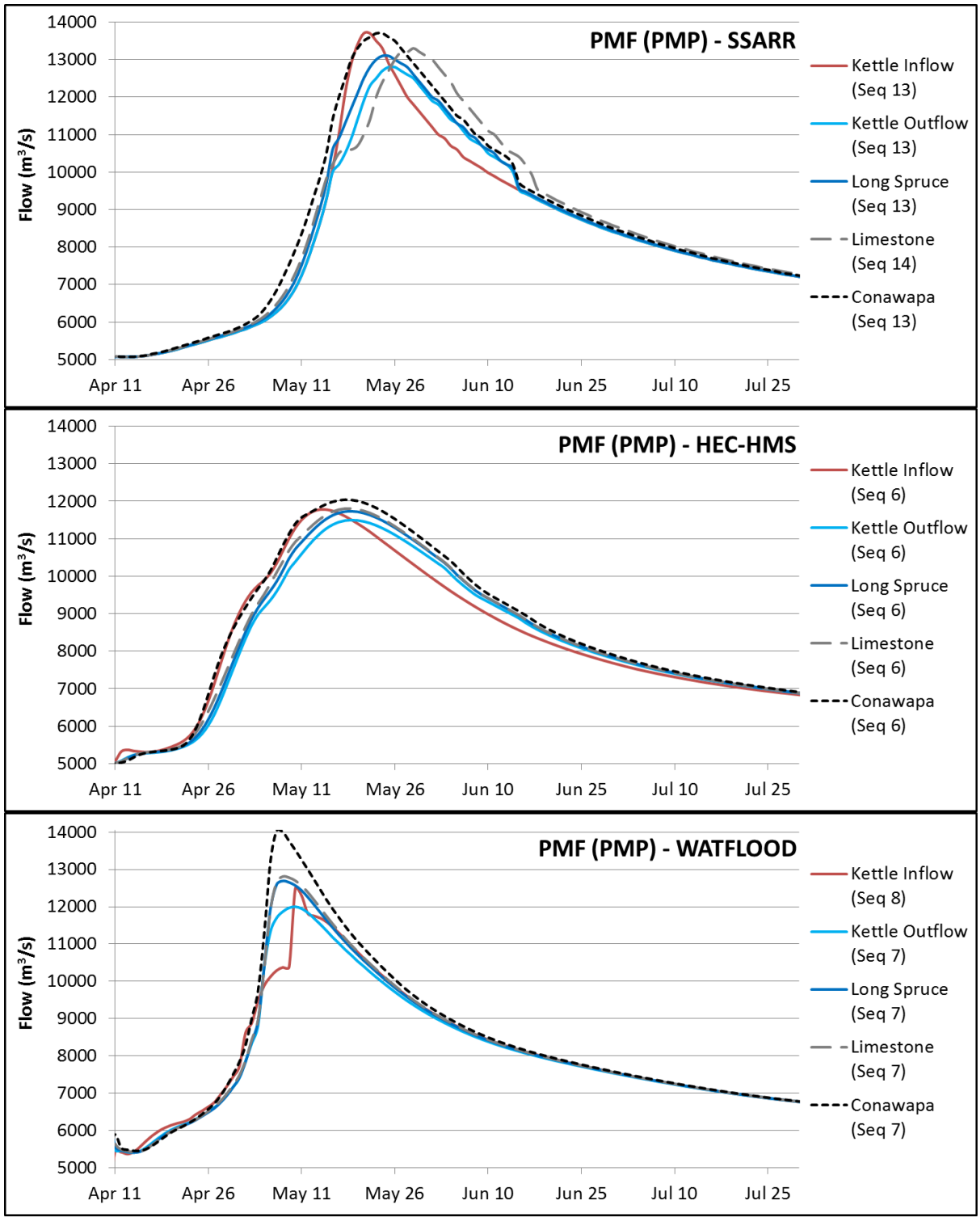

Figure 58: Baseline PMF (PMP scenario) results from all three hydrological models for generating stations downstream of Keeyask in the Lower Nelson River Complex

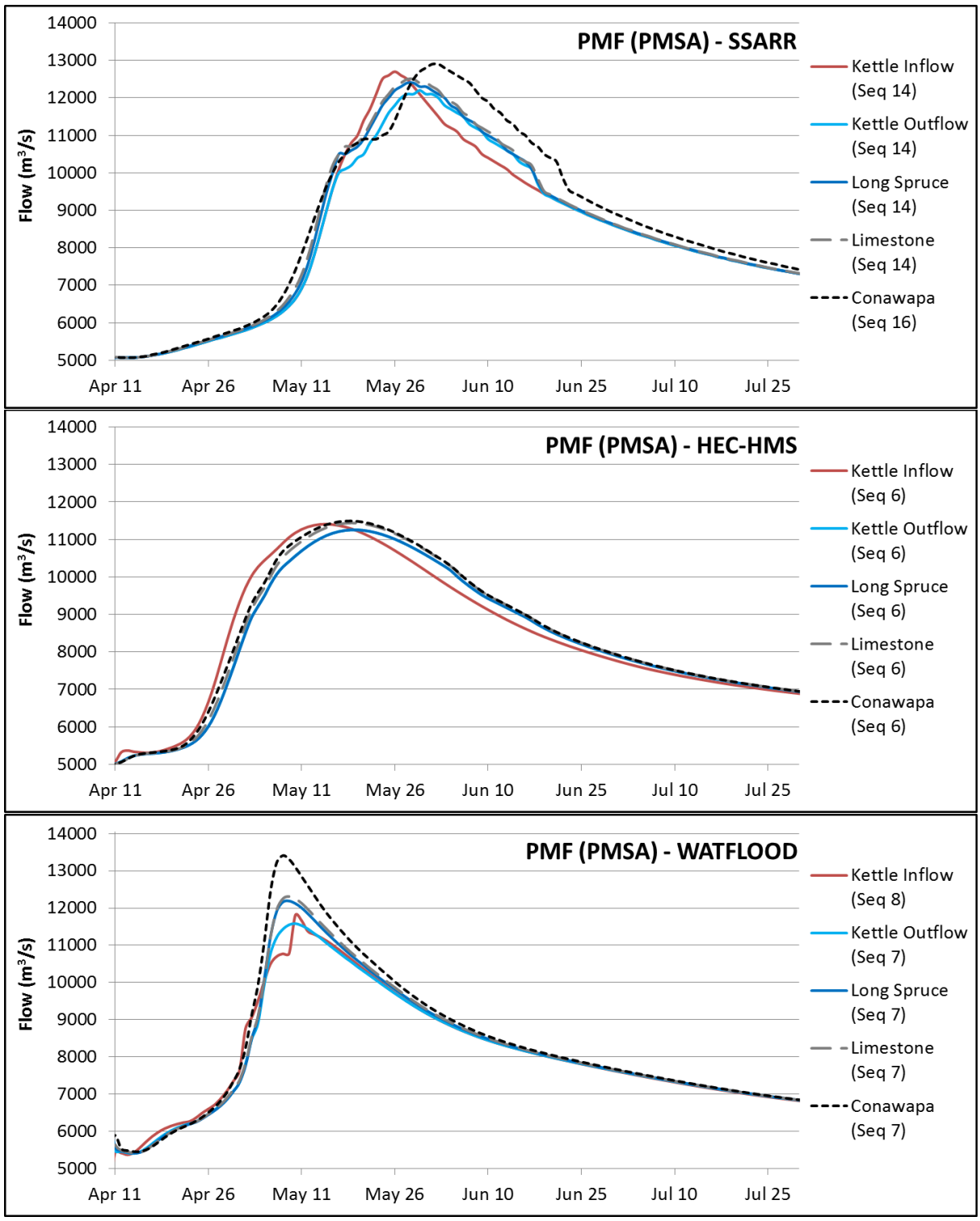

Figure 59: Baseline PMF (PMSA) results from all three hydrological models for generating stations downstream of Keeyask in the Lower Nelson River Complex

F.2. PROJECTED FUTURE PERIOD

Projected changes to PMF inputs from the fourteen future climate scenarios are given in Table 35. The corresponding impacts on PMF peak flows, illustrated as the maximum, median, and minimum index scenarios, are shown in Tables 36 through 43.

Table 35: Projected climate change impacts on PMF inputs

	Projected Changes to Baseline Inputs (%)								
	PMF (PMP) Scenario		PMF (PMSA) Scenario		Lake Winnipeg Outflows – Common to all PMF Scenarios				
RCM	PMP	1/100 YR SWE	1/100 YR Rain	PMSA	Apr	May	June	July	Aug
aet_aet	-17.5	-12.1	54.7	-42.0	-0.1	-0.2	-0.3	-0.4	-0.4
aev_aev	-0.5	18.6	20.6	43.1	-0.8	-2.3	-3.4	-4.1	-4.5
aey_afb	29.2	16.8	1.2	18.3	2.2	6.1	9.0	10.9	12.1
aez_afc	-11.5	14.5	-13.4	30.1	1.3	3.8	5.5	6.7	7.4
afa_afd	10.6	-10.6	11.8	-35.4	3.7	10.4	15.4	18.6	20.5
agx_agx	-2.8	12.3	10.7	40.7	0.6	1.8	2.7	3.2	3.5
ahi_ahk	-10.2	1.3	35.4	7.4	0.8	2.4	3.5	4.2	4.6
ahj_ahj	-14.5	20.9	28.3	56.6	2.8	7.7	11.4	13.8	15.3
crcm_ccsm	-32.2	5.5	41.0	13.4	-1.4	-3.9	-5.8	-7.0	-7.7
ecp2_gfdl	1.1	-1.5	2.2	-5.0	1.1	3.1	4.6	5.5	6.1
mm5i_ccsm	-29.7	-7.2	16.6	-9.9	0.2	0.5	0.8	0.9	1.0
mm5i_hadcm3	-19.2	-5.4	3.0	1.7	2.0	5.6	8.3	10.1	11.1
rcm3_cgcm3	-34.8	-13.0	26.7	-21.6	0.3	0.8	1.1	1.4	1.5
rcm3_gfdl	12.6	3.1	-7.3	12.3	2.3	6.5	9.7	11.7	12.9
Median	**-10.8**	**2.2**	**14.2**	**9.9**	**1.0**	**2.7**	**4.0**	**4.9**	**5.4**

Table 36: Change in PMF (PMP) after incorporating climate change impacts on PMP

		Keeyask G.S.	Kettle G.S. Inflows	Kettle G.S. Outflows	Long Spruce G.S.	Limestone G.S.	Conawapa G.S.
SSAR	MAX	6.1	5.8	10.9	11.5	9.8	10.2
	MED	-1.5	-2.2	-1.6	-1.5	-2.3	-2.2
	MIN	-6.9	-7.3	-6.3	-6.1	-6.8	-6.6
HEC-HMS	MAX	4.7	5.3	4.1	4.6	4.7	5.1
	MED	-1.4	-1.6	-1.3	-1.4	-1.5	-1.6
	MIN	-5.0	-5.4	-4.7	-5.0	-5.1	-5.5
WAT-FLOOD	MAX	4.2	5.6	4.3	5.1	5.4	6.8
	MED	-1.4	-1.9	-1.5	-1.8	-1.8	-2.3
	MIN	-4.9	-6.5	-5.1	-6.0	-6.1	-7.5

Table 37: Change in PMF (PMSA) after incorporating climate change impacts on 1/100 year rainfall

		Keeyask G.S.	Kettle G.S. Inflows	Kettle G.S. Outflows	Long Spruce G.S.	Limestone G.S.	Conawapa G.S.
SSAR	MAX	6.5	7.1	5.7	5.6	6.4	6.2
	MED	2.4	3.1	1.6	1.6	1.6	1.6
	MIN	-0.8	-1.6	-1.6	-1.6	-1.6	-1.6
HEC-HMS	MAX	4.1	4.5	3.8	4.2	4.2	4.6
	MED	1.2	1.3	1.1	1.2	1.3	1.4
	MIN	-0.8	-1.1	-0.7	-0.9	-1.0	-1.0
WAT-FLOOD	MAX	4.3	5.7	4.3	5.1	5.1	6.4
	MED	1.2	1.7	1.3	1.6	1.5	1.9
	MIN	-1.0	-1.4	-1.1	-1.2	-1.3	-1.6

Table 38: Change in PMF (PMP) after incorporating climate change impacts on PMP and 1/100 year SWE

		Keeyask G.S.	Kettle G.S. Inflows	Kettle G.S. Outflows	Long Spruce G.S.	Limestone G.S.	Conawapa G.S.
SSAR	MAX	11.5	11.7	18.0	19.8	18.8	19.7
	MED	0.0	0.0	0.0	0.0	-0.8	0.0
	MIN	-9.9	-10.9	-9.4	-9.9	-10.5	-10.2
HEC-HMS	MAX	10.9	11.4	10.3	10.7	10.9	11.2
	MED	-0.3	-0.3	-0.4	-0.3	-0.3	-0.3
	MIN	-9.6	-10.1	-9.2	-9.5	-9.5	-9.8
WAT-FLOOD	MAX	11.0	12.5	11.3	12.5	12.4	12.6
	MED	-0.4	-0.4	-0.4	-0.4	-0.3	-0.4
	MIN	-8.8	-11.6	-9.0	-10.0	-10.2	-12.3

Table 39: Change in PMF (PMSA) after incorporating climate change impacts on 1/100 year rainfall and PMSA

		Keeyask G.S.	Kettle G.S. Inflows	Kettle G.S. Outflows	Long Spruce G.S.	Limestone G.S.	Conawapa G.S.
SSAR	MAX	19.5	20.5	24.6	26.6	27.2	27.9
	MED	7.3	7.1	6.6	6.5	6.4	6.2
	MIN	-11.4	-11.0	-10.7	-10.5	-10.4	-10.9
HEC-HMS	MAX	25.3	25.6	27.2	28.2	28.6	31.3
	MED	5.5	5.8	5.4	5.6	5.7	5.9
	MIN	-13.9	-14.0	-13.5	-13.5	-13.4	-13.4
WAT-FLOOD	MAX	26.3	27.2	26.6	28.7	28.7	30.9
	MED	6.0	7.3	6.0	6.4	6.4	6.9
	MIN	-14.6	-13.9	-14.7	-15.1	-15.4	-16.5

Table 40: Change in PMF (PMP) after incorporating climate change impacts on PMP, 1/100 year SWE, and daily temperature

		Keeyask G.S.	Kettle G.S. Inflows	Kettle G.S. Outflows	Long Spruce G.S.	Limestone G.S.	Conawapa G.S.
SSAR	MAX	10.7	10.9	17.2	18.3	17.3	18.2
	MED	-0.8	-0.7	0.0	-0.8	-0.8	-0.7
	MIN	-11.5	-12.4	-10.2	-10.7	-11.3	-11.7
HEC-HMS	MAX	11.0	11.2	10.5	10.7	10.8	10.9
	MED	0.3	0.3	0.1	0.1	0.2	0.1
	MIN	-9.1	-9.5	-8.7	-9.1	-9.1	-9.5
WAT-FLOOD	MAX	9.2	9.6	9.5	11.6	11.5	12.3
	MED	-1.3	-1.6	-1.1	-1.8	-2.1	-3.6
	MIN	-10.5	-12.0	-10.8	-12.2	-12.3	-14.5

Table 41: Change in PMF (PMSA) after incorporating climate change impacts on 1/100 year rainfall, PMSA, and daily temperature

		Keeyask G.S.	Kettle G.S. Inflows	Kettle G.S. Outflows	Long Spruce G.S.	Limestone G.S.	Conawapa G.S.
SSAR	MAX	20.3	21.3	25.4	27.4	27.2	28.7
	MED	6.5	6.3	4.9	5.6	5.6	5.4
	MIN	-13.0	-13.4	-13.1	-12.1	-12.0	-12.4
HEC-HMS	MAX	26.2	26.4	28.1	28.1	29.6	31.9
	MED	6.5	6.7	6.2	6.2	6.4	6.5
	MIN	-13.1	-13.4	-12.8	-12.8	-12.9	-13.0
WAT-FLOOD	MAX	26.6	27.3	26.7	26.7	27.1	27.3
	MED	3.4	4.6	4.1	4.1	4.1	3.7
	MIN	-17.0	-17.0	-17.0	-17.0	-18.1	-19.5

Table 42: Change in PMF (PMP) after incorporating climate change impacts to all four PMF inputs (PMP, 1/100 year SWE, temperature, Lake Winnipeg outflows)

		Keeyask G.S.	Kettle G.S. Inflows	Kettle G.S. Outflows	Long Spruce G.S.	Limestone G.S.	Conawapa G.S.
SSAR	MAX	12.2	12.4	18.8	19.8	18.8	19.7
	MED	0.8	0.0	0.8	0.0	0.0	0.0
	MIN	-11.5	-12.4	-10.2	-10.7	-11.3	-11.7
HEC-HMS	MAX	12.5	12.7	12.1	12.2	12.2	12.2
	MED	1.0	1.0	0.8	0.7	0.7	0.6
	MIN	-8.8	-9.3	-8.6	-8.9	-8.9	-9.3
WAT-FLOOD	MAX	10.4	10.4	10.6	12.5	12.3	13.0
	MED	-1.5	-1.3	-1.3	-1.6	-2.0	-3.2
	MIN	-10.4	-11.9	-10.7	-12.1	-12.3	-14.4

Table 43: Change in PMF (PMSA) after incorporating climate change impacts to all four PMF inputs (1/100 year rainfall, PMSA, temperature, and Lake Winnipeg outflows)

		Keeyask G.S.	Kettle G.S. Inflows	Kettle G.S. Outflows	Long Spruce G.S.	Limestone G.S.	Conawapa G.S.
SSAR	MAX	22.0	22.8	27.9	29.8	29.6	31.0
	MED	7.3	7.9	6.6	6.5	6.4	7.0
	MIN	-11.4	-11.0	-11.5	-10.5	-10.4	-10.1
HEC-HMS	MAX	28.6	28.6	30.3	31.1	31.3	33.1
	MED	7.2	6.9	7.0	6.8	6.7	6.4
	MIN	-13.1	-12.8	-12.8	-12.6	-12.4	-12.2
WAT-FLOOD	MAX	28.5	29.0	28.4	28.5	28.6	28.6
	MED	4.6	6.7	5.5	6.0	5.8	6.3
	MIN	-14.9	-13.9	-14.9	-15.3	-15.6	-16.6

APPENDIX G: REGIONAL SENSITIVITY ANALYSIS FIGURES

The figures below illustrate regional sensitivity analysis graphics output by the MCAT tool in MATLAB (Wagener, Wheater, & Lees, 2004). They are based on 10,000 randomly sampled parameter sets in WATFLOOD and 20,000 samples in HEC-HMS, each simulated over the PMF period; sensitivity is defined based on the change in the PMF peak flow.

The figures are best considered in the context of the following description from the MCAT User Manual (Wagener et al., 2004):

> The parameter population is sorted according to the currently selected objective function and split into ten equally sized groups. The cumulative distributions for each group are plotted. A difference in the distributions suggests sensitivity of the model performance to the parameter analysed. (p. 13)

These figures are the basis for qualitative and relative assessments of sensitivity among decision variables in HEC-HMS and WATFLOOD, provided in Section 5.5.

(Figures begin on next page)

G.1. HEC-HMS – PARAMETER SENSITIVITY RESULTS

G.1.1. SOIL MOISTURE ACCOUNTING (SURFACE) PARAMETERS

Maximum Surface Storage (mm; by sub-basin)

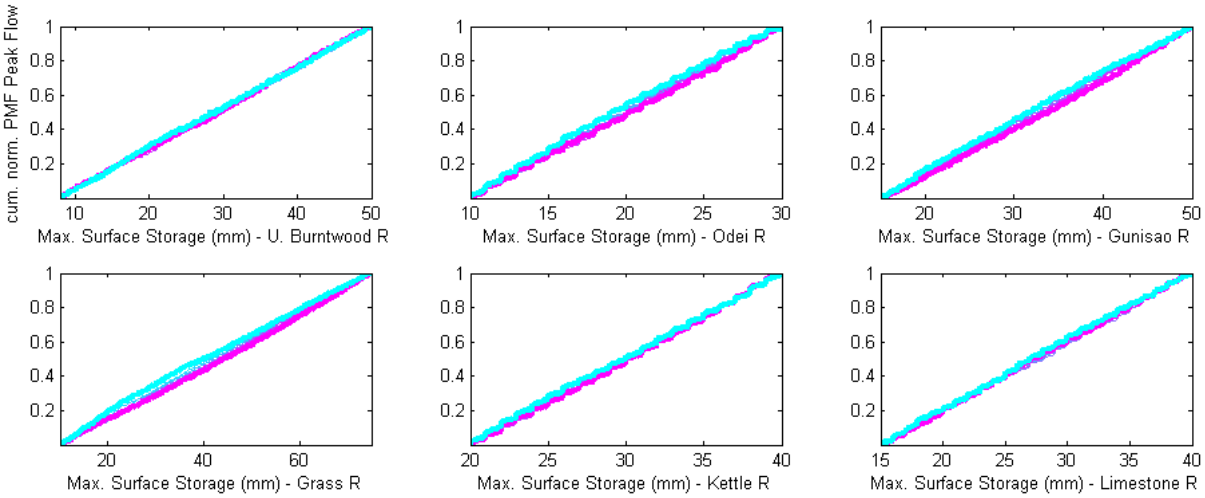

Maximum Infiltration Rate (mm/hr; by sub-basin)

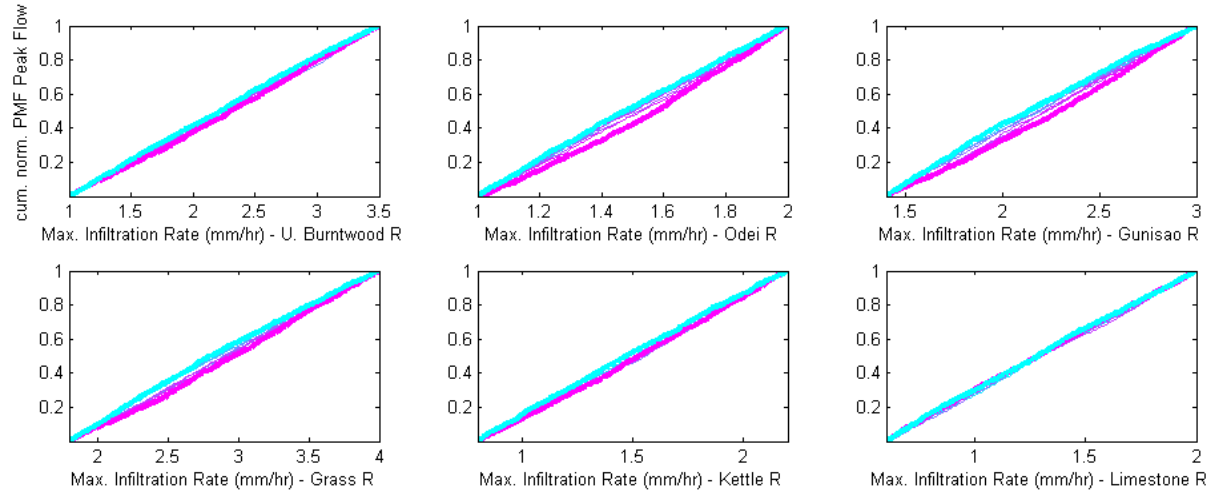

Percent Impervious Area (%; by sub-basin)

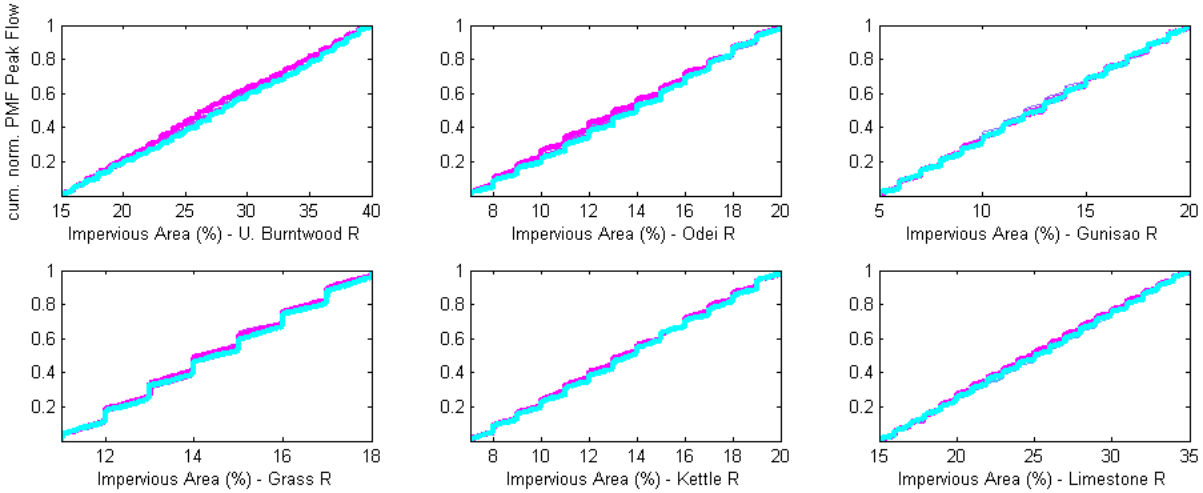

G.1.2. SOIL MOISTURE ACCOUNTING (SOIL) PARAMETERS

Soil Tension Storage (mm; by sub-basin)

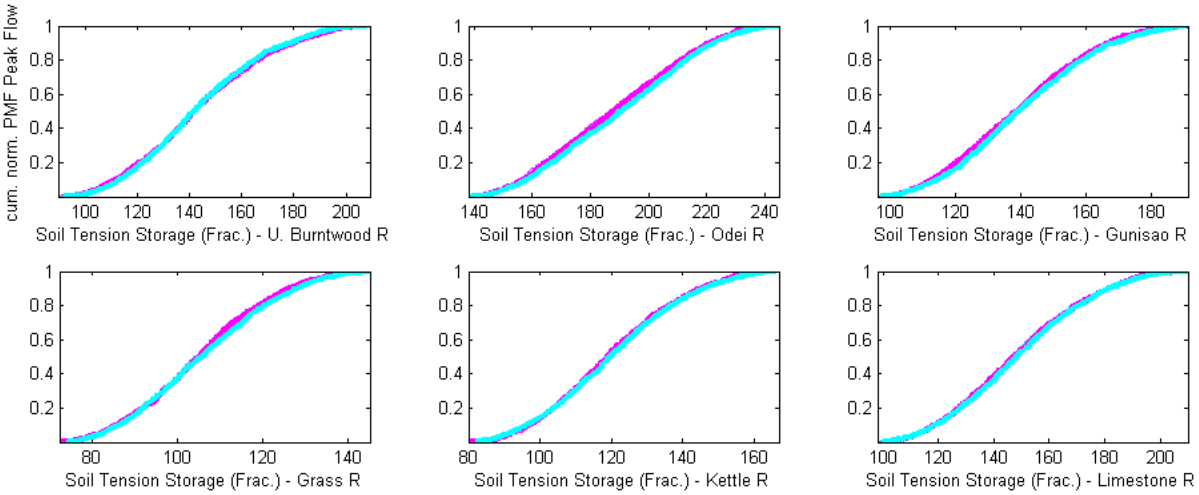

Maximum Soil Storage (mm; by sub-basin)

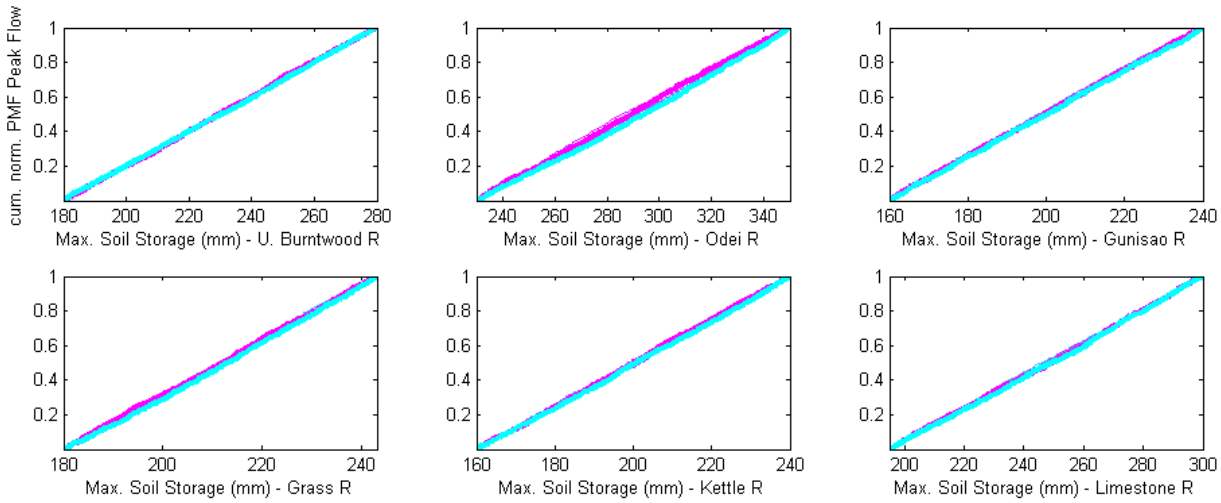

Maximum Soil Percolation (mm/hr; by sub-basin)

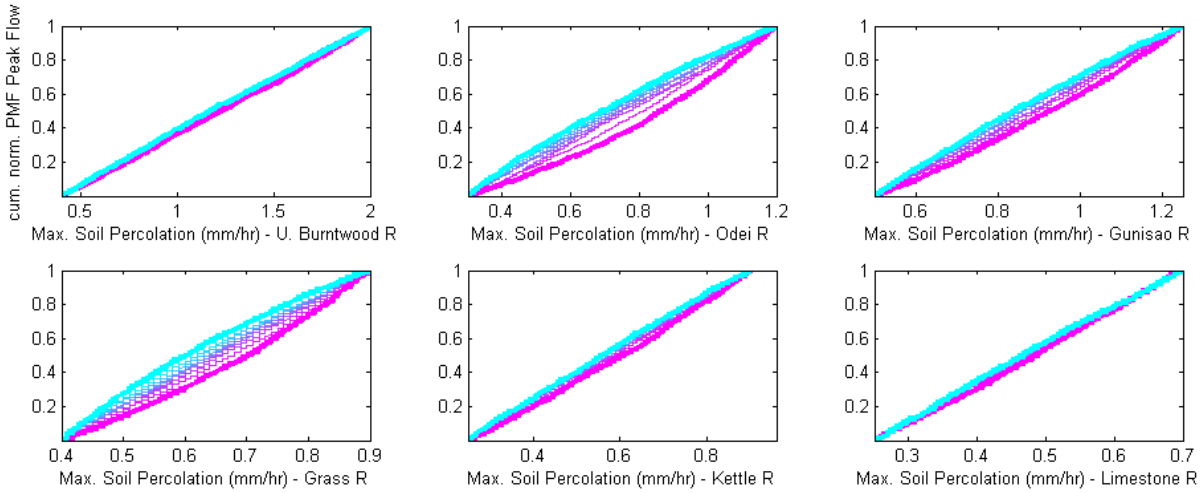

G.1.3. SOIL MOISTURE ACCOUNTING (GROUNDWATER LAYER 1) PARAMETERS

Upper Groundwater - Maximum Storage (mm; by sub-basin)

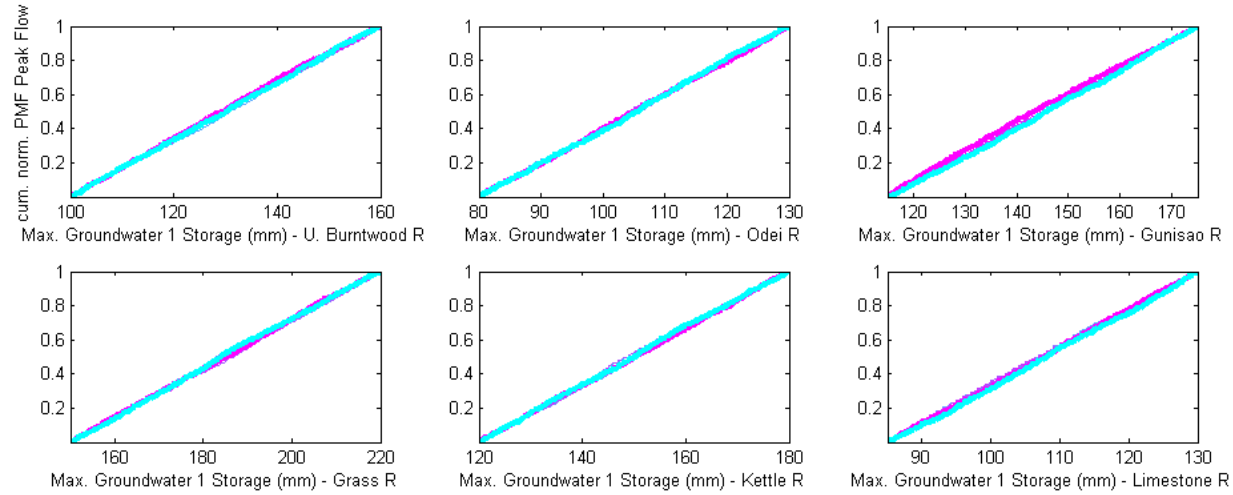

Upper Groundwater - Storage Coefficient (hr; by sub-basin)

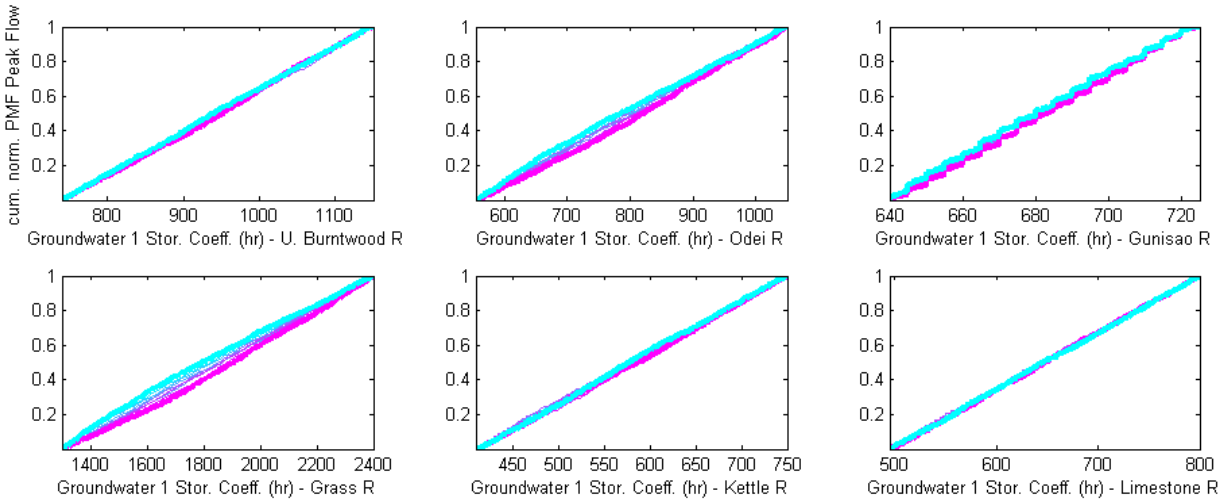

Upper Groundwater - Maximum Percolation (mm/hr; by sub-basin)

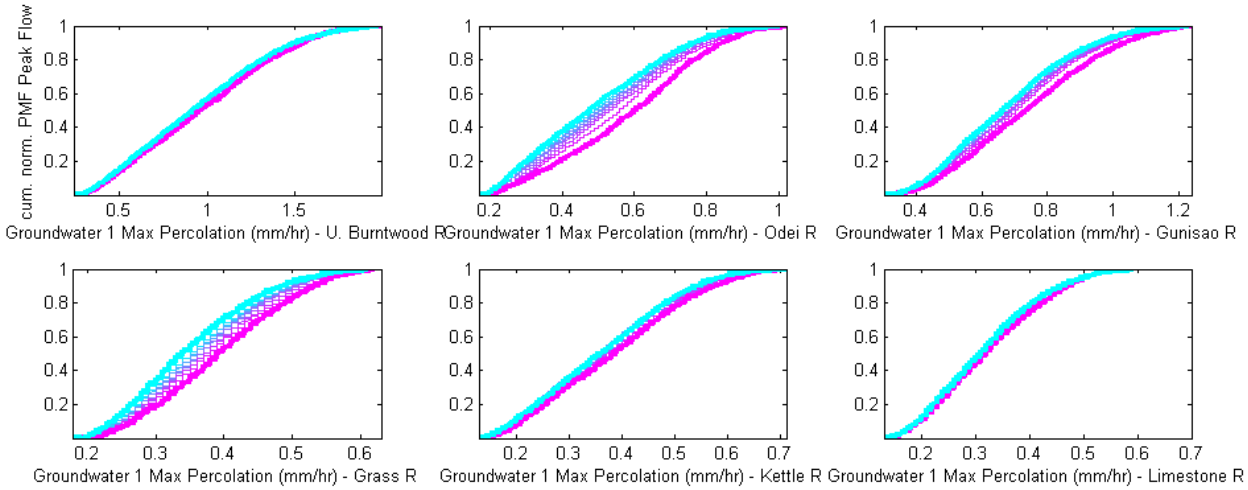

G.1.4. SOIL MOISTURE ACCOUNTING (GROUNDWATER LAYER 2) PARAMETERS

Lower Groundwater – Maximum Storage (mm) and Storage Coefficient (hr) (by sub-basin)

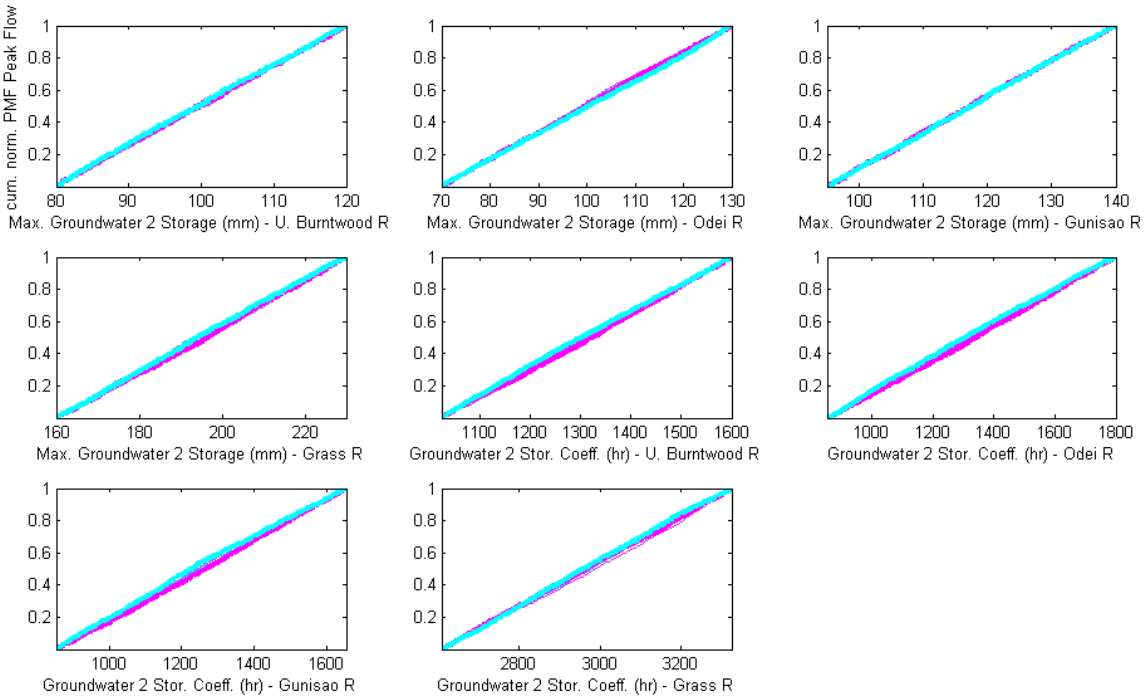

Lower Groundwater – Maximum Percolation (mm/hr) (by sub-basin)

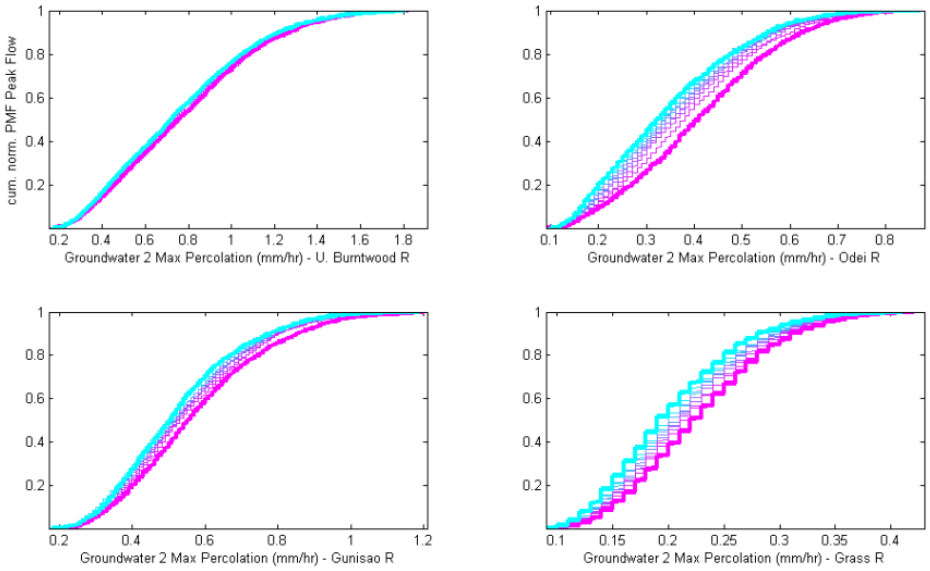

G.1.5. CLARK UNIT HYDROGRAPH PARAMETERS

Time of Concentration (hr; by sub-basin)

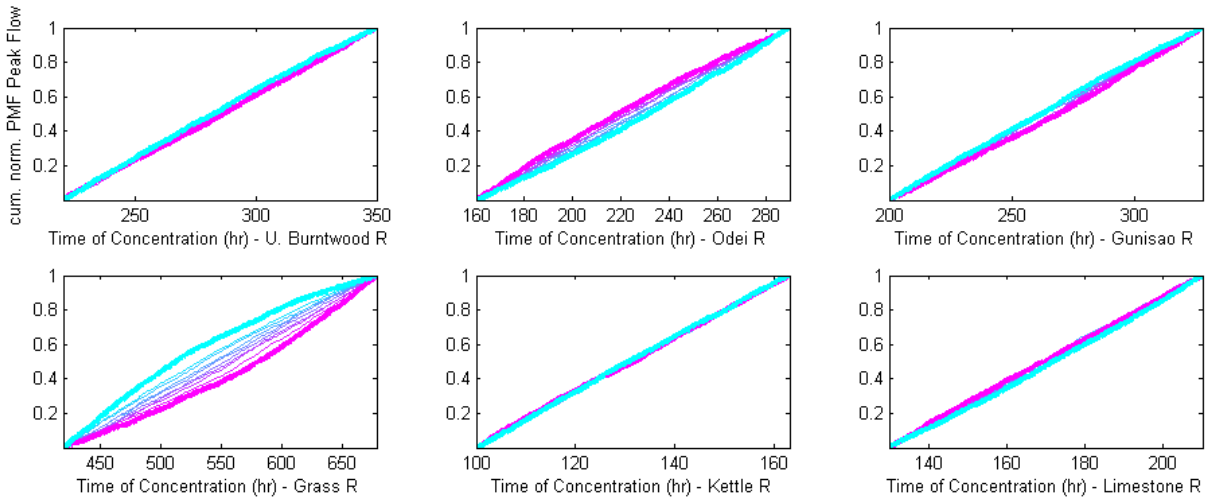

Surface Storage Coefficient (hr; by sub-basin)

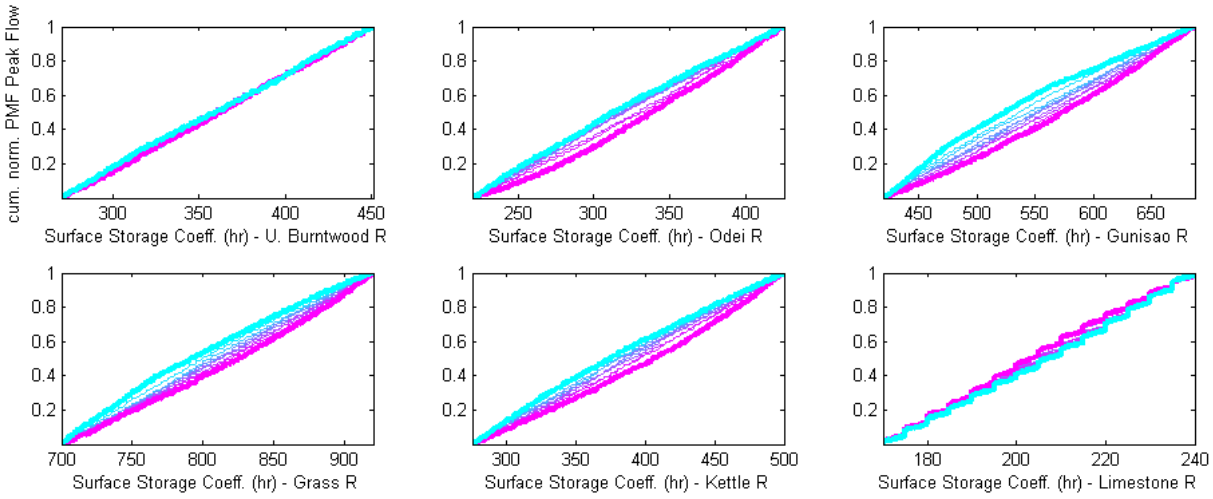

G.1.6. SNOWMELT PARAMETERS

Snowmelt Rate (mm/°C/day) and Base Melt Temperature (°C) (global parameters)

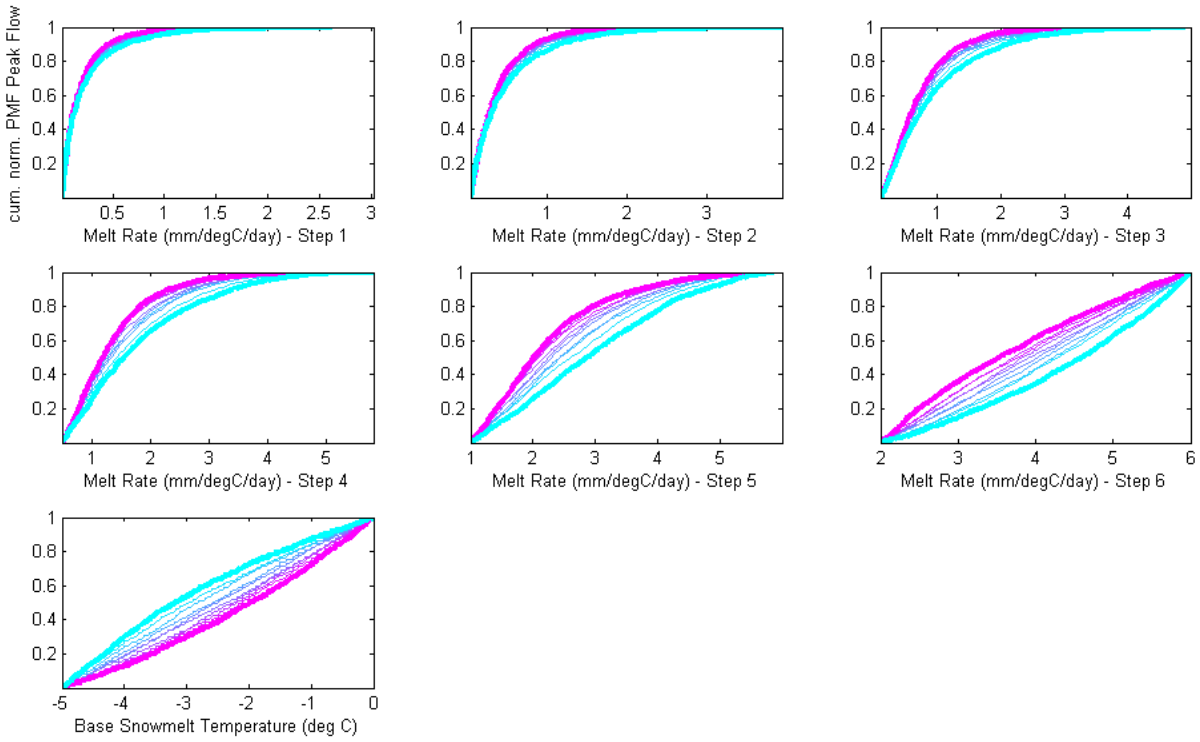

G.2. WATFLOOD – PARAMETER SENSITIVITY RESULTS

G.2.1. RIVER CLASS PARAMETERS

Manning's Roughness – Channel (by river class)

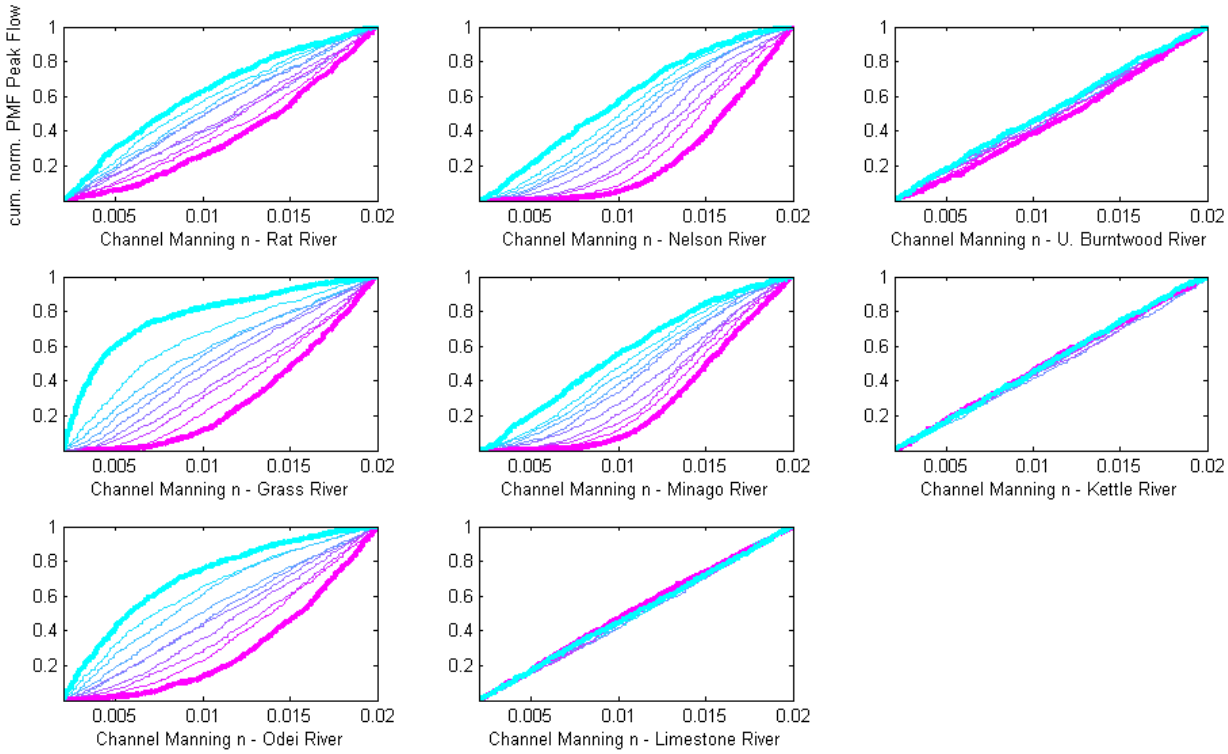

Wetland Bank Porosity (by river class)

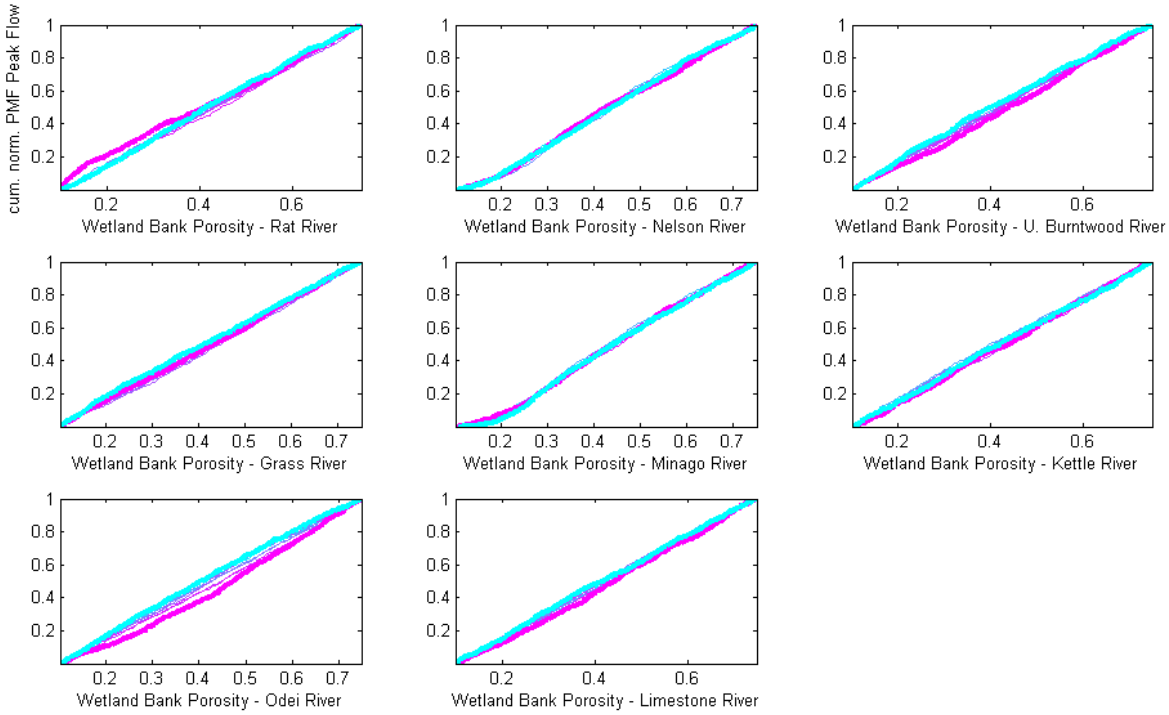

Wetland Lateral Conductivity (by river class)

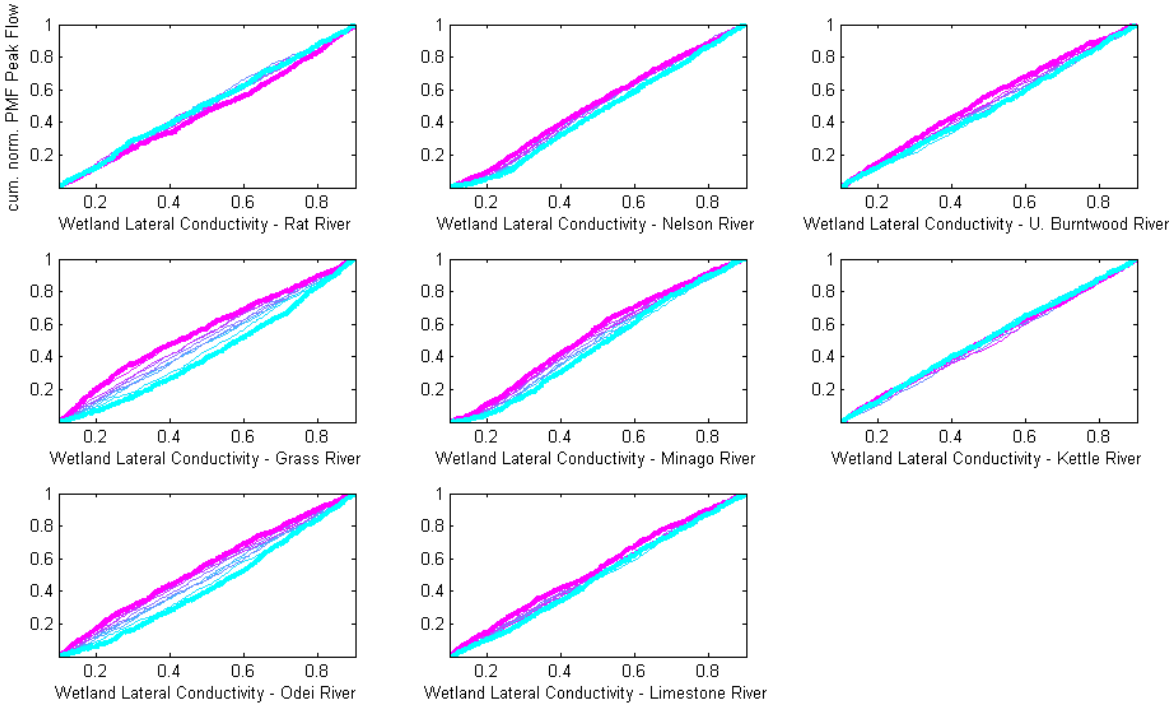

G.2.2. LAND CLASS PARAMETERS – SUBSURFACE PROCESSES

Interflow Coefficient (by land class)

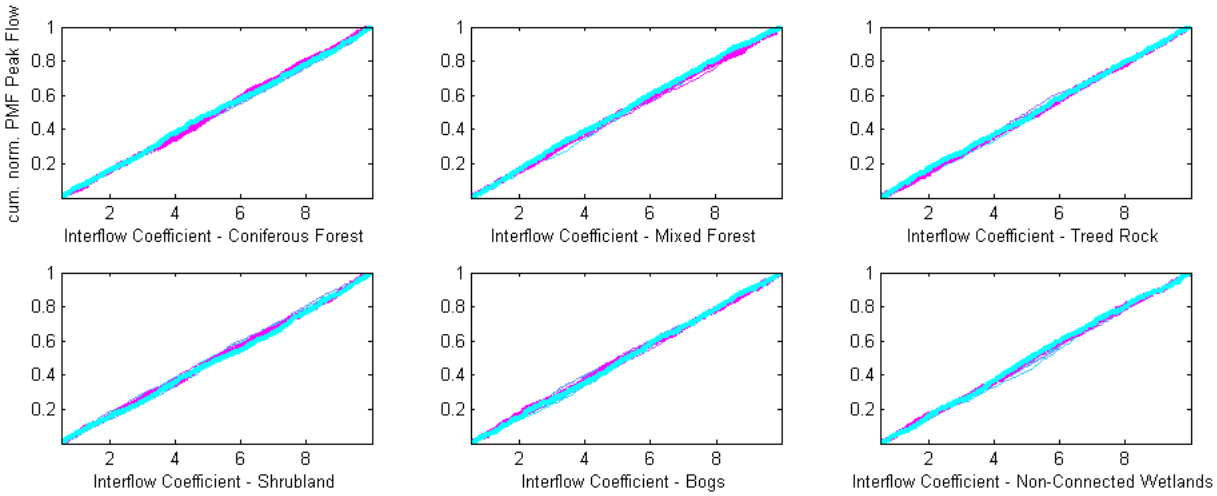

Infiltration Coefficient – Bare Ground (by land class)

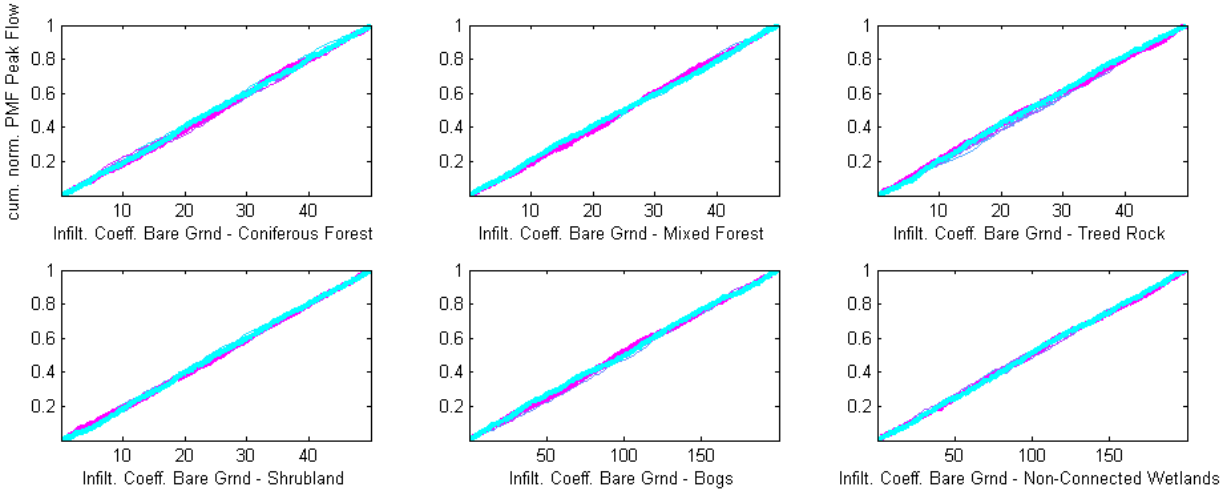

Upper Zone Retention (mm; by land class)

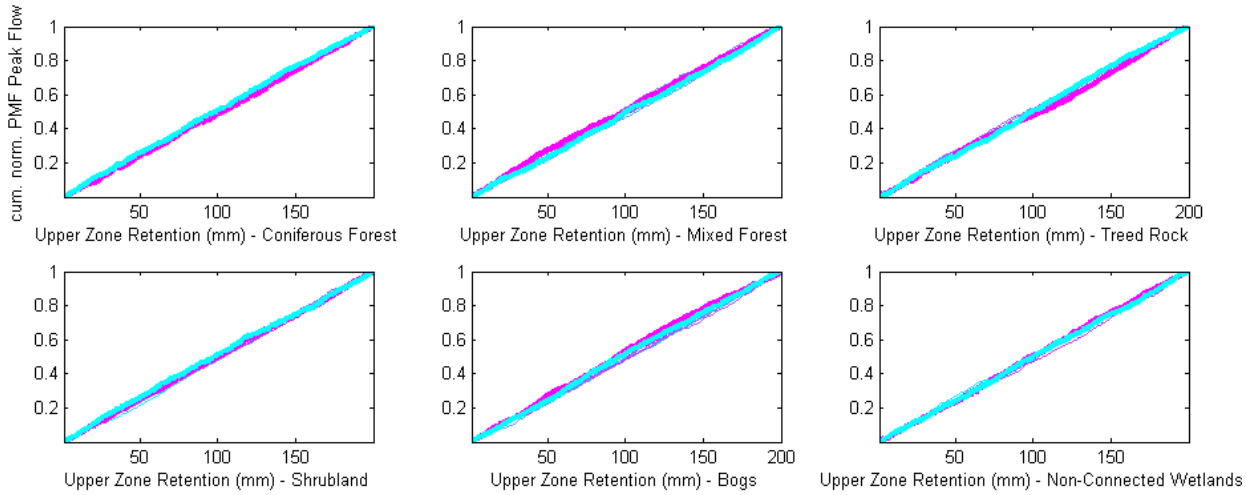

Recharge Coefficient – Bare Ground (by land class)

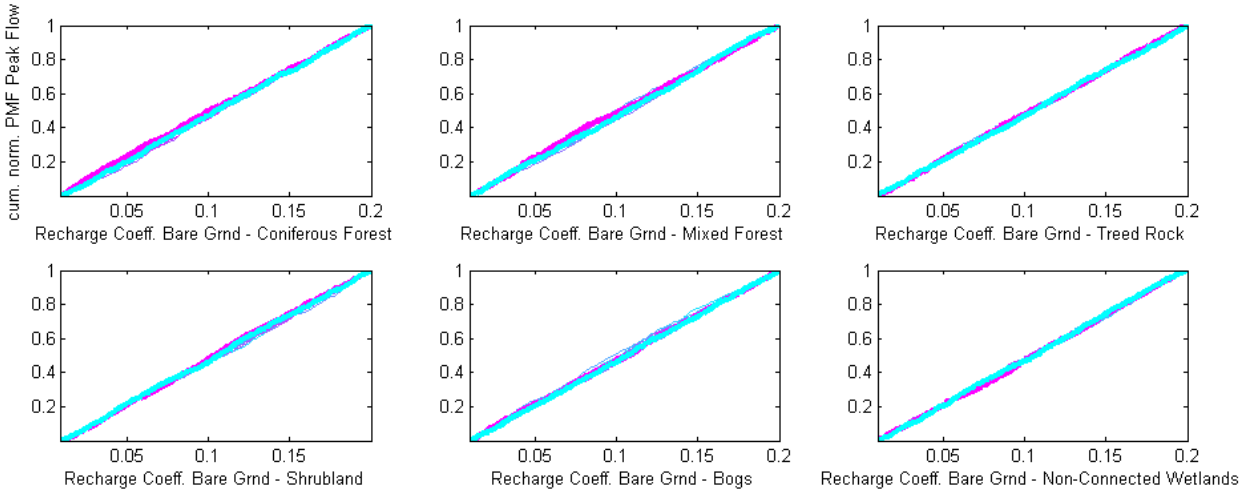

G.2.3. LAND CLASS PARAMETERS – SNOWMELT

Snowmelt Rate (mm/°C/hr; by land class)

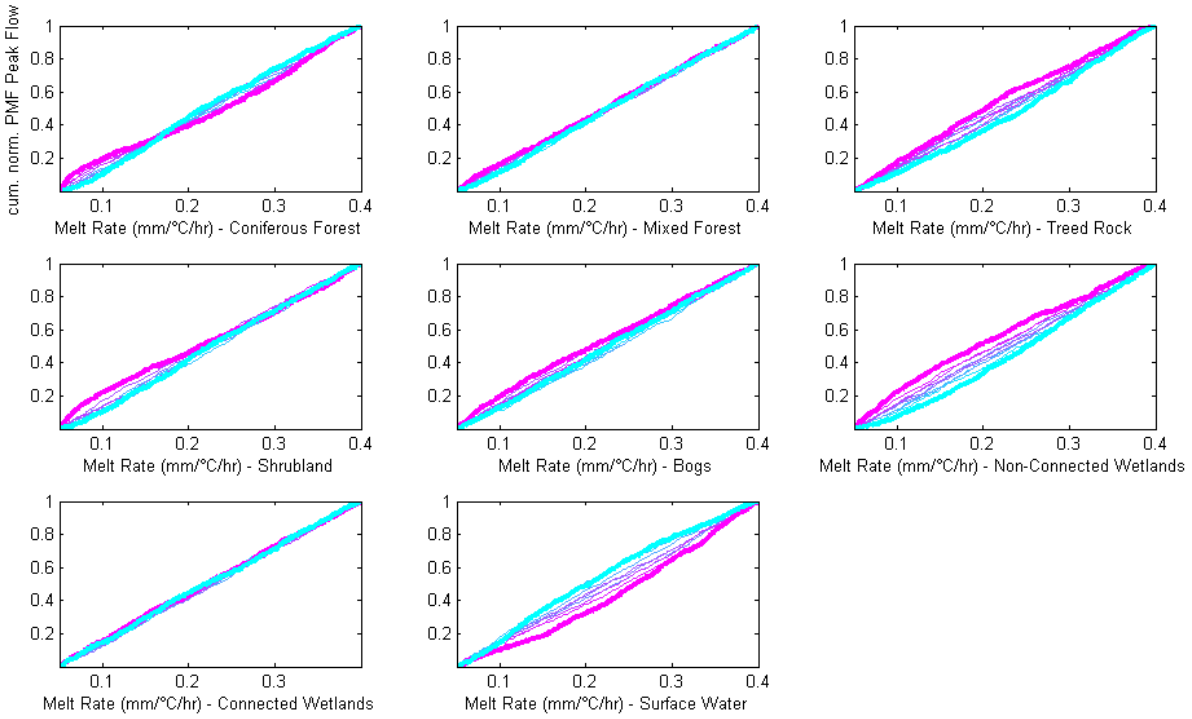

Base Melt Temperature (°C; by land class)